

Sedimentology of the Paleogene succession at Calypsostranda, Svalbard

Louise Kristiansen Poole

Master of Science Thesis
In Sedimentology/ Petroleum geology

January 2018



Department of Earth Science

University of Bergen¹



Department of Arctic Geology

The University Centre in Svalbard²

Abstract

The following study encompasses sedimentological investigations of the Calypsostranda Group. The Calypsostranda Group is comprised of Paleogene sediments where outcrops are well exposed in a coastal section at Renardodden (Calypsostranda area), on the southern shores of Bellsund in western Spitsbergen.

The aim of the study is to: i) generate reliable depositional models for the evolution of the sediments of the Calypsostranda Group, through facies recognition and break-down ii) investigate and discuss source-to-sink perspectives including provenance and possible basin-development scenarios in accordance with different age datings and the tectonic history of western Spitsbergen.

A limited amount of research has been conducted on the deposits of the Calypsostranda Group, however they are important to understand in the context of the regional sedimentation and tectonic history of western Spitsbergen. The succession encompasses delta plain sediments of the Skilvika Formation and paralic to marine sediments of the Renardodden Formation. Through sedimentological outcrop investigations, sixteen lithofacies have been identified from the studied sedimentary succession of the Calypsostranda Group (F1-F16) by means of facies recognition and break-down. The lithofacies were further grouped into seven sub facies associations, which can be divided into two main facies associations: i) a sub-aerial delta plain (Skilvika Formation) and ii) a paralic to marine regime (Renardodden Formation).

The deposits in the Calypsostranda area were initially deposited in a prograding fluvial dominated, storm-wave influenced delta system. The fluvial dominance can be deduced from a number of observations; the abundance of distributary channels on the delta plain, coarse-grained debris flow deposition from hyperpycnal flows on the delta front, mouth bar deposits and turbidites. The dominance of very-fine to fine-grained sand and abundancies of coal fragments in the marine deposits are indicators of a fluvial dominated system. The deposits have further been divided into a five-stage depositional model that involves a major transgressive phase drowning previously subaerial deposits, followed by normal regression with delta progradation.

Evidence from the petrographical and sedimentological analysis points to a potential dual source area for the deposits in the Calypsostranda area. Findings of metasedimentary rock fragments, silica-rich biofragments and chloritoid in the thin sections account for a potential metamorphic basement derived source. In addition, a sand-rich system and coal fragments suggests an uplifted sedimentary source. Given the uncertainty of the ages of the deposits, three different palaeogeographical scenarios are presented and described.

Acknowledgements

This study is a master's thesis within sedimentological research at the University of Bergen. Several contributors have supported with discussions, guidance and assistance throughout the writing process. Parts of this research was conducted in relation to the ARCEX project, which is funded by the Research Council of Norway (grant number 228107).

First of all, I would like to thank my supervisor Prof. William Helland-Hansen at the University of Bergen for invaluable guidance and interesting discussions throughout the whole writing process. I would also like to thank my co-supervisor Sten-Andreas Grundvåg at the University of Tromsø for proof reading and valuable feedback.

Thank you to logistics at UNIS for providing safety training for both field seasons so that field work could be carried out in a safe manner. Malte Jochmann (UNIS), Dirk Knaust (Statoil ASA) and Karoline Thu Skjærpe are thanked for assistance during the field season of -17 and for engaging discussions.

Olav Walderhaug (Statoil ASA) is thanked for discussions related to the thin sections and Helge Kommedal for assistance with Adobe Illustrator.

Irina Dumitru is thanked for preparing the thin sections and assistance with the RAMAN microscope. Irene Heggstad at the ELMILAB for guidance with the scanning electron microscope.

Thank you to all my friends at the University in Bergen for so many enjoyable times and for all your support during our years of study. Special thanks to Heidi and Marthe for proof reading parts of this thesis.

Finally, I would like to give a very special thanks to my family and Øyvind. To my family for your continuous support and affection, it has meant everything. And thank you to Øyvind for your encouragement, both in the field and at home, and for always being patient and believing in me.

Louise Kristiansen Poole

Stavanger, 14 January 2018

Table of Contents

1. Introduction	1
1.1. Preface	1
1.2 Previous work	1
1.2.1 Age correlations	2
1.3 Aims and objectives	3
1.4 Geographic location and geological setting	4
1.5 Study area	5
2. Methods	7
2.1 Field work	7
2.2 Post-field work	7
2.2.1 Digitisation	7
2.2.2 Light microscopy	8
2.2.3 Scanning electron microscopy	8
2.2.4 Textural analyses	9
3 Geological framework	11
3.1. Introduction	11
3.2. Pre- Caledonian era	13
3.3. Caledonide and Post- Caledonide era	13
3.3.1 Caledonian era	14
3.3.2 Devonian	15
3.3.3. Carboniferous	15
3.3.4. Permian	16
3.3.5 Mesozoic era	16
3.3.6. Cretaceous	17
3.4. Cenozoic era	18
3.4.1. Rifting and uplift	18
3.4.2. Stratigraphy	19
3.4.3. The West Spitsbergen fold- and thrust belt	22
3.5. Lithostratigraphic and geological setting of the study area	24
3.5.1. Structural setting	24
3.5.1. Kapp Lyell sequence	25
3.5.2. Calypsostranda Group	25
4 Lithofacies and facies associations	27
4.1 Introduction	27
4.2 Lithofacies	28
4.3 Facies associations with subsequent lithofacies	33
4.3.1 Facies association 1: Continental depositional environment	33
4.3.2 Facies association 2: Open marine depositional environment	59
5. Petrography	75
5.1 Textural analysis	76
5.2 Composition	78
5.2.1 Framework constituents	80
5.2.2 Diagenetic minerals	84
5.2.3: Presence of organic matter	87
5.2.4 Classification	87
6 Geological development	93
6.1 Depositional environments	93
6.2 Modern analogues	95
6.3 Depositional history of the Calypsostranda Group	98

6.3.1 Stage 1: Tectonic faulting and mass transport deposition	98
6.3.2 Stage 2: Development of a meandering river system	99
6.3.3 Stage 3: Transgressive phase with retrogradational delta system	100
6.3.4 Stage 4: Continued transgressive phase and development of major flooding surfaces	101
6.3.5 Stage 5: Normal regressive phase and delta progradation	102
7 Source to sink perspectives	105
7.1 Provenance	105
7.2 Age	107
7.3 Implications of a Paleocene/ early Eocene age (Fig. 7.2)	107
7.3.1 Possible connection to the Central Tertiary Basin	108
7.3.2 Accumulation in an outlier basin off the western coast of Spitsbergen (Fig. 7.3)	112
7.4 Implications of a late Eocene/ early Oligocene age (Fig. 7.4)	113
7.4.1 Possible correlation to the Central Tertiary Basin	114
7.4.2 Development of a fault-bounded graben	116
7.5 Summary	118
7.6 Outlook	119
8. Conclusions	120
References	122
Appendix A	129
Appendix B	159

1. Introduction

1.1. Preface

The Svalbard archipelago has a distinct stratigraphy, is a good analogue for the sedimentary succession in the Barents Sea and displays rocks from Precambrian to Paleogene in age (Steel and Worsley, 1984). As a result, it has been an interest area for geological research for decades. Some of the basins with Paleogene accumulations are less studied and are important in understanding the context of regional sedimentation and tectonic history of western Spitsbergen. This thesis provides detailed sedimentological research and analysis of the Paleogene outcrops at Skilvika and Renardodden, from now on referred to as the Calypsostranda area.

1.2 Previous work

Of the Paleogene basins at Svalbard, the Central Tertiary Basin in the central part of Spitsbergen has been the main interest area of numerous studies. The basin represents sediments of early Paleocene to late Eocene and possibly Oligocene in age (Steel et al., 1985) and comprises sediments of fluvio-deltaic, shallow-marine and marine deep origin. The spectacular clinoforms of the Battfjellet Formation (Eocene) are especially well studied (e.g. Mellere et al., 2002; Helland-Hansen and Helland-Hansen, 2010; Gjelberg, 2010; Grundvag et al., 2014). Detailed sedimentary analysis of the Paleogene outcrops in the Calypsostranda area have been few, although studies describing the tectonic elements and unconformities (Dallmann, 1989; Birkenmajer, 2006), floras and plant remains (e.g. Heer 1876; Nathorst 1910; Livsic 1974) and biostratigraphy (Head, 1984) have been conducted. Vonderbank (1970) conducted sedimentological descriptions of the deposits and found traces of *Ophiomorpha nodosa* in the upper part of the section.

Recent studies have provided detailed sedimentological and structural studies of the deposits. *Kleinspehn*. in Dallmann (1999) logged the Skilvika and Renardodden Formation and estimated the succession to be over 260 meters thick. Dallmann (1989) published a study on the boundary between the metamorphic basement rocks of the

Kapp Lyell sequence and the Cenozoic strata where he presents evidences for a fault contact that divides the Precambrian basement from the overlying sedimentary rocks. Birkenmajer (2006) studied tectonic features including faults within the sedimentary succession. Birkenmajer and Gmur (2010) conducted sedimentological analyses and corresponding coal petrography of the main Paleogene outcrops in the Calypsostranda area (Fig. 1.1).

1.2.1 Age correlations

Several age correlations to deposits of the Central Tertiary Basin have been suggested for the Paleogene deposits at Calypsostranda (e.g. Heer, 1876; Nathorst, 1910; Livsic, 1974; Thiedig et. al 1979). The first published work is that of Heer (1876) and later Nathorst (1910) who studied floras in the succession and suggested an equivalent age to the Aspelintoppen Formation, based on similarities in floristic findings. Livsic (1974) conducted studies of pollen, mineral composition, spores and plant remains of the deposits and suggest a correlation with the Storvola Formation (referred to as the Aspelintoppen Formation in present literature). Thiedig et. al (1979) correlate the succession to the lower parts of The Central Tertiary Basin succession, due to discoveries of a certain type of mollusc, *Conchocele conradii* which has in previous studies been found in the Basilika Formation of the Central Tertiary Basin (Rosenkrantz, 1942). Head (1984) studied dinocyst assemblages in the Renardodden Formation and sporomorph assemblages in the Skilvika Formation. From these results, he suggested the age of the deposits to be late Eocene to early Oligocene.

A palynological analysis conducted late 2017 on a sandstone sample from the Skilvika Formation, pointed towards a late Paleocene/early Oligocene age for the deposits, based on assemblages of dinocysts, diatoms, pollen and spores in the sample (Lenz, 2017).

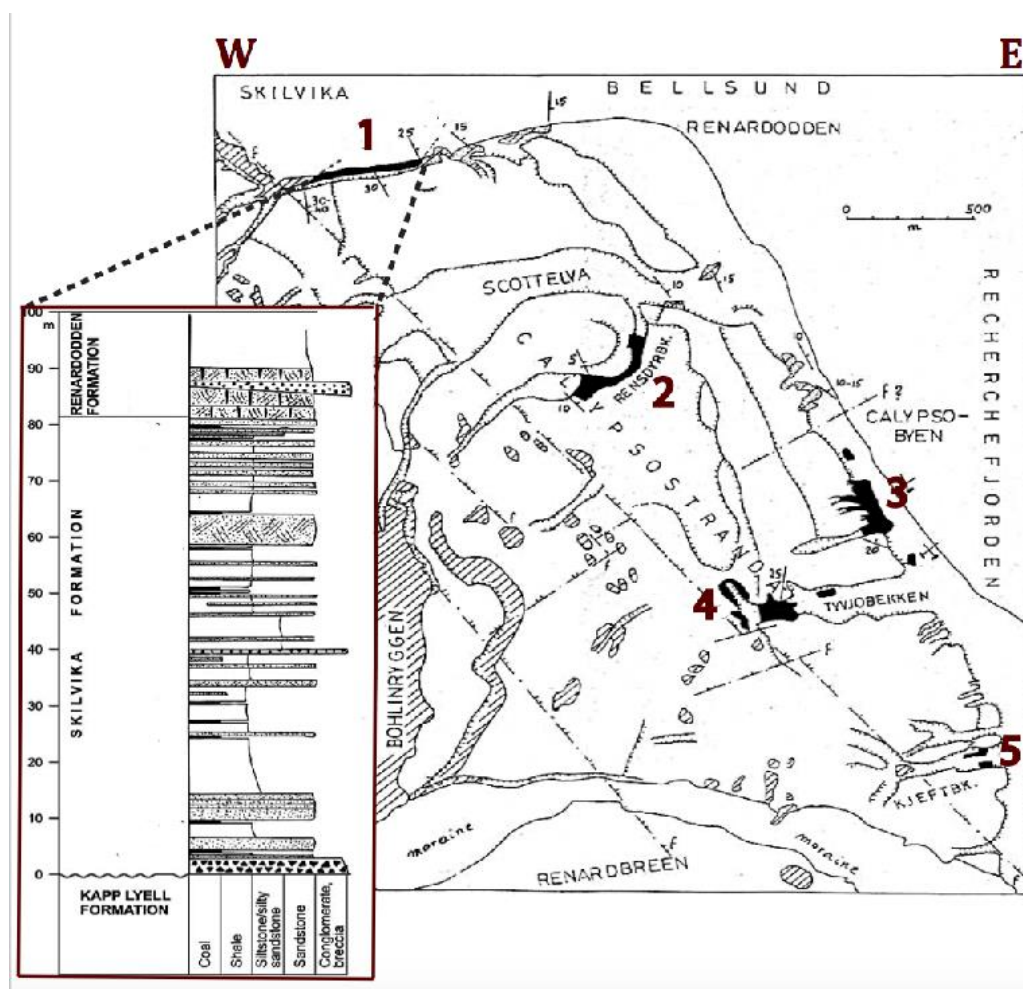


Figure 1.1: Map and stratigraphy of the study area displaying the five localities of Paleogene outcrops in the Calypsostranda area. 1-Skilvika (with corresponding log) , 2-Reinsdyrbekken, 3-Calypsobyen, 4-Tyvjobekken, 5-Kjeftbekken. Modified from Birkenmajer and Gmur (2010) after Birkenmajer and Zastawniak (2005).

1.3 Aims and objectives

The aim of this study is to: i) generate reliable depositional models for the evolution of the sediments of the Calypsostranda Group, through facies recognition and break-down ii) investigate and discuss source-to-sink perspectives including provenance and possible basin-development scenarios in accordance with different age datings.

The scientific method for this thesis is based on sedimentological outcrop analyses and petrographical studies from sample-taking. In-depth sedimentological investigations through logging, sketching, photography and sample-taking were conducted during field work in the summer 2016 and 2017. Specifically, the objectives are:

- Provide a detailed lithostratigraphic log and facies break-down to understand sedimentary processes involved in the deposition of the sediments.
- Conduct thin section analyses of samples from the facies identified in order to study textures and mineral compositions to investigate source-to-sink perspectives of the Calypsostranda Group.

1.4 Geographic location and geological setting

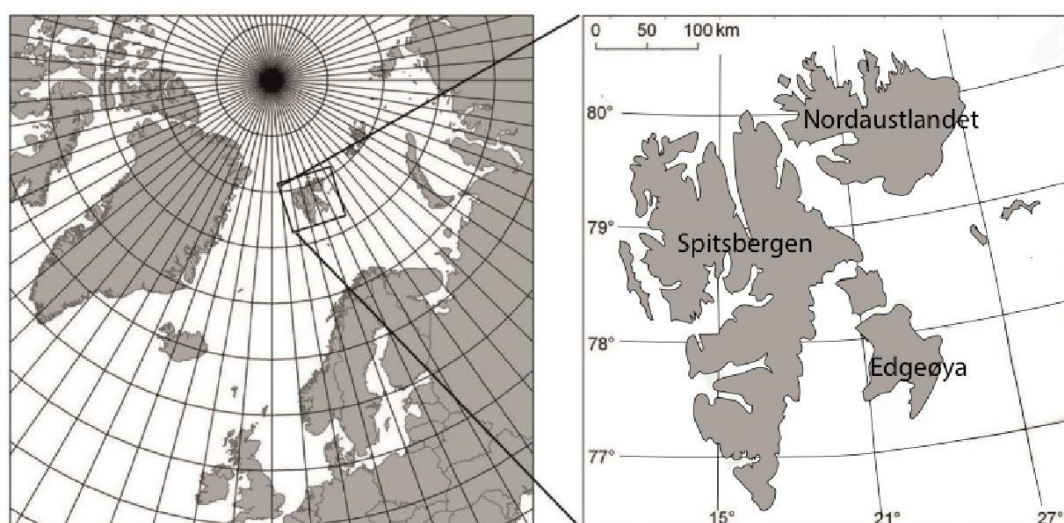


Figure 1.2: Geographic location of Svalbard in the Barents Sea, showing the three islands of Spitsbergen, Nordaustlandet and Edgeøya. Modified from Joly et al. (2016)

The Svalbard archipelago is situated in the northern Barents Sea where the main island of Spitsbergen is located between 74°-80° N latitude and 10°-21° E longitude (Fig. 1.2). The archipelago is an uplifted part of the Barents Sea shelf (e.g. Worsley, 2008). Svalbard was connected to Greenland until early Cenozoic, when a major rifting phase occurred, which led to the opening of the Fram strait (Faleide et al, 1993). The Norwegian-Greenland Sea had its configuration in the early Eocene (e.g. Døssing et al., 2010) . As a result of the extension, basins developed containing sediments from late Eocene to Oligocene age (Dallmann et al., 2015). The Hornsund Fault Complex (Fig. 3.5a), dividing the Greenland and Barents shelves, was initially acting as a transform fault system in the Paleocene and early Eocene. This movement eventually resulted in a transpressional regime taking place in western Spitsbergen as Greenland moved further north along the De Geer Fault Zone, which led to the formation of the West Spitsbergen fold-and-thrust-belt (Døssing et al., 2010).

1.5 Study area

The study was conducted on the coastal Paleogene deposits at Calypsostranda (Fig. 1.3; Fig 1.4). Fieldwork was conducted during two weeks in August 2016. The outcrops were also studied for a three-day period in August 2017. Both field seasons were spent at the Calypsobyen cabin, an old coal mining community.

The topography in the area is relatively flat as there is a major plateau stretching from the Renardbreen in the south up to the Rochesterpynten and Kapp Lyell coastal areas in the north (Fig.1.3B). The plateau has small topographic highs and is vegetated with moss. A river running from Scottbreen crosses between the camp area in Calypsobyen and the outcrops at Calypsostranda. In the study area, the cliffs are fairly steep with extensive mass transport. Parts of the outcrops were therefore covered in debris. 247.5 meters of the coastal section was logged and studied.

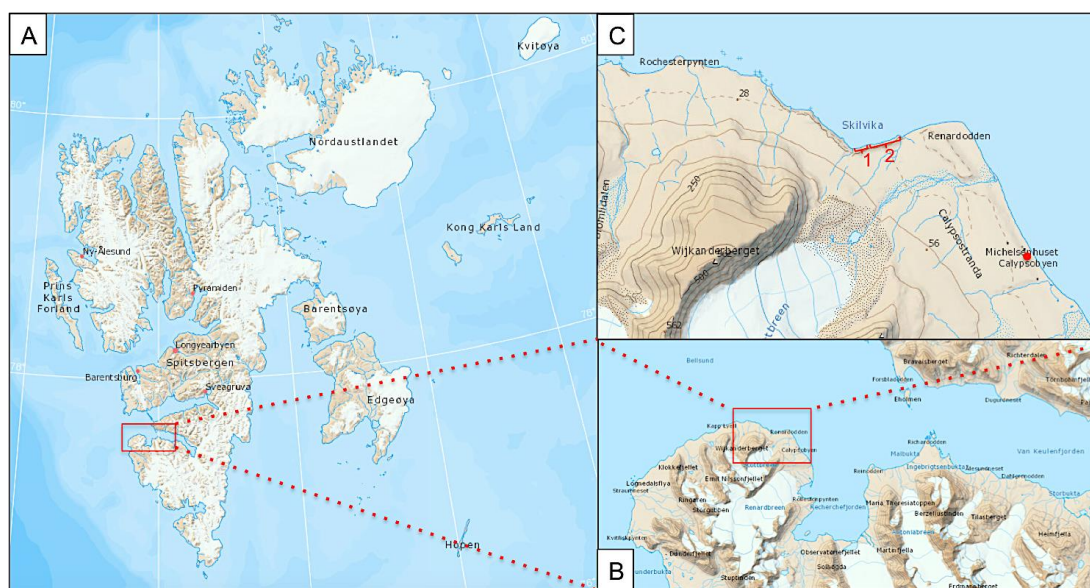


Figure 1.3: Study area: A) The Svalbard archipelago with study area outlined. B) Map of the Bellsund area C) Local map with study area marked. 1 denotes the beach area where the Skilvika Formation was studied. 2 denotes the beach where the Renardodden Formation was studied. The red dot marks the Calypsobyen cabin, which was the base during both field seasons. Maps from Norsk Polarinstitutt. (<http://toposvalbard.npolar.no/>).



Figure 1.4: View of the coastal section at Calypsostranda with the Skilvika- and Renardodden Formation labelled. Photo: Øystein Grasdøl

2. Methods

2.1 Field work

Most of data was collected during the field season in August 2016. Data collection during field work was conducted by means of sediment logging on paper, collection of sedimentary rocks- and coal samples, paleocurrent measurements, photography and strike/dip measurements of faults and bedding planes. Logging in a 1:50 scale of the Skilvika- and Renardodden Formations were conducted, a 1:20 scale was used in cases where more detailed sedimentological study was required. The dip of the beds (20 degrees) made it achievable to log by following bed boundaries upwards in the succession. Where gaps were present, two rulers were used to display the bed dip and to accurately measure the gap to the next visible outcrop. Sedimentary structures, bed boundary types, bioturbation, grain size, presence of organic detritus and roots were recorded in the logs. Samples were taken for each facies type. Measurements were done through use of a compass. Palaeocurrent measurements were conducted on cross-stratified beds, but due to surface erosion, such measurements were few and unreliable. Strike and dip measurements were taken on well exposed beds and faults.

2.2 Post-field work

Post-field work included digitisation of the lithostratigraphic logs and thin section studies of the samples from the outcrops. These studies involved usage of the light microscope and scanning electron microscope to conduct textural and compositional analysis. In addition, the thin sections were point counted. All thin section studies were carried out at the University of Bergen.

2.2.1 Digitisation

Digitisation of the lithostratigraphic logs was performed through drawing in Adobe Illustrator CC 2017. Logs were drawn in a 1:50 meter scale displaying lithology, sedimentary structures and grain-size (Appendix B). Several of the figures used in this thesis were also modified in Adobe Illustrator.

2.2.2 Light microscopy

Compositional and textural studies of the thin sections were conducted through an optical light microscope of type Nikon ECLIPSE E200. Point counts were conducted through the light microscope, by counting 300 points per sample on 10x optical zoom using PetroMod version 2.34. The point counts were carried out in order to classify the sedimentary rock type based on Dott (1964) classification diagram (Fig.5.10). Photographs in plane-polarized (PPL) and cross-polarized light (XPL) were taken through a Nikon ECLIPSE LV100 POL light-microscope using a built-in camera of the type Nikon Digital Sight DS-U3. Studies were conducted on 4x, 10x and 20x optical zoom. The RAMAN microscope was used to distinguish between minerals.

2.2.3 Scanning electron microscopy

Scanning Electron Microscopy (SEM) using backscattered electron imaging (HdAsB) was performed to determine mineralogical composition in the studied samples (Fig. 2.1). A ZEISS Supra 55VP Field Emission Scanning Electron Microscope (SEM) was utilized.

Each thin section was individually prepared through the following workflow: 1) Removing epoxy glue with acetone 2) Applying a layer of carbon which increases conductivity in the samples in preparation for HdAsB (Pers.com Heggestad, 2017. 3) Carbon tape was used to attach the thin sections to an aluminium plate which was then inserted face-up into the microscope. A maximum of four thin sections could be attached simultaneously. HdAsB was used with 15 kilovolt (EHT) applied on the electrons that were exerted on the samples.

From the resultant backscattered images, light-colored minerals reflect higher atomic number, hence heavy minerals (e.g. zircon). Dark colored minerals display lower atomic number and consequently light minerals (e.g. quartz). This is a result from the emission of electrons. More collisions will occur between the electrons and the heavy elements, hence influencing backscattering of the electrons and the lighter color of the minerals (Zhou and Wang, 2007).

The production of X-rays by electrons (X-ray micro-analysis) permits atomic identification and quantitative analysis to be performed. From the emitting of x-ray beams with differing wavelengths, a photon is produced characteristic for a specific atom, and the element can be determined. A line scan through each thin section was

produced to distinguish between K-feldspar and quartz, to quality control the point counts. K-feldspar was detected as a spike in potassium (K) occurring simultaneously with an elevation in aluminium (Al), oxygen (O) and silicon (Si). Through this method, K-feldspar could be distinguished from quartz (elevation in Si and O), and a ratio between the two minerals could be obtained by measurements with a ruler on the line scan.

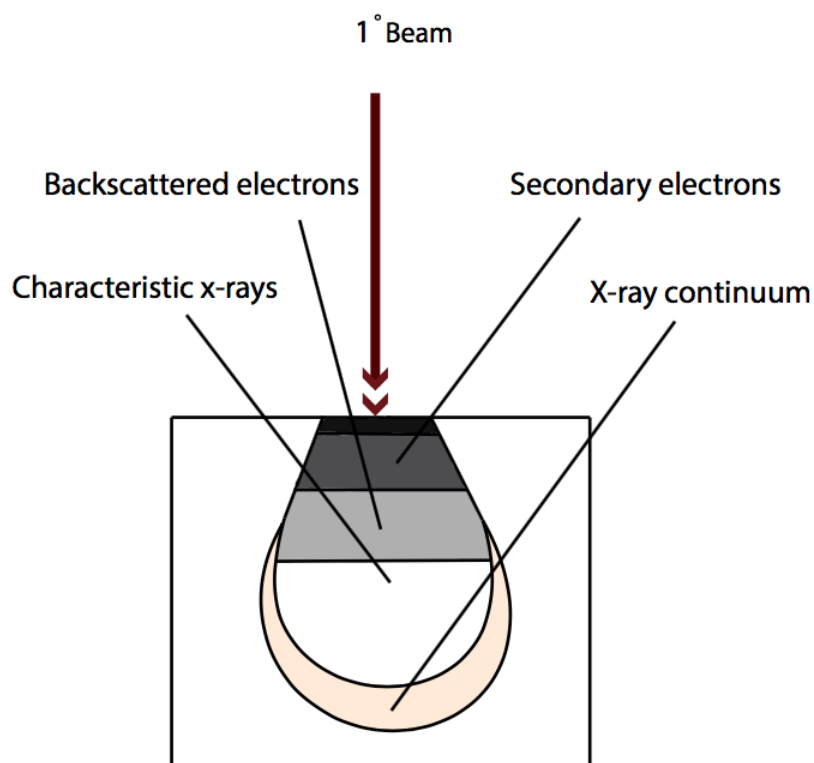


Figure 2.1: Drawing showing generated signals and detection regions in the scanning electron microscope (SEM). Modified from Zhou and Wang (2007)

2.2.4 Textural analyses

Textural analyses were studied in the NIKON ECLIPSE E200 light-microscope for each of the 13 samples that were prepared, and carried out in 10x optical zoom. The thin sections were coloured with blue epoxy to make textural characterisation and pore space more visible and easily determined. Each of the samples were characterised based on their degree of sorting, grain sizes, rounding, sphericity, porosity and fabric (grain or matrix supported). Grain sizes were determined through measuring approximately 30 random grains per sample and averaging these values

before converting to micrometers (μm). The smallest and largest observed grain size was also measured per sample to determine the grain size distribution in the entire sample and comparing to the sorting. The degree of sorting was determined from Jerram (2001) based on sorting in 2D samples (Fig. 2.2) and was visually viewed in the light microscope through comparison. Fabric and porosity were determined from modal point counts. Fabric was classified as grain-supported (<50% matrix) or matrix supported (>50% matrix). Porosity was divided into primary or secondary porosity and determined as a percentage composition from the point counts.

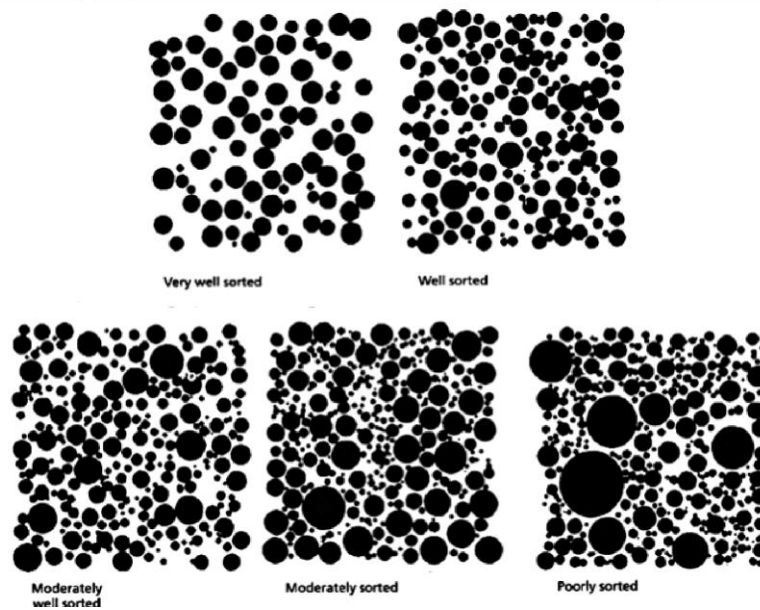


Figure 2.2: Model used for determining sorting in 2D view of the thin sections. Modified from Jerram (2001)

Sphericity and rounding are based on Pettijohn et al.'s (1987) redrawn version from Powers (1953) (Fig. 2.3) and was determined visually in the light microscope from the average of at least 30 random grains per thin section sample.

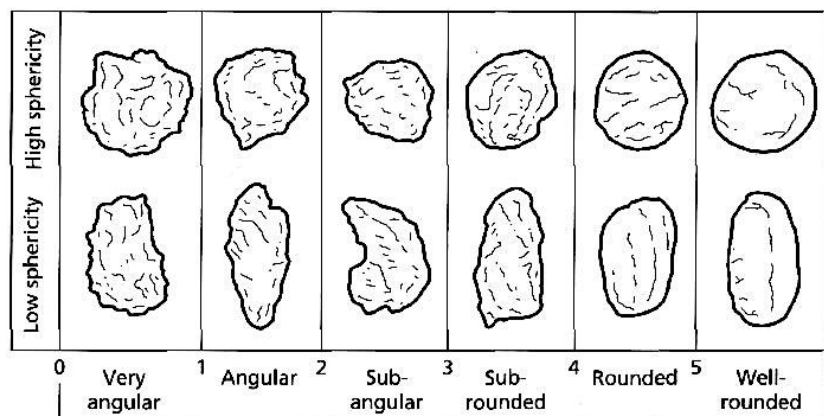


Figure 2.3: Model used to determine the sphericity of grains in the studied samples. From Pettijohn et al., (1987), redrawn from Powers (1953)

3 Geological framework

3.1. Introduction

The Svalbard archipelago is an uplifted and subaerially exposed part of the northwestern Barents Sea shelf (Worsley, 2008) where the bedrock geology provides an excellent analogue for sedimentary deposits in the Barents Sea. Svalbard has a diverse stratigraphy representing layered rocks from Palaeoproterozoic to Cenozoic age (*Fig.3.1;Fig 3.2*) (Dallmann et al., 2015). Paleogene deposits and Proterozoic strata are well exposed at Calypsostranda. (Fig 3.1)

Svalbard is the only part of Norway where sediments of Paleogene age can be found well preserved on land (Martinsen and Nøttvedt, 2006). The focus for this study is the Paleogene succession in the Calypsostranda Group, which comprise the Renardodden Formation and Skilvika Formation. The following chapter will provide a regional description of the geological history and stratigraphic structure of Svalbard from the pre-Caledonian era to Cenozoic times.

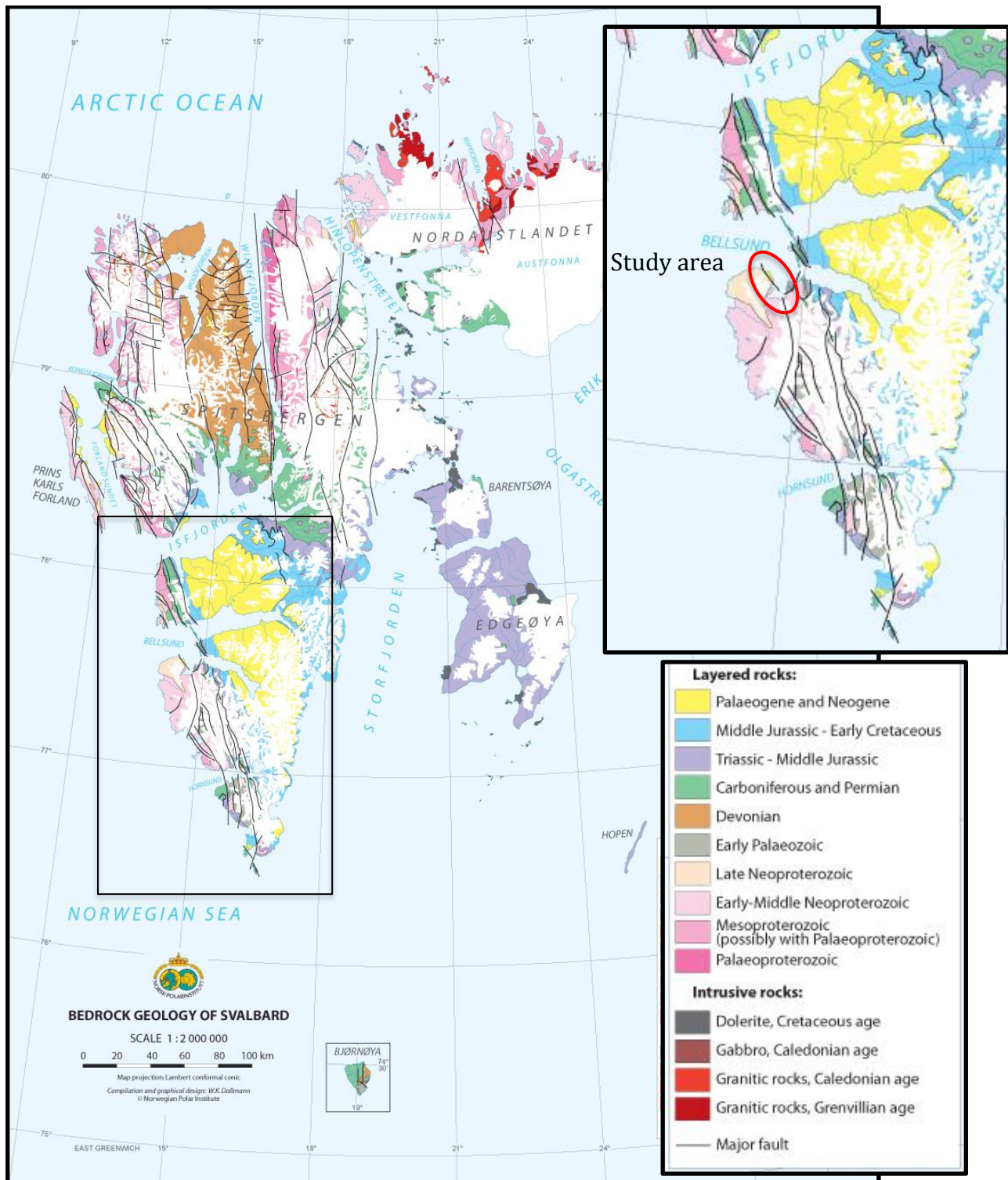


Figure 3.1: Geological map portraying the bedrock geology of Svalbard with study area circled. Modified from Dallmann (2015).

3.2. Pre- Caledonian era

The oldest rocks, the pre-Caledonian basement, on the Svalbard archipelago, are present in three provinces: North- eastern, North- western and the South- western. The provinces are characterised and differentiated based on their rock types and regional structural grain (Dallmann et al., 2015). The pre-Caledonian rocks ranging from Late Riphean age to Silurian in age are generally referred to as the Hecla Hoek basement (Worsley et al., 1986)

There are significant similarities between the Neoproterozoic succession of Svalbard, and the Eleonore Bay Supergroup of Neoproterozoic age in Central East Greenland. Both of these Neoproterozoic successions, are overlain of Vendian age tillites and carbonates (Dallmann et al., 2015). The similarities in rock type may be an indication that East Greenland and eastern Svalbard were situated on the same continental margin of Laurentia, during the Neoproterozoic and Early Paleozoic (Dallmann et al., 2015). The Late Neoproterozoic rocks of Vendian age can be observed in the mountain area between Bellsund, Chamberlindalen and Dunderdalen (Fig 3.1), and consist of mainly tilloid rocks (Dallmann et al., 2015). The Paleoproterozoic Kapp Lyell diamictites adjacent to the study area are strongly tectonized, both in terms of folding and faulting (Dallmann, 1989) and may be altered due to a late tectonothermal event that has been recorded in the Southwestern Province.

3.3. Caledonide and Post- Caledonide era

A number of tectonic events have occurred subsequent to the Caledonian orogeny, these have been fundamental with regards to provenance and transport of post Caledonian sediments (Steel and Worsley, 1984; Dallmann et al., 1999; Smelror et al., 2009).

	Age	Lithology	Age	Min./max. Th. (m)	Group	Facies			
Regional uplift	0 Mill. years	Tertiary	Tertiary deformation						
			Eocene Paleocene	0/3000	Van Mijenfjorden	Deltaic marine clastics, Paleocene coals			
Eurekan	100	Cretaceous	Albian Aptian	550/1700+	Adventdalen	Marine clastics, major deltaic advance in lower Cretaceous			
Callovian									
Uplift of Uralides	200	Jurassic	Bathonian Rhaetian Ladinian	70/510+	Kapp Toscana	Deltaic/shallow marine clastics			
			Lad Griesb.				60/870	Sassendalen	Fg marine clastics
			Artinskian				0/460	Tempelfjorden	Silicified marine clastics/lsts
			Artinskian				0/1800	Gipsdalen	Lsts/dms/evaporites, local red clastics along faulted block margins
?Bashkirian									
Uplift	300	Carbon.	?Namurian Famennian	0/1250	Billefjorden	Grey fluvial/alluvial clastics & coal			
Rifting									
Svalbardian Event	400	Devon.	Svalbardian deformation						
			Givetian	0/8000	Andrée Land, Red Bay, Siktefjellet	Old Red Sandstone up into grey fluvial clastics			
Caledonian	Downtonian								

Figure 3.2: The Devonian to Cenozoic stratigraphic column of Svalbard. Modified from Worsley et al. (1986).

3.3.1 Caledonian era

The opening of the Iapetus Ocean between Baltica and Laurentia occurred in the Cambrium. Within 100 million years, the Iapetus Ocean closed leading to a collision between Laurentia and Baltica and the formation of the Caledonides (Fossen et al., 2006). The collision led to compression and folding of the rocks in the collision zone, and high temperature and pressure conditions resulted in metamorphism of certain rocks that can be seen on the Svalbard archipelago today. In Svalbard, high-pressure metamorphic eclogites and blueschists can be observed in Western Spitsbergen on Biscayahalvøya, Motalafjella and Nordenskiöld land (Dallmann et al., 2015).

3.3.2 Devonian

The assemblage of the supercontinent Pangaea began in Early Devonian when Gondwana drifted northwards towards Euramerica (Dallmann et al., 2015). What had previously been a regime dominated by compression in Svalbard that had given rise to the Caledonian orogeny, became an extensional regime which eventually led to the break-down and collapse of the mountain range. The Devonian period was thus highly influenced by weathering and denudation. Extension led to the formation of subsiding crustal blocks, where eroded material would accumulate in fault-bounded rift basins. This Devonian terrestrial bedrock is commonly referred to as the “Old Red Sandstone” represented by the fining upwards successions of the Siktefjellet Group, the Red Bay Group and the Wood Bay Formation. (Fig.3.2) (Harland and Wright, 1979; Worsley et al., 1986; Dallmann et al., 2015). Towards the end of the Devonian period, the Svalbardian event took place with pronounced tectonic activity (Friend and Moody-Stuart, 1972; Worsley, 2008). This event can be documented in the upper parts of the Mimerdalen Subgroup with the presence of conglomerates (Dallmann et al., 2015). An unconformity surface between Devonian strata and overlying carboniferous strata (Billefjorden Group) developed as a result of the tectonic phase (Hellem, 1980; Harland et al., 1997).

3.3.3. Carboniferous

A hot, humid climate in Early Carboniferous accommodated widespread vegetation on the Svalbard archipelago and coal deposits are characteristic of this time (Dallmann et al., 2015). The Billefjorden Group comprise the tropical non-marine siliciclastics deposited from Late Devonian (Famennian) to late early Carboniferous (Visèan) (Fig 3.2) (Gjelberg and Steel, 1981; Worsley, 2008).

Rifting and an extensional regime began in late early Carboniferous and led to the formation of a horst-and- graben landscape. Pronounced rifting occurred between Greenland and Svalbard, and in the Barents Sea (Stemmerik, 1997; Golonka et al., 2003). An unconformable contact is present between the Billefjorden and Gipsdalen groups, and is an indication of major regional uplift followed by a sudden shift in climate (Worsley, 2008). A marine transgression following sea level rise occurred in

Late Carboniferous. This led to a steady submergence of most land areas in Svalbard, and marginal marine deposits like carbonates and evaporites replaced the previous terrestrial deposits.

The Gipsdalen Group are of Early Carboniferous to Early Permian age and comprise mixed clastic, evaporite and carbonate successions (Dallmann et al., 2015). The deposits are representative of the advancement from a terrestrial setting to a stable, shallow-marine shelf.

3.3.4. Permian

The bedrocks deposited during this period are greatly diversified due to varying climatic conditions as Svalbard drifted 15 degrees north during a 50 million year time span (Dallmann et al., 2015). The Permian rocks are subsequently divided into two main lithostratigraphic groups:

- i) Gipsdalen Group: Comprised of carbonates and evaporites of Early Carboniferous to Early Permian age, deposited in a dry and warm climatic environment (Blomeier et al., 2009).
- ii) Tempelfjorden Group: Comprised of open-marine sediments such as limestone, sandstone and chert (Dallmann et al., 2015). The sediments were deposited on an exposed sub-aerial surface, with renewed flooding episodes (Worsley 2008).

3.3.5 Mesozoic era

The Svalbard archipelago was relatively stable during the Mesozoic and thick successions of clastic deposits characterize this era. The period is important in the context of hydrocarbon exploration in the Barents Sea today (Leith et al., 1993; Vorren, 1993; Henriksen et al., 2011).

The Lower and Middle Sassendalen Group (Fig. 3.2) of Early to Middle Triassic age comprise clastic sediments of shale, siltstones and sandstones (Steel and Worsley,

1984). It has been noted that the basal shales are possibly Late Permian in age (Worsley, 2008).

The Kapp Toscana Group (Fig 3.2) represents the Upper Triassic and Lower Jurassic clastic sediments and denotes a remarkable shift in the depositional setting. Uplift and erosion of the Uralides most likely led to the entrance of a large delta system from the southeast of the basin, which favored the deposition of sandstones, shales and siltstones in a shallow-marine to deltaic setting (Steel and Worsley, 1984; Riis et al., 2008; Henriksen et al., 2011; Dallmann et al., 2015).

In the Late Jurassic, conditions favored the formation and preservation of organic rich sediments. These black shales of the Upper Jurassic are source rocks for hydrocarbons in the western parts of the Barents shelf (Hekkingen Formation) (Leith et al., 1993; Worsley, 2008; Henriksen et al., 2011).

The Jurassic sediments are generally divided into two main lithostratigraphic units (Dallmann et al., 2015):

- i) Wilhelmøya of the Kapp Toscana Group: Sandstones with heterolithic successions ranging from lower to middle Jurassic age.
- ii) Agardhfjellet Formation of the Janusfjellet Subgroup: A succession that is largely shale-dominated and is representative of Middle to Late Jurassic in age.

3.3.6. Cretaceous

In the Cretaceous, Pangaea was in its final break-up phase, which led to extensive volcanism due to sea-floor spreading (Dallmann et al., 2015). High eustatic sea levels were contained throughout the period. The Atlantic Ocean started to form as Eurasia and Laurasia broke apart at the onfall of the period. The Early Cretaceous basins of the Barents shelf were mainly dominated by shale and sandstone deposition (Worsley, 2008).

Sedimentary, volcanic and intrusive rocks are found in Svalbard up until the late Albian stage. The Jurassic-Cretaceous Adventdalen Group (Fig. 3.2) consists of

siltstones, sandstones, shales, subordinate coals, rare bentonites and conglomerates. The Lower Cretaceous Strata in Spitsbergen includes the Rurikfjellet, Helvetiafjellet and Carolinefjellet formations (Dallmann et al., 2015). Upper cretaceous sediments are not observed on the Svalbard archipelago as a major stratigraphic break is present between lower cretaceous sediments of the Carolinefjellet Formation and the Cenozoic strata above. Conglomeratic, laterally irregularly developed sediments of the Grønfjorden bed are the oldest deposited sediments in the Cenozoic succession. Where the Grønfjorden bed is absent, delta plain sediments of the Firkanten Formation bound to the underlying unconformity (Dallmann et al., 1999).

3.4. Cenozoic era

Uplift and erosion ensued in parts of Svalbard and surrounding areas of the Barents Sea during the Cenozoic era (Cavanagh et al., 2006). Tectonics and sediment deposition on the Svalbard archipelago was largely controlled by a transpressional regime that occurred as a result of the partitioning of Greenland from The Barents Shelf in Paleogene, and subsequent rise of the Spitsbergen fold-and-thrust belt (Eurekan orogeny). The creation of this tectonic belt has tectonically affected the entire stratigraphy in Western Spitsbergen (*Fig. 3.5*) (Braathen et al., 1999).

3.4.1. Rifting and uplift

Three main periods of exhumation occurred in the Barents sea region from late Paleocene to late Pliocene- Pleistocene (Cavanagh et al., 2006). The first uplift developed prior to the North Atlantic rifting in late Paleocene when igneous activity was high. The second phase occurred in Oligocene- Miocene and was related to rifting and the development of passive margins. The last period was related to the ice scouring in Pliocene- Pleistocene when erosion of the shelf area occurred. The different periods of exhumation led to erosion and re-deposition of sediments west of the Barents Sea shelf.

Tectonic activity along the margins of the western Barents Sea shelf dominated the development of the Svalbard region in Paleogene (Worsley, 2008) where first a major compressional phase (Eurekan orogeny) and thereafter a rifting phase occurred

(Faleide et al., 1993; Dallmann et al., 2015). Formation of the Atlantic Ocean proliferated further North during the Paleogene period and eventually led to the partitioning of Svalbard from Greenland and the opening of the Fram Strait (Dallmann et al., 2015). This allowed for an exchange of water between the Arctic and more southerly latitudes.

The Hornsund Fault Complex, dividing the Greenland and Barents shelves, was initially acting as a transform fault system in the early Eocene (e.g. Leever et al., 2011). At the end of the Eocene, the Fault Complex shifted from a transform regime to an extensional regime and led to the division of Eurasia from Greenland. As a result of this extension, depositional basins developed containing sediments from late Eocene to Oligocene age (Dallmann et al., 2015). These sediments are well-exposed in the Forlandssundet Graben, but are also present in other basins off the west coast of Spitsbergen (Blinova et al., 2009).

3.4.2. Stratigraphy

The sedimentary rocks from Paleogene are restricted to two larger depositional basins (Dallmann et al., 2015):

- i) The Central Tertiary Basin (CTB): The Central Tertiary Basin formed as a depression in the initial stages of the Paleogene as a result of continued rifting in the Labrador Sea and Baffin Bay (Dallmann et al., 2015). The sedimentary fill of this basin is the Van Mijenfjorden Group (Fig. 3.3) which lie unconformably on Mesozoic strata, and consists of sandstones, siltstones, shales and subordinate coals and conglomerates. The transport directions of the deposits, are reflected by alternating transtensional and transpressive regimes along the western margin (Worsley 2008). The Van Mijenfjorden group is comprised of the Firkanten Formation, Basilika Formation, Grumantbyen Formation, Frysjaodden Formation, Battfjellet Formation and the upper Aspelintoppen Formation (Fig 3.3).
The Firkanten Formation is further subdivided into the basal conglomeratic Grønfjorden Bed, the predominantly delta plain deposits of

the Todalen Member, the delta front sandstones of the Endalen Member and the lower delta front to prodelta sediments of the Kolthoffberget Member (Steel et al., 1981; Dallmann et al., 1999). Type sections for these members (which will further be discussed in Chapter 7) are shown in fig. 3.4.

- ii) The Forlandssundet Graben with sedimentary deposits of Eocene-Oligocene age. These comprise the clastic sedimentary formations of the Buchananisen Group, consisting of conglomerates, sandstones, siltstones and shales (Dallmann et al., 2015).

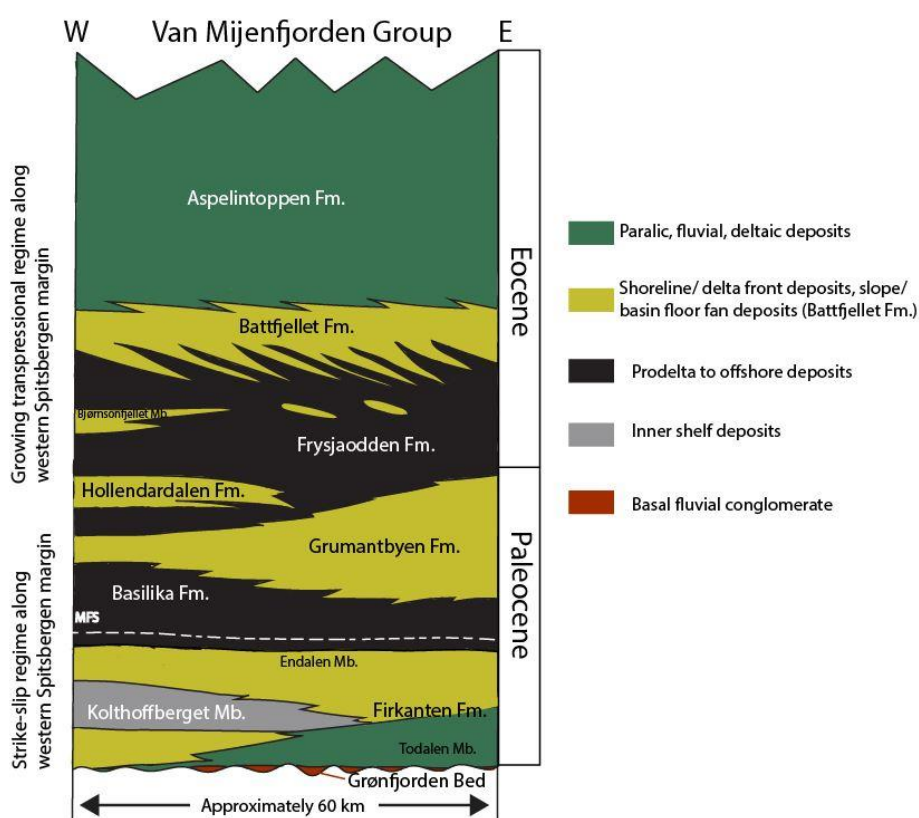


Figure 3.3: Stratigraphy of the Central Tertiary Basin with tectonic events outlined. Modified after Steel et al. (1985), Grundvag et al. (2014), Gjelberg (2010) and Petersen et al. (2016)

Paleogene sediments also occur on Øyrlandsodden, Brøggerhalvøya and south of Bellsund, on the Renardodden Fault Block, which is the focus of this study (Dallmann et al., 2015).

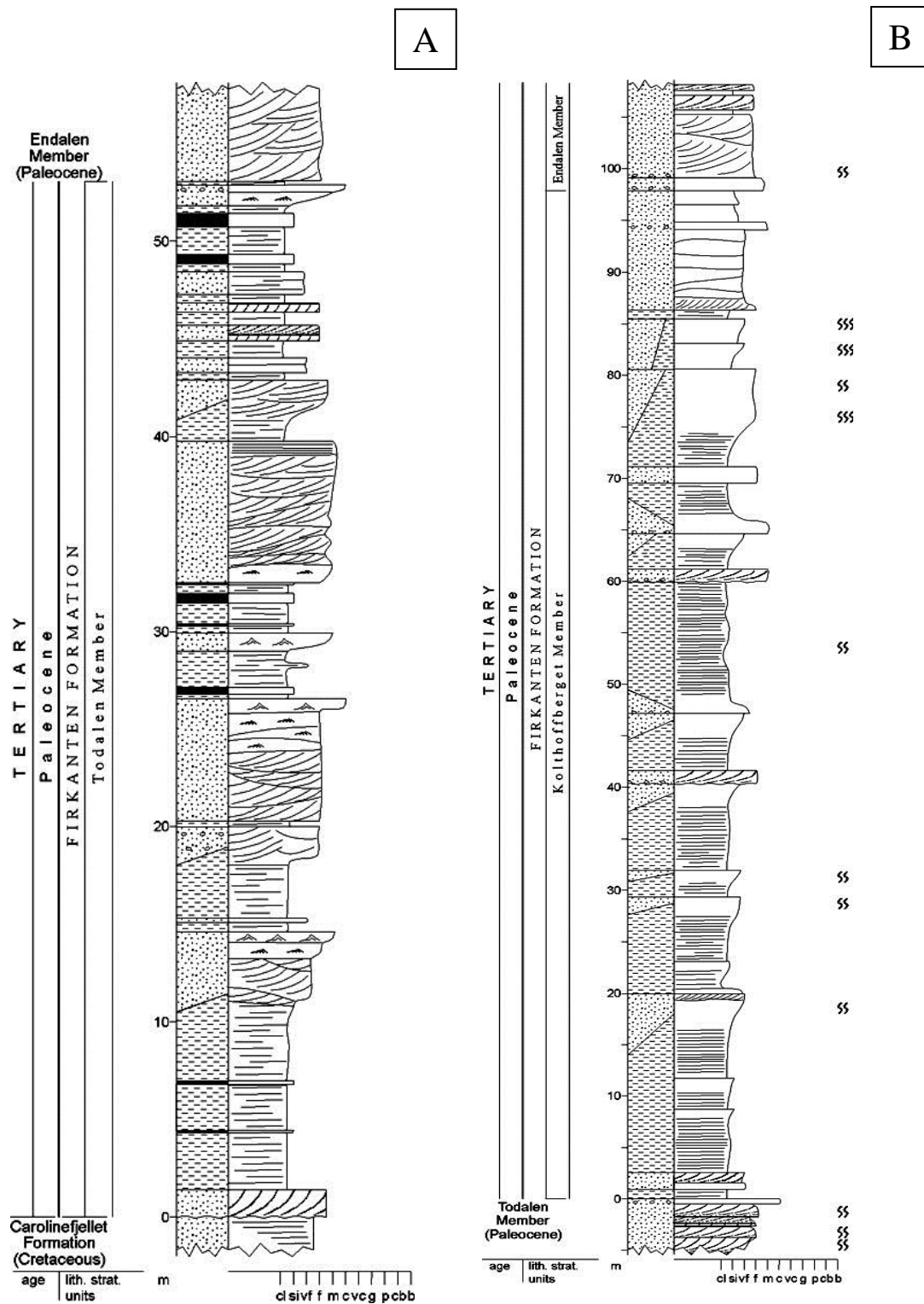


Figure 3.4: Type section logs from the Firkanten Formation for A) The Totalen Member and parts of the Endalen Member. Locality: Bayfjellnosa. B) The Kolthoffberget Member and parts of the Totalen and Endalen members. Locality: Kolthoffberget. From Dallmann et al. (1999)

3.4.3. The West Spitsbergen fold- and thrust belt

The West Spitsbergen fold and thrust belt is an orogenic belt, which measures 100-200 km wide and 500 km long and is situated along the Western flank of Spitsbergen (Leever et al., 2010). The fold-and thrust belt developed mainly in the Eocene, and acted as a main sediment source to the Central Tertiary Basin (Fig. 3.3) (Steel et al., 1985). Sideways movement in the transform zone between the Barents Sea and Greenland, and transpression between Svalbard and Greenland at a given time contributed to the formation of this fold-and-thrust belt (Martinsen and Nøttvedt, 2006).

The West Spitsbergen fold and thrust belt has previously been subdivided into three main zones (Bergh et al., 1997; Braathen et al., 1999), however it has more recently been split into four specific zones (Leever et al., 2011). (Fig. 3.5C)

From west to east:

- i) The western hinterland zone comprising metamorphic basement rocks of Caledonian age that have been influenced by extensional deformation in Oligocene
- ii) A basement-involved fold-thrust complex comprising metamorphic basement rocks of Caledonian age
- iii) The Central Zone consisting of a decoupled unit that has been prone to thin-skinned deformation above a detachment zone in Permian evaporites
- iv) An Eastern foreland province characterised by thick-skinned deformation associated with structural inversion of two fault zones in the east (Billefjorden and Lomfjorden)

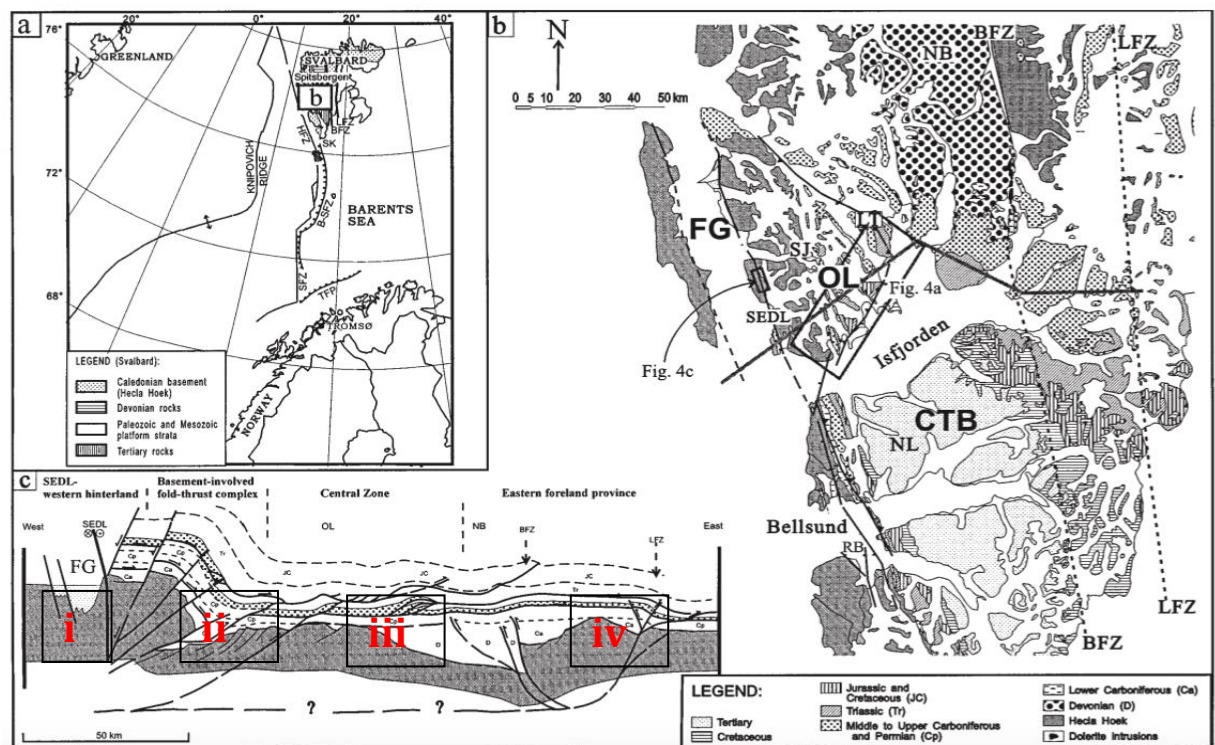


Figure 3.5: (A) Position of the Svalbard archipelago in the Barents Sea (B) Geological map with the Central Tertiary Basin (CTB) and Forlandssundet Graben outlined (FG). Study area is outlined (RB) (C) Cross section through central Spitsbergen from a westerly to easterly direction with the four main provinces outlined. Modified from Braathen et al., 1999.

In order to describe the relative timing of events and when deformational structures were formed, Bergh et al. (1997) proposed a 5-stage kinematic model for the creation of the West Spitsbergen fold-and-thrust belt based on its physical development (Bergh et al., 1997):

- i) Stage 1 involved north-northeast shortening parallel to the beds in the cover sequence, and occurred in Late Cretaceous times. This shortening resulted in folded decollements within Carboniferous and Permian cover strata in the Western Zone and represents the first deformational structures that were formed as a result of the formation of the Spitsbergen fold-and thrust belt.
- ii) Stage 2 involved a major shortening phase and subsequent uplift in the Western Zone. As a result of this, thick-skinned deformation with associated thrusts and macrofolds developed in the Western zone. In the Central zone, in-sequence thrusting of hinterland dipping imbricates occurred in addition to folding of previously formed decollement structures. In the Eastern zone,

older strata were superpositioned above younger strata in stacked in-sequence successions that were eastward propagating.

- iii) Stage 3 involved thick-skinned deformations in the Eastern zone, through the reactivation and uplift of the Gipshuken and Bravaisberget basement thrusts. This resulted in folding of overlying previously formed decollement structures.
- iv) Stage 4 was an out-of-sequence thrust phase and involved decapitation of structures in the Western and Eastern zones that had previously been prone to in-sequence thrusting.
- v) Stage 5, the last stage in the formation of the Spitsbergen fold-and thrust belt, involved extensional deformation in the western zone, in the form of extensional faulting.

3.5. Lithostratigraphic and geological setting of the study area

Cenozoic strata of the Paleogene Calypsostranda Group occur adjacent to Precambrian basement rocks of Vendian age, the Kapp Lyell sequence, in the cliffs between Renardodden and Skilvika in Bellsund (Fig 1.1). The basement rocks are comprised mainly of tilloid rocks (Dallmann, 1989), whereas the Paleogene sediments include clastic sediments (Dallmann et al., 2015). Most previous interpretations support or suggest a fault contact dividing the two domains (Fig. 3.5B) (Dallmann, 1989). There is however, still a controversy whether the smaller unconformity between the Skilvika Formation and the Proterozoic Kapp Lyell diamictites is of sedimentary (Vonderbank, 1970; Birkenmajer, 2006) or tectonic (Thiedig et al., 1979; Dallmann, 1989; Dallmann et al., 1999) origin.

3.5.1. Structural setting

Dallmann (1989) suggests that the Precambrian and Cenozoic domains are separated through a fault system and that the fault at Calypsostranda is part of a long-lived tectonic lineament, like the Inner Hornsund Fault Zone. He supports the notion of a fault contact in his studies through observations based on the tectonic history of the area. Another theory suggests that the fault could possibly be connected to the

Central-west fault zone, which separates two basement provinces of Svalbard (western and central) (*Fig 1.* in Harland and Wright (1979)).

3.5.1. Kapp Lyell sequence

The basement rocks in the coastal section are for the most part comprised of metamorphic quartzite-clast-supported diamictite and a dark grey mica schist with yellow to dark green coating (Birkenmajer, 2006). These are separated by a major fault. The diamictites are strongly tectonized and have varying dips. The mica schist directly underlies the contact to the Skilvika Formation and overly the diamictite. They have a dip towards the northeast where the matrix consists of subrounded fine sandstone clasts with organic-rich drapes, in addition to angular quartzite clasts (Birkenmajer, 2006). There is a possible palaeo-weathering surface on top, which is stained yellow by jarosite coating (Birkenmajer, 2006).

3.5.2. Calypsostranda Group

The Calypsostranda Group comprises the basin fill sediments outcropping in the Calypsostranda area, with an assemblage of sandstones, shales, subordinate conglomerates and coal seams. (Dallmann et al., 2015). The Group encompasses the Skilvika- and Renardodden formations. *K. Kleinspehn* in Dallmann (1999) has previously logged the Calypsostranda Group and estimated the entire succession to be 265 m.

There is still uncertainty regarding the exact age of the deposits within the Calypsostranda Group, as discussed in Chapter 1: Introduction.

Skilvika Formation

The Skilvika Formation comprises fluvio- deltaic facies (Dallman et al. 1999; 2015) and encompasses the lower part of the Calypsostranda Group. The deposits consist of fine-grained sediments with thin coal seams (Birkenmajer & Gmur, 2010), and have previously been interpreted to be terrestrial strata deposited in a deltaic environment. The coal seams are interpreted as having been deposited in swamps, marshes or

stagnant pools of water (Birkenmajer & Gmur, 2010). Abundant plant remains are observed (Dallmann, 1999, and references therein).

There are five exposures of the Skilvika Formation in the Calypsostranda region (from north to south) (Fig. 1.1):

- 1) Skilvika
- 2) Reinsdyrbekken
- 3) Calypsobyen
- 4) Tyvjobekken creek
- 5) Kjeftbekken Creek

The best-preserved deposits are found in the main section located in the coastal section at Skilvika in the Calypsostranda area.

Renardodden Formation

The Renardodden Formation is the upper unit of the Calypsostranda group. The Renardodden Formation has previously been interpreted as having been deposited in a shallow-marine environment (Dallmann et al., 1999; Birkenmajer and Gmur, 2010). According to Dallmann (1999), the formation is composed of fine-to medium sandstones with interbeds of siltstones and claystones. Siderite concretions and *Ophiomorpha* burrows are present. Vonderbank (1970) has previously noted the presence of *Ophiomorpha* in the upper part of the succession. The top of the unit bounds to quaternary deposits through an unconformity surface (Dallmann, 1999 and references therein).

4 Lithofacies and facies associations

4.1 Introduction

In this study, 16 lithofacies are recognized in the investigated section of the Calypsostranda Group (Table 4.1) They are recognized and sub-divided into lithofacies based on their lithological composition, grain size, primary sedimentary structures, bioturbation and colour. Descriptions and subdivision into lithofacies are based on outcrop investigations and thin section studies of selected samples in a light microscope (Chapter 5). A detailed description of the various lithofacies follows in section 4.3, a summary is captured in Table 4.1.

The lithofacies are further grouped into two facies associations (Table 4.2) which represent two primary depositional environments:

- **FA 1:** A continental regime including sediments deposited in a delta plain environment (FA 1).
- **FA 2:** A marine regime including sediments deposited in delta front to prodelta regions (FA 2).

The two facies associations also include a wide range of sub- associations (Table 4.2) reflecting proximal to distal trends and lateral variability within the continental and marine regimes.

4.2 Lithofacies

Table 4.1: Summary of lithofacies recognized in the present study

Facies	Name	Lithology and grain-size	Sedimentary structures and bed geometry	Formation	Colour	Thickness (cm)	Sedimentary process
F 1 <i>Fig. 4.3</i>	Mica-rich, poorly sorted basal breccia	Silty, brecciated, schist matrix with abundant mica. Granules, pebbles and occasional boulders appear in the matrix	No structures observed, rather chaotic fabric.	Skilvika	Greyish with some yellow stains	375	Tectonically-induced mass wasting and slumping possibly triggered by activity in the underlying fault
F 2 <i>Fig. 4.5</i>	Coal and coaly shale	Shimmering characteristic, some layers are very well cleated. Locally interbedded shale	Cleated	Skilvika and Renardodden	Black	<u>Coal:</u> 2-20 <u>Coaly shale:</u> 5-50	Coal is a product of alteration processes of peat and organic material through compaction. Formation under anoxic conditions
F 3 <i>Fig.4.6</i>	Structureless to faintly laminated very-fine to fine sandstone	Sharply based and topped, very-fine to fine-grained sandstone. Rootlets occur in places, as well as undulating internal surfaces	Massive and structureless to faintly laminated appearance Plane parallel lamination	Skilvika	Light grey to light beige	10-135	Structureless appearance points to rapid deposition and aggradation of sand from a sustained-type flow. Faint lamination may indicate upper flow regime conditions.
F 4 <i>Fig. 4.7</i>	Very fine flaser laminated sandstone	Very fine-grained sandstone with coarse to very coarse-grained sandstone lenses/horizons. Organic draped flaser bedding. Coal fragments and rootlets occur	Flaser bedding. Plane parallel lamination in places.	Skilvika	Light beige to light grey	45	Lamination may indicate sediment transport and deposition under upper flow regime conditions

F 5 <i>Fig. 4.8</i>	Siltstone	siltstone containing coal fragments, or fractured silty shale with roots and siderite concretions. Fractured silty shale may contain very fine-grained sandstone layers/lenses and intercalations of mud and coal fragments	No structures observed	Skilvika	Consolidated shale is whitish beige, with some yellow stains. Fractured silty shale is very light grey to dark grey	5-280	Transport of fine grained material by currents and rapid deposition by fallout from suspension when carrying capacity is decreased
F6 <i>Fig. 4.9</i>	Soft sediment deformed siltstone/sandstone and mudstone	Siltstone/sandstone and mudstone with internal soft sediment deformation. Erosion at base. Medium to coarse-grained sandstone lenses with coal fragments.	Various Deformational structures including load casts, ball-and-pillow structures and convolute lamination	Skilvika	Light to dark grey	235	Load casts (ball-and-pillow) formed in unconsolidated sediment as a result of loading (due to density contrasts) of the original sand/silt bed (Bridge and Demicco, 2008)
F7 <i>Fig. 4.10</i>	Mudstone	Clayey to silty mudstone. Very-fine and fine-grained sandstone lenses may occur. Variable content of organic material, and coal fragments may be present	Laminated or structureless	Skilvika and Renardodden	Light to very dark grey. Red stained or beige sandstone lenses.	2-140	Fallout of mud particles and floccules from suspension due to low flow rate and low carrying capacity. Drainage and flow is limited
F 8A <i>Fig. 4.12</i>	Sandstone with gravel conglomerate	Fine and coarse sandstone beds with rounded to subrounded, and occasional angular granules. Quartz pebbles are dominating	Matrix-supported fabric. Clast supported in two thin horizons.	Skilvika	Matrix is light to dark grey with yellow/red oxidation stains	25-35	Breakup of rocks through weathering and erosion (Stow, 2005). Deposition under upper flow regime conditions acquiring a high rate of flow and a large carrying capacity

F 8B <i>Fig. 4.17</i>	Thick bedded gravel conglomerate with angular clasts	Poorly sorted unconsolidated granule-rich beds. Sub-rounded to angular granules. Quartz pebbles are dominating	Clast supported fabric	Renardodden	Matrix is light grey	30-220	Breakup of rocks through weathering and erosion (Stow, 2005). Deposition under upper flow regime conditions acquiring a high rate of flow and a large carrying capacity
F9 <i>Fig. 4.13</i>	Sandstone with sigmoidal to tangential cross-stratification	Consolidated fine to medium sandstone with organic/coal draped stratification. Very coarse-grained sandstone to quartz granules is present	Sigmoidal or tangential cross stratification. Commonly, the prograding dunes have a sharp top and are slightly aggradational.	Skilvika and Renardodden	Light grey with yellow/red rust stains	25-100	The cross-stratification is formed by the migration and deposition of two to three-dimensional dunes formed in the upper flow regime.
F 10 <i>Fig. 4.14</i>	Trough cross-stratified sandstone	Sandstones ranging from very fine to medium, where some beds are fining upwards. Roots and siderite concretions are observed.	Trough cross-stratified sandstone <i>Palaeophycus</i>	Skilvika	Light grey to light beige	45-275	Migrating three-dimensional dunes form in the upper part of the lower flow regime as a result of increased rate of flow
F11 <i>Fig. 4.15</i>	Plane-parallel stratified /laminated sandstone	Very-fine to medium grained sandstone with coal draped plane parallel stratification/ lamination. Coal fragments are present in addition to mud draped laminations	Plane parallel stratification/ lamination	Renardodden and Skilvika	Light to dark grey with yellow/red rust stains	10-90	Migration of sand beds in a setting dominated by upper flow regime conditions, with high suspension load and fluctuating between smooth and rough flow

F 12 <i>Fig. 4.18</i>	Bioturbated homogeneous sandstone	Homogeneous very-fine and very-fine to fine tabular sandstone beds. Coal fragments are common and clay clasts and a sandstone clast are observed.	Lack of sedimentary structures, some planar laminations and wave ripple laminations is visible in places when the degree of bioturbation is low.	Renardodden	Light grey	3-200	Various organisms stirring and burrowing into underlying unconsolidated sand
F 13 <i>Fig. 4.19</i>	Sandstone with <i>Ophiomorpha</i> trace fossils	Fine grained, consolidated sandstone bed with sharp boundaries and <i>Ophiomorpha</i> trace fossils ranging from 4 cm to 10 cm in length. Organic detritus and coal fragments are present	Some wave ripple cross- laminations	Renardodden	Light grey with yellow/red rust stains	15-220+	Burrowing of <i>Ophiomorpha</i> trace fossils into underlying fine grained marine sand
F14 <i>Fig. 4.20</i>	Soft sediment deformed sandstone	Very-fine to fine-grained sandstone beds with sharp or erosional bed boundaries. Coal fragments. Some silt between sandstone beds	Deformational structures and <i>skolithos-type</i> burrows are present. <i>Teichichnus</i> and possibly <i>Macaronichnus</i>	Renardodden Crude laminator	Light grey with reddish rust stains	10-40	Deformation of unconsolidated sand due to the influence of storm waves
F 15 <i>Fig. 4.21</i>	Highly bioturbated organic rich sandstone	Consolidated or unconsolidated bioturbated very-fine to fine sandstone. Coal fragments and concretions are present.	Overall relatively structureless. Some ripples, Plane parallel laminations and coal draped laminations in addition to a deformation structure (scour) are observed	Renardodden	Dark grey with yellow weathering cracks	30 - 1005	Bioturbation in a setting with little sediment input, in addition to low fallout of sediments from suspension

F 16A <i>Fig.</i> 4.23A	Heterolithics comprising alternating silt, mud and sand	Alternating beds of silt, mud and very-fine to fine sandstone. Coal fragments and siderite concretions are common in sandstone intervals	Plane parallel laminations and slight discontinuous wavy bedding in sand-rich units <i>Skolithos</i> burrows	Renardodden	<u>Sandstone:</u> light beige	0.5-27	Alternations in lithology are a result of fluctuations in sediment input from the coast in combination with fluctuations in current strengths
					<u>Silty mudstone:</u> grey to dark grey	0.5-50	
F16B <i>Fig.</i> 4.23B	Highly bioturbated heterolithics comprising alternating shale and silt/sand	Discontinuous bioturbated beds of shale and silt/sand with shale dominating. Organic material abundant. Coal granules and roots are present.	Plane parallel laminations and wavy bedding <i>Skolithos</i> burrows	Renardodden	Mostly dark grey, sands are light beige with red and yellow stains. Some areas have a greenish colour	Irregular layers	Alternations in lithology are a result of fluctuations in sediment input from the coast in combination with fluctuations in current strengths. Burrowing of organisms into unconsolidated strata.

4.3 Facies associations with subsequent lithofacies

In the following section, sixteen lithofacies are classified, described and interpreted in regard to the corresponding sub facies association. Seven different sub facies associations have been detected from the logged succession of the Calypsostranda Group (Table 4.2). The whole succession has previously been interpreted to be 265 meters in the stratotype (Dallmann, 1999). As part of this study, 247,5 meters of the section was covered, as part of detailed sedimentary outcrop analysis along two beaches in the Calypsostranda area where the majority of the outcrops are observed.

Table 4.2: Summary of the two facies associations and their sub-associations and lithofacies recognized in the present study.

<i>Facies association</i>	<i>Sub-associations</i>	<i>Lithofacies</i>	<i>Depositional environment</i>
FA1 Continental regime	SUB FA1.1	F1	Tectonically generated mass transport complex
	SUB FA 1.2	F4, F7, F3, F5, F9, F6, F2	Floodplain
	SUB FA 1.3	F8A, F10, F11, F9	Distributary channel fills
FA2 Paralic to marine	SUB FA 2.1	F8B, F11, F9, F13, F12	Upper delta front
	SUB FA 2.2	F13, F14, F12, F11	Middle delta front
	SUB FA 2.3	F15, F11	Lower delta front
	SUB FA 2.4	F16A, F16B	Prodelta

4.3.1 Facies association 1: Continental depositional environment

This facies association includes SUB FA 1.1: Tectonically generated mass transport deposits, SUB FA 1.2: Floodplain deposits and SUB FA 1.3: Distributary channel fill deposits. These sub-associations represent depositional environments that were not or only little affected by open marine processes. The investigated sediments stratigraphically belong to the Skilvika Formation and are interpreted to be of predominantly continental origin, part of a subaerial delta plain environment. The formation is mostly composed of fine-grained sandstone and siltstone (Fig. 4.1), with

the presence of a few conglomeratic horizons and *in-situ* coal deposits (F1, F2, F3, F4, F5, F6, F7, F8, F9, F10, F11, Table 4.1).

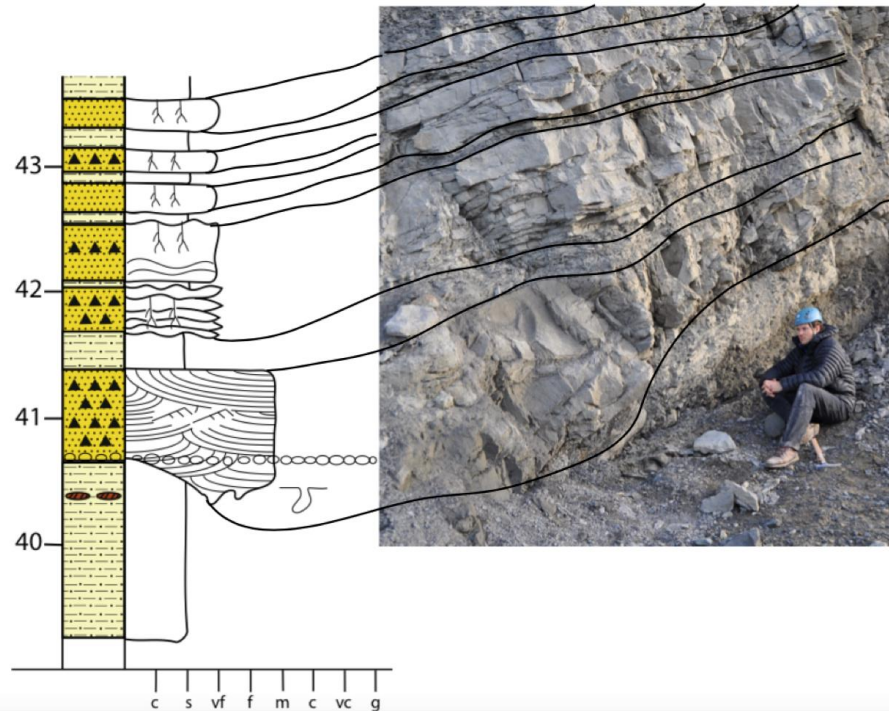


Figure 4.1: Example of a lithostratigraphic log from the Skilvika Formation displaying deposits part of Facies association 1: Continental depositional environment. A distributary channel with trough-cross stratification erodes overbank silty deposits below. Tabular sandstone beds with root growth representing crevasse deposits are present above the channel. Person as scale

4.3.1.1 SUB FA 1.1: Tectonically generated mass transport complex

Facies included within the sub facies association is; **F1:** Mica-rich, poorly sorted basal breccia. The stratigraphic position is displayed in the log in fig. 4.2.

The association includes brecciated, poorly sorted deposits overlying the unconformity at the base of the Skilvika Formation. The deposits have been transported and reworked as a result of tectonic processes.

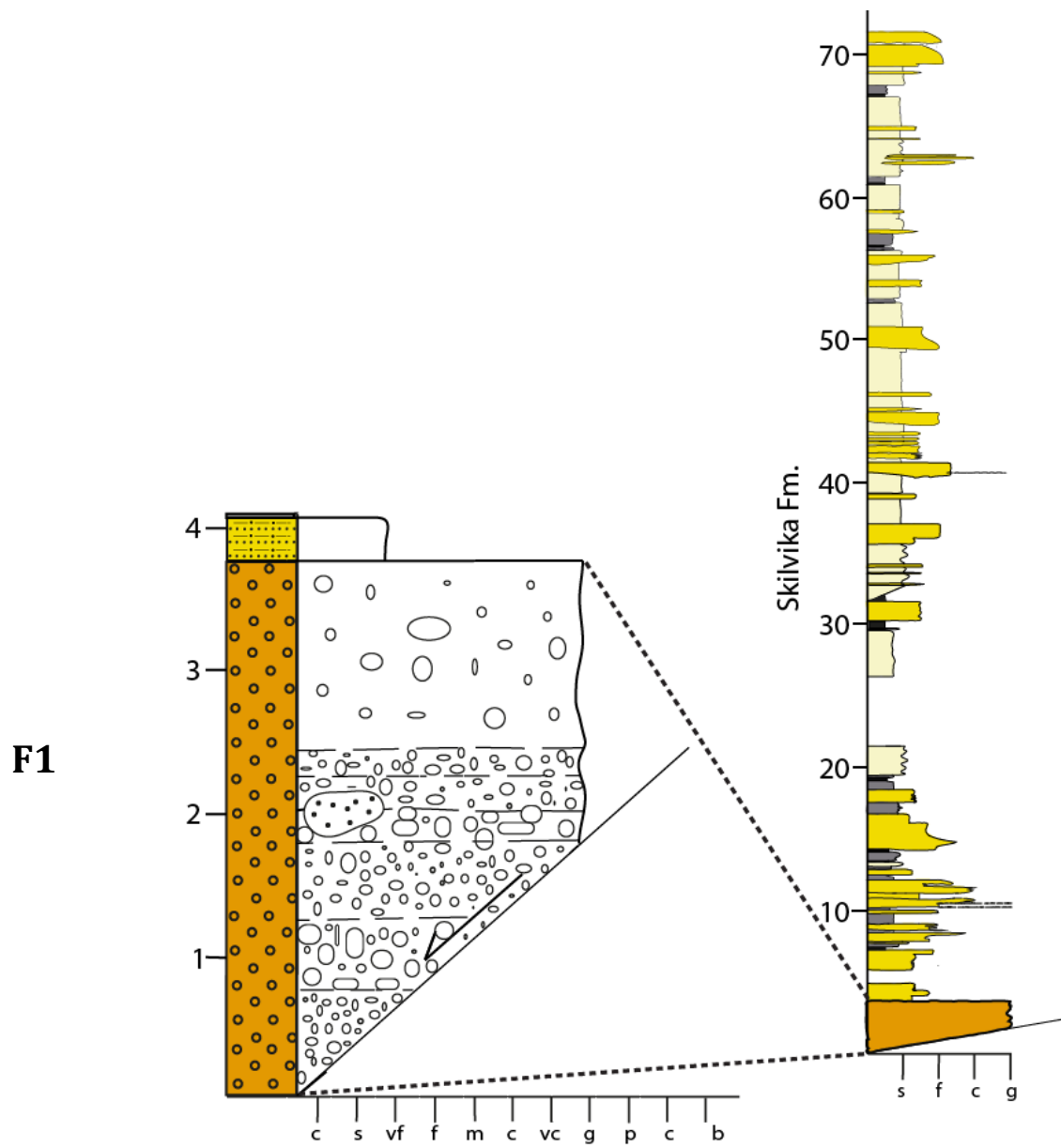


Figure 4.2: Lithostratigraphic log with stratigraphic position of SUB FA 1.1: Tectonically mass generated slump, at the base of the Skilvika Formation. F1 is highlighted

*Facies 1 (F1): Mica-rich, poorly sorted basal breccia**Description*

A 375 cm thick brecciated unit is present at the base of the Skilvika Formation. The entire unit unconformably overlies basement rocks composed of brecciated mica schist (Fig 4.3), and is separated by a faulted contact with an apparent dip 70–80 degrees towards northeast. A second large fault cuts nearly vertically through the section in the upper part of the unit, and several micro faults are present within the unit. The deposit displays slight rotation of the original bedding. The lower 245 cm of the unit comprises a chaotic breccia where sandstone and quartzite granules, pebbles and occasional boulders appear in a brecciated schist matrix interbedded with mica schist clasts derived from the basement below. The fine sandstone clasts are subrounded in shape whereas the quartzite clasts well-rounded to angular. MPS of the clasts was measured to be 22.4 cm in the lowermost 2 meters of the unit. The top 130 cm of the unit has a significant decrease in the amount of granules and is matrix supported. The matrix consists of a light grey silty mica schist matrix.

Interpretation

Based on the faulted contact in combination with the chaotic fabric, poor sorting of the breccia and slight bedding, this facies is interpreted to be part of a larger slump complex that has been activated as a response to movements on the underlying fault. This interpretation is in line with previous interpretations by Birkenmajer (2006) who mentions that it could be considered “a fossilized incipient slump”. No primary structures were observed, but due to the slight bedding, it is not considered to be a cohesive debris flow deposit. The slump deposit and sediments directly overlying the deposit do not portray any sedimentary structures, trace fossils or shell remnants indicative of a marine environment suggesting a continental environment for the deposit.

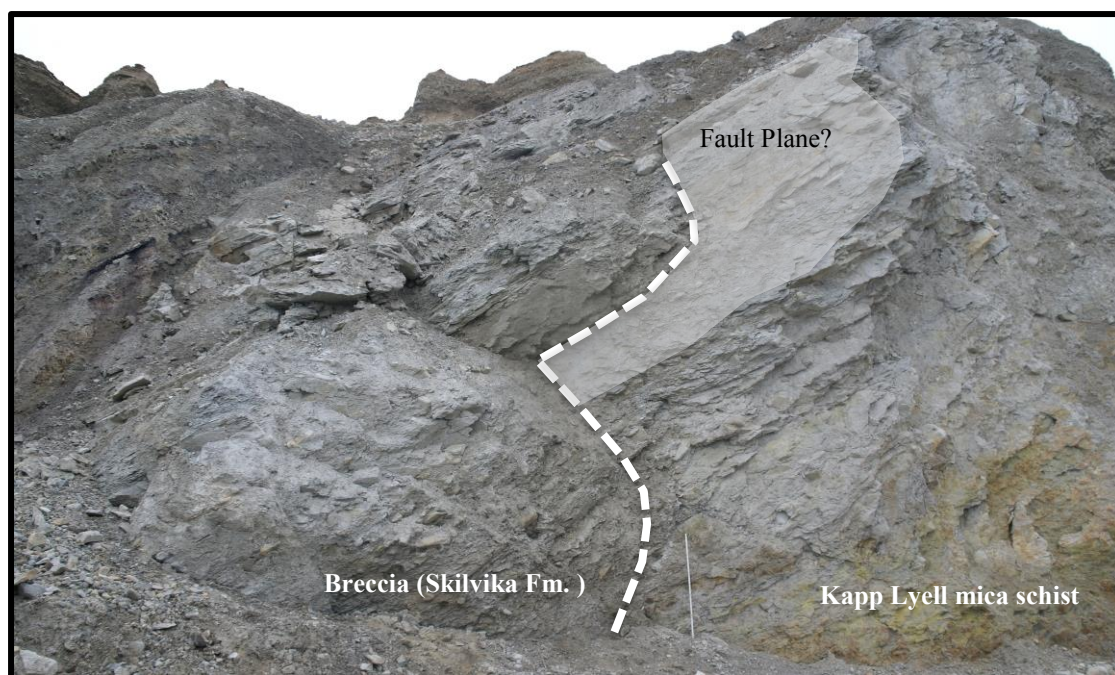


Figure 4.3: Mica-rich basal breccia with contact to underlying mica schist basement rocks of the Kapp Lyell succession. A suggested fault plane is marked by a stippled line. Ruler for scale, 1 m.

4.3.1.2. SUB FA 1.2: *Floodplain deposits*

Seven lithofacies are described within facies assemblage SUB FA1; **F2**: Coal or coaly shale **F7**: Mudstone, **F3**: Structureless or faintly laminated very fine- to fine-grained sandstone, **F4**: Very fine-grained flaser laminated sandstone, **F5**: Siltstone, **F6**: Soft-sediment deformed silt-/sandstone and shale, and **F9**: Very fine- to medium-grained sandstone with sigmoidal to tangential cross-stratification.

Based on the combination of lithofacies in the studied succession (Fig 4.4), the facies assemblage is interpreted as floodplain deposits. A number of indicators, which will be described in more detail under each lithofacies, point to this interpretation.

The floodplain deposits are abundant in the Skilvika Formation (Fig 4.4) and are generally composed of fine sandstone, siltstone and mudstone. Coal (F2) and organic material such as rootlets and organic detritus is abundant. Sedimentary structures indicating unidirectional flow like tabular cross-stratification (F9) is observed. Sediments derived from the floodplain environment, have been transported and

deposited as overbank deposits on a relatively flat substrate. The sediments are essentially deposited during flooding events, predominantly by suspension fallout in the overbank flood basins (Reading, 1996).

According to Miall (2013), sediments that are developed outside the main fluvial channels can be restricted to three different classes:

1. Deposits formed as a result of overbank flow. These are relatively coarse-grained and include crevasse-channel, crevasse-splay and levee deposits (**F3, F4, F6, F9**).
2. Sediments laid down in low-energy environments. The deposits are relatively fine-grained and can develop for instance from ephemeral sheet floods or accumulate in floodplain ponds (**F2, F7, F5**).
3. Deposits that have developed as a result of paedogenesis, organic activity or evaporation and are classified as biochemical sediments (Not present in the studied succession).

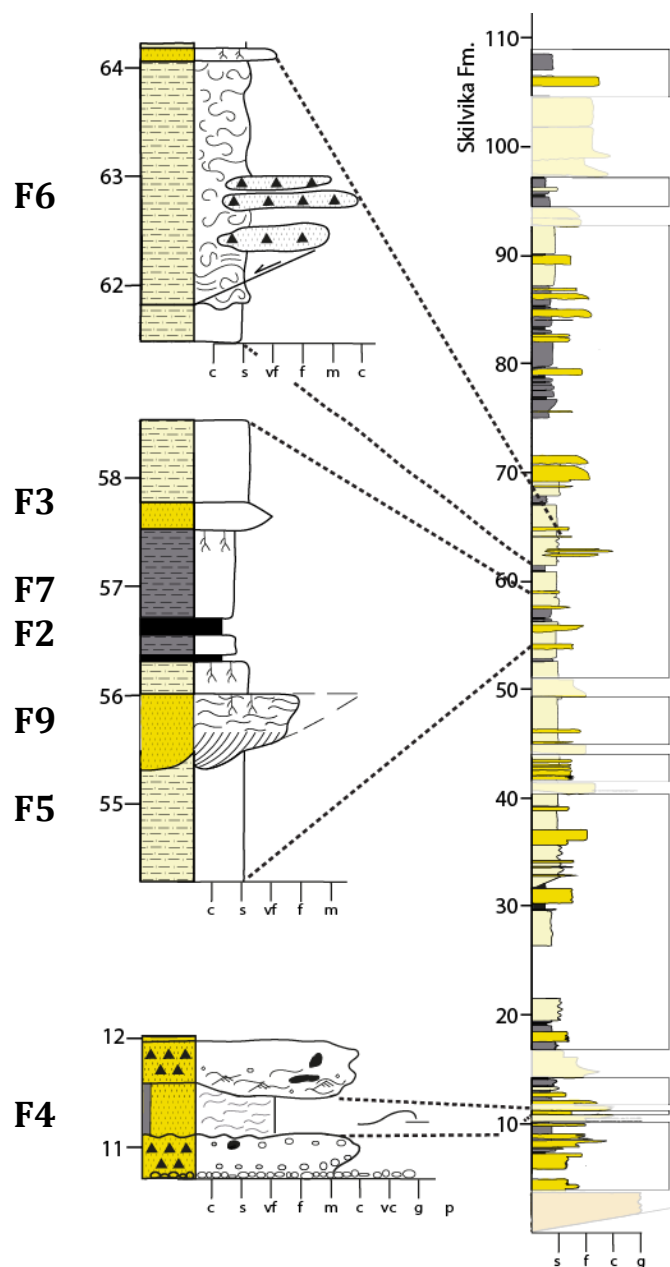


Figure 4.4: Composite log of the entire Skilvika Formation displaying where floodplain deposits (SUB FA 1.2) are present (black outline). Examples of each facies is shown on a lithostratigraphic log. Refer to legend in Appendix B.

Facies 2 (F2): Coal or coaly shale

Description

The facies occur either as pure coal with a shimmering appearance (Fig. 4.5) or as coaly shale. In the Skilvika Formation, the coal seams range from 2 to 20 cm, whereas the coaly shales range from 5 to 50 cm. Some pure coal layers are very well cleated, and iron rich concretions may be observed. The coal has a black colour, but yellow oxidation stains may be present. The coal seams are under- and overlain by mudstone,

siltstone and sandstone belonging to SUB FA 1.2: Floodplain deposits, and SUB FA 1.3: Distributary channels and infill deposits. Deposits underlying the coal seams are commonly penetrated by rootlets.

Interpretation

Coals are organic-rich sedimentary rocks and a product of alteration processes of peat and organic material through compaction. The coal horizons in the Skilvika Formation that overlie paleosols are interpreted to be autochthonous coals, due to the presence of rootlets in the underlying strata (e.g. Reading 1996). Formation and diagenesis has occurred under anoxic conditions in either swamps, marshes or bodies of still-standing water (Birkenmajer and Gmur, 2010).

Coals are common sedimentary rocks of both paralic- (coastal and deltaic) and limnic (lacustrine and fluvial) environments (e.g. Stow, 2005). The studied coal seams of the Skilvika Formation are thin and laterally extensive, suggesting a nearshore environment in a deltaic setting. In fluvial sequences, coal seams are frequently more restricted (Stow, 2005).



Figure 4.5: *In-situ* laterally extensive coal seam in the Skilvika Fm, The hammer is 13 cm from top to base.

Facies 3 (F3): Structureless or faintly laminated very-fine to fine sandstone

Description

The facies is abundant in the Skilvika Formation and is observed throughout the whole formation as predominantly non-graded, tabular sandstone beds with characteristic sharp tops and bases (Fig. 4.6 A&B). Some beds exhibit a slight normal grading with undulating base boundaries. The lithology is mostly homogeneous and consists of very-fine to fine-grained sandstone, with occasional siltstone interbeds. Units range from 10 cm to 135 cm in thickness, but are mostly relatively thin and rarely exceed 40 cm in thickness. Unconsolidated muddy and/or silty overbank deposits (F5, table 4.1) under- and overlay the sandstones of F3. Rootlets, organic detritus and coal fragments are common, as well as undulating internal surfaces. Organic draped laminations are present and help in identifying discontinuous wavy or planar parallel laminations. Small Fe-concretions may be observed, as well as occasional quartz granules. Coals (F2, table 4.1) overlie some of the sandstone beds and represent *in-situ* deposition as evidenced by root growth in the sandstone. One sandstone bed shows distinct relief at the base, as well as tangential cross-stratification. The sandstone beds are grey to light beige in colour, and some reddish oxidation stains may be observed at weathered surfaces.

Interpretation

Based on the occurrence of rootlets in addition to a sheet-like architecture, the facies is interpreted to be floodplain deposits occurring laterally to a distributary system. Furthermore, due to the predominantly sharp tops and bases and dominance of sandstone, the sediments are interpreted to be mainly crevasse channel and splay deposits. The rarity of sedimentary structures may be an indication of rapid transportation and deposition.

The thinner intervals (<65 cm) could represent crevasse splay deposits, whereas the thicker (>65 cm) are most likely crevasse channel deposits. This assumption is based on the observations of a 65-cm thick sandstone bed interpreted to be a crevasse channel deposit due to its lensoid shape and pronounced tangential cross stratification at the base. This is the only bed where one can use geometric criteria to distinguish between crevasse splay deposits and crevasse channels; the outcrops are generally not laterally

extensive enough to use such criteria to differentiate between types of crevasse deposits. Some of the beds show an upwards-fining characteristic which is typical for channel deposits.

A breach in the levee of a main or distributary channel due to high runoff (e.g. Miall, 2010) and episodic flooding, has led to the transportation of silt and finer sand particles that were previously in suspension in the channel. These have been transported onto the floodplain and deposited as crevasse deposits. The sediments may also be channel infill deposits of small crevasse channels with enough flowing capacity to transport sand. Sand will be deposited out of suspension when flow rate is decreased. Crevasse channels on the floodplain have transported the organic material and deposited it as organic draped discontinuous and parallel laminations in the crevasse splay deposits (Fig 4.6 B). Crevasse channels may have had strong enough flowing capacity to transport larger sized grains, like the observed quartz granules and coal fragments.

Tangential cross-stratification (F9, table 4.1) is observed in one of the beds (Fig 4.4 C). Tangential termination of foresets within dunes is common where sediments falls out of suspension on the lee face of the migrating dune (Cheel, 2005). Such stratification may be indicative of deposition in small streams, like crevasse channels on the floodplain, and deposition more distal to the main channel source, but can be deposited in a variety of environments where currents and sediment load are sufficient enough.

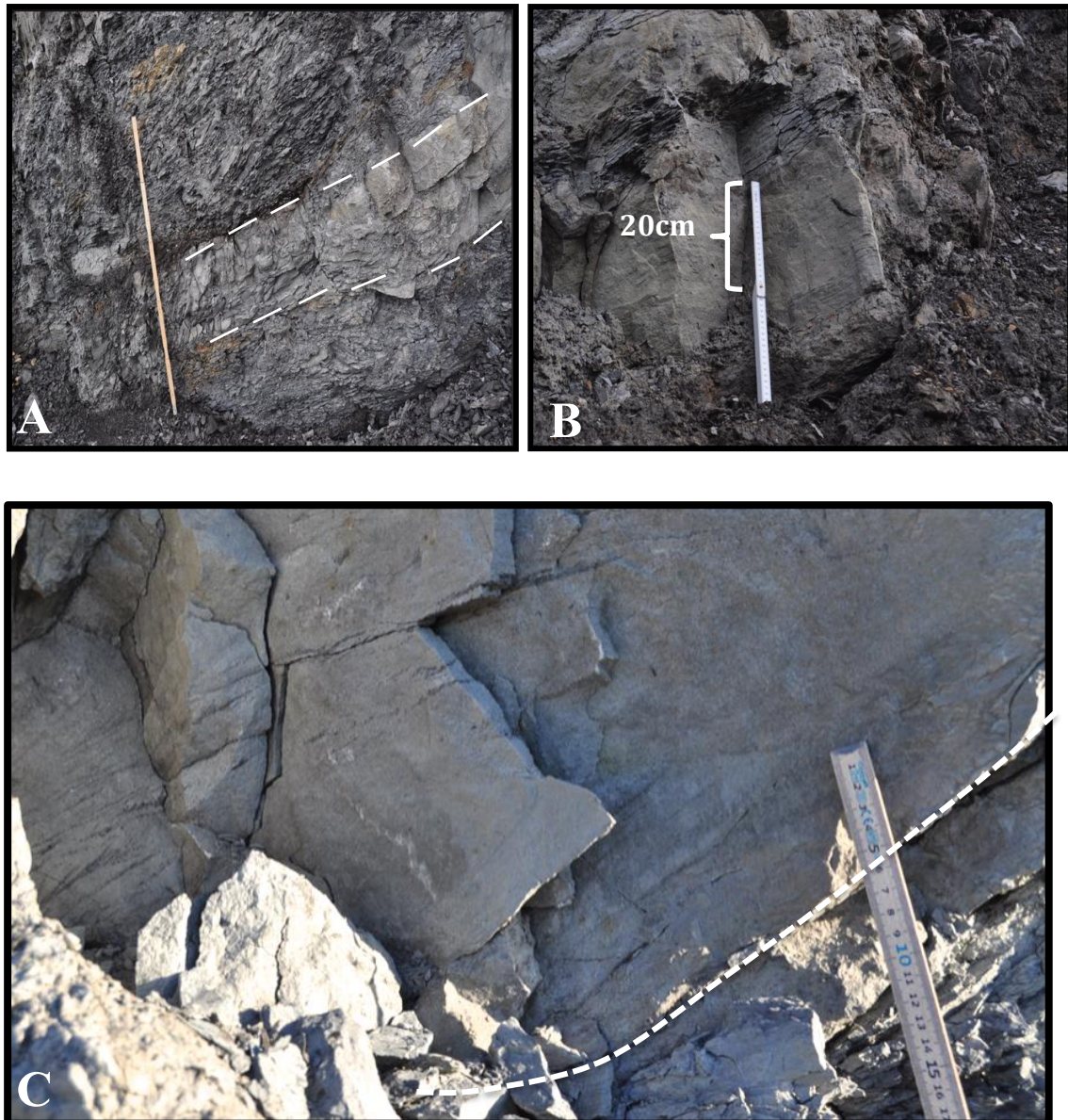


Figure 4.6: Structureless or faintly laminated very-fine to fine sandstone. The crevasse splay deposits are characterised by sharp tops and bases (A), and internal planar parallel and discontinuous laminations (B). The crevasse channel deposits show a more curved basal part (C) with the presence of tangential cross-stratification. The scale as represented by the ruler is 1m in A, and 20cm in B.

Facies 4 (F4): Very fine-grained flaser bedded sandstone

Description

The facies can be observed in a 45-cm thick very fine-grained sandstone unit near the base of the Skilvika Formation (Fig 4.7). Mud-draped flaser lamination in discontinuous and undulating bedding characterise the sandstone. Coarse to very coarse-grained sandstone is inter-bedded as lenses and thin horizons throughout the finer-grained sandstone bed. Coal fragments and roots perpendicular to the bedding can be observed. The facies has undulating boundaries to the under- and overlying units

comprising of medium to coarse-grained sandstone above, and a coarse-grained to granule-rich sandstone below. The bed is light beige to light grey in colour with some reddish oxidation stains due to weathering of the rock. The bed has a slight heterolithic lithology with a sand-mud ratio of approximately 90-10.

Interpretation

Due to the presence of coarser grained sand in the deposits, as well as the dominance of sand over mud, the slightly heterolithic sediments of F4 are interpreted to be floodplain deposits, generated by episodic flooding events and deposited as proximal levee deposits on the channel banks, close to the edges of the channel. Finer grained sediments are typically more abundant more distal to the channel (e.g. Guccione, 2009). Fine-grained sandstone and siltstone typically dominate the composition of levee deposits (Reading, 1996).

Flaser bedding is typical in areas with low amounts of mud in suspension and where stronger currents are present to erode previously deposited mud (Dalrymple, 2010). The deposits may be derived from transport and deposition in the overbank area during periods of flooding. Vegetation growth in periods with few flood-events is evidenced by the presence of roots. Ripple-bedded units with interlayered horizontal bedding is common for levee deposits (e.g. Singh, 1972), although lamination may be disrupted as a result of bioturbation (e.g. Reading, 1996).

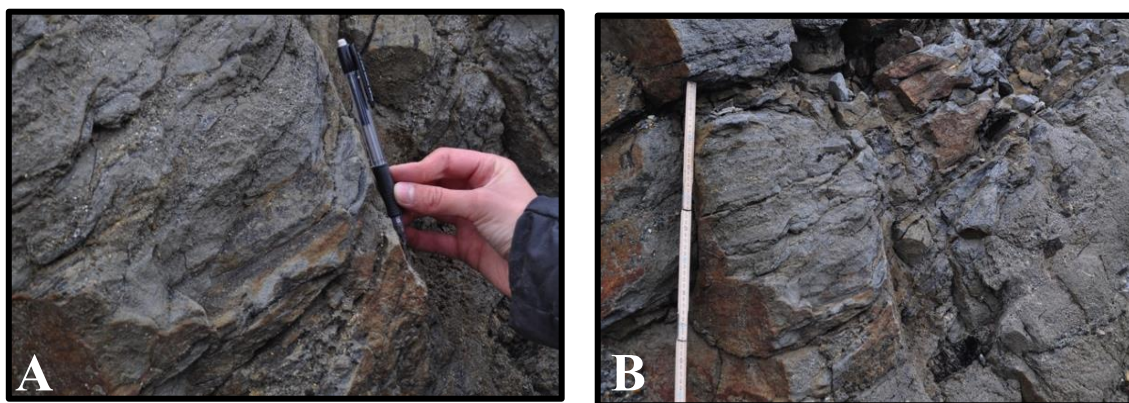


Figure 4.7: Very fine-grained flaser laminated sandstone near the base of the Skilvika Formation. Outcrops displaying flaser bedding and the characteristic undulating bedding

*Facies 5 (F5): Siltstone**Description*

The facies consists of consolidated siltstone or highly fractured silty shale and is abundant throughout the Skilvika Formation. The silt beds/units generally have sharp tops and bases with a vast variety in thickness ranging from 5 cm to 280 cm.

The consolidated siltstones appear as thin homogeneous beds ranging from 10 cm to 60 cm (Fig 4.8 A). The beds are non-graded and may contain small coal fragments. Colour ranges from whitish beige to light grey with some yellow stains. No internal sedimentary structures can be identified.

The highly fractured silty shale units comprise thicker intervals where silt and mud are mixed or intercalated with one other (Fig 4.8 B). Silt is the most pronounced lithology. Some roots, coal fragments and large Fe-concretions are observed, in addition to very fine sandstone layers and lenses. Thicknesses vary in the range of 5cm to 280 cm, but the majority of the units are above 1 meter thick. Units are separated by thin sandstone layers (average 10 cm) and structureless to faintly laminated sandstone (F3). The sediments are light grey to dark grey in colour.

Interpretation

Based on the siltstone-dominated character, the presence of coal fragments, and the occurrence of roots, this association is interpreted to be deposits derived from the transport and deposition of fine-grained material by fluvial processes during episodic flooding of the floodplain. Fallout from suspension of silt and mud has occurred when the transport capacity of the flow has decreased. The grain sizes in the deposits may convey information regarding the distance from the channel source, where the amount of fine silt and clay particles will be greater with increasing distance from the channel source (Guccione, 2009).

The deposition of the more homogeneous silt layers may have occurred in closer proximity to the channel source than that of the thicker intervals with silty shale. This

assumption is based on studies showing that the total amount of silt and clay fractions in overbank sediments, derived from a large stream, will increase with distance from the source (Guccione, 2009). The homogeneous silt layers may also have been deposited in aqueous environments containing little suspended sediments (Guccione, 2009).

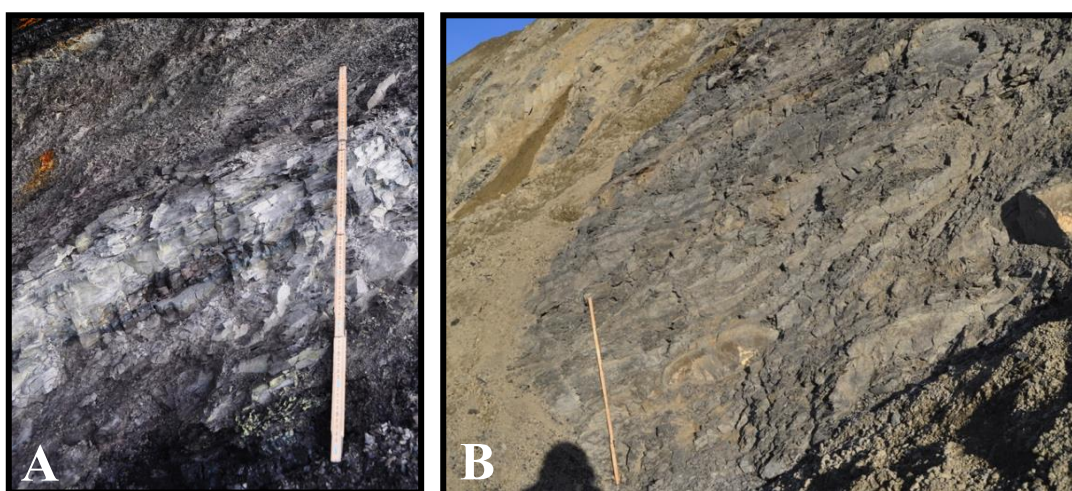


Figure 4.8: Siltstone represented in the outcrops, portraying the general thickness contrasts between the two sub-facies. A) Consolidated siltstone. B) Highly fractured silty shale. The scale represented by the ruler is 1 m in both photographs.

Facies 6 (F6): Soft sediment deformed siltstone/sandstone and shale

Description

The facies is comprised of siltstone/sandstone and mudstone and is only observed at one level in the Skilvika Formation within a 235 cm thick chaotic unit (Fig. 4.9) containing calcrete nodules. Medium to coarse-grained sandstone with coal fragments and root traces are identified as isolated lenses in surrounding deformed mudstone. The unit is under- and overlain by silty shale overbank deposits (F5) and is light grey with reddish oxidation stains (Fig 4.9). Erosion of the underlying unit can be observed at the base.

Interpretation

Due to the pronounced deformation of fine-grained sediment and presence of isolated sandstone lenses, the facies is interpreted to be a typical example of soft sediment deformation characterised by load casts in finer-grained sediments. The well-

developed load casts, so called “ball- and pillow” structures are formed in unconsolidated sediment due to loading of the original sand/silt bed (Bridge and Demicco, 2008). Such deformational structures form as a result of a Rayleigh-Taylor instability due to density contrasts between the overlying and underlying unit (Kaus and Podladchikov, 2001). A larger density contrast will generally produce more pronounced load casts. “Ball- and pillow” structures form when the casts are completely isolated from the original overlying unit, which is the case in the Skilvika Formation, where a medium to coarse sandstone bed has been deposited on top of a fine mudstone. A suggestion for such a setting, may be in an alluvial environment where channel avulsion, such as crevasse splays, has led to deposition of sediments on top of unconsolidated fine-grained floodplain deposits.



Figure 4.9: Soft sediment deformed siltstone/sandstone and shale in the Skilvika Formation. Characteristic “ball and pillow” structures can be observed with isolated sandstone lenses in surrounding mudstone. The scale represented by the ruler is 1 m from base to top.

Facies 7: Mudstone:

Description

The mudstones in the studied succession have varying lithological compositions and are composed of unconsolidated non-laminated to slightly laminated clay-rich mudstones to consolidated shaley mudstone. Mudstone beds are most abundant in the Skilvika Formation, but are also present near the base of the Renardodden Formation. Their thicknesses range from 2-3 cm to 75 cm in the Skilvika Formation and from 2 cm

to 140 cm in the Renardodden Formation. In general, the shaley mudstones are very fissile, whereas the clay-rich mudstones are non-fissile. The clay-rich mudstones are usually very water-saturated and are easily broken apart. There is a varying content of organic material and coal fragments may be present. The facies is light to dark grey whereas intervening very-fine and fine-grained sandstone lenses and concretions are beige or red stained. Root traces, concretions, and coal fragments are observed. The mudstones are under- and overlain by coal (Fig 4.10) or sandstones, and may have rootlet growth where coal horizons overly the mudstone.

Interpretation

Based on the fine-grain size, the relatively homogeneous composition and occurrence of lamination in most of the deposits, the deposits and the mudstones in the Skilvika Formation are interpreted to be mainly lacustrine deposits of the alluvial environment where drainage and flow is limited. Due to their marine influence the mudstones in the Renardodden Formation are interpreted to be deposited in wetlands on the lower delta plain, as part of a flood basin setting. The mudstones have been deposited as a result of fallout of mud particles from suspension due to low flow rate and low transport capacity.

The clay-rich mudstones with slight laminations (Fig. 4.10) may be interpreted to be similar to varve laminations due to rhythmic bedding, and have been deposited in restricted oxbow lakes or in more vast lakes belonging to the floodplain environment (Reading, 1996). Neck cut-offs in a meandering river environment are likely processes for transporting of finer overbank sediments (Reading, 1996). Neck-cut offs are predecessors to the formation of oxbow lakes, and are produced in sinuous rivers where cut banks meet (Bridge and Demicco, 2008). As disconnection from the main channel flow occurs, an oxbow lake is produced (Bridge and Demicco, 2008). Flow rate is decreased leading to fallout and accumulation of finer-grained particles.

The colour the mudstones exhibit can be a good indicator of how well the floodplain is drained. Due to their grey colour and conservancy of organic material, the mudstones are indicated to be prone to waterlogged conditions (Reading, 1996).



Fig 4.10: Mudstone deposits of facies 7, interbedded with coal seams. The ruler represents 1 m.

4.3.1.4. SUB FA 1.3: Distributary channel fill deposits

The following lithofacies are included within SUB FA 1.3 and are portrayed in the log in Fig. 4.11; **F8A:** Sandstone with gravel conglomerate, **F9:** Very fine to medium-grained sandstone with sigmoidal cross-stratification, **F10:** Trough cross-stratified sandstone and **F11:** Sandstone with plane parallel stratification.

Based on the combination of lithofacies in the studied succession (Fig. 4.11), the close proximity to floodplain deposits, the well-rounded grains and granules in the sediments and presence of unidirectional sedimentary structures indicating unidirectional flow, the facies included within sub association FA 1.3 are interpreted as having been deposited within distributary channels. The interpretations of the specific lithofacies are based on the assumption of them being deposited in distributary channels through processes directly related to fluvial channel infilling, on the delta plain.

Sediments included within distributary channel fills are composed of sandstone and gravel conglomerate with well-rounded grains and frequent occurrences of organic detritus such as root traces and coal fragments. Sedimentary structures are observed through unidirectional bedforms produced under i) lower flow regime conditions:

tabular cross-stratification (**F9**) and trough cross-stratification (**F10**) to ii) upper flow regime conditions: plane parallel stratification (**F11**).

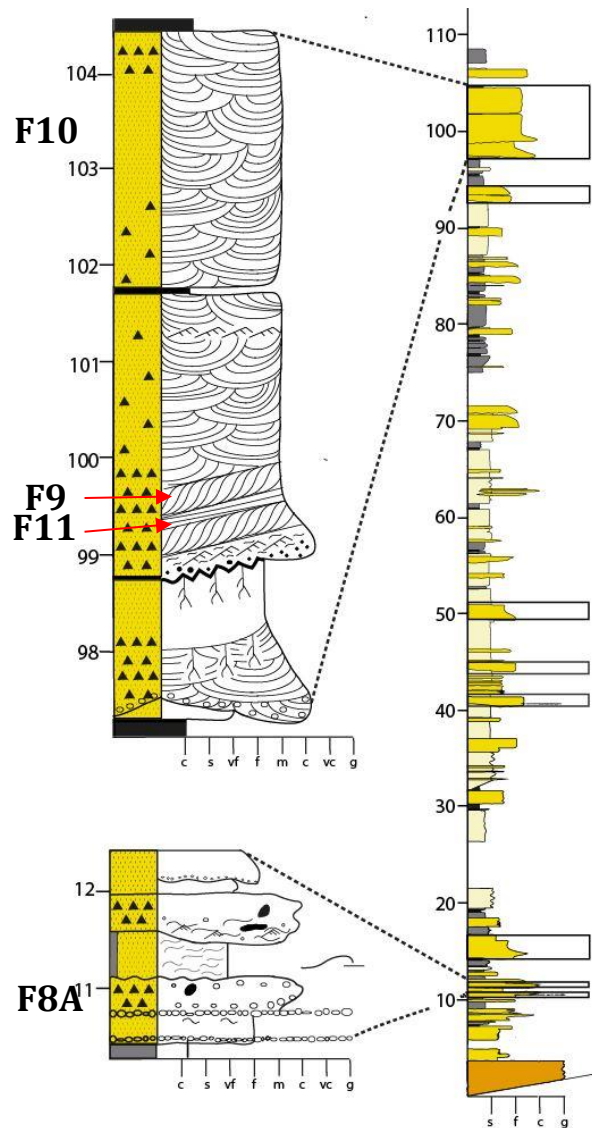


Figure 4.11: Composite log of the entire Skilvika Formation displaying where floodplain deposits (SUB FA 1.3) are present (black outline). Examples of each facies is shown on a lithostratigraphic log. Refer to legend in Appendix B.

Facies 8A (F8A): Sandstone (fine and coarse-grained) with gravel conglomerate

Description

This facies is characterised by three upwards fining sandstone beds ranging from 25 to 35 cm in thickness, containing gravel conglomerate. Unidirectional ripples are observed in one of the sandstone beds, otherwise the beds are structureless. One of the beds is eroding underlying strata. There are two clast-supported gravel conglomerate

horizons (Fig 4.12) with thicknesses of 4 and 5 cm respectively near the base of two of the upwards-fining beds, otherwise the sandstones are matrix supported with occasional isolate granules. The granules are sub-rounded to rounded with some angular and sub-rounded pebbles in a medium to very coarse sandstone matrix. Quartz is the dominating clast component, although coal and mudstone clasts are also observed. The matrix is light to dark grey in colour, whereas the quartz clasts are milky white to light beige with reddish and yellow oxidation stains. The conglomeratic horizons are embedded in poorly laminated fine-grained sandstone, and are overlain by inversely graded fine to coarse-grained sandstone bed.

Interpretation

Due to the upwards fining beds and large, isolated clasts, the beds are interpreted to be bedload deposits derived from channel runoff (Reading, 1996). The transport and deposition of the sandstone beds with conglomerate beds of the Skilvika Formation has occurred in an alluvial environment through fluvial processes where rivers or streams have a high rate of flow and a capacity to transport larger clasts and coarser grained sand. The deposits are interpreted to be mature due to their high content of rounded quartz clasts. Transport and reworking in a distributary channel, and deposition far from the source area is likely for these deposits.

The granule-rich beds in the Calypsobyen Group have various environmental interpretations and are therefore classified into two different sub facies-associations. The granule-bearing beds of the Skilvika Formation are classified as SUB FA 1.3: Distributary channel fill deposits, whereas the thicker conglomerate beds of the Renardodden Formation are classified as SUB FA 2.1: Upper delta front deposits.

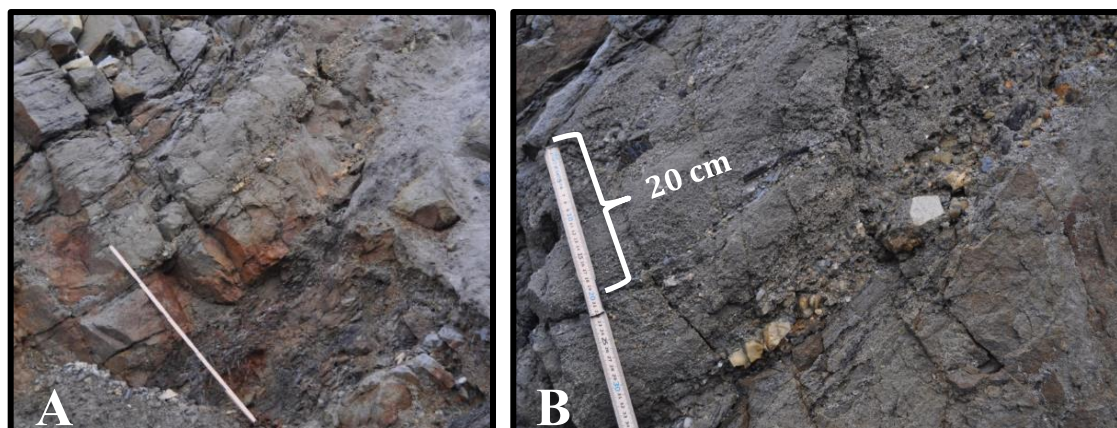


Figure 4.12: Clast-supported gravel conglomerate near the base of the Skilvika Formation. Quartz is the dominating clast component. Ruler in A is 1 m.

Facies 9 (F9): Very fine to medium-grained sandstone with sigmoidal cross-stratification

Description

The facies is characterised by very fine to medium-grained sandstone with sigmoidal organic-draped cross-stratified sets (Fig 4.13). Often, the cross-stratified sets have a sharp erosional top surface and very coarse-grained to granule size quartz grains are present within the stratifications (Fig 4.13B). The cross-stratified sets are 25 cm to 100 cm thick and occur within a homogeneous 495 cm to 700 cm thick sandstone units in the top section of the Skilvika Formation. Trough cross-stratification (F10, table 4.1, Fig 4.14 A&B) is observed above the sigmoidal cross-stratified sets and represents increasing flow strength. The sandstone is light grey with yellow to reddish oxidation stains.

Interpretation

Sigmoidal internal strata are common in bedforms, like washed out dunes, that have characteristic long crests and short lee faces (Cheel, 2005). The sigmoidal foresets can be traced up into horizontally laminated topsets (Fig 4.13). These topsets indicate dunes or bars deposited as plane beds as a result of transitional to upper-phase flow conditions (Reading, 1996). As observed in Fig 4.13 B, the strata sets are truncated by an upper bounding surface, which is typical for sigmoidal strata (Cheel, 2005) .

Cross-stratification is common in both deltaic environments and shallow-marine clastic environments (Stow, 2005) and form as a result of the migration and deposition of sand in dunes from unidirectional currents under lower to transitional flow regime conditions.

The stratification may be indicative of deposition within a distributary channel where there is a sufficient amount of sediment supply and strength of the unidirectional flow. The high abundance of coal and organic material in the stratifications indicates a high amount of suspended organic matter within the channel.

The sediments may also be part of SUB FA 2.1: Upper delta front deposits, where deposition has occurred within coastal environments where distributaries flow into an open body of water.

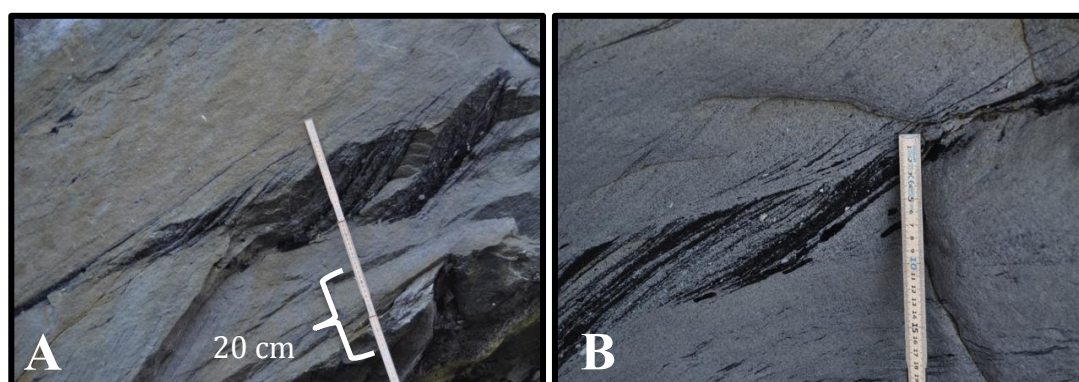


Figure 4.13: Sigmoidal cross stratification with organic- draped sigmoidal internal strata (B and C)

Facies 10 (F10): Trough cross-stratified sandstone

Description

Trough cross-stratification is observed in very fine to fine-, fine-, fine- to medium- and coarse-grained sandstone. Trough cross-stratification is most commonly observed within 50 cm to 275 cm thick normal graded beds with sharp or erosive concave-up lower boundaries. In other areas, the trough cross-stratification is present in 45 cm to 80 cm thick non-graded beds with sharp tops and sharp or undulating lower boundaries.

In-situ rootlets at the top of upwards-fining units, coal fragments, pebbles and siderite concretions are observed within the beds containing trough cross-stratified sandstone, in addition to climbing ripple lamination. The trace fossil *Palaeophycus* is observed at the base of a 50-cm thick trough cross-stratified sandstone bed. The sandstones are

light grey to light beige in colour and yellow jarosite coating is observed (Fig. 4.14 A&B).

The facies is under- and overlain by plane parallel stratification/lamination (F11), coal (F2), structureless or faintly laminated sandstone (F3), siltstone (F5), sandstone with flaser bedding (F4) and sandstone with sigmoidal cross-stratification (F9).

Interpretation

Based on the undulating trough-cross bedding, presence of *in-situ* root growth and occurrence of unidirectional climbing ripple cross-lamination in predominantly upwards-fining units, the trough cross-stratified sandstones are interpreted to be fluvial deposits belonging to SUB FA 1.3: Distributary channel fill deposits.

Trough cross-stratification is formed in the upper part of the lower flow regime, with the development of three-dimensional dunes with undulating ridges, through the migration of sand. Based on the thickness, grading and surface geometry of the individual trough-cross stratified sandstone beds, they can be subdivided into type of distributary: i) Low sinuosity minor distributary: ii) High sinuosity meandering distributary:

- i) Given an overall interpretation in terms of distributary channel fills, it is suggested that the trough-cross stratified sandstone bodies less than 2 meters thick, showing non-graded and normal graded grain size trends, are classified as delta distributaries based on the Gibling (2006) classification of fluvial-channel bodies. The concave up bases (Fig. 4.14 C), observed sedimentary structures and the presence of coal clasts and gravels support this classification. The aggradational fill is recorded in the channel bodies within dominantly upwards fining units. Absence of lateral accretion surfaces, points to deposition within short-lived, low-sinuosity channels, perhaps distributaries deviating from the main channel. The sandstones are under and overlain by floodplain sediments (SUB FA 2.1, Table 4.1) and are on this basis interpreted to be part of a sub-aerial upper delta plain

environment. The environmental interpretation is further supported by to the presence of roots in the sandstones, and *in-situ* coal deposits directly overlying the sandstone beds.

- ii) The trough-cross stratified beds above 2 m thick are part of a 7 m thick multi-storey sandstone body observed near the top of the Skilvika Formation (Fig. 4.14 A). Due to its pronounced lateral-accretion sets (with epsilon cross-beds), thickness and fining upwards trend (Fig. 4.14 A), the deposit is classified as a meandering channel body (Gibling, 2006) with multi-storey channel bodies and banks which migrate. The presence of pronounced unidirectional sedimentary structures in the multi-storey channel body and the occurrence of the mineral *glauconite* (section 5.2.2) and marine-derived dinoflagellate cysts (Lenz, 2017) in the older fluvial sediments, may indicate either a transitional marginal-marine environment influenced by fluvial and marine processes or a drowned fluvial system. Deposition within a meandering system, which is later drowned due to a transgression, is a likely interpretation for the large channel body.



Figure 4.14: A: A large scale multi-storey channel body at the base of the Renardodden Fm., with person as scale. B: Low angle trough cross stratification as part of the multistorey channel deposit in (A) where ruler represents 30 cm. C: Trough cross stratified delta distributary deposit in the Skilvika Fm.

Facies 11 (F11): Plane-parallel stratified/laminated sandstone

Description

The facies occurs as continuous parallel laminations/stratifications (Fig. 4.15 B) or discontinuous laminations (e.g. Paola et al., 1989) in very-fine, very-fine to fine, fine, fine-to medium and medium sandstone throughout the entire stratigraphic unit. Individual lamina is characterised by normal grading and are topped by either an organic-rich or mudstone-rich interval. Coal fragments in individual laminae,

Ophiomorpha trace fossils and wave-ripple cross-lamination (Fig 4.15 A) are observed in places.

The laminations are observed in either isolated beds with sharp tops and bases, or as part of upwards-fining sandstone units. The isolated beds range from 10 cm to 90 cm in thickness, whereas the sections within upwards fining units range from 37 cm to 90 cm. The lamina is observed in dark grey sandstones which may be yellow/reddish due to rust stains, where the top of the individual laminae are dark brown to black in colour.

The facies is abundant in both the Skilvika- and Renardodden Formation and is therefore under and overlain by a large number of facies: Trough cross stratified sandstone (F10), structureless or faintly laminated sandstone (F3), mudstone (F7), unconsolidated siltstone (F5), sigmoidal cross-stratified sandstone (F9), bioturbated homogeneous sandstone (F12), highly bioturbated organic rich sandstone (F15) and sandstone with *Ophiomorpha* trace fossils (F13). Plane-parallel lamination also occurs within sandstone intervals in Facies 16: Heterolithics comprised of alternating sand, silt and mud.

Interpretation

Plane parallel lamination/stratification is produced by migration and deposition of sand under upper flow regime conditions where the currents have a high suspension load and fluctuate between smooth and rough flow. Experiments conducted by Paola et al. (1989) demonstrate that the superposition of laterally extensive parallel lamina is a result of turbulence induced frequent erosion and deposition, and migration of bed forms with low amplitude.

Two interpretations for this lithofacies can be suggested. Based on the occurrence of both cross-stratification and wave ripple-cross lamination in close association with the plane-parallel stratified/laminated sandstones in the succession, the plane-parallel stratification is interpreted to be influenced either by unidirectional currents in a i) continental regime (SUB FA 1.3) or ii) by strong oscillatory wave currents or combined currents in a shallow-marine setting (SUB FA 2.1, 2.2 and 2.3).

- i) The lamina that are under-and/or overlain by fine-grained floodplain deposits (F3 and F5) are usually present within upwards fining sandstone units and are interpreted to be part of channel deposits in a continental regime. Discontinuous parallel laminations are observed within crevasse splay deposits (F3, Table 4.1) and may be produced by sudden flooding events.
- ii) Due to the presence of *Ophiomorpha* trace fossils and wave-ripple cross-laminations within the sandstone units, these deposits are interpreted to be deposited in a high-energy upper to (mid) delta front environment. The presence of organic material in the form of coal draped laminations and/or coal fragments is indicative of an environment with high suspension load of sediments from the continental regime. Abundant terrestrial organic material has previously been found in slope deposits of a fluvial dominated delta system in Spitsbergen (Petter & Steel, 2006).

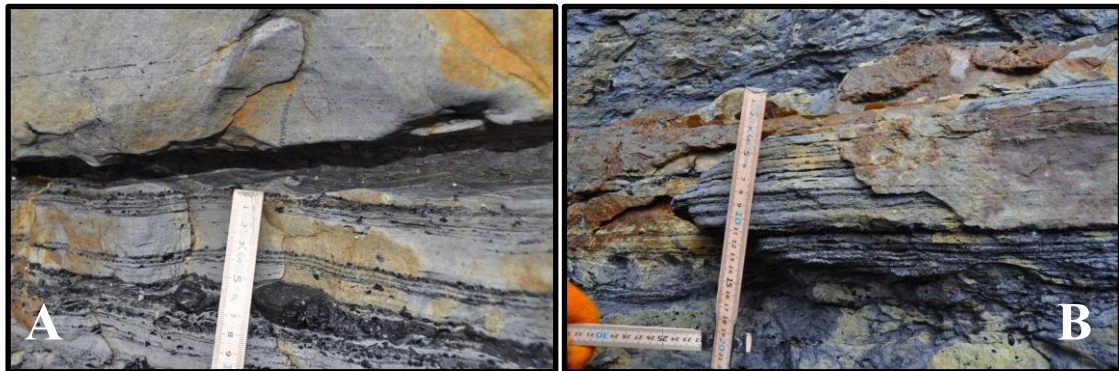


Figure 4.15: A: Organic draped plane parallel stratification and laminations with *Ophiomorpha* trace fossils, coal clasts and wave-ripple laminations B: Sandstone with organic draped plane parallel stratification. Both sandstones are near the top of the Renardodden Formation.

4.3.2 Facies association 2: Open marine depositional environment

Sub-associations that have been subject to marine processes include SUB FA2.1: Upper delta front deposits, SUB FA2.2: Middle delta front deposits, SUB FA2.3: Lower delta front deposits, and SUB FA 2.4: prodelta deposits (Table 4.2).

The majority of the deposits of the Renardodden Formation have been subject to marine processes, and FA 2 is therefore dominating this part of the investigated succession. The sediments are mostly composed of very-fine to fine sandstone, silt and some mudstone (F11, F12, F13, F14, F15, F16A&B, Table 4.1). A few conglomerate units are present near the base of the Renardodden Formation (F8B, Table 4.1). Coal fragments and bioturbation are abundant features in the sandstone units.

4.3.2.1. SUB FA 2.1: Upper delta front deposits

The following lithofacies are included within SUB FA 2.1 and are portrayed in the log in Fig. 4.16; **F8B**: Thick bedded gravel conglomerate with angular clasts, **F9**: Sandstone with sigmoidal cross-stratification, **F11**: Sandstone with plane parallel stratification, **F13**: Sandstone with *Ophiomorpha* trace fossils and **F12**: Bioturbated homogeneous sandstone (Table 4.1).

Based on the combination of lithofacies in the studied succession (Fig 4.16), the facies assemblage is interpreted as Upper delta front deposits. A number of indicators, which will be described in more detail under each lithofacies, point to this interpretation.

Fluvial processes (hyperpycnal flows) may interfere in the upper delta front, which has been the case for the granule-rich deposits of Facies 8B in the Renardodden Formation.

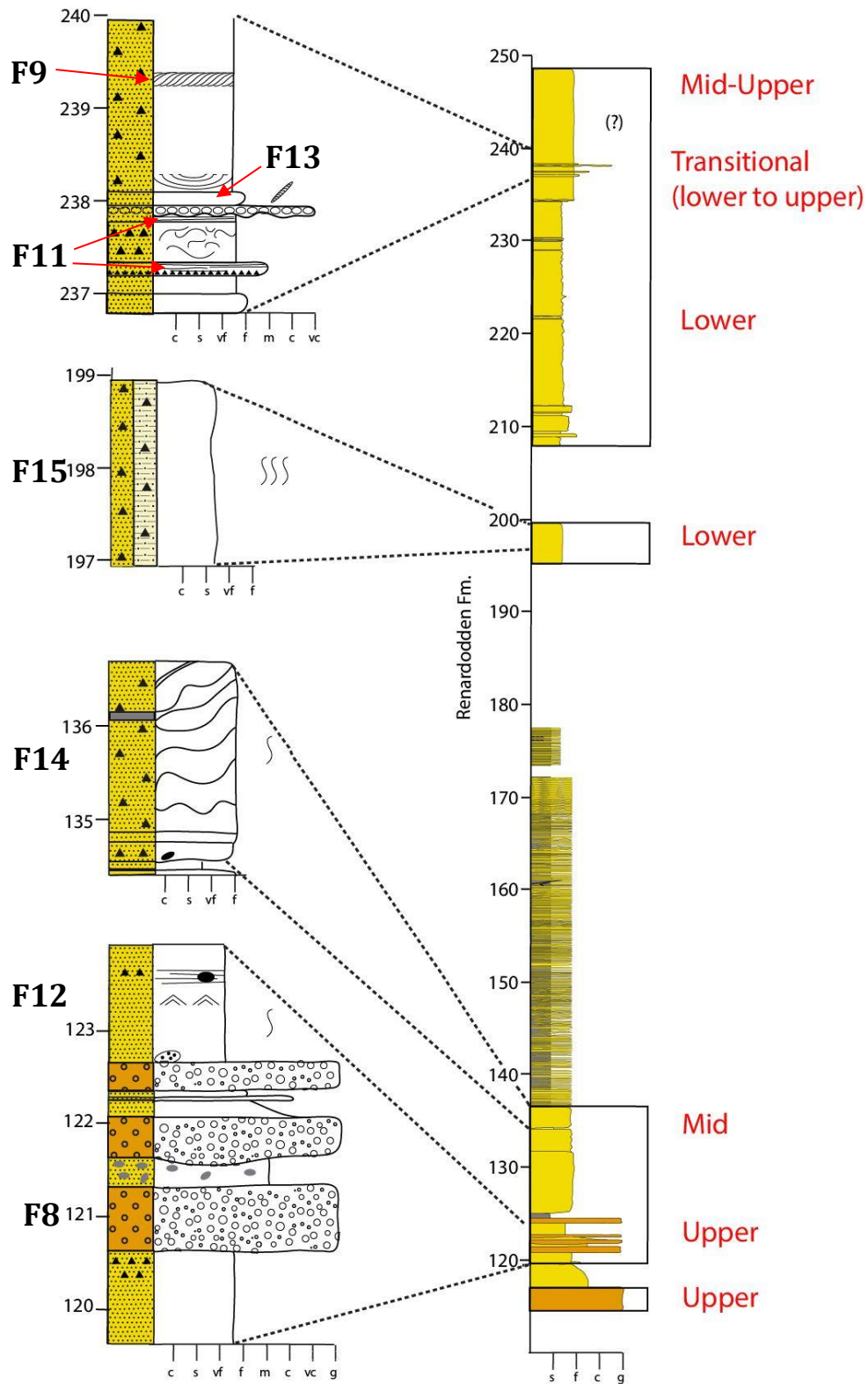


Figure 4.16: Composite log of the entire logged section of the Renardodden Formation displaying where delta front deposits (upper, mid and lower) (SUB FA 2.1-SUB FA 2.3) are present (black outline). Examples of each facies is shown on a lithostratigraphic log. Refer to legend in Appendix B.

Facies 8B (F8B): Thick bedded gravel conglomerate with angular clasts

Description

These conglomerates occur as poorly sorted unconsolidated granule-rich beds (Fig. 4.17). In addition to granules, the conglomerate contains occasional pebbles in fine and very-fine sandstone matrix. The clasts are composed of quartz, unconsolidated mud, mudstone and coal. In one conglomerate bed, very fine-grained sandstone lenses are present. Quartz and coal clasts are generally sub-rounded to rounded in shape, whereas the clay clasts have an angular shape. The beds are 30 cm to 220 cm in thickness and have sharp and distinct top boundaries, but the basal part is erosive to the underlying non-graded sandstone deposits. The conglomerate beds have a light grey matrix with milky white to beige quartz clasts, coal clasts and dark grey mudstone and clay clasts. The over- and underlying successions are composed of very-fine, medium and coarse sandstone units belonging to F12; Bioturbated homogeneous sandstone.

Interpretation

On the basis of their poor sorting and the angularity of the mudstone/unconsolidated mud clasts, the conglomerate beds are interpreted to be much more immature than the conglomerates belonging to the Skilvika Formation (F8A, section 4.3.1). The poorly sorted beds are interpreted as being deposited in an upper delta front environment during flood events where short transport from the source area is likely (due to the angularity of the clasts). Rounded quartz clasts are also present in the deposits suggesting several stages of transport and deposition of the sediments. A suggestion is debris flow deposits from high density underflows, where the mudstone/unconsolidated mud clasts are rip-up clasts from underlying marine shale. A study conducted by (Prior and Bornhold, 1989) from a submarine fan in British Columbia explained similar deposits of coarse sediments (including coarse gravel) suggested to be gravity flows, which were induced during flood events. The erosion of the underlying substrate may be caused by high density hyperpycnal flows as a result of their high energy (Petter and Steel, 2006).

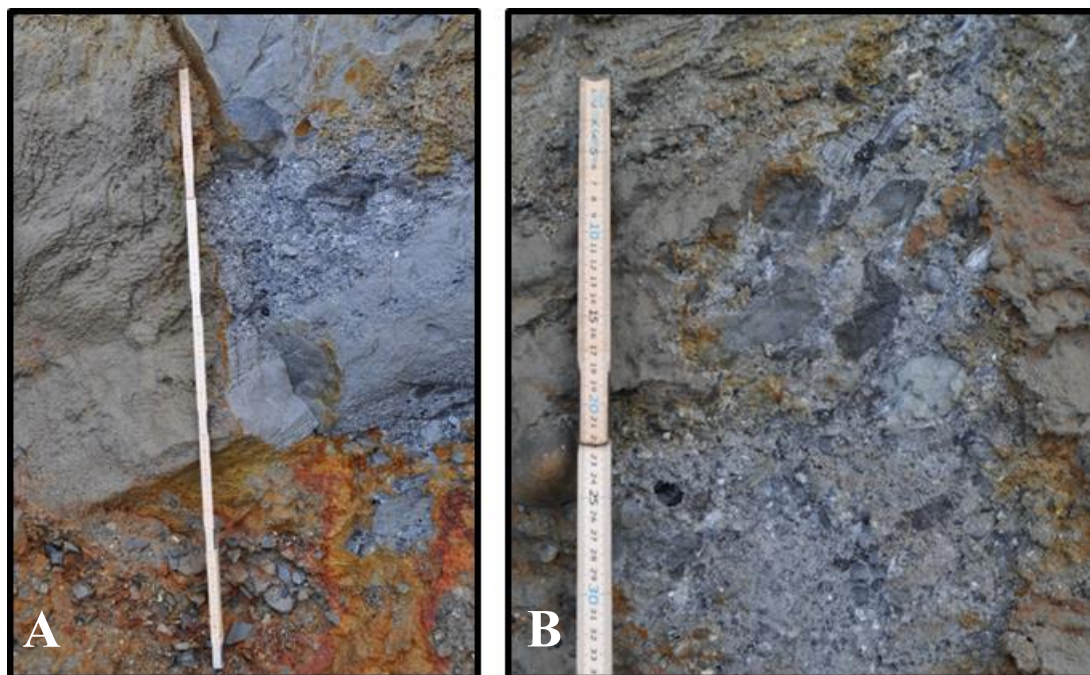


Figure 4.17: Unconsolidated immature debris flow deposits. Ruler represents 1 m in A.

Facies 12 (F12): Bioturbated homogeneous sandstone

Description

Bioturbated homogeneous very-fine and very-fine to fine tabular sandstone beds are observed near the base of the Renardodden Formation ranging in thicknesses from 3 cm to 200 cm. In addition, medium-, fine and a coarse-grained sandstone beds belonging to the same facies is observed between conglomeratic beds of F8B (Fig 4.17). Roots are observed in a 10-cm thick sandstone bed in the uppermost part of the facies unit. The lack of sedimentary structures, apart from some planar lamination and wave-ripple cross-lamination, suggests high degree of bioturbation in the sandstone. The thickest bed of the facies (upper part of Fig 4.18 A) shows no primary sedimentary structures and is highly bioturbated. Coal fragments are common, and a larger coal clast (4 cm in diameter) (Fig. 4.18B), a medium to coarse sandstone clast in addition to clay clasts are distinguished in the facies. Sharp tops and bases mostly bound the tabular sandstone beds, although some undulating and erosive boundaries are observed. Slight deformation in the upper part of the section is present.

The bioturbated homogeneous sandstone beds are over- and underlain by granule-rich conglomerate (F8B), mudstone (F7), very-fine to medium sandstone with sigmoidal cross-stratification (F9) and soft sediment deformed sandstone (F14).

The entire unit of the specific facies is underlain by sigmoidal cross-stratified sandstone, and terminated with the onset of deformed sandstone beds. The colour of the beds is light grey with reddish and orange oxidation stains.

Interpretation

Tabular conglomerates interfingered with sandstone with muddy drapes, in addition to well-rounded clasts are typical for nearshore deposits of clastic coasts (Fig 4.18) (Reading, 1996). On the basis of this, and the bioturbated sandstone beds, the deposits are interpreted to be beach deposits belonging to SUB FA 2.1: Upper delta front deposits and Mid delta front deposits of SUB FA 2.2. The slight deformation of the upper part of the facies show indication of wave reworking perhaps during storm events. The presence of roots in the uppermost part of the unit suggests a more nearshore environment and an overall regression throughout the unit from a mid-delta front environment to a upper delta front depositional environment.

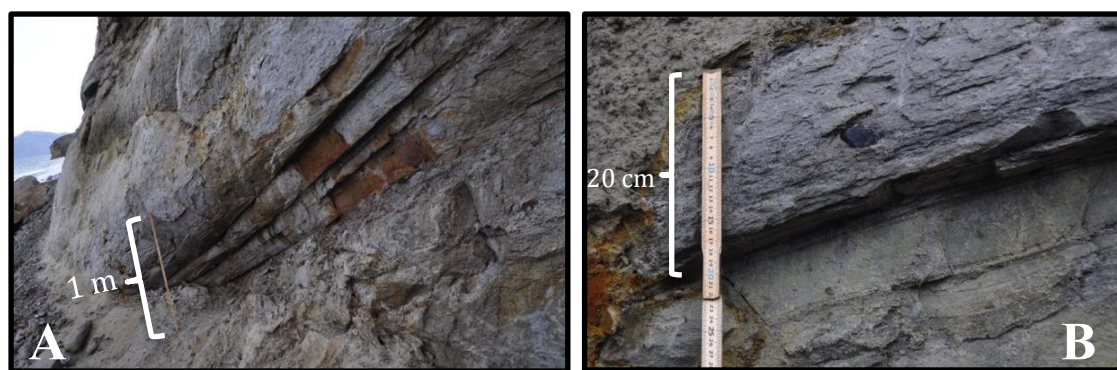


Figure 4.18: A: Tabular bioturbated sandstone beds near the base of the Renardodden Formation with B: muddy drapes and well-rounded coal clasts. Ruler represents 1 m in A and 28 cm in B.

4.3.2.2. *SUB FA 2.2: Mid delta front deposits*

The following lithofacies are included within SUB FA 2.2 and are portrayed in the log in Fig. 4.16; **F11**: Sandstone with plane parallel stratification, **F13**: Sandstone with *Ophiomorpha* trace fossils and **F12**: Bioturbated homogeneous sandstone and **F14**: Soft-sediment deformed sandstone (Table 4.1).

Based on the combination of lithofacies in the studied succession (Fig 4.16), the facies assemblage is interpreted as mid delta front. A number of indicators, which will be described in more detail under each lithofacies, point to this interpretation.

Deposits included within the middle part of the delta front zone are generally very-fine grained to fine-grained sandstone with little or no silt or mud content. The zone bounds to the upper delta front and to the lower delta front where finer grained sediments accumulate.

Facies 13 (F13): Sandstone with Ophiomorpha trace fossils

Description

The facies occur in very-fine to fine and fine-grained consolidated sandstones. Organic detritus and coal fragments are present. Trace fossils in the form of *Ophiomorpha* are observed in a 15 cm thick bed and in the uppermost 220 cm of the entire 148 m logged section. The burrows in the 15 cm thick bed are 5 cm to 10 cm long.

The burrows have dominantly a shaft configuration (Fig.4.19 A&C), although some Y-shaped regular mazes can be seen in the upper sandstone unit of the logged marine succession (Fig. 4.19 B) (e.g. Fig 2. Frey et al. 1978). A pelletal lining is a common feature for the shafts (Fig 4.19A), although some are smooth and elongated, and some shafts portray meniscoid laminae. The colour of the sandstones is light grey with yellow and reddish rust stains.

The 15 cm bed has sharp boundaries to underlying very coarse to granule- and iron-rich sandstone and overlying bioturbated organic rich sandstone (F15).

The burrowed sandstone in the 220 cm thick unit has an undulating lower boundary and appears to be erosional towards the underlying sandstone.

Interpretation

Due to the dominance of shafts in the facies, the sandstone is interpreted as having been prone to high-energy environments; boxworks and mazes will usually be more abundant in low-energy environments (Frey et al., 1978). Due to their mostly vertical shafts and pelletal lining, the burrows are interpreted to be *Ophiomorpha nodosa* (Fig. 1, Frey et al., 1978). *Ophiomorpha nodosa* is common in shallow-water deposits (Tchoumatchenco and Uchman, 2001) and are common globally in marginal marine and shallow marine environments (Nagy et al., 2016)

The sandstone containing *Ophiomorpha* is interpreted to be deposited in an upper delta front (SUB FA 2.1) and/or mid delta front (SUB FA 2.2) depositional setting. *Ophiomorpha cf. nodosa* and *Ophiomorpa cf. irregulaire* have previously been identified in lower parts (Paleocene) of the Central Tertiary Basin succession in Spitsbergen (Nagy et al., 2016).

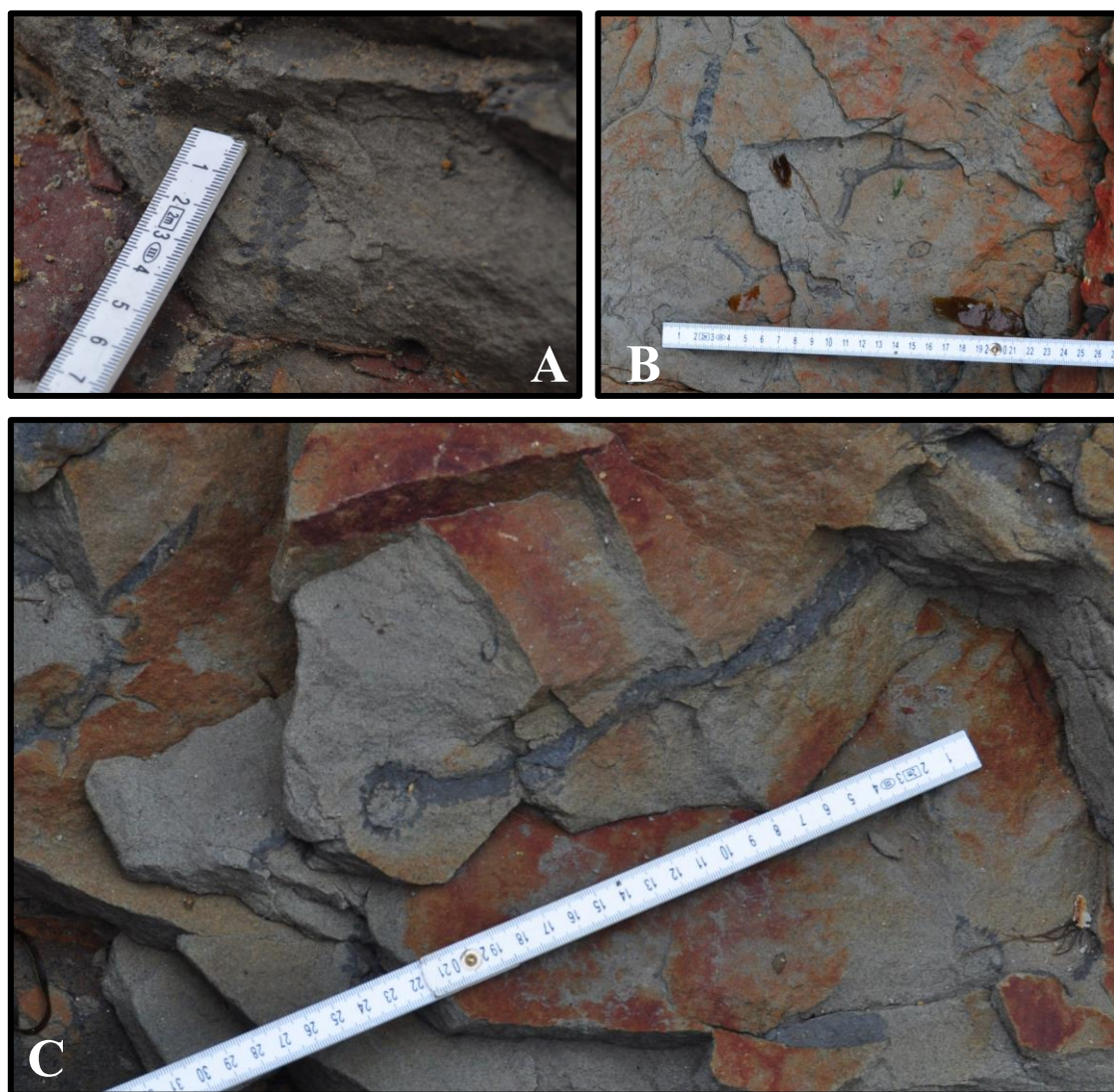


Figure 4.19: Ophiomorpha trace fossils in consolidated fine sandstone sections in the upper part of the Renardodden Fm. A: Pelletal lining on the shafts B: Y-shaped regular maze C: Trace fossil with a shaft configuration

Facies 14 (F14): Soft-sediment deformed sandstone

Description

The facies can be observed in a dominantly very-fine to fine-grained 215 cm thick sandstone unit. The sandstone unit is divided into thinner beds ranging from 10 to 40 cm in thickness, where the average thickness is 15 cm. These thinner beds portray sharp bed boundaries to each other, and the top of the unit is distinguished by an erosional boundary. Some silt with coal fragments is observed between sandstone beds within the unit. Coal fragments and bioturbation (*Skolithos* burrows) can be distinguished in the sandstone.

The basal 70 cm of the unit is composed of beds planar to one another and shows little deformation. Overlying these, there is pronounced deformation in the northeastern part of the outcrops, whereas the outcrops towards the southwest show little deformation and include tabular, planar beds (Fig. 4.20). In the top metre of the unit, there is pronounced soft-sediment deformation throughout the whole section. The unit is overlain by heterolithic alternating silt, mud and sand (F16A), and underlain by a silt-rich coal seam (F2). The sandstone unit is light grey with reddish and orange oxidation stains. *Teichichnus* trace fossils was observed *in-situ* whereas *macaronichnus* trace fossils was observed in loose sandstone blocks immediately beneath the outcrop.

Interpretation

Due to the presence of *in-situ* *Teichichnus* and possibly *Macaronichnus* in the facies, one may assume that the base of the facies represents a flooding surface or a rapid transgression from the underlying F12 displaying root growth. *Teichichnus* is common in shallow-marine environments (Knaust, 2017).

The deformed sandstone beds are interpreted to be mouth bar deposits and deposited in the delta front of a fluvial dominated, storm-wave influenced delta. The delta front deposits form part of a deltaic succession, which are overlain by a transgressive surface with prodelta heterolithics (Bhattacharya, 2010).

A trigger, for instance fluctuations in pressure due to storm waves, is required in order to change the state and thereby cause deformation of a material (Owen, 1987). There may be several causes for the deformation. Storm waves are active in the upper delta front region, making waves a likely candidate to trigger the specific type of deformation. Soft-sediment deformation occurred soon after deposition, with storm waves interacting with partly unconsolidated sediment.

An alternative interpretation for these deposits are lower delta front sediments similar to those exposed in the Karoo mixed-delta system, and described by Jones et al. (2013). In such a scenario, the beds would have been deformed *in-situ* by loading, resulting in the vertical movement of fluids and sediment (Jones et al., 2013).



Figure 4.20: Soft sediment deformed sandstone with pronounced deformation in the upper meter of the unit. Ruler is 1 m.

4.3.2.3. SUB FA 2.3: Lower delta front deposits

The following lithofacies is included within SUB FA 2.3 and are portrayed in the log in Fig. 4.16; **F15:** Highly bioturbated organic rich sandstone and **F11:** Sandstone with plane parallel stratification (Table 4.1).

Based on the combination of lithofacies in the studied succession (Fig 4.16), the facies assemblage is interpreted as floodplain deposits. A number of indicators, which will be described in more detail under each lithofacies, point to this interpretation.

The lower delta front region encompasses fine-grained sand with increasing amount of silt for sediments deposited deeper into the basin. The deposits are organic-rich and display high amounts of bioturbation. The zone transitions into the middle delta front proximally and distally into the prodelta.

Facies 15 (F15): Highly bioturbated organic rich sandstone

Description

Consolidated or unconsolidated bioturbated very-fine to fine and silty to very-fine sandstone is present near the top of the Renardodden Formation with units in the range

of 30 cm to 10.5 meters in thickness. This part of the succession is poorly exposed, inhibiting detailed thickness measurements. The lowermost unit is more fine-grained than the upper part and is composed of fine-grained sediments including silt and very fine sand. Otherwise, the facies is composed of sandstone and organic matter. Large sand concretions (Fig.4.21 A) and well-rounded coal clasts are abundant throughout the whole facies. Small coal draped laminations/horizons (Fig 4.21 B) are present as well as plane parallel lamination. A scouring structure and loading into the underlying bed is observed in the uppermost part of the facies unit. Yellow weathering cracks are abundant features in the facies. Fine and very-fine to fine sandstone layers with less organic material are occasionally observed. Coal fragments are abundant and are concentrated in layers that are 5-10 cm thick (Fig 4.21 C). The colour of the facies is dark grey with reddish oxidation stains, where the weathering cracks are beige to light yellow.

The bioturbated organic rich sandstone units are under-and overlain by very-fine to fine and fine sandstone beds, coal fragment layers, sandstone with plane parallel stratification (F11), very fine to fine sandstone with sigmoidal cross-stratification (F9) and sandstone with *Ophiomorpha* trace fossils (F13).

Interpretation

Due to the high sand content and the abundance of organic material including coal clasts and fragments, these deposits are interpreted to have derived from a fluvial dominated delta according to the coastal system classification of Reading (1996). A system dominated by large sediment supply from the alluvial environment is likely to include large quantities of organic material and large coal clasts, not only on the delta plain, but also in the open marine environment. The facies is interpreted to have been deposited on the lower delta front within a fluvial dominated, storm-wave influenced delta system (Bhattacharya, 2010).

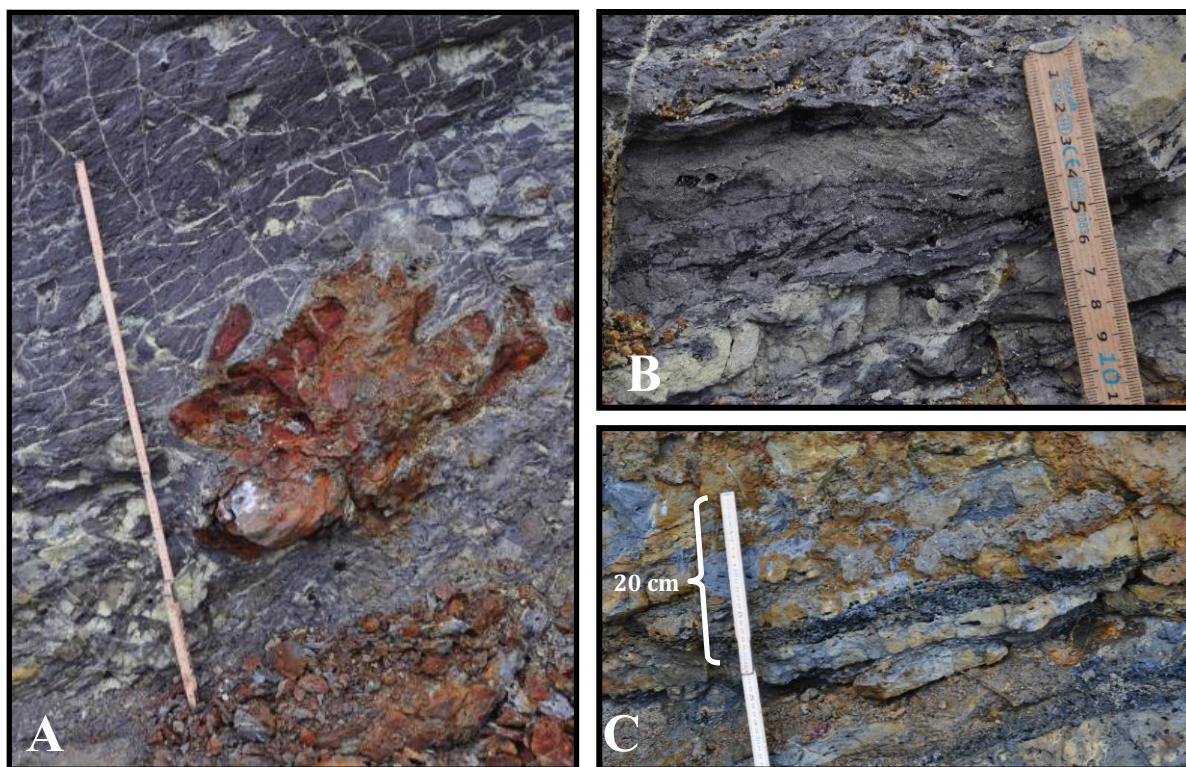


Figure 4.21: Bioturbated organic rich sandstone with yellow weathering cracks A: Large iron-rich sandstone concretion. Ruler represents 1 m. B: Small organic-draped laminations. C: Coal fragment layer

4.3.2.4. SUB FA 2.4: Prodelta deposits

The following lithofacies is presented in the text and are portrayed in the log in Fig. 4.22; **F16(A+B):** Heterolithics comprising alternating sandstone, siltstone and mudstone.

Based on the combination of lithofacies in the studied succession (Fig. 4.22), the facies assemblage is interpreted as prodelta deposits. A number of indicators, which will be described in more detail under each lithofacies, point to this interpretation.

As observed in the deposits at Renardodden, the prodelta region has increasing amounts of bioturbation and finer-grained sediments compared to the delta front. The prodelta region transitions proximally to the lower delta front region.

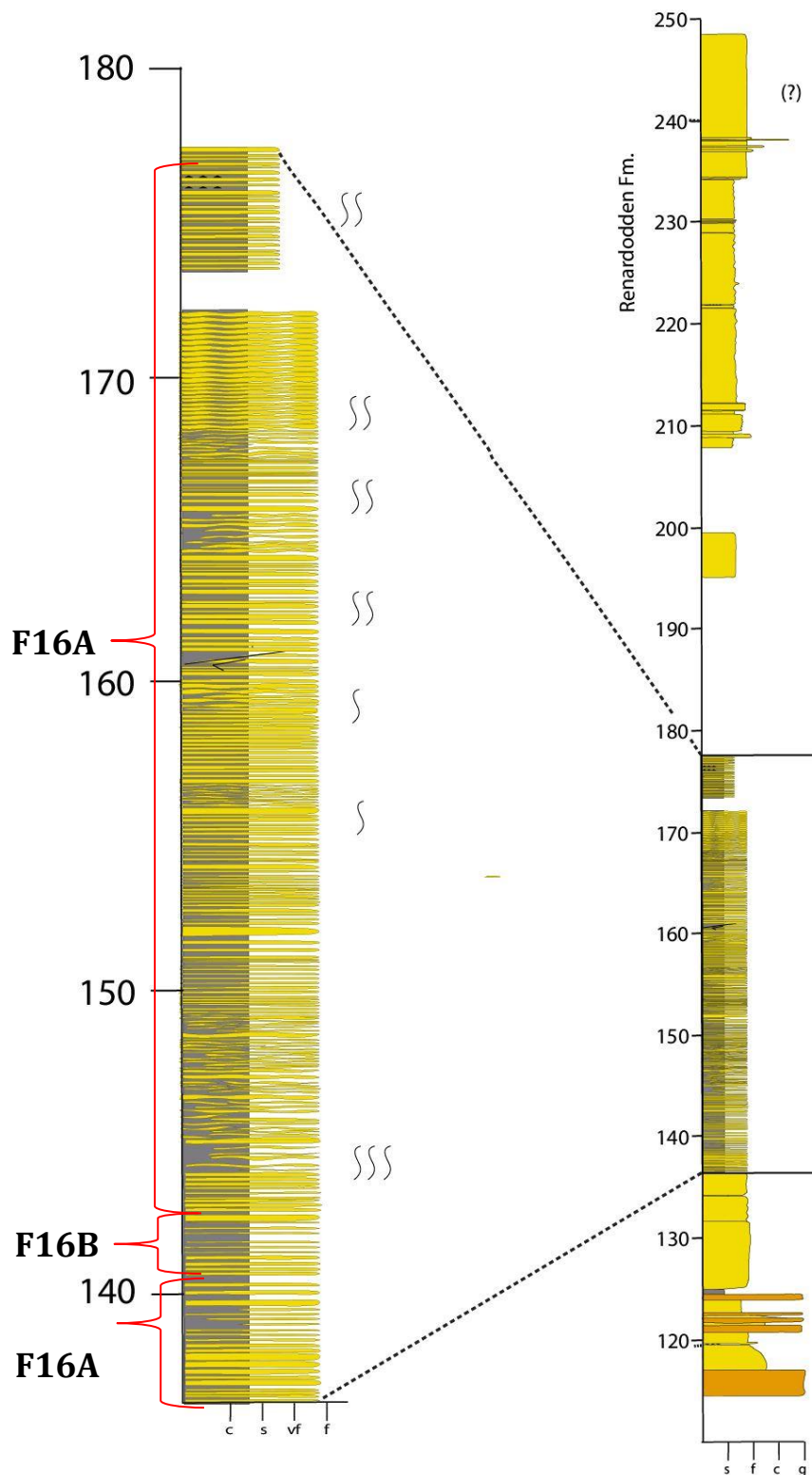


Figure 4.22: Composite log of the entire logged section of the Renardodden Formation displaying where prodelta deposits (SUB FA 2.4) are present (black outline). Examples of each facies is shown on a lithostratigraphic log. Refer to legend in Appendix B

Facies 16 (F16): Heterolithics comprising alternating sand, silt and mud

The facies is divided into two sub-facies based on the continuity of beds and the degree of bioturbation:

Facies 16A: Heterolithics comprising alternating silt, mud and sand

Facies 16B: Highly bioturbated heterolithics comprising alternating shale and silt/sand

Description

Facies 16A (Fig 4.23 A) is observed in the Renardodden Formation and is composed of alternating continuous beds of dark grey silt-and mudstone and light beige to grey very-fine to fine sandstone, where the ratio of sand/silt-mud ranges from 10-90 to 90-10. The sandstone beds range from 0,5 cm to 27 cm in thickness, whereas the siltstone/mudstone beds range from 0,5 cm to 50 cm. The beds are tabular and continuous with sharp or undulating top and base boundaries. Coal fragments are abundant in the sandstone intervals, and organic detritus in addition to quartz pebbles are also observed. Burrows, planar-parallel laminations, organic draped laminations, wave ripples and slight discontinuous bedding is observed in some of the sand-rich beds.

The facies unit is underlain by soft sediment deformed sandstone (F14) and overlain by a gap, but it is assumed that the organic-rich bioturbated sandstone (F15) may directly be overlying the heterolithic unit due to the large gap present between the two facies. Throughout the heterolithic unit, beds rich in coal fragments and sandstone concretion layers are observed. The facies show mostly normal graded beds within the heterolithic deposits. Two faults cut the facies and a distinct drag affecting heterolithic layers are observed near one of the fault boundaries.

Facies 16B (Fig. 4.23 B) is an approximately 200 cm thick unit occurring as a separate body within Facies 16A which is distinguished based on the presence of discontinuous bioturbated beds of shale and silt/sand. Shale is the dominating lithology with a ratio of 80-20 relative to sand/silt. Organic material is abundant and organic detritus including coal granules are present. Plane-parallel lamination and wavy geometry of

bedding is observed, as well as bioturbation in the form of *Skolithos*-type burrows. Due to the discontinuity of internal sandstone layers, the sandstone and mudstone layers in the facies are difficult to measure individually. The unit is under- and overlain by heterolithics comprising alternating silt, mud and shale (Facies 16A). The colour of the facies is mostly dark grey, sands are light beige with red and yellow oxidation stains. Some areas have a greenish colour

Interpretation

Heterolithic deposits are typical for prodelta sediments in a fluvial dominated delta (Bhattacharya, 2010), but can be found in several different environments. The heterolithic sediments are interpreted as deposits of the prodelta region due to their high content of mud, very-fine to fine grained sand, bioturbation and normal grading resembling turbidites. The stratigraphic context of the underlying (older) deposits where an overall transgression is observed, also suggests a gradual transition into a more distal environment. The alterations of silt, mud and sand are a result of fluctuations in sediment input from the coast in combination with fluctuations in current strengths. Finer material will be deposited during periods of still stand, whereas coarser material is suggested to be deposited as a result of large sediment loads brought down the delta slope by gravity flows initiated by floods (such as turbidity currents). Normal or inverse grading in the deposits indicate deposition as a result of hyperpycnal density underflows discharged under floods and storms (Bhattacharya, 2010). Similar occurrences of sharp-based sandstones, siltstones and mudstones are found in a prodelta turbidite succession from the Lower Kenilworth Member of the Book Cliffs in Utah. Similarly, these deposits have been interpreted as being derived from a storm-influenced delta system (Pattison, 2005).

The greenish colour that characterises parts of Facies 16B, may be an indication of the presence of glauconite. This has been confirmed in thin section (Chapter 5, section 4.2.2). Due to the high mudstone content, and assumed high amount of bioturbation due to reworked and discontinuous internal layers, F16B is interpreted to be deposited deeper in the basin than F16A. Thus, they mark the deepest deposits in the entire succession.

The coal fragment layers in the Renardodden Formation are transported fragments from the alluvial system. Transportation has occurred during periods of high sediment input to the coast with deposition of coal fragments in concentrated layers in deeper waters. Thus, such coal fragment layers are present within sediments deposited in the deeper basin such as heterolithic sediments (F16, Table 4.1) and bioturbated organic rich sandstone (F15, table 4.1).

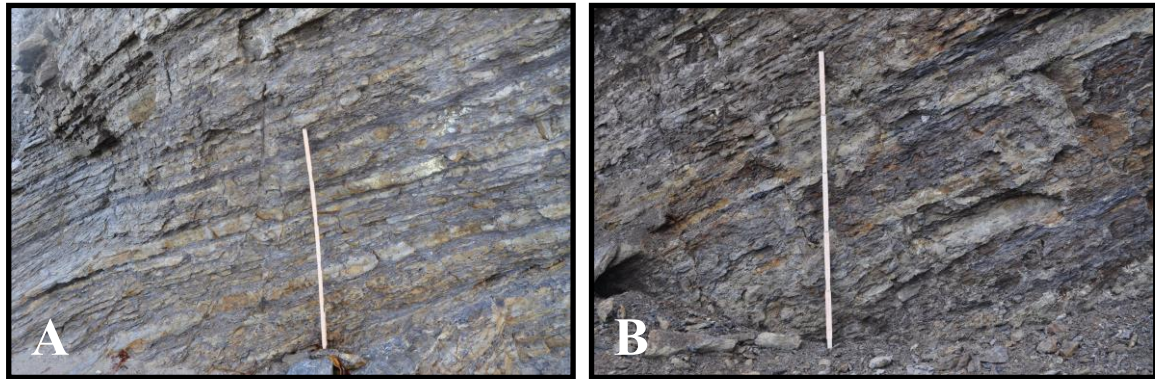


Figure 4.23: A: facies 16A: Heterolithics comprising alternating silt, mud and sand. B: facies 16B: Highly bioturbated heterolithics comprising alternating shale and silt/sand. The ruler represents 1 m in both photographs.

5. Petrography

The following study includes in-depth analysis of the facies, through thin-section analysis of the samples through a light microscope and a scanning electron microscope (SEM) and RAMAN microscope. 13 samples were analysed from the studied outcrops, 7 samples from the Skilvika Formation and 6 samples from the Renardodden Formation (Appendix B). Textural and compositional analyses were conducted, in addition to point counts of framework minerals and matrix to determine the sedimentary rock type. Classification was determined by comparing composition of framework constituents of quartz, feldspar and rock fragments to the amount of matrix using Dott's (1964) modified classification of sedimentary rocks (Fig 5.11). Analyses and comparisons were based on arranging the samples into lithofacies and depositional environments (Table 5.1). It is important to note that 13 samples are not sufficient enough to obtain accurate values for all the sediments in the entire studied outcrop. This study focuses on the general trend in the facies and hence environmental interpretations to be able to link the observations to the outcrop observations of the facies.

Table 5.1. Summary of the samples analysed and their subsequent facies and depositional environments.

Depositional environment	Thin section sample number	Lithofacies
(?)Continental slump deposit	2.1	F1
Floodplain	2.2	F4
	2.8	F6
	2.10	F3
Distributary channel fills	2.3	F10
	2.5	F8
	4.1	F11
Upper delta front	4.5	F12
	4.10	F11
	4.11	F13
Mid delta front	4.3	F14
Prodelta	4.2	F16
	4.6	F16

5.1 Textural analysis

Analyses were conducted through determining the textural properties; roundness (Fig 5.2), sphericity (Fig 5.1), fabric, grain size (Appendix A) and sorting (Fig 5.3) in order to compare the samples and hence the corresponding depositional environments.

All samples, apart from two, are grain supported and are predominantly composed of grains above 0.03 mm in diameter. Sample 2.10 and 2.8, which are both interpreted to be part of the floodplain environment, are matrix-supported and calcite cemented respectively. 77.7% of the total composition in sample 2.10 is composed of matrix (less than 0.03 mm (Dott, 1964)) and 54,7% of sample 2.8 is supported by pore-filling calcite cement.

Sphericity (Fig 5.1), roundness (Fig 5.2) and degree of sorting (Fig 5.3) are classified according to depositional environments. The floodplain system includes grains with

varying textural characteristics, which have low-moderate to high sphericity, are subangular to subrounded with moderate to well degree of sorting. Samples from distributary channel fills and the open marine environment (delta front and prodelta) have moderate and high sphericities, subrounded to rounded grains and are moderately (distributary channels) to well- sorted (marine environment).

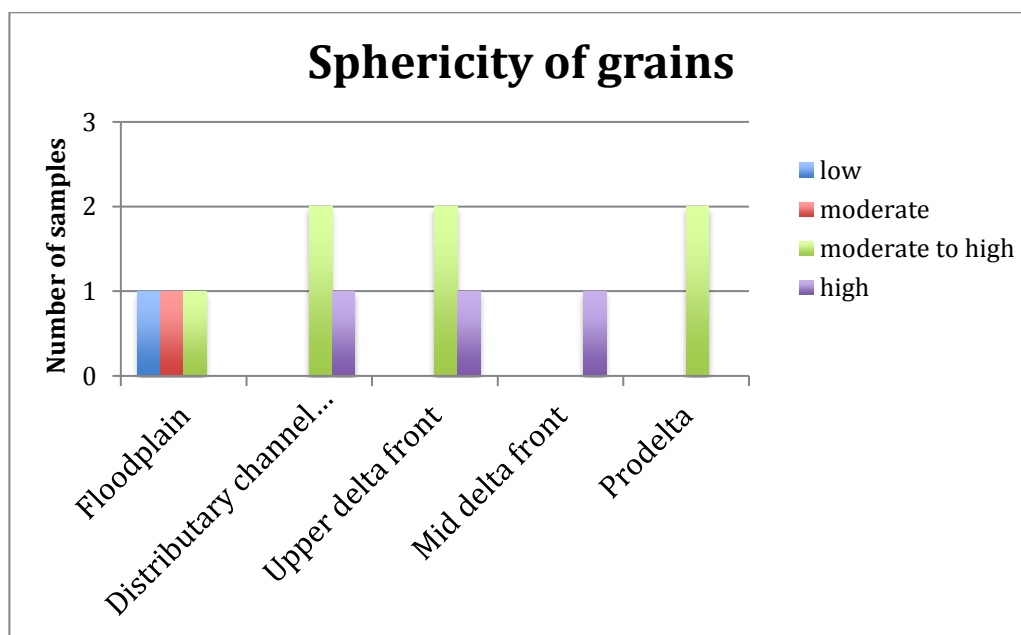


Figure 5.1: Measure of grain sphericity, subdivided on the basis of depositional environments

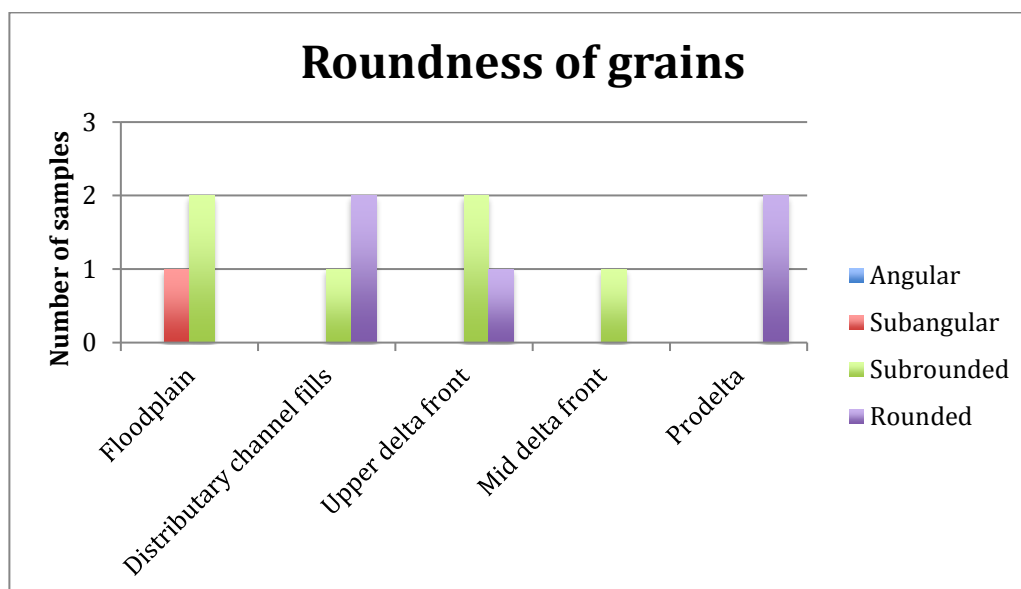


Figure 5.2: Measure of the roundness of the grains, subdivided on the basis of depositional environment

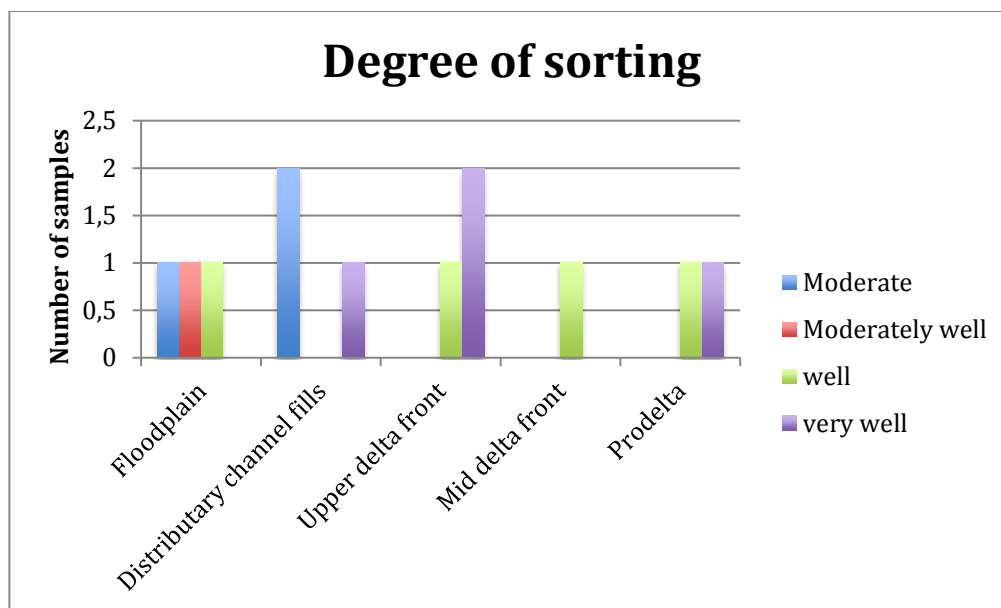


Figure 5.3: Measure of the sorting of the grains in the samples, subdivided on the basis of depositional environments

5.2 Composition

Modal analyses were conducted through 300 point counts per sample on a Nikon Eclipse LV100 POL light-microscope with 10x10 optical zoom where results are presented in Table 5.2. Framework grains including quartz, feldspar, mica and rock fragments in addition to authigenic minerals, organic fragments, cement and matrix are counted. Primary and secondary porosity were also differentiated. Primary porosity is the original intergranular pore space created during lithification of the rock, whereas secondary porosity presents pore space formed through removal of previously deposited grains through dissolution.

Table 5.2. Summary of the samples studied and their subsequent facies and depositional environments

Sample number	Framework minerals			Authigenic minerals							Organic detritus	Matrix	Porosity		
	Quartz	Feldspar K-feldspar	Plagioclase	Rock fragments	Mica	Heavy minerals	Glauconite	Calcite cement	oxide cement (organic, pyrite)	Spiculite			Chlorite	Primary porosity	Secondary porosity
2.1	60	-	-	-	38.7	0.3	-	-	-	-	-	1	-	-	-
2.2	64.7	0.7	1	9	1	0.3	-	-	5.3	-	0.7	0.3	8.7	3.3	5
2.3	67	1	-	8.3	2.3	-	-	-	3.7	0.3	-	1.3	7.7	4.7	3.7
2.10	13.3	-	-	-	0.7	3.3	-	-	-	-	-	5	77.7	-	-
2.5	68	11.7	0.3	8.4	1.7	0.6	0.3	-	1.0	-	-	-	4	1.3	3.0
2.8	30.3	9.3	0.3	-	0.3	4	0.3	54.7	2.7	-	-	0.3	-	-	-
4.1	64.3	2.3	-	3	0.3	1.3	-	0.3	6	-	-	0.7	5.7	12.3	3.7
4.5	58.3	3.7	1.3	9.7	-	1.4	0.3	-	3.7	-	-	1.3	4	8.7	7.7
4.3	51.3	7.7	0.7	4.6	-	1.2	-	-	5.3	-	0.7	1.3	11.3	11.7	3.7
4.6	61.3	3	0.7	4	-	2	-	-	4	-	-	1.3	7	15.6	1
4.2	46.7	5.7	0.7	3.6	0.3	1.5	-	-	4.0	-	-	18.3	6.0	10	2.7
4.10	50.3	11	0.3	6.3	0.3	1	-	-	3.7	-	-	10	7	7.7	2.3
4.11	54.6	6.3	0.3	7.6	0.3	3.3	0.3	-	4.7	-	-	0.3	6.0	13.3	2.7

5.2.1 Framework constituents

The framework grains in the analysed thin sections are quartz (monocrystalline and polycrystalline), feldspar (alkali feldspar and plagioclase), rock fragments, mica and heavy minerals. Quartz is the most abundant framework mineral in the thin sections and constitute over 50% in 9 out of the 13 samples. Rock fragments and feldspars are more abundant than micas whereas heavy minerals are subordinate.

Altered quartz and alkali feldspar may be difficult to distinguish in the light microscope due to absence of twinning in the feldspars. The RAMAN microscope and SEM microscope were used to differentiate between the two. A line scan was drawn through each thin section in the SEM microscope and a general measure of the proportions of each mineral were used to quality control the point counts in order to classify the rock on more accurate terms.

Quartz appears in all the samples as mono-, poly- (Fig.5.4 A) or microcrystalline grains (detrital chert) (Fig 5.4 B). Quartz is characterised based on its undulatory extinction, first-order birefringence, low relief and absence of pleochroism. In several samples, the quartz grains are fractured and altered where secondary fluid inclusions in the form of vacuoles are observed. Polycrystalline quartz is observed displaying elongated grains with sutured contacts or as grains without sutured internal grain boundaries.

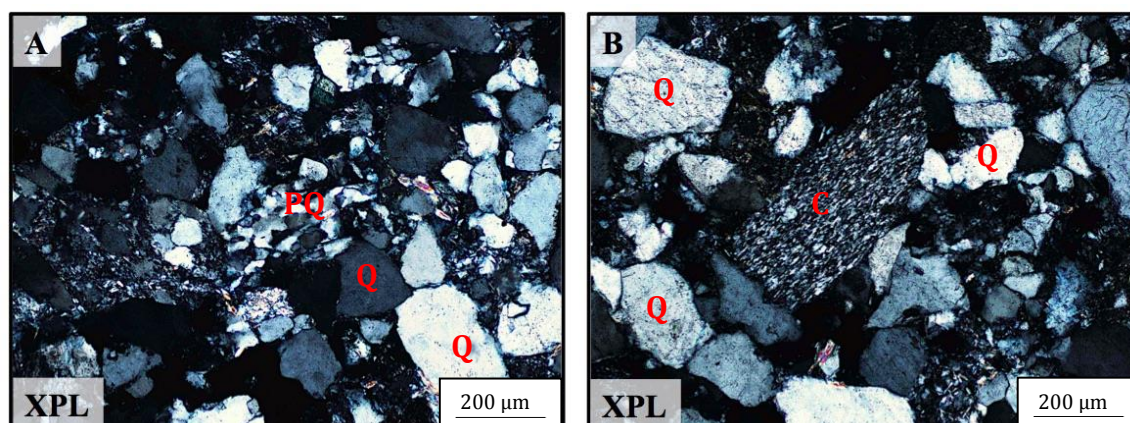


Figure 5.4: : A) Grain constituents of Polycrystalline quartz (PQ) with elongated quartz crystals, surrounded by monocrystalline quartz grains (Q) B) A Chert (C) fragment

Feldspar is observed as both alkali feldspars and plagioclase in the studied thin sections,

where the SEM scanlines revealed that alkali feldspar is more ample than plagioclase. Feldspars are distinguished based on their low relief, first-order birefringence colours and absence of pleochroism. Some of the feldspars are highly fractured and some have secondary alteration through reaction with aqueous fluids, in the form of sericitization of feldspar to muscovite. In a light microscope, plagioclase is more pronounced and easily identifiable due to its characteristic albite twinning (Fig 5.5 B) in cross-polarized light (XPL). The K-feldspar microcline is also easily identified due to the presence of tartan twinning, which are polysynthetic twins in two directions (Fig 5.5 A) (Ulmer-Scholle et al., 2014).

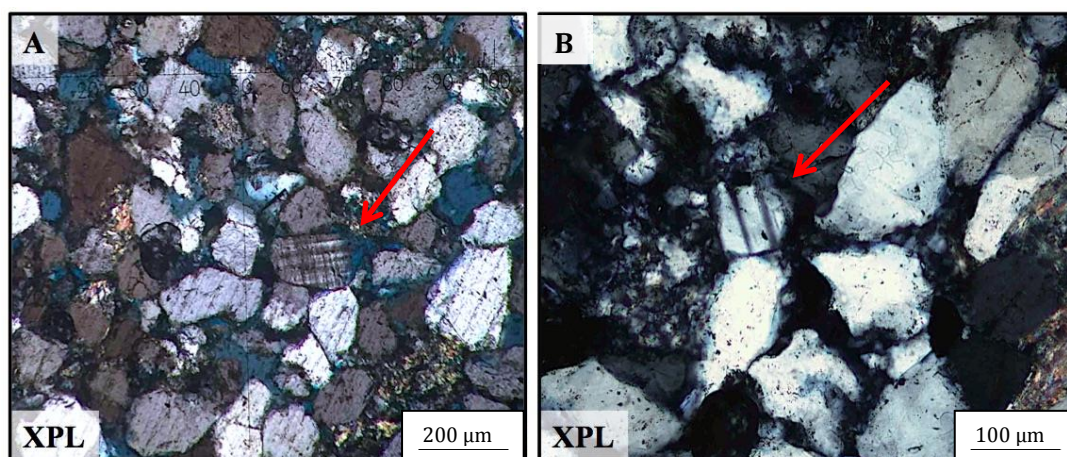


Figure 5.5: A) Microcline feldspar displaying cross-hatched twinning. B) Plagioclase feldspar with polysynthetic twins in the form of albite

A large variety of rock fragments with differing origins have been observed in the studied samples. Skeletal silica- rich fragments are observed in a fining upwards trough-cross stratified sandstone in the Skilvika Formation displaying an abundance of spiculite (Fig 5.6A). Chert (Fig 5.4 B), in addition to ductile shale rock fragments and siltstone rock fragments are identified to be of sedimentary origin, whilst crenulated mica-rich shale rock fragments are identified to be of metamorphic origin. This classification is mainly based on the assumption that the shale rock fragments of sedimentary origin have no preferred orientation and are highly ductile, whereas the micas in the metamorphic rock are well-foliated (Ulmer-Scholle et al., 2014). The ductility of shale rock fragments and micaceous rock fragments can make them challenging to distinguish from pseudomatrix. Shale rock fragments and micaceous rock fragments are therefore considered matrix constituents in the final classification (Table 5.3). The term pseudomatrix was first introduced by Dickinson (1970) and is

explained as a interstitial paste that is discontinuous and has formed as a result of the deformation of ductile rock fragments.

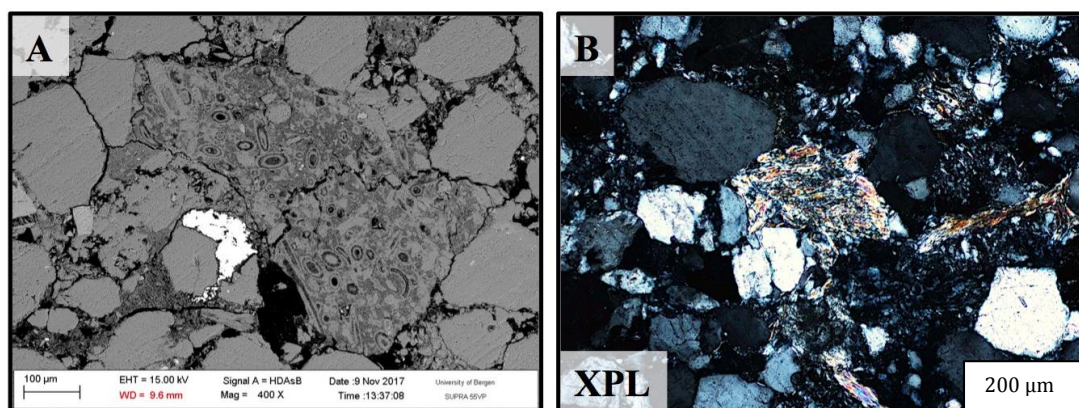


Figure 5.6: A) Backscattered image from the scanning electron microscope (SEM) displaying a spiculite-rich skeletal fragment from a sublitharenite B) A slightly crenulated well-foliated rock fragment with a metamorphic origin

Other framework minerals identified in the thin sections include the light micas: muscovite, biotite, phlogopite and chlorite (Fig 5.7A-B), in addition to the heavy minerals: chloritoid, rutile, zircon, epidote, tourmaline, monazite and apatite (Fig 5.7C-F). Mica is present in all the samples whereas the heavy minerals are subordinate. The SEM-microscope was helpful in identifying several of the heavy minerals as they will have a lighter colour in the backscatter image and are therefore easily identifiable. Zircon, tourmaline and chloritoid are especially abundant and are observed in 11/13 (85%), 11/13 (85%) and 9/13 (69%) of the samples respectively.

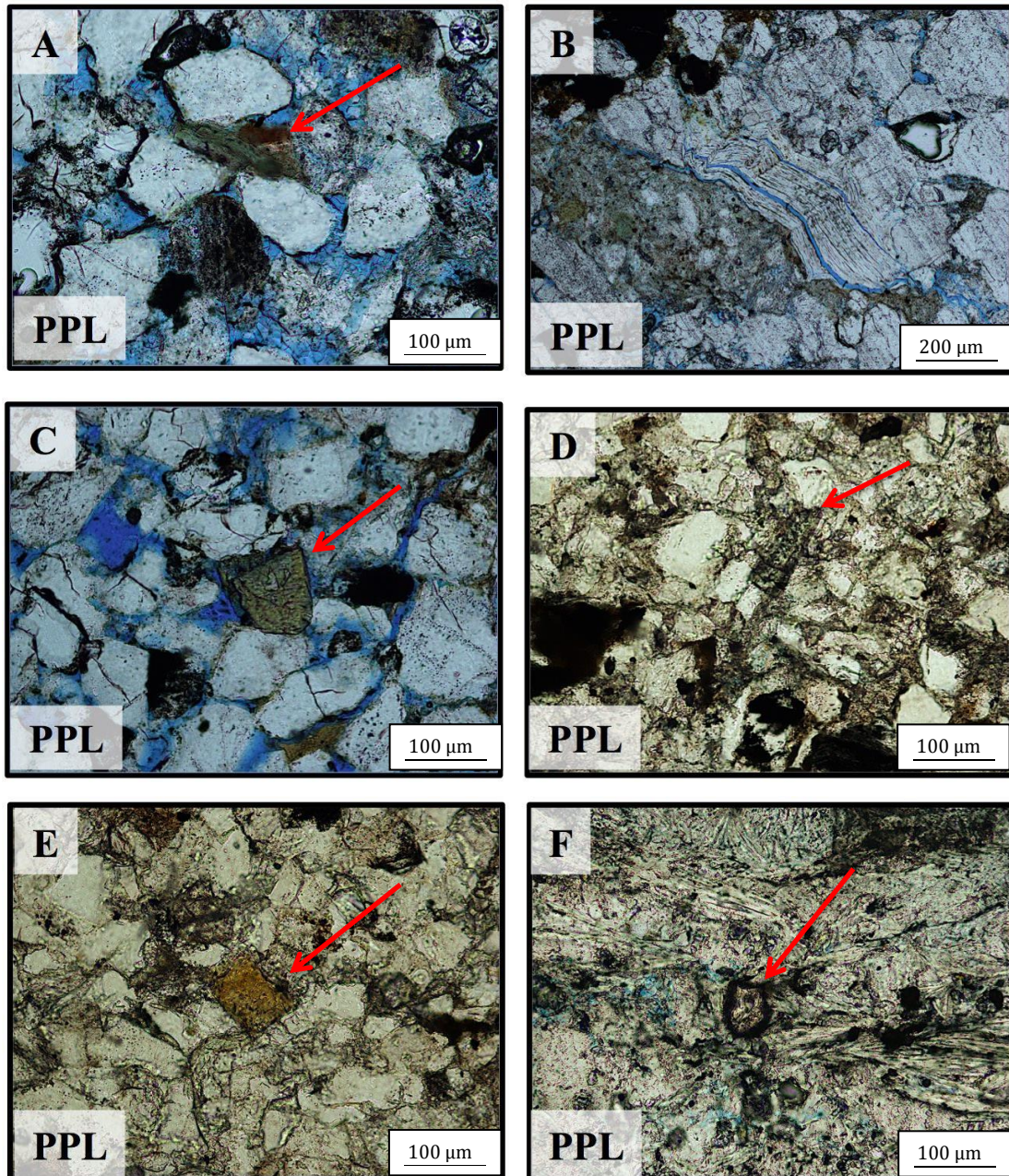


Figure 5.7: Micas and heavy minerals from the studied samples taken through plane polarized light (PPL) in a light microscope. A) Authigenic chlorite as a replacement mineral for biotite. B) A crenulated muscovite grain C) Epidote grain with a light brown pleochroism and well-developed cleavage D) An elongated chloritoid grain portraying cleavage and a slight blue pleochroism E) Tourmaline indicated by a bright yellow pleochroism E) A rounded Zircon grain surrounded by mica grains portraying a very high relief.

5.2.2 Diagenetic minerals

Glauconite

Distribution:

Glauconite is present in 8 (61,5%) of the studied samples, where 4 are from the fluvial Skilvika Formation and 4 from the marine Renardodden Formation. Of the samples from the Skilvika Formation, glauconite is found in samples from the floodplain environment (Fig 5.8) and from distributary channels and infills. The phyllosilicate clay mineral is characterised based on its light-to olive green pleochroism and the generally small grain size of less than 1 mm wide (pers.comm Walderhaug, 2017). The aggregates are subrounded to rounded and often have graphite inclusions.

Origin:

Glauconite is a syngenic to diagenetic clay mineral in marine sediments and commonly appears in sandstones (Pichler and Schmitt-Riegraf, 1997). Oceanographic surveys depict that the sheet silicate forms at the boundary between the ocean floor sediments and open water, between 60- 500 m under the water surface (Wilson et al., 2013). It is commonly formed on continental shelves, but has also been found on greater depths on subsided submarine highs and active margins (Odin and Matter, 1981). Glauconitization favors pH values that are slightly alkaline (between 7-8) and a mildly reducing to mildly oxidizing oxidation reduction-potential (Eh conditions) (Wilson et al., 2013). Due to the turbulency and oxidizing Eh-conditions of shallow waters, formation of glauconite is not favored in shallow waters below 50 meters (Odin and Matter, 1981).

Odin and Matter (1981) states that a marine transgression, where detrital near-shore sediments are submerged, is a favorable setting for the formation of glauconite.

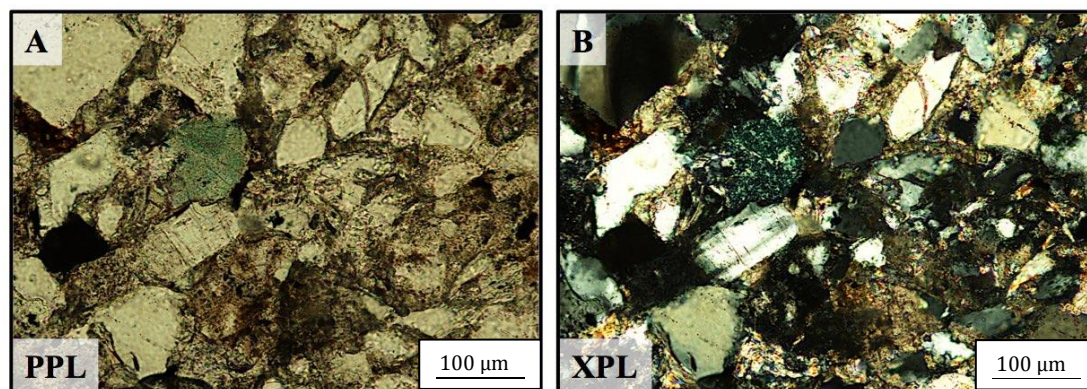


Figure 5.8 A subrounded glauconite grain from sample 2.8 (floodplain environment) in PPL (A) and XPL (B).

Pyrite

Distribution:

Through analyses in the SEM microscope, pyrite is detected as small spherical framboids, in close association with organic detritus (Fig 5.9) and as iron oxide cementation bounding framework grains. Pyrite is observed in samples derived from the marine depositional environment (Renardodden Formation), although the cementation is also observed in a sample from a distributary channel system in the Skilvika Formation. The iron oxide cementation and framboids are opaque in the light microscope.

Origin:

The distribution of authigenic pyrite is closely associated with sedimentary rocks and the presence of organic detritus (Berner, 1970). Formation of pyrite is initiated by the deposition of organic matter in non-turbulent waters, followed by induced activity from sulfate-reducing bacteria under anaerobic conditions during the production of hydrogen sulfide (H_2S) (Berner, 1970). Hydrogen sulfide will thereby react with detrital iron derived from the organic matter to form non-crystalline FeS. Formation of crystalline pyrite is a long process taking several years, and involves the oxidation of H_2S to form elemental sulfur which will further react with FeS and lead to crystallization of pyrite in the form of framboidal microspheres (Berner, 1970).

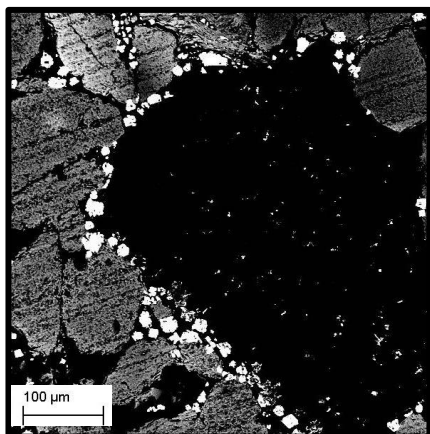


Figure 5.9: Backscattered image from the scanning electron microscope (SEM) displaying spherical pyrite framboids surrounding a coal clast.

Calcite

Distribution:

Calcite cement in the form of pore-filling sparite (“sparry”) calcite is observed in one sample in the Skilvika formation (2.8), interpreted as having been deposited on the floodplain. Syntaxial overgrowth of cement on framework grains is observed in the calcareous sandstone. In XPL, the cementation can be identified with a 4th order birefringence colour. Porosity and permeability is nearly non-existent in the sample due to the presence of cementation.

Origin:

Calcite cementation in sandstones is initially produced by precipitation, as solutions pass through pore spaces in the sediment. Calcite cement can have both external-and internal sources, where the internal sources like carbonate rock fragments-and fossils, in addition to plagioclase are present within the sandstone. In such cases, diffusion can occur due to that the distance from dissolution to precipitation of calcite is short. With external sources, transportation usually occurs through fluid flow (Bjørkum and Walderhaug, 1990). Although calcite cementation is widespread in shallow-marine environments, calcite-cemented sandstones originating from fluvial environments have also been previously studied (e.g. Hall et al., 2004; Wanas, 2008; Zhang et al., 2015). The calcite cement from the floodplain environment has been interpreted to form as a result of supersaturation of CaCO₃ in pore water following a wet period, ultimately leading to calcite precipitation (Mueller et al., 2004).

Chlorite

Chlorite is a subordinate mineral in the thin section samples from both formations and is present as either components in close association with mica and quartz minerals in internally foliated rock fragments (phyllite) or as replacement minerals for framework sheet minerals like biotite (Fig 5.7 A). Chlorite can be easily misinterpreted as glauconite in the light microscope due to their similar green pleochroism in plane polarized light (PPL, from now on), but chlorite is distinguished based on its relatively low birefringence colour when studied in XPL-light, its fibrous plate appearance and a well-developed cleavage. Chlorite is a significant constituent in the formation of metamorphosed rocks such as phyllite and is a secondary alteration mineral for biotite to form pseudomorphs through the process of chloritization. (Pichler and Schmitt-Riegraf, 1997).

5.2.3: Presence of organic matter

Organic matter is a major constituent in several of the studied samples, where it may be pore-filling (oxide cement) or present as rounded coal and elongated plant fragments (organic detritus). Organics are characterised by their opacity in the light microscope and the high content of carbon, which could be measured in an X-ray micro analysis in the SEM microscope. An important note is the abundance of organic detritus in the marine environment, constituting 18.3% in sample 4.2 (prodeltaic heterolithics) and 10% in sample 4.10 (delta front sandstone). This abundance of organic matter is supported by outcrop observations, where an abundance of coal clasts/fragments were observed throughout the whole marine Renardodden Formation.

5.2.4 Classification

In this section, the samples are classified based on their primary constituents (%) of quartz, feldspar, rock fragments and matrix content. The classifications are based on Dott`s (1964) modified classification of sandstones (Fig. 5.10) and are further classified in QFL and QmFL diagrams as described by (e.g. Dickinson et al., 1983) (Fig. 5.11). Framework constituents classify the type of rock as a quartz arenite, feldspathic or

lithic, whereas matrix content highlights the dominant grain size and classifies the rock as an arenite, wacke or mudstone. A quartz arenite will have a clear abundance of detrital quartz above 90%, whereas an arkose or litharenite will have more than 25% feldspar and rock fragments respectively. Amount of matrix is crucial in the classification as a total matrix percentage less than 15% classifies the rock as an arenite, whereas between 15% and 75% matrix constitutes a wacke. A mudstone is classified as having above 75% matrix. In the following classification, matrix percentage is calculated from the total point counts per sample, whereas the type of rock is determined from framework constituents relative to one another (quartz+ feldspar+ rock fragments =100%). Alkali feldspar and quartz were often difficult to distinguish in the light microscope due to visual similarities, and therefore classification based on this method has uncertainties involved. To quality control point counts from the light microscope, a scan line from the SEM microscope was used to check approximate amounts of K-Feldspar.

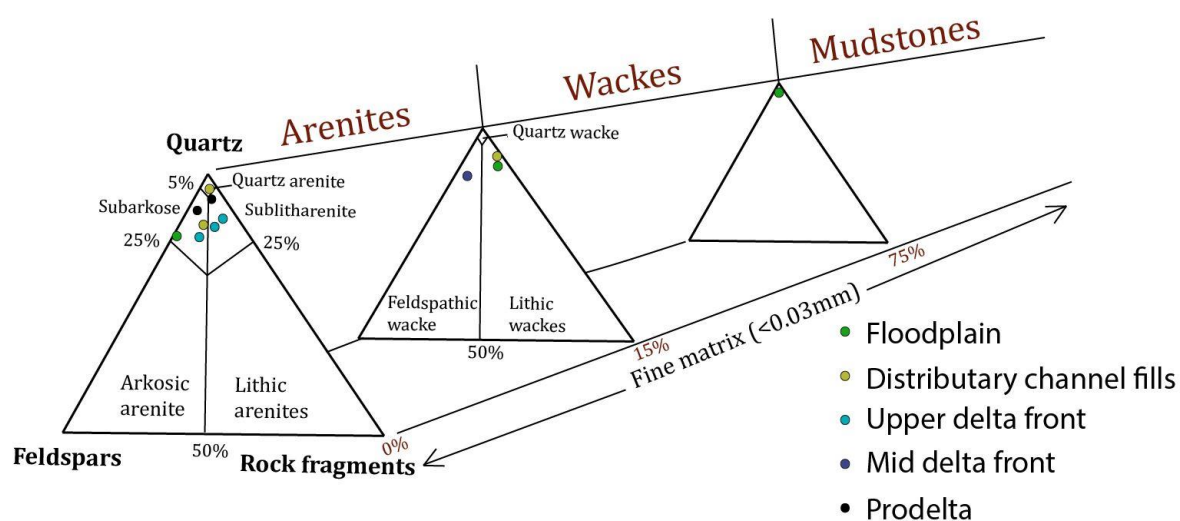


Figure 5.10: Classification of sandstones based on framework constituents (quartz, feldspar and rock fragments) and matrix content. Classified based on depositional environments. Modified from Dott Jr (1964).

As displayed in Table 5.3, most of the samples are classified as subarkose or sublitharenite with a relatively subordinate content of feldspar and/or rock fragments of less than 25%. Matrix content is dominantly below 15% and most of the samples are therefore classified as arenites based on Dott's (1964) classification (Fig 5.10). Only one mudstone is observed, in the floodplain environment, with a matrix content of 77.7%. Sample 4.1 is classified as a quartz arenite and is from the large channel body

with trough cross- stratification (Facies 10 in section 4.3.1). The ratio between quartz and feldspar in the samples may be a representation of the maturity of the rock, where a higher amount of quartz and less feldspar accounts for a higher maturity for the sandstone, and hence vice versa. In terms of this, the most compositionally immature rock may be found in the floodplain environment (24% feldspar) whereas the most compositionally mature rock may be interpreted to derive from distributary channels (92% quartz).

Table 5.3. Summary of the framework constituents, matrix composition and subsequent rock classification based on point counts. Percentage of quartz, feldspar and rock fragments are given by accounting for a 100% composition of the three framework minerals. Matrix percentage is given from a total percentage of all constituents counted in each sample.

Depositional environment	Thin section sample number	Quartz (%)	Feldspar (%)	Rock fragments (%)	Matrix (% of total)	Rock classification
Tectonically generated slump complex	2.1	100				<i>Metamorphic origin</i>
Floodplain of upper delta plain	2.2	85.9	2.2	11.9	17.4	<i>Lithic wacke</i>
	2.8	75.8	24.2	0	0	<i>Subarkose</i>
	2.10	100	0	0	77.7	<i>Mudstone</i>
Distributary channel fills	2.3	87.8	1.3	10.9	15.3	<i>Lithic wacke</i>
	2.5	77	13.6	9.4	12.5	<i>Subarkose</i>
	4.1	92.4	3.3	4.3	8.7	<i>Quartz arenite</i>
Upper delta front	4.5	80	6.8	13.2	13.4	<i>Sublitharenite</i>
	4.10	74	16.7	9.3	13.7	<i>Subarkose</i>
	4.11	79.2	9.7	11.1	13.6	<i>Sublitharenite</i>
Mid delta front	4.3	79.8	13	7.2	16	<i>Feldspathic wacke</i>
Prodelta	4.2	81.4	11	7.6	9.4	<i>Subarkose</i>
	4.6	88.9	5.3	5.8	11	<i>Sublitharenite</i>

5.2.4.1 QFL-QmFLt diagrams

The arenites are further classified in QFL (Fig. 5.11 A) and QmFLt (Fig. 5.11 B) ternary diagrams similar to those described by e.g. Dickinson et al. (1983) and

Pettijohn et al. (1987). This is beneficial in order to discuss possible provenance areas for the deposits of the Calypsostranda Group in accordance with the provenance classification presented by Dickinson and Suczek (1979) (Chapter 7). QFL diagrams are based on total composition of quartz, feldspar and lithic rock fragments (e.g. Dickinson, 1970). In the QFL diagram, quartz grains include the total amount of monocrystalline, polycrystalline and microcrystalline (chert) quartz in the samples (Dickinson et al., 1983). In the QmFLt diagram, only monocrystalline rock fragments are considered quartz grains. Polycrystalline and microcrystalline quartz are thereby classified as part of total lithic fragments (Lt), in addition to rock fragments derived from igneous or sedimentary origin (Dickinson et al., 1983). Due to the relative abundancy of polycrystalline grains in the studied samples, the samples will contain a higher lithic component in the QmFLt classification than in the QFL classification, and more of the samples will therefore be classified as sublitharenites and lithic arenites.

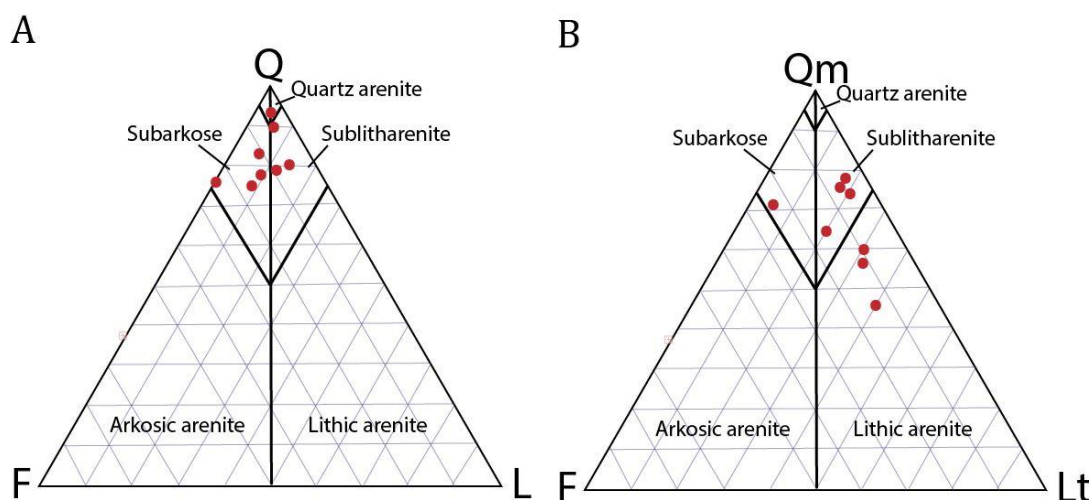


Figure 5.11: Results from the arenites presented in A) QFL and B) QmFLt diagrams modified from Dott (1964) and Dickinson and Suczek (1979)

5.2.4.2 Error percentage

An error percentage for the samples was calculated based on SEM scan lines to determine the composition of alkali feldspar (Table 5.4). Figure 5.12 shows a typical x-ray spectrum measured through the SEM microscope where K-Feldspar (KAlSi_3O_8) is detected. A higher value of potassium (K) and aluminium (Al) will differentiate

between K-Feldspar and quartz (SiO_2) and an expected value of K-feldspar could be calculated.

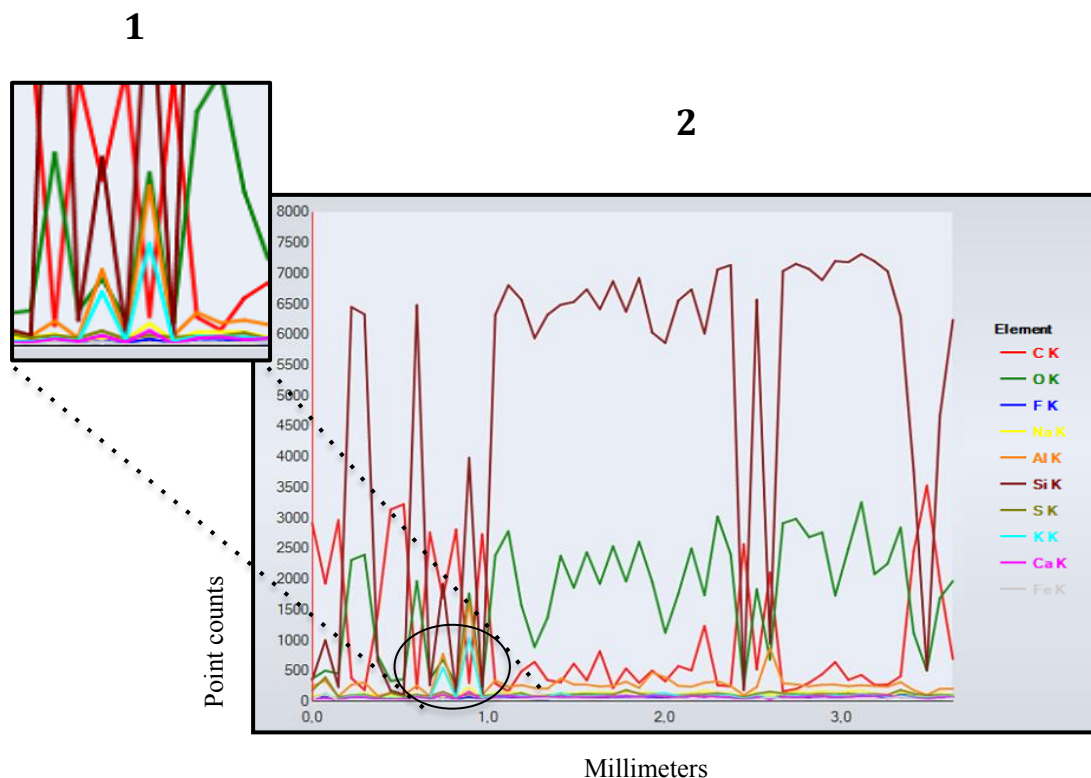


Figure 5.12: (2) A scan line from sample 4.2 displaying X-ray spectrums of the element compositions in the studied sample based on point counts of each element. (1) K-Feldspar is identified based on readings of potassium (K) and aluminium (Al), in addition to silicon (Si) and oxygen (O).

Table 5.4. Error percentages from the studied samples, showing classifications estimated from point counts and from scan line analysis in the scanning electron microscope (SEM).

Sample	Error percentage (Point count- SEM)	Classification (point count)	Classification (SEM analysis)
2.2	- 4.8 %	Lithic wacke	Lithic wacke
2.3	- 6.6 %	Lithic wacke	Lithic wacke
2.5	- 1.6 %	Subarkose	Subarkose
2.8	- 1.2 %	Subarkose	Arkose
2.10	-	Mudstone	Mudstone
4.1	- 2.4 %	Quartz arenite	Quartz arenite
4.2	- 3.8 %	Subarkose	Subarkose
4.3	- 3.3 %	Feldspathic wacke	Feldspathic wacke
4.5	- 1.6 %	Sublitharenite	Sublitharenite
4.6	- 1.6 %	Sublitharenite	Subarkose
4.10	- 1.61 %	Subarkose	Subarkose
4.11	+3.2	Sublitharenite	Subarkose

Table 5.4 displays the necessity of calculating errors in point counts, where the samples marked in red are important to note due to that they may be classified as different rocks based on the amount of K-feldspar. The values show that K-Feldspar is underestimated in manual point counts, most likely due to the visual similarities it has to quartz in both XPL and PPL view in the light microscope, in terms of relief, birefringence and pleochroism. An underestimation of K-feldspar may result in a misrepresentation of the compositional maturity when comparing ratio of quartz to feldspar.

6 Geological development

The following chapter presents depositional models and discusses the geological development for the sediments of the Calypsostranda Group. The interpretations are based on outcrop observations, including sedimentary structures, grain sizes and architectural elements (in particular for the fluvial deposits). Petrography is also linked to depositional environments and will be briefly discussed. More detailed discussion of the mineralogy and coal diagenesis is presented in Chapter 7: Source to sink perspectives.

6.1 Depositional environments

The section at Calypsostranda has previously been logged by *Kleinspehn K.* in Dallmann (1999). Similarities to the log by *Kleinspehn K.* was found in the following study:

- A fault bounds the basal part of the Skilvika Formation to underlying basement rocks.
- The Skilvika Formation is dominated by silt, upwards fining sandstone units and *in-situ* coal deposits.
- Very-fine and fine sandstone is the dominating grain size in the Renardodden Formation

However, some differences are also noted. The first 30 meters of the Skilvika Formation are more fine-grained in this study than that has been logged by *Kleinspehn*. In addition, the deposits in the Renardodden Formation are much more heterolithic (Facies 16) than what has been indicated on the corresponding log.

The Paleogene strata at Calypsostranda have previously been interpreted to be deposits of terrestrial origin (the Skivika Formation) and marine origin (the Renardodden Formation) (e.g. Livsic, 1974; Harland et al., 1997; Dallmann et al., 1999; Birkenmajer, 2006). Based on the sedimentological observations, the present study supports these interpretations. Two main depositional environments for the deposits have been recognized: 1) Sediments of the Skilvika Formation accumulated

in an alluvial delta plain environment, and 2) The deposits of the Renardodden Formation were deposited in a littoral to offshore environment. More specifically, the Skilvika Formation is linked to a meandering river system composed of channel- and floodplain deposits (Fig. 6.4) (SUB FA 1.2, SUB FA 1.3, Table 4.2) and the Renardodden Formation to a marine environment with deposits belonging to delta front and prodelta regions (SUB FA 2.1, SUB FA 2.2, SUB FA 2.3, SUB FA 2.4, Table 4.2). The vertical stacking of the deposits suggests the presence of a prograding river-dominated delta system that was subsequently transgressed (Fig. 6.1).

The interpreted depositional environments are supported by the petrographic analysis. The sphericity, roundness and sorting of the grains in the samples can all be a measure of the textural maturity of the sandstone and can be linked to the depositional environment in which the samples are derived from. Low sphericity (Fig 5.1) in addition to angular and subangular grains (Fig 5.2) are linked to sediments deposited in the floodplain environment. Contrary to this, deposits from the marine environment and from distributary channels show moderate to high sphericity in addition to subrounded and rounded grains indicating a higher textural maturity and higher energy environments than that of the continental deposits. All samples show a degree of sorting which is moderate or higher, but the degree is linked to depositional environments. The very well sorted samples are linked to marine and distributary channel environments (Fig 5.3). On the basis of these results, it can be deduced that texturally mature grains in terms of roundness, sphericity and sorting are all linked to environments where fluvial or marine processes have influenced the grains.

The lower half of the studied succession is interpreted to be deposits from a river - dominated delta. This interpretation is based on the assumed high sediment load from the coast evident by high ratios of sandstone in SUB FA 1.3 (highly bioturbated sandstone of the lower delta front region (F15)) and SUB FA 2.4 (heterolithic deposits of the prodelta region (F16)). Both these facies also include rounded allochthonous coal fragments suggesting a river dominated system. A dominating fluvial system with several distributaries is a suggested model for such large amounts of sediment load to be transported to the lower delta front and prodelta depositional environments. The sediments do not portray sedimentary structures prone to tidal

influence (e.g. double mud drapes or tidal bundles), wave ripples are only observed in F11 (belonging to the delta front environment in the Renardodden Formation). This indicates that neither waves nor tides were major contributors in such a delta system. However, a possible interpretation is that F14 (soft sediment deformed sandstone) may have been deformed by storm waves suggesting a fluvial river dominated delta system occasionally influenced by storm wave action.

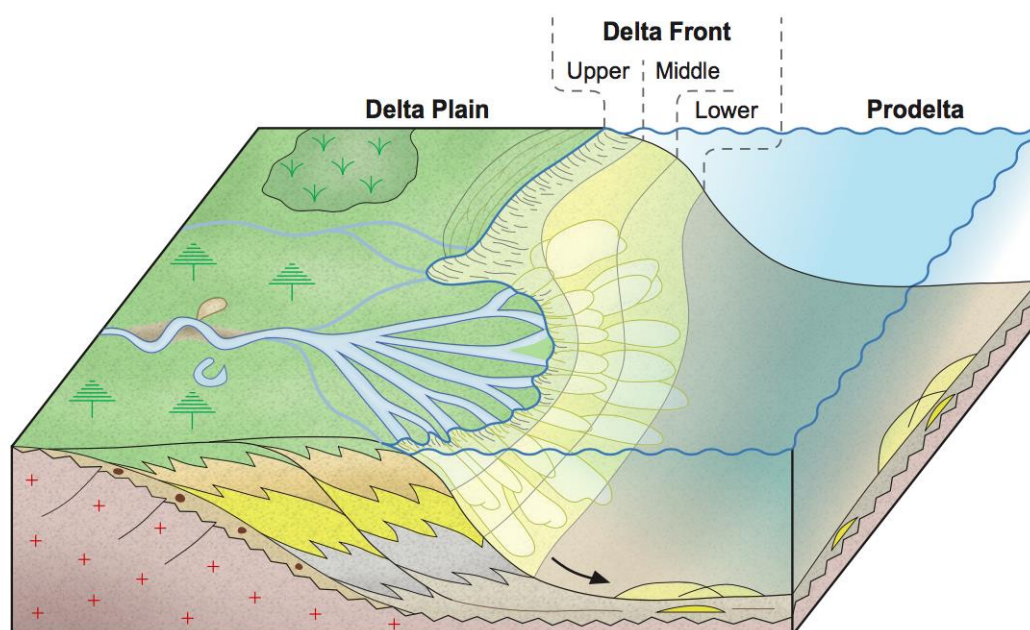


Figure 6.1: Depositional environment for the deposits of the Calypsostranda Group at time of deposition of the Skilvika Formation: Prograding fluvial dominated delta system with depositional zones marked.

6.2 Modern analogues

Potential analogues have been investigated to better understand the depositional environments and the development of the succession. The Mississippi Delta and the Wax Lake Delta (Wellner et al., 2005) are perhaps the most known modern analogues of river dominated deltas where distributaries reach far out to the basin and where the delta front is very little affected by tide or wave processes. Due to their large size,

they are not considered ideal analogues for the smaller delta system at Calypsostranda.

The Burdekin Delta in NE Australia is a likely candidate due to its size, geomorphology and sediment distribution (Fig 6.2) (Fielding et al., 2005). The Burdekin Delta has similarities to the proposed delta system in Calypsostranda in terms of the stratigraphic development, distribution of facies, climate and geomorphological features. The pronounced development of a meandering river system on the delta plain (Fig. 6.2) and high sediment discharge are especially analogous to the proposed delta system at Calypsostranda. Other similarities include:

- The Burdekin delta is exposed to a humid climate (Fielding et al., 2005), which was also the case for Svalbard in the Early Paleogene (Dallmann, 2015).
- The depositional model for the Burdekin Delta features delta plain sediments transitioning into mouth bar sands at the river mouth and on the delta front, and further transition into lower delta front sediments (Fielding, 2005).
- It has been suggested that hyperpycnal underflows may at times be produced at the river mouth of the Burdekin Delta (Amos et al., 2004), as has been suggested for the system at Calypsostranda.

Despite similarities, there are also differences between the facies of the two delta systems:

- The Burdekin Delta has very coarse-grained mouth bar deposits (medium to very coarse-grained sandstone) (Fielding et al., 2005), whereas the mouth bar deposits of the Calypsostranda Group are much finer-grained.
- The lower delta front of the Burdekin delta is mud-dominated, whereas the lower delta front of the Calypsostranda Group is almost entirely comprised of sand (F15).



Figure 6.2: Modern analogue of a river dominated delta system, the Burdekin delta in NE Australia. Distributaries develop on the upper delta plain when the main channel divides. Meandering channels are shown on the delta plain and are a visual interpretation of how the delta system at Calypsostranda might have looked like. Photo is taken from Google Earth.

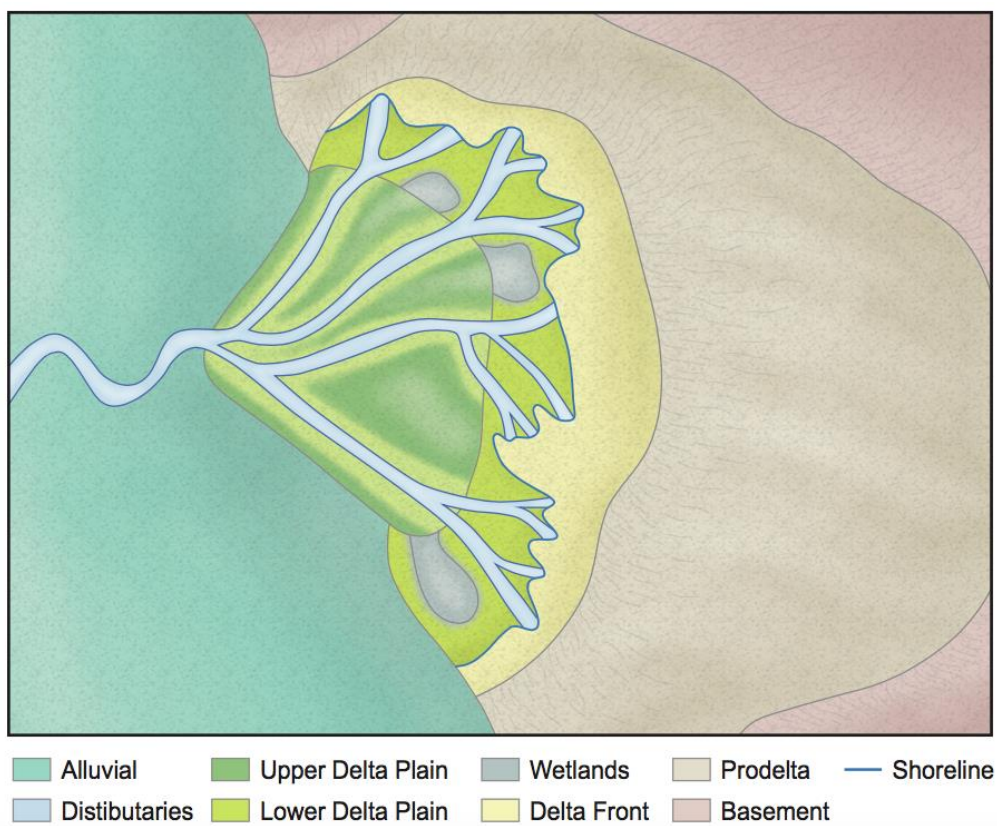


Figure 6.3: Illustrated fluvial delta system for the deposits at Calypsostranda

6.3 Depositional history of the Calypsostranda Group

The depositional development of the vertical facies succession recorded in the Calypsostranda Group is outlined below. Based on the stratigraphic architecture, the depositional development of the succession can be divided into five stages:

Stage 1: Accumulation of (?)Paleogene strata on Neoproterozoic rocks, followed by faulting between the two domains and associated slump development (SUB FA 1.1).

Stage 2 (Fig 6.4): A river-dominating delta system progrades into the area, depositing delta plain sediments (SUB FA 1.2 & SUB FA 1.3)

Stage 3 (Fig 6.5): A transgression follows leading to deposition of sediments on the middle and upper delta front (SUB FA 2.1 & SUB FA 2.2). A flooding surface is noted between F12 (Bioturbated homogeneous sandstone) and F14 (Soft sediment deformed sandstone) representing a gradual transgression from a nearshore (Upper delta front) to a more distal delta front environment.

Stage 4 (Fig. 6.6): A rapid transgression follows, indicated by a flooding surface, marked at the boundary between F14 (soft sediment deformed sandstone) and the heterolithic prodelta deposits (F16A). A shift in relative sea level is denoted with a maximum flooding surface at the finest measured grain size in the association (F16B; SUB FA 2.4).

Stage 5 (Fig 6.7): Normal regression and delta progradation with lower delta front deposits (SUB FA 2.3) followed by mid delta front deposits (SUBFA 2.2).

6.3.1 Stage 1: Tectonic faulting and mass transport deposition

A possible interpretation for the initial stage of the deposits is faulting with accompanying mass wasting. (?) Paleogene sediments were deposited on top of the precambrian unconformity with accommodation space being created as a result of tectonic activity in the area. As the Paleogene sediments accumulated and started to lithify, a weakness was developed between the Cenozoic and Precambrian sediments, and a fault developed. As a result, a coherent mass of Cenozoic sediments was transported and deposited as mass transport/ slump deposits and was later fossilized (F1). This small fault may be further connected to the fault dividing the Precambrian

and Calypsostranda domains, as described by Dallmann (1989), which is further connected to the inner Hornsund Fault Zone.

6.3.2 Stage 2: Development of a meandering river system

The majority of the floodplain deposits are interpreted as being deposited in a meandering channel environment (Fig 6.4). The environmental interpretation is based on the presence of a large channel body at the base of the Renardodden Formation and its classification as a meandering channel body based on Gibling (2006) classification of river systems. In addition, the presence of *in-situ* rootlets and coal horizons in the Skilvika Formation point to an alluvial setting, where anoxic swamps and vegetation was abundant. Figure 6.4 illustrates the depositional environment for a meandering system on the sub-aerial upper delta plain and it can be directly linked to the floodplain and distributary deposits on the upper delta plain (SUB FA 1.2; SUB FA 1.3). Crevasse splay deposits (F3), swamp areas with coal accumulations (F2), restricted lakes with mud deposition (F7), levee deposits (F4), overbank deposits (F5), distributary channel deposits (F8, F9, F10, F11) and meander point bar deposits (F10) are all deposited in such an environmental setting.

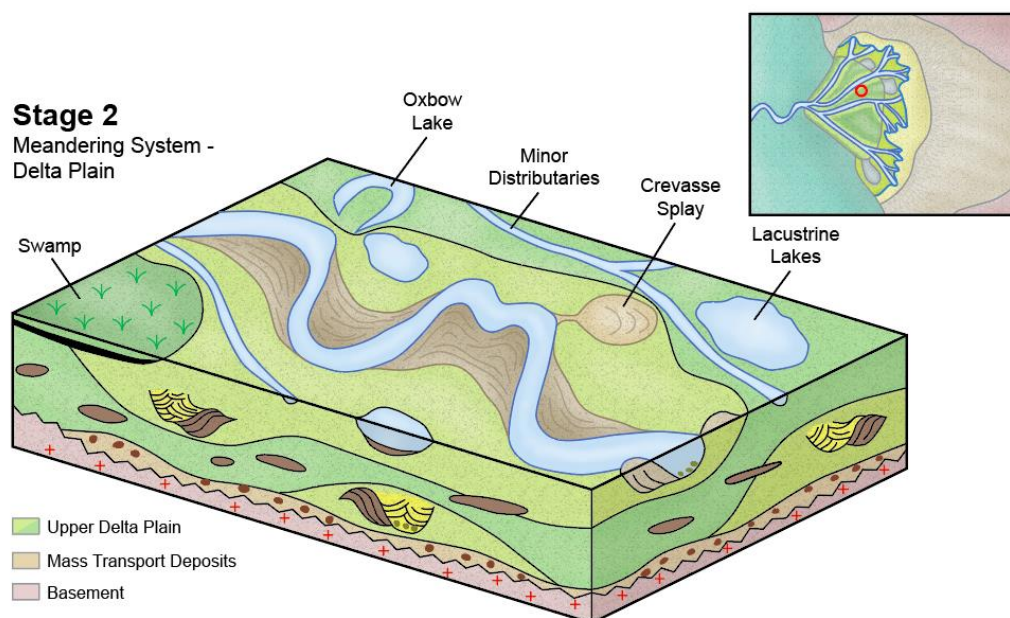


Figure 6.4: Illustration of a meandering river system on an upper delta plain with accumulations of floodplain deposits viewed in cross-section.

6.3.3 Stage 3: Transgressive phase with retrogradational delta system

Stage 3 marks a transgression and the drowning of the previously deposited alluvial delta plain deposits (stage 2). This leads to a retrogradation of the entire delta system and deposition of upper delta front and subsequently middle delta front deposits (SUB FA 2.1; SUB FA 2.2). Upper delta front sediments mainly include fine-grained homogeneous bioturbated beach deposits (F12) and gravel conglomerate (F8 B). Gravel conglomerate in the upper delta front have been interpreted as being hyperpycnal debris flow deposits with rip-up mud clasts. It is highly probable that distributaries still have a high sediment load at this stage evidenced by the transport of fine-grained sediments with coal fragments down the delta slope and into the lower delta front and prodelta environments. The presence of the diagenetic clay mineral glauconite in 4 of the thin sections from the fluvial Skilvika Formation further strengthens the interpretation of a marine transgression and drowning of previously upper delta plain deposits, as this is a mineral that only forms in marine environments (e.g. Pichler and Schmitt-Riegraf, 1997). Odin and Matter (1981) states that a marine transgression, where detrital near-shore sediments are submerged, is a favorable setting for the formation of glauconite. As a result, the sediments will be drowned below turbulent waters and deposition of sediments will be absent allowing glauconitization to take place on top of previously deposited sediments.

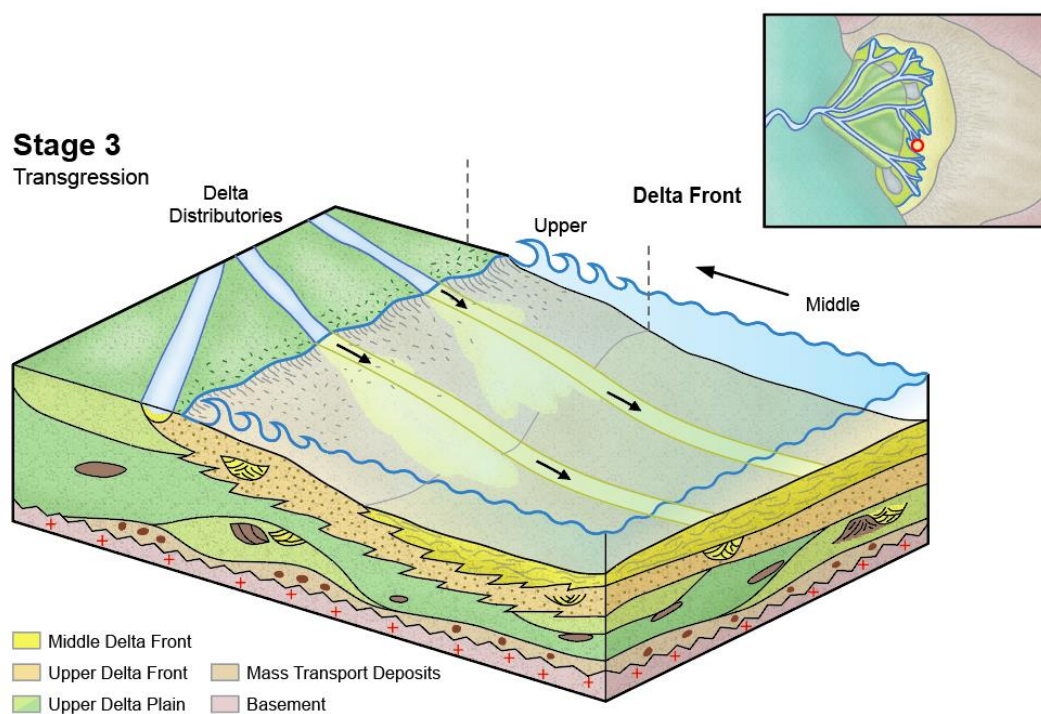


Figure 6.5: Transgressive phase and drowning of upper delta plain deposits. Development of hyperpycnal flows where a large amount of sediments are by-passed the delta front.

6.3.4 Stage 4: Continued transgressive phase and development of major flooding surfaces

This stage marks further transgression and subsequent retrogradation of the delta with the occurrence of two pronounced flooding surfaces, one major surface between middle delta front deposits and overlying prodelta deposits, and one major flooding surface associated with the finest measured grain size in the prodelta heterolithic deposits (F16B) (Fig 6.6). The maximum flooding surface marks the most distal part of the delta in the whole studied succession at Calypsostranda and thus bounds two contrasting systems, a retrogradational sequence below from a progradational sequence above. Prodelta deposits (F16) are composed of heterolithic alternating mudstone, sandstone and siltstone with high amounts of coal clasts. For such a high concentration of sand-grained lithology to be transported to the lower delta front and prodeltaic zone, a fluvial dominated system is required. Therefore, sand-rich sediments are interpreted to be transported by distributaries on the delta plain, down the delta slope and further deposited on the basin floor.

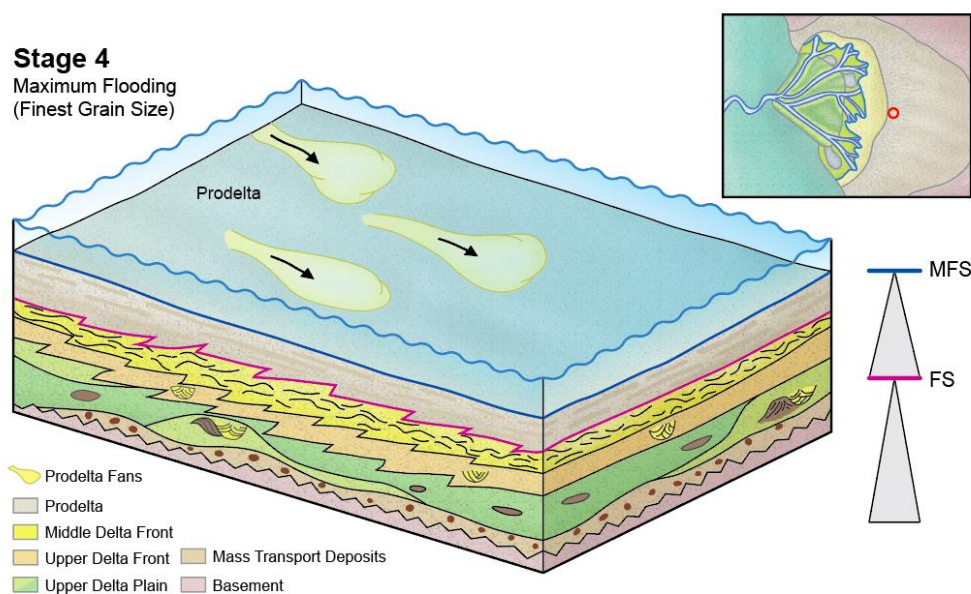


Figure 6.6: Continued transgressive phase and development of a major flooding surface (FS), and a maximum flooding surface (MFS). Prodelta fans/turbidites are shown where sediments have been transported down the delta flow by hyperpycnal flows and deposited further downslope in the lower delta front and prodelta environments

6.3.5 Stage 5: Normal regressive phase and delta progradation

Stage 5 (Fig 6.7) denotes the last depositional phase and is characterised by a normal regression and delta progradation following the major flooding surface in stage 4. The regression is initiated in prodelta deposits (F16A) where sand- and mud rich heterolithic deposits (F16A) overlay finer grained silt- and mud-rich heterolithic deposits (F16B). As the delta builds out, bioturbated organic-rich sands (F15) belonging to the lower delta front are deposited directly above prodelta deposits of facies 16B. With further progradation, mid delta front deposits are deposited on lower delta front deposits. These deposits mark the upper part of the logged section of the Renardodden Formation, and also indicate a turbulent, and highly energetic nearshore environment due to the abundance of *Ophiomorpha* trace fossils with shaft configurations in the fine-grained sandstone (F13) (Frey et al., 1978).

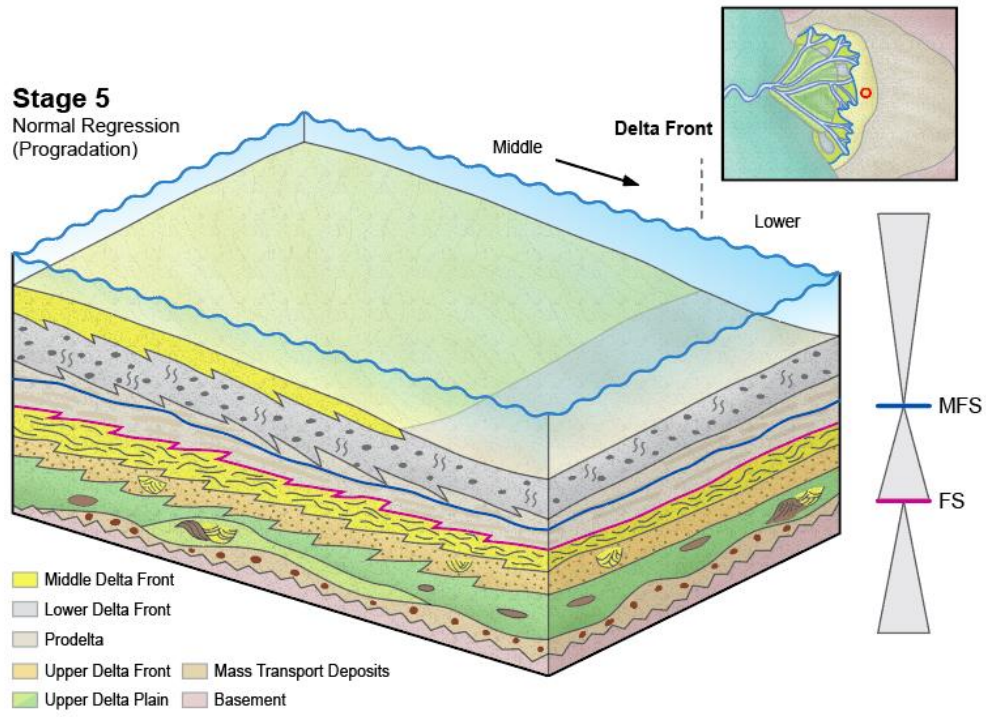


Figure 6.7: Stage 5: normal regressive phase and delta progradation.

7 Source to sink perspectives

The following chapter provides perspectives on provenance and possible basin-development scenarios for the Paleogene succession at Calypsostranda, based mainly on petrographic and sedimentological results presented in this study, as well as other relevant literature. Paleogene outcrops located in the coastal section at Calypsostranda are isolated from other Paleogene sediment accumulations in Spitsbergen, and have been affected by post-depositional and possibly syn-depositional tectonic activity. There is also a discussion of the age of the Calypsostranda Group and in the following chapter alternative ages of the succession will be discussed with regards to possible basin settings and the tectonic influence at time of deposition.

7.1 Provenance

In this study, 13 thin section samples from the Paleogene succession at Calypsostranda were analysed and classified. 8 arenitic sedimentary rocks were subsequently classified in QFL and QmFLt ternary diagrams (Dickinson, 1970; Dickinson et al., 1983; Pettijohn et al., 1987). According to the classification presented by Dickinson & Suczek (1979), the ternary diagrams (Fig. 7.1 A&B) show that the probable provenance area for the Paleogene deposits at Calypsostranda are within recycled orogens either within foreland upland- or collision orogeny provenances.

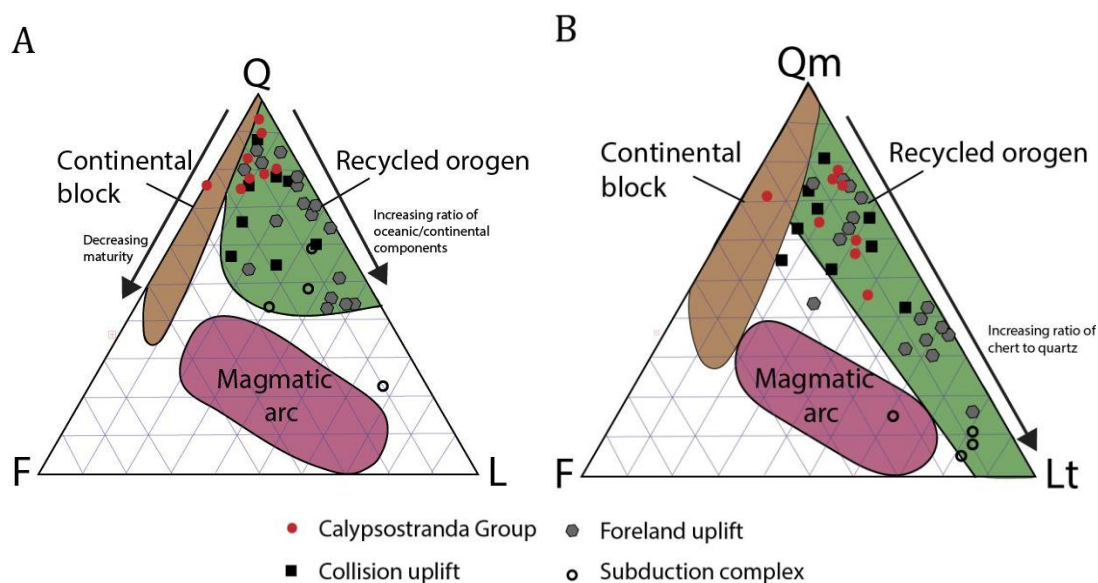


Figure 7.1: Provenance area ternary diagrams showing modal point counts of the arenites in the Calypsostranda succession compared to different provenances. Red dots are samples from Calypsostranda. Grey, black and transparent dots are values from foreland uplift, collision uplift and subduction complexes within recycled orogens, taken from studies conducted by Dickinson and Suczek (1979). A) QFL diagram where mono-macro- and microcrystalline quartz grains are classified as quartz grains B) QmFLt diagram where only monocrystalline quartz grains are included as quartz grains. Polycrystalline and microcrystalline grains are considered rock fragments in the specific ternary diagram.

The modal point counts also suggest two potential interpretations with regards to provenance:

- 1) The mature framework grains with an abundance of quartz and subordinate feldspar grains (<12%, Table 5.1) indicates deposition in a distal environment with a provenance from a quartzose sedimentary source area (e.g. Schlegel et al., 2013).
- 2) The samples also inhibit a presence of polycrystalline quartz grains and crenulated micaceous rock fragments in addition to heavy minerals such as chloritoid indicating a potential basement provenance for the sedimentary succession.

It is critical to understand the development and deformation of the West Spitsbergen fold-and-thrust belt in relation to deposition of the sediments at Calypsostranda as the interpretations of the provenance are inconclusive.

7.2 Age

Early Paleocene to Oligocene ages have been proposed for the Paleogene deposits at Calypsostranda. The majority of recent literature (e.g. Dallmann, 1989; Dallmann et al., 1999; Birkenmajer and Gmur, 2010) refers to Head (1984) late Eocene to early Oligocene age dating for the deposits. The datings are based on his findings of sporomorph and dinocyst assemblages. However, a palynological analysis conducted late 2017 on a sandstone sample from the Skilvika Formation, pointed towards a late Paleocene/early Eocene age for the deposits. This is based on assemblages of dinocysts, diatoms, pollen and spores in the sample (Lenz, 2017) and in particular, Lenz's findings of diatoms belonging to *Coscinodisus spp.* This is important since the species have proven to be typical of the Paleocene/Eocene boundary in the North Sea in earlier studies (Gradstein et al., 1992).

Younger ages have also been proposed for the deposits by Livsic (1974) who suggested an Oligocene age based on findings of pollen and spores. In his published work, he also mentions a correlation with the Forlandssundet Graben, which is dated as Eocene/early Oligocene (eg. Dallmann, 2015). Braathen et.al (1999) also suggests an Oligocene(?) age for the deposits at Calypsostranda linking the deposition to the latest stage of the formation of a critical wedge for the West-Spitsbergen fold-and – thrust-belt.

Although several more age propositions for the deposits have been made (e.g. Thiedig et al., 1979; Manum and Throndsen, 1986), the following two age scenarios will be the focus of this discussion; 1) a Paleocene/ early Eocene age, and 2) a late Eocene/early Oligocene-age.

7.3 Implications of a Paleocene/ early Eocene age (Fig. 7.2)

Based on the palynological age dating from Lenz (2017), a late Paleocene/early Eocene age for the deposits at Calypsostranda point to deposition before or at the onset of the main deformation phase of the West Spitsbergen fold-and-thrust belt (WSFTB) (eg. Leveer et. al, 2011).

7.3.1 Possible connection to the Central Tertiary Basin

The Central Tertiary Basin (CTB) consists of sediments ranging from early Paleocene (Firkanten Formation) to late Eocene/ possibly early Oligocene (Aspelintoppen Formation) (Steel et al., 1985).

The source direction for the Paleocene Firkanten Formation in the CTB has been broadly discussed (e.g. Petersen et al., 2016). There are two main interpretations of the provenance for the Firkanten Formation in the literature:

- i) An uplifted peripheral bulge source to the east-northeast (Kellogg, 1975; Bruhn et al., 2003; Petersen et al., 2016)
- ii) A westerly and northerly source reflecting early uplift of the western thrust belt (Lüthje, 2008)

The main deformation phase of the fold and thrust belt is correlated with the shift in source area for the Central Tertiary Basin, expressed by the income of the westerly derived Hollendardalen Formation in latest Paleocene (Steel et al., 1981; Harding et al., 2011). Sediments of latest Paleocene (Hollendardalen Formation) to Eocene age (Frysjaodden, Battfjellet and Aspelintoppen formations) are generally agreed upon to be sourced from the west as a result of the rise of the fold and thrust belt.

A Zircon age dating conducted by Petersen et al (2016) supported Bruhn & Steel's (2003) model proposing an easterly to northeasterly source for the sediments of the Firkanten Formation of the CTB (Fig. 7.2 a). If the sediments at Calypsostranda are of Paleocene age, a northeastern to eastern source area and direct connection to the CTB would be the most viable option and not a source derived from the WSFTB. This is based on:

- i) The occurrence of relatively fine-grained sediments (siltstone and sandstone) and subordinate conglomerates in the succession suggest deposition from an uplifted sedimentary source. Sandstones of the Firkanten Formation have been classified as arkosic (Schlegel et al., 2013), whereas the samples from Calypsostranda display a more quartz-rich composition. The fine-grained sediments and the mineral composition indicate a potential distal depositional environment for the Calypsostranda succession compared to the Firkanten

Formation (Fig 7.2a). Large parts of the Barents Sea Platform (including Svalbard) was in the late Mesozoic covered with thick successions of mesozoic clastic deposits (Sassendalen Group and Kapp Toscana Group) (Dallmann, 2015). Through uplift, these successions can provide important source areas.

- ii) The large amount of coal clasts present in the Renardodden Formation suggest a source area with continental sediments.
- iii) Polycrystalline quartz grains have previously been observed in the lowermost succession of the Firkanten Formation of the CTB (Schlegel et al., 2013). There is a relatively large component of polycrystalline quartz in the sandstone samples from Calypsostranda compared to other rock fragments with 1.4% to 10.5% of the total volume being polycrystalline quartz.
- iv) There are similarities between the stratigraphy of the Firkanten Formation and the deposits at Calypsostranda. The coal-bearing, delta plain sediments of the Todalen Member (Fig. 3.4 A) and the fluvial, coal-bearing Skilvika Formation at Calypsostranda could potentially be time-equivalent and laterally connected at the time of deposition. In addition, the Kolthoffberget Member (Fig. 3.4 B) of the Firkanten Formation, has significant similarities to the delta front-prodelta sediments at Calypsostranda (Facies 15) with both having very fine-grained, highly bioturbated, organic-rich sandstones (Dallmann et al., 1999; Nagy, 2005). The similarities in stratigraphy indicates a delta-dominated regime for both systems with the deltas feeding large amounts of sand into the prodelta environment. There are however differences in thicknesses where the Skilvika (approx. 110 m) and Renardodden formations (>135 m) are significantly thicker than the Todalen Member (53 m (Dallmann, 1999)) and the Kolthoffberget Member (up to 120 m, Dallmann, 1999). If the formations are time-equivalent, these differences may be explained by significant erosion of parts of the Firkanten Formation.
- v) The Firkanten Formation displays a similar intermediate-scale transgressive sequence to the geological model proposed for the succession at Calypsostranda. The Firkanten Formation has an overall transgressive trend from the basal Todalen member with the delta front sediments of the Endalen member and transition into prodelta sediments of the Basilika Formation (Steel et al., 1981). This delta plain to prodelta sequence is similar to that of the

sediments at Calypsostranda suggesting a possible connection between the two successions during time of deposition. However, the intermediate-scale transgressive cycle in the Firkanten Formation is the overall trend of several small-scale cycles (Bruhn et al., 2003). In the Calypsostranda Group, such small scale cycles cannot be observed.

- vi) The fluvial conglomerates of the Grønfjorden beds have well-rounded quartzite pebbles (Bruhn et al., 2003). Rounded quartzite pebbles are also observed in high abundancies in the slump deposit at the base of the Skilvika Formation (F1), suggesting a possible correlation to the basal parts of the Firkanten Formation. In such a case, the conglomerates in the Skilvika Formation would be a slumped fluvial deposit.

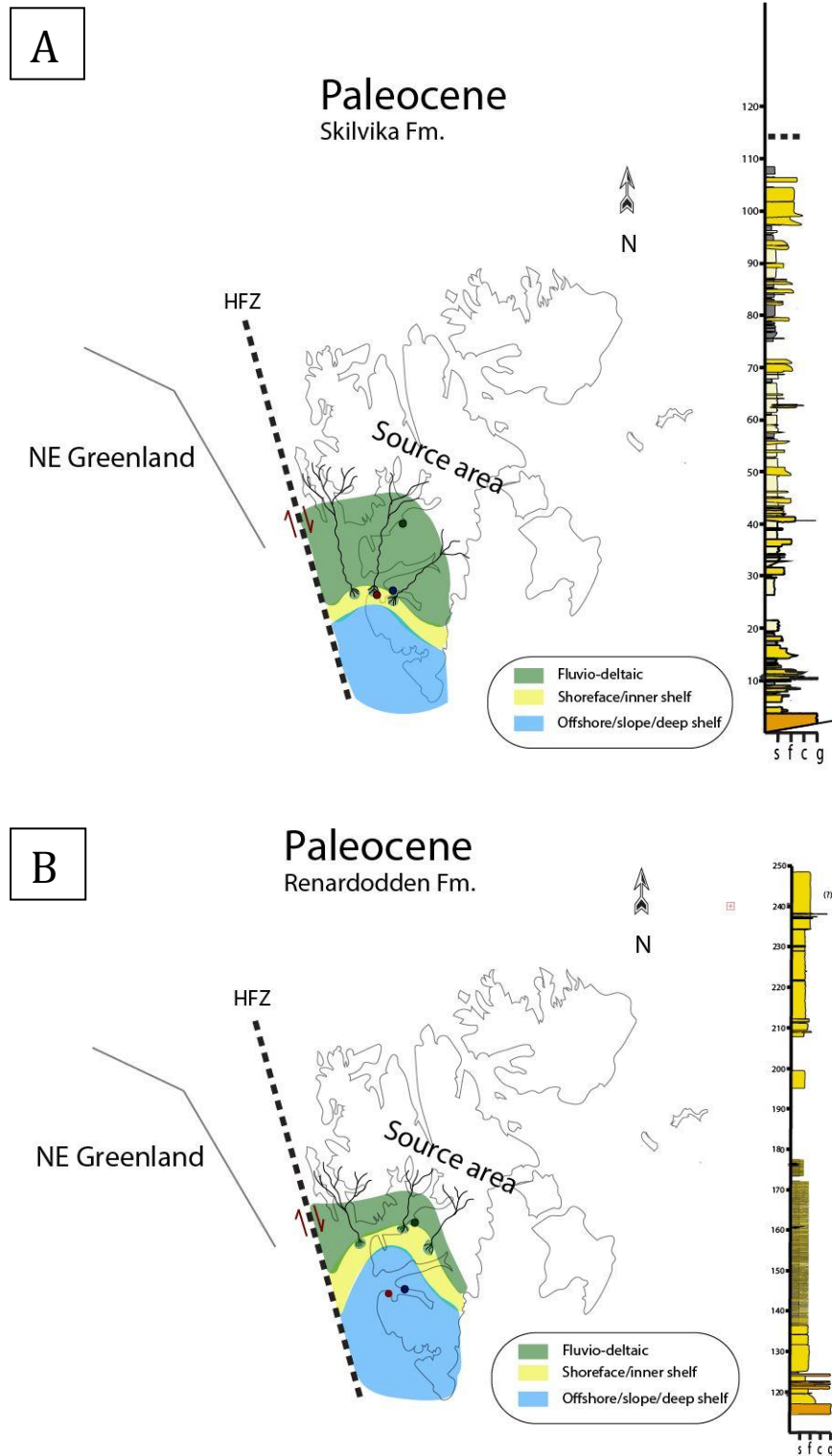


Figure 7.2: Sediment source area for the Central Tertiary Basin (CTB) in early Paleocene where present study area is marked with a red dot. Sediments in the study area may have been originally deposited further west and been shifted eastwards during rise of the WSFTB. The green dot marks the location of the logged section of the Todalen Member (Fig. 3.4 A), whereas the blue dot marks the location of the logged section of the Kolthoffberget Member (Fig. 3.4 B).

A) Deposition of the Skilvika Formation with composite log displayed B) Deposition of the Renardodden Formation with composite log displayed. HFZ-Hornsund Fault Zone. Modified (redrawn) from Petersen et.al 2016.

7.3.2 Accumulation in an outlier basin off the western coast of Spitsbergen (Fig. 7.3)

It has previously been suggested that the sediments may be a remainder of an offshore Cenozoic sedimentary basin, situated off the west coast of Spitsbergen, although a specific basin is not stated (Dallmann, 1999; Dallmann 2015). A possible accumulation area for the sediments at Calypsostranda is disconnection from the CTB and deposition in a pull-apart basin formed in the early Paleocene as a result of the dextral transtension that developed between Greenland and Svalbard.

In Late Paleozoic, NE-SW rifting occurred in the basins north and east of Greenland. This rifting was followed by an E-W extension in the Late Mesozoic, which subsequently led to dextral transtension laterally to the margin of eastern North Greenland and the formation of pull-apart basins in early Paleocene (Fig.7.3)(Døssing et al., 2010). One such pull-apart basin, the Central Wandel Sea Basin (CWSB) developed north of Greenland along the Hornsund Fault Zone, and formed a depocenter for Paleogene sediments sourced from northern Greenland (Fig 7.3) (Døssing et al., 2010). It may be possible that the basin in which the potential Paleogene sediments at Calypsostranda were deposited in, are age correlative to the Central Wandel Sea Basin (CWSB), perhaps also in connection with the CWSB. Hence, deposition in a pull-apart basin in Paleocene, along the Hornsund Fault Zone is a possibility. Thus, deposition prior to the rise of the fold and thrust belt could account for an isolated system to the west of the Spitsbergen archipelago, with deposition and sourcing disconnected from the CTB. As a result, the deposits of the isolated basin may have been shifted eastward in thrust sheets as a transpressional regime between Greenland and Svalbard was initiated, giving rise to the Spitsbergen fold-and-thrust belt (Fig 7.3) (e.g. Braathen et al., 1999; Leever et al., 2011).

The fault dividing the Neoproterozoic domain from the Calypsostranda domain described by e.g. Dallmann (1989) (Fig. 3.1) may thus be a reverse fault, that arose as a result of the transpression in the early stages of the formation of the WSFTB, and not a normal fault as previously suggested (e.g. Livsic, 1974).

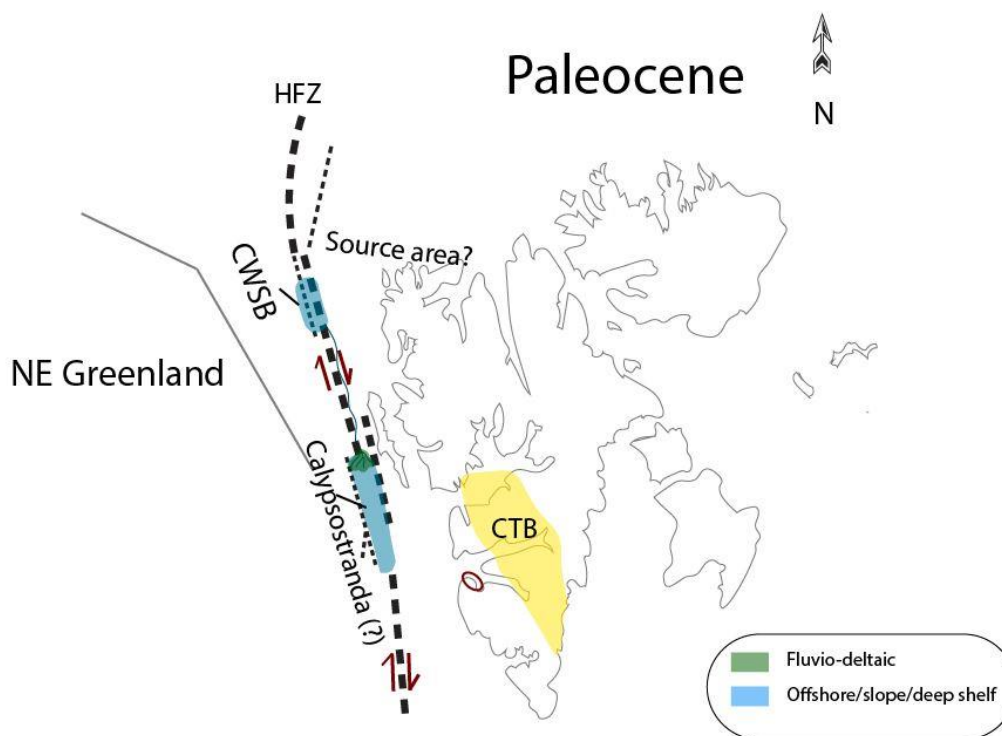


Figure 7.3: Transpressional regime and possible formation of pull-apart basins during early break up between Greenland and Svalbard in Paleocene. Present study area is outlined in red. HFZ- Hornsund Fault Zone. CWSB- Central West Wandel Sea. CTB- Central Tertiary Basin. The Dead Sea is used as a modern day analogue (Noda, 2013).

7.4 Implications of a late Eocene/ early Oligocene age (Fig. 7.4)

Another suggestion is a late Eocene/ early Oligocene age for the deposits at Calypsostranda (Head, 1984). This would suggest deposition in a period where the WSFTB was well-developed in western Spitsbergen. In late Eocene, extensional faulting and basin formation was taking place in the Western Hinterland region giving room for basin formation (Fig. 7.4) (e.g. Braathen et. al, 1999). Age correlations to the Aspelintoppen Formation in the CTB and the Marchaislaguna Formation (of Buchananisen Group in the Forlandssundet Graben) have been suggested for the deposits at Calypsostranda, based on palaeontology, structural evidence and lithological comparisons (Livsic, 1974).

7.4.1 Possible correlation to the Central Tertiary Basin

In the latest Paleocene, sediment sourcing had shifted from easterly to westerly for the Central Tertiary Basin (Steel et. al, 1985).

A late Eocene/ early Oligocene age for the deposits suggest sourcing from the WSFTB as formation of the fold-and-thrust belt was nearly completed at this time. As discussed in section 7.3.1, the sedimentological and petrographical observations suggest that the deposits at Calypsostranda are most likely distal in regards to proximity to the source area. There are however, some petrographical observations which may indicate a local source within the WSFTB:

- i) Findings of polycrystalline quartz rock fragments, crenulated micaceous rock fragments and phyllite in the studied samples. Several of the polycrystalline grains which were detected are composed of elongated, sutured grains with diffuse boundaries. Such grains are interpreted as being derived from a metamorphic source area (Ulmer-Scholle et al., 2014). This implies potential metasediments or metamorphic rocks in the provenance area in addition to a sedimentary source signature. In addition, silica-rich rock fragments found in one of the samples (Fig 5.6A), may indicate remnants from uplifted Permian strata in the WSFTB where spiculites were common (e.g. Blomeier et al., 2011).
- ii) Shale rock fragments present in several of the studied thin section samples indicate short transportation from a nearby sedimentary source, which may be derived from uplifted strata within the WSFTB.
- iii) The presence of the mineral chloritoid in 69% of the studied samples indicates a nearby uplifted source of basement rocks (Müller and Spielhagen, 1990).

One potential explanation for such differing observations is that there is a dual source system including the WSFTB and parts of an uplifted foreland basin. This foreland basin could potentially be uplifted and eroded parts of the CTB particularly the Firkanten Formation with its pronounced coal successions (e.g. Nøttvedt, 1985; Nagy, 2005). The Calypsostranda succession contains an abundance of allochthonous coal fragments. The coal fragments in the basal part of the Renardodden Formation have

previously been interpreted as being sourced from the Skilvika Formation (Birkenmajer and Gmur, 2010). Observations from the field show that these coal fragments are well rounded and are therefore classified as allochthonous “coal pebbles”. This questions the original interpretation of Birkenmajer and Gmur (2010) that the source is the Skilvika Formation as the coal would have to be diagenetic coal and not peat during deposition, which would require a hiatus between the two formations for burial and coalification to occur (pers. comm. Jochmann, 2017). Such a hiatus is not observed in the sediments at Calypsostranda and a different source area should be considered for the coal fragments in the Calypsostranda Group.

Given a late Eocene/ early Oligocene age, the coal in the Firkanten Formation would potentially already be coalified and the upper package of the Van Mijenfjorden Group partly eroded by the time of deposition of the Calypsostranda Group, so transport of sediments from the Firkanten Formation could potentially have taken place (pers. comm. Jochmann, 2017). Petrographical similarities to the Hollendardalen Formation have also been observed in the samples. The heavy mineral chloritoid is relatively abundant in the samples from Calypsostranda and are present in 69 % of the studied samples. Chloritoid has been recorded in the Hollendardalen Formation, but is absent in underlying beds (Müller and Spielhagen, 1990). Low amounts of feldspar have also been recorded in the Hollendardalen Formation (Müller and Spielhagen, 1990) in addition to samples taken from the CTB that were Paleocene to Eocene age (Schlegel et.al, 2013). The Central Tertiary Basin may have thus served as a source area for the deposits of the Calypsostranda Group, if they are of Eocene/Oligocene age.

late Eocene/early Oligocene

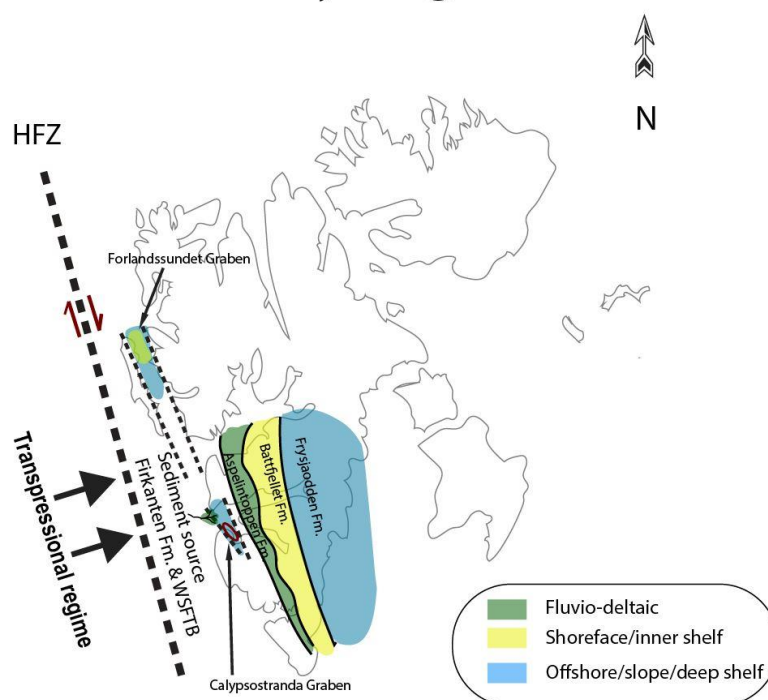


Figure 7.4: Development as a fault-bounded graben in late Eocene/ early Oligocene and sourcing from the WSFTB in addition to uplifted and eroded parts of the Firkanten Formation. HFZ- Hornsund Fault Zone. Modified from Petersen et al. (2016)

7.4.2 Development of a fault-bounded graben

For the late Eocene/early Oligocene age model to be viable, the Paleogene sediments at Calypsostranda would most likely have been deposited in a fault-bounded graben (Fig 7.4) (Birkenmajer and Gmur, 2010). Correlation with the Buchananisen Group of the Forlandssundet graben has been suggested and is also supported in recent literature (Dallmann, 2015). Onset of sedimentation in the Forlandssundet Graben has been suggested to have taken place in the late Paleocene/ early Eocene, although graben formation did not occur before the late Eocene (e.g. Blinova et al., 2009). A similar tectonic system to the Forlandssundet Graben may have occurred further south with deposition of the sediments at Calypsostranda in a graben that developed during the Oligocene extensional faulting.

A possible connection of the suggested graben in Calypsostranda to the Forlandssundet Graben can be discussed in terms of seismic imaging and sedimentological observations at Calypsostranda. A seismic research conducted by Blinova et. al (2009) documented the connection between the Forlandssundet Graben

and the southern Bellsund Graben (Fig. 7.5). The seismic image shows a southern termination of the Bellsund Graben with no connection to Calypsostranda. This may thus indicate an isolated graben structure for the sediments at Calypsostranda, with deposition of sediments in late Eocene-early Oligocene (Head, 1984) or in Oligocene (Livsic, 1974; Braathen et al., 1999) when the opening of the North Atlantic Ocean occurred, and extensional faulting took place in the western Hinterland region of Spitsbergen (eg. Braathen et al., 1999).

In terms of sedimentological investigations, the deposits in Forlandssundet Graben contain an abundance of locally-derived conglomerates (e.g. Kleinspehn and Teyssier, 1992; Dallmann et al., 2015). Observations from the present field work only indicate subordinate occurrences of conglomerates in the succession at Calypsostranda. If the deposits were fed by a nearby uplifted source (like the WSFTB), the sediments at Calypsostranda would be expected to be much more immature and contain even larger amounts of basement derived conglomerates. The subordinate conglomerate beds in the Calypsostranda succession are mostly linked to distributary channel deposits (SUB FA 1.3); specifically, the rounded conglomerates may be long transported clasts from the source area that have been rounded in channel systems.

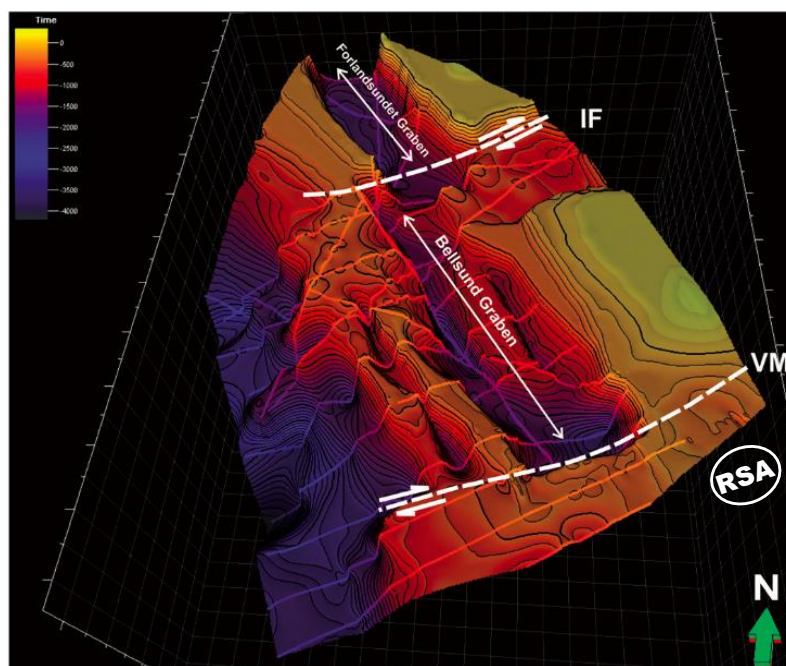


Figure 7.5: Time-depth map from Petrel displaying the basement interface highlighting the Forlandssundet and Bellsund graben in addition to strike-slip faults. IF- Isfjorden VM-Van Mijenfjorden RSA- study area. From Blinova et. al, (2009).

7.5 Summary

In summary, the exact age of the Paleogene deposits at Calypsostranda are uncertain and have been widely discussed. In this study, two likely settings have been proposed for the sediments at Calypsostranda based on different age datings. Based on palynological studies, Lenz (2017) suggests a late Paleocene/ early Eocene age, whereas Head (1984) suggests a late Eocene/ early Oligocene age for the deposits.

A Paleocene age would suggest deposition in either: i) connection with lower parts of the CTB succession (Firkanten Formation) or ii) deposition in a pull-apart basin before the major deformational phase of the West Spitsbergen fold-and-thrust belt. A possible suggestion is an isolated basin off the western coast of Spitsbergen, age correlative to the Central West Wandel Sea, which has later been shifted eastward as a response to the formation of the WSFTB.

A late Eocene/ early Oligocene age would favor deposition as a result of extensional faulting in the last stage of the formation of the WSFTB. A dual source area may be present where both lower parts of the Central Tertiary Basin succession (CTB) and uplifted strata of the WSFTB have possibly contributed as sediment sources.

Although the provenance area and exact age for the Paleogene deposits in this study are inconclusive, a preferred age and provenance area for the deposits at Calypsostranda is suggested: Based on similarities between the Firkanten Formation and the Calypsostranda Group in terms of the stratigraphic setting, lithostratigraphy and petrographic composition, it is likely that the sediments are of Paleocene age. A plausible provenance would be an uplifted bulge to the northeast-east contributing with both basement derived- or recycled sediments in addition to clastic sediments (perhaps uplifted Mesozoic strata). A Paleocene/ early Eocene age and deposition in an outlier pull-apart basin off the west coast of Spitsbergen is also a possible interpretation, but more studies on likely sedimentary provenance areas in Paleocene need to be considered, before such an assumption can be made.

7.6 Outlook

The deposits at Calypsostranda have previously not been extensively studied compared to other major Paleogene basins in Spitsbergen, but are very important to understand in the context of the regional sedimentation and tectonic history of western Spitsbergen. On the basis of inconclusive provenance results and varying age datings, this study suggests the following topics for further research:

- The thin section samples contained a relative abundance of zircon grains. A zircon age dating could be conducted for the deposits at Calypsostranda to better understand the age of the provenance area. Such datings can further be compared to similar age datings that have been conducted for the CTB in order to investigate a possible connection between the two Paleogene basins.
 - Palynological analysis for the autochthonous and allochthonous coal deposits of the Calypsostranda Group is necessary to more accurately determine the age of the deposits and to aid in understanding of the provenance area for the allochthonous coal clasts.
 - Detection of possible Paleogene accumulation basins northwest of Svalbard along the Hornsund Fault Zone (through e.g. reflection seismology) and provenance studies for these should be conducted. This would verify the hypothesis that the sediments at Calypsostranda are part of a pull-apart basin off the west coast of Spitsbergen, which was later shifted east as a result of the rise of the West Spitsbergen fold-and-thrust belt.
 - A comparative sedimentological study between Paleogene successions at Svalbard to Paleogene successions in Greenland would be very interesting in terms of better understanding the sedimentation patterns and possible connections between the two archipelagos before the major rifting phase in the North Atlantic Sea.
-

8. Conclusions

The aim of this study was to generate depositional models for the Calypsostranda Group and to discuss source-to-sink perspectives for the deposits in terms of age, provenance and possible accumulation basins. A multi-stage depositional model was constructed on the basis of facies break-down, analysis and process interpretations for the studied deposits. Source-to-sink aspects were discussed mainly on the basis of petrographical results from the present study incorporated with relevant literature, although sedimentological observations from the field were also taken into account. Based on sedimentological investigations from fieldwork at Calypsostranda, petrographical studies of thin section samples, and discussions on provenance; the following can be concluded:

- The deposits at Calypsostranda were initially deposited in a prograding fluvial dominated, storm-wave influenced delta system. The fluvial dominance can be deduced from the abundance of distributary channels with associated channel fill sediments on the delta plain, coarse-grained debris flow deposition from hyperpycnal flows on the delta front and delta front mouth bar deposits. Very-fine and fine-grained sand and abundancies of coal fragments in the marine deposits are essential indicators of a fluvial dominating system.
- Sixteen lithofacies were distinguished from the studied sedimentary succession of the Calypsostranda Group (F1-F16). The lithofacies can further be divided into two main facies associations; FA1: A sub-aerial delta plain and FA2; A paralic to marine regime. FA1 comprises tectonically generated mass deposits (SUB FA1.1), floodplain deposits (SUB FA 1.2) and distributary channel fill deposits (SUB FA 1.3). FA2 comprises delta front deposits (SUB FA 2.1-SUB FA2.3) and prodelta deposits (SUB FA 2.4).
- The Skilvika Formation comprises sediments deposited on the upper delta plain as part of a meandering distributary floodplain environment (FA1),

whereas the Renardodden Formation comprises sediments deposited in a marine environment including the delta front and prodelta regions (FA2).

- The deposits at Calypsostranda can be divided into a five-stage depositional model that involves a major transgressive phase drowning previously subaerial deposits, followed by normal regression with delta progradation. The shift in relative sea level is marked with a maximum flooding surface (MFS) in the finest grained sediments of the heterolithic prodelta deposits (F16).
- Based on petrographical and sedimentological analysis, a dual source area for the deposits at Calypsostranda are suggested. Findings of metasedimentary rock fragments, silica-rich biofragments and chloritoid in the thin sections account for a metamorphic basement derived source, whereas a sand-rich system and coal fragments account for an uplifted sedimentary source.
- Based on palynological age datings in combination with sedimentological observations in the present study, two likely age models are presented for the deposits at Calypsostranda: i) a Paleocene/early Eocene age either with deposition in a pull-apart basin off the western coast of Spitsbergen, or in connection with the lower parts of the Central Tertiary Basin succession ii) a late Eocene/early Oligocene age with deposition in a fault bounded graben and sourcing from lower parts of the CTB in addition to the WSFTB .
- There are similarities between the Firkanten Formation and the Calypsostranda Group in terms of the stratigraphic setting, lithostratigraphy and petrographic composition and it is likely that the succession at Calypsostranda is of Paleocene age. A plausible provenance would be an uplifted bulge to the northeast-east contributing with both basement derived sediments and clastic sediments (perhaps uplifted Mesozoic strata).

References

- Amos, K. J., Alexander, J., Horn, A., Pocock, G. D., & Fielding, C. R. (2004). Supply limited sediment transport in a high-discharge event of the tropical Burdekin River, North Queensland, Australia. *Sedimentology*, 51(1), 145-162.
- Bergh, S. G., Braathen, A., & Andresen, A. (1997). Interaction of basement-involved and thin-skinned tectonism in the Tertiary fold-thrust belt of central Spitsbergen, Svalbard. *AAPG bulletin*, 81(4), 637-661.
- Berner, R. A. (1970). Sedimentary pyrite formation. *American Journal of Science*, 268(1), 1-23.
- Bhattacharya, J. (2010). Deltas. In N. P. James & R. W. Dalrymple (Eds.), *Facies Models 4* (pp. 233-265): Geological Association of Canada.
- Birkenmajer, K. (2006). Character of basal and intraformational unconformities in the Calypsostranda Group (late Palaeogene), Bellsund, Spitsbergen. *Polish Polar Research*, 27(2), 107-118.
- Birkenmajer, K., & Gmur, D. (2010). Coals of the Calypsostranda Group (Palaeogene) at Bellsund, Spitsbergen. *Studia Geologica Polonica*, 133, 51-63.
- Birkenmajer, K., & Zastawniak, E. (2005). A new late Palaeogene macroflora from Bellsund, Spitsbergen. *ACTA PALAEOBOTANICA-KRAKOW-*, 45(2), 145.
- Bjørkum, P. A., & Walderhaug, O. (1990). Geometrical arrangement of calcite cementation within shallow marine sandstones. *Earth Science Reviews*, 29(1), 145-161.
- Blinova, M., Thorsen, R., Mjelde, R., & Faleide, J. I. (2009). Structure and evolution of the Bellsund Graben between Forlandsundet and Bellsund (Spitsbergen) based on marine seismic data.
- Blomeier, D., Dustira, A., Forke, H., & Scheibner, C. (2011). Environmental change in the Early Permian of NE Svalbard: from a warm-water carbonate platform (Gipshuken Formation) to a temperate, mixed siliciclastic-carbonate ramp (Kapp Starostin Formation). *Facies*, 57(3), 493-523.
- Blomeier, D., Scheibner, C., & Forke, H. (2009). Facies arrangement and cyclostratigraphic architecture of a shallow-marine, warm-water carbonate platform: the Late Carboniferous Ny Friesland Platform in eastern Spitsbergen (Pyefjellet Beds, Wordiekammen Formation, Gipsdalen Group). *Facies*, 55(2), 291-324.
- Braathen, A., Bergh, S. G., & Maher, H. D. (1999). Application of a critical wedge taper model to the Tertiary transpressional fold-thrust belt on Spitsbergen, Svalbard. *Geological Society of America Bulletin*, 111(10), 1468-1485.
- Bridge, J., & Demicco, R. (2008). *Earth Surface Processes, Landforms and Sediment Deposits*: Cambridge University Press.
- Bruhn, R., Steel, R., & Bruhn, R. (2003). High-resolution sequence stratigraphy of a clastic foredeep succession (Paleocene, Spitsbergen): An example of peripheral-bulge-controlled depositional architecture. *Journal of Sedimentary Research*, 73(5).

- Cavanagh, A. J., Di Primio, R., Scheck-Wenderoth, M., & Horsfield, B. (2006). Severity and timing of Cenozoic exhumation in the southwestern Barents Sea. *Journal of the Geological Society*, 163(5), 761-774.
- Cheel, R. (2005). Introduction to clastic sedimentology. *ERSC 2P10 Course Notes. Brock University, Ontario*.
- Dallmann, W. K. (1989). The nature of the Precambrian-Tertiary boundary at Renardodden, Bellsund, Svalbard. *Polar Research*, 7(2), 139-145.
- Dallmann, W. K., Blomeier, D., & Elvevold, S. (Cartographer). (2015). Geoscience atlas of Svalbard
- Dallmann, W. K., Stratigrafisk komité for, S., Norsk, p., & Norges Svalbard- og, I.-u. (1999). *Lithostratigraphic lexicon of Svalbard : review and recommendations for nomenclature use : Upper Palaeozoic to Quaternary bedrock*. Tromsø: Norsk polarinstitutt.
- Dalrymple, R. W. (2010). Tidal depositional systems. In N. P. James & R. W. Dalrymple (Eds.), *Facies Models 4* (pp. 201-232): Geological Association of Canada.
- Dickinson, W. R. (1970). Interpreting detrital modes of graywacke and arkose. *Journal of Sedimentary Research*, 40(2).
- Dickinson, W. R., Beard, L., Brakenridge, G., Erjavec, J., Ferguson, R., Inman, K., . . . Dickinson, W. (1983). Provenance of North American Phanerozoic sandstones in relation to tectonic setting. *Bulletin of the Geological Society of America*, 94(2), 222-235.
- Dickinson, W. R., & Suczek, C. A. (1979). Plate tectonics and sandstone compositions. *AAPG bulletin*, 63(12), 2164-2182.
- Dott Jr, R. H. (1964). Wacke, Graywacke and Matrix--What Approach to Immature Sandstone Classification? *Journal of Sedimentary Research*, 34(3).
- Døssing, A., Stemmerik, L., Dahl-Jensen, T., & Schlindwein, V. (2010). Segmentation of the eastern North Greenland oblique-shear margin — Regional plate tectonic implications. *Earth and Planetary Science Letters*, 292(3), 239-253.
- Faleide, J. I., Vågnes, E., & Gudlaugsson, S. T. (1993). Late Mesozoic-Cenozoic evolution of the south-western Barents Sea in a regional rift-shear tectonic setting. *Marine and Petroleum Geology*, 10(3), 186-214.
- Fielding, C. R., Trueman, J. D., & Alexander, J. (2005). Sharp-Based, Flood-Dominated Mouth Bar Sands from the Burdekin River Delta of Northeastern Australia: Extending the Spectrum of Mouth-Bar Facies, Geometry, and Stacking Patterns. *Journal of Sedimentary Research*, 75(1), 55-66.
- Fossen, H., Pedersen, R. F., Bergh, S. G., & Andresen, A. (2006). En fjellkjede blir til, oppbygningen av kaledonidene; ca. 500-405 millioner år. In I. B. Ramberg, I. Bryhni & A. Nøttvedt (Eds.), *Landet blir til* (pp. 178-229). Trondheim: Norsk Geologisk Forening.
- Frey, R. W., Howard, J. D., & Pryor, W. A. (1978). Ophiomorpha: Its morphologic, taxonomic, and environmental significance. *Palaeogeography, Palaeoclimatology, Palaeoecology*, 23(C), 199-229.
- Friend, P. F., & Moody-Stuart, M. (1972). *Sedimentation of the Wood Bay Formation (Devonian) of Spitsbergen : regional analysis of a late orogenic basin* (Vol. nr 157). Oslo: Norsk polarinstitutt.

- Gibling, M. R. (2006). Width and Thickness of Fluvial Channel Bodies and Valley Fills in the Geological Record: A Literature Compilation and Classification. *Journal of Sedimentary Research*, 76(5), 731-770.
- Gjelberg. (2010). *Facies analysis and sandbody geometry of the paleogene Battfjellet Formation, central western Nordenskiöld Land, Spitsbergen*. H.K. Gjelberg, Universitetet i Bergen Institutt for, geovitenskap.
- Gjelberg, & Steel, R. (1981). An outline of lower-middle Carboniferous sedimentation on Svalbard: effects of tectonic, climatic and sea level changes in rift basin sequences.
- Golonka, J., Bocharova, N. Y., Ford, D., Edrich, M. E., Bednarczyk, J., Wildharber, J., & Golonka, J. (2003). Paleogeographic reconstructions and basins development of the Arctic. *Marine and Petroleum Geology*, 20(3), 211-248.
- Gradstein, F. M., Kristiansen, I. L., Loemo, L., & Kaminski, M. A. (1992). Cenozoic Foraminiferal and Dinoflagellate Cyst Biostratigraphy of the Central North Sea. *Micropaleontology*, 38(2), 101-137.
- Grundvag, S. A., Johannessen, E., Helland-Hansen, W., & Plink-Bjorklund, P. (2014). Depositional architecture and evolution of progradationally stacked lobe complexes in the Eocene Central Basin of Spitsbergen. In *Sedimentology* (Vol. 61, pp. 535-569).
- Guccione, M. (2009). Grain-size distribution of overbank sediment and its use to locate channel positions. *Alluvial Sedimentation*. Blackwell Publishing Ltd, 185-194.
- Hall, J., Mozley, P., Davis, J., Delude-Roy, N., & Hall, J. (2004). Environments of formation and controls on spatial distribution of calcite cementation in Plio-Pleistocene fluvial deposits, New Mexico, USA. *Journal of Sedimentary Research*, 74(5).
- Harding, I. C., Charles, A. J., Marshall, J. E., Pälike, H., Roberts, A. P., Wilson, P. A., . . . Moremon, R. (2011). Sea-level and salinity fluctuations during the Paleocene–Eocene thermal maximum in Arctic Spitsbergen. *Earth and Planetary Science Letters*, 303(1), 97-107.
- Harland, W. B., Anderson, L. M., & Manasrah, D. (1997). *The geology of Svalbard* (Vol. 17). London: Geological Society.
- Harland, W. B., & Wright, N. (1979). Alternative hypothesis for the pre-Carboniferous evolution of Svalbard. *Norsk Polarinstitutt Skrifter*, 167, 89-117.
- Head, M. (1984). A palynological investigation of Tertiary strata at Renardodden, West Spitsbergen. *Abstract, 6th International palynological Conference, Calgary 1984*, 61.
- Heer, O. (1876). Florafossilisarctica.IV(1).InK. *Svenska Vetensk. Akad. Handl*, 14(5), 141 pp. 132 pls.
- Helland-Hansen, W., & Helland-Hansen, W. (2010). Facies and stacking patterns of shelf-deltas within the Palaeogene Battfjellet Formation, Nordenskiöld Land, Svalbard: implications for subsurface reservoir prediction. *Sedimentology*, 57(1), 190-208.
- Hellem, T. (1980). *En sedimentologisk og diagenetisk undersøkelse av utvalgte profiler fra Tempelfjordgruppen (Perm) i Isfjordområdet, Spitsbergen*. MSc thesis, University of Oslo, Norway,
- Henriksen, E., Ryseth, A., Larssen, G., Heide, T., Roenning, K., Sollid, K., . . . Henriksen, E. (2011). Chapter 10 Tectonostratigraphy of the greater

- Barents Sea: implications for petroleum systems. *Geological Society, London, Memoirs*, 35(1), 163-195.
- Jerram, D. A. (2001). Visual comparators for degree of grain-size sorting in two and three-dimensions. *Computers and Geosciences*, 27(4), 485-492.
- Joly, D., Geir, A., Eirik, M., & Lennart, N. (2016). Building an indicator to characterize the thermal conditions for plant growth on an Arctic archipelago, Svalbard. *Building an indicator to characterize the thermal conditions for plant growth on an Arctic archipelago, Svalbard*, 66, 623-631.
- Jones, G. E., Hodgson, D. M., & Flint, S. S. (2013). Contrast in the process response of stacked clinothems to the shelf-slope rollover. *Geosphere*, 9(2), 299-316.
- Kaus, B. J. P., & Podladchikov, Y. Y. (2001). Forward and reverse modeling of the three-dimensional viscous Rayleigh-Taylor instability. *Geophysical Research Letters*, 28(6), 1095-1098.
- Kellogg, H. E. (1975). Tertiary stratigraphy and tectonism in Svalbard and continental drift. *AAPG bulletin*, 59(3), 465-485.
- Kleinspehn, K. L., & Teyssier, C. (1992). Tectonics of the Palaeogene Forlandsundet Basin, Spitsbergen: a preliminary report. *Norsk Geologisk Tidsskrift*, 72(1), 93-104.
- Knaust, D. (2017). The ichnogenus *Teichichnus* Seilacher, 1955. *Earth-Science Reviews*.
- Leever, K. A., Gabrielsen, R. H., Faleide, J. I., & Braathen, A. (2011). A transpressional origin for the West Spitsbergen fold-and-thrust belt: Insight from analog modeling. *Tectonics*, 30(2), n/a-n/a.
- Leith, T. L., Weiss, H. M., Mørk, A., århus, N., Elvebakk, G., Embry, A. F., . . . Borisov, A. V. (1993). Mesozoic hydrocarbon source-rocks of the Arctic region. In T. O. Vorren, E. Bergsager, Ø. A. Dahl-Stamnes, E. Holter, B. Johansen, E. Lie & T. B. Lund (Eds.), *Norwegian Petroleum Society Special Publications* (Vol. 2, pp. 1-25): Elsevier.
- Lenz, O. (2017). Report on palynostratigraphic analysis of sediment samples WJL-17-3 to WJL-17-12. *Institut für Angewandte Geowissenschaften, Fachgebiet Angewandte Sedimentgeologie (Unpublished report)*
- Livsic, J. (1974). Palaeogene deposits and the platform structure of Svalbard.
- Lüthje, C. J. (2008). Transgressive development of coal-bearing coastal plain to shallow marine setting in a flexural compressional basin, Paleocene, Svalbard, Arctic Norway.
- Manum, S. B., & Throndsen, T. (1986). Age of Tertiary formations on Spitsbergen. *Polar Research*, 4(2), 103-131.
- Martinsen, O., & Nøttvedt, A. (2006). Av hav stiger landet: Paleogen og Neogen (Kenozoikum), kontinentene av i dag formes; 66-2,7 millioner år In I. B. Ramberg, I. Bryhni & A. Nøttvedt (Eds.), *Landet blir til* (pp. 447-477). Trondheim: Norsk Geologisk Forening.
- Mellere, D., Plink-Bjorklund, P., & Steel, R. (2002). Anatomy of shelf deltas at the edge of a prograding Eocene shelf margin, Spitsbergen. *Sedimentology*, 49(6), 1181-1206.
- Miall, A. D. (2010). Alluvial deposits. In N. P. James & R. W. Dalrymple (Eds.), *Facies Models 4* (pp. 105-137): Geological Association of Canada.
- Miall, A. D. (2013). *The geology of fluvial deposits: sedimentary facies, basin analysis, and petroleum geology*: Springer.

- Mueller, R., Nystuen, J., Wright, V., & Mueller, R. (2004). Pedogenic mud aggregates and paleosol development in ancient dryland river systems: Criteria for interpreting alluvial mudrock origin and floodplain dynamics. *Journal of Sedimentary Research*, 74(4).
- Müller, R. D., & Spielhagen, R. F. (1990). Evolution of the Central Tertiary Basin of Spitsbergen: towards a synthesis of sediment and plate tectonic history. *Palaeogeography, Palaeoclimatology, Palaeoecology*, 80(2), 153-172.
- Nagy, J. (2005). Delta-influenced foraminiferal facies and sequence stratigraphy of Paleocene deposits in Spitsbergen. *Palaeogeography, Palaeoclimatology, Palaeoecology*, 222(1), 161-179.
- Nagy, J., Tovar, F. J. R., & Reolid, M. (2016). Environmental significance of Ophiomorpha in a transgressive–regressive sequence of the Spitsbergen Paleocene. *Polar Research*, 35(1), 24192.
- Nathorst, A. G. (1910). Beitrage zur Geologie der Bareninsel. *Uppsala*, 10, 261-416.
- Noda, A. (2013). Strike-Slip Basin–Its Configuration and Sedimentary Facies. In *Mechanism of Sedimentary Basin Formation-Multidisciplinary Approach on Active Plate Margins*: InTech.
- Nøttvedt, A. (1985). Askeladden Delta Sequence (Palaeocene) on Spitsbergen–sedimentation and controls on delta formation. *Polar Research*, 3(1), 21-48.
- Odin, G. S., & Matter, A. (1981). De glauconiarum origine. *Sedimentology*, 28(5), 611-641.
- Owen, G. (1987). Deformation processes in unconsolidated sands. *Geological Society, London, Special Publications*, 29(1), 11-24.
- Paola, C., Wiebe, S. M., & Reinhart, M. A. (1989). Upper-regime parallel lamination as the result of turbulent sediment transport and low-amplitude bed forms. *Sedimentology*, 36(1), 47-59.
- Pattison, S. A. (2005). Isolated highstand shelf sandstone body of turbiditic origin, lower Kenilworth Member, Cretaceous Western Interior, Book Cliffs, Utah, USA. *Sedimentary Geology*, 177(1), 131-144.
- Petersen, T. G., Thomsen, T. B., Olaussen, S., & Stemmerik, L. (2016). Provenance shifts in an evolving Eurekan foreland basin: the Tertiary Central Basin, Spitsbergen.(Report)(Author abstract). *Journal of the Geological Society*, 173(4), 634.
- Petter, A. L., & Steel, R. J. (2006). Hyperpycnal flow variability and slope organization on an Eocene shelf margin, Central Basin, Spitsbergen. *AAPG bulletin*, 90(10), 1451-1472.
- Pettijohn, F., Potter, P., & Siever, R. (1987). Sand and Sandstone, 2nd. In: Springer, New York.
- Pichler, H., & Schmitt-Riegraf, C. (1997). *Rock-forming minerals in thin section*: Chapman & Hall.
- Powers, M. C. (1953). A new roundness scale for sedimentary particles. *Journal of Sedimentary Research*, 23(2).
- Prior, D. B., & Bornhold, B. D. (1989). Submarine sedimentation on a developing Holocene fan delta. *Sedimentology*, 36(6), 1053-1076.
- Reading, H. G. (1996). Sedimentary Environments: Processes, Facies and Stratigraphy. 3rd. Edition. *Blackwell Science. Oxford*.
- Riis, F., Lundschieen, B. A., Hoy, T., Mork, A., Mork, M. B. E., Mork, A., . . . Weitschat, W. (2008). Evolution of the Triassic shelf in the northern Barents Sea

- region. In (Vol. 27, pp. 318-338). Oxford: Oxford, United Kingdom: Blackwell in partnership with the Norwegian Polar Institute.
- Rosenkrantz, A. (1942). Slregten Thyasira's geologiske Optraeden. *Meddel. Dansk Geol. For.*, 10, , 277-278.
- Schlegel, A., Lisker, F., Dörr, N., Jochmann, M., Schubert, K., & Spiegel, C. (2013). Petrography and geochemistry of siliciclastic rocks from the Central Tertiary Basin of Svalbard—implications for provenance, tectonic setting and climate [Petrografie und Geochemie siliziklastischer Gesteine aus dem Zentralen Tertiärbecken auf Spitzbergen—Folgerungen für das Liefergebiet, seine tektonische Stellung und das Klima.]. *Zeitschrift der Deutschen Gesellschaft für Geowissenschaften*, 164(1), 173-186.
- Singh, I. B. (1972). On the bedding in the natural-levee and the point-bar deposits of the Gomti river, Uttar Pradesh, India. *Sedimentary Geology*, 7(4), 309-317.
- Smelror, M., Basov, V. A., & Norges geologiske, u. k. (2009). *Atlas: geological history of the Barents Sea*. Trondheim: Geological Survey of Norway.
- Steel, R. J., Dalland, A., Kalgraff, K., & Larsen, V. (1981). The Central Tertiary Basin of Spitsbergen: sedimentary development of a sheared-margin basin.
- Steel, R. J., Gjelberg, J., Helland-Hansen, W., Kleinspehn, K., Nøttvedt, A., & Rye-Larsen, M. (1985). The Tertiary strike-slip basins and orogenic belt of Spitsbergen.
- Steel, R. J., & Worsley, D. (1984). Svalbard's post-Caledonian strata—an atlas of sedimentational patterns and palaeogeographic evolution. In *Petroleum geology of the North European margin* (pp. 109-135): Springer.
- Stemmerik, L. (1997). Permian (Artinskian Kazanian) Cool-Water Carbonates in North Greenland, Svalbard and the Western Barents Sea.
- Stow, D. A. (2005). *Sedimentary rocks in the Field: a color guide*: Gulf Professional Publishing.
- Tchoumatchenco, P., & Uchman, A. (2001). The oldest deep-sea Ophiomorpha and Scolicia and associated trace fossils from the Upper Jurassic–Lower Cretaceous deep-water turbidite deposits of SW Bulgaria. *Palaeogeography, Palaeoclimatology, Palaeoecology*, 169(1), 85-99.
- Thiedig, F., Pickton, C., Lehmann, U., Harland, W., & Anderson, H. (1979). Das Tertiär von Renardodden (östlich Kapp Lyell, Westspitzbergen, Svalbard). *Mitteilungen Geologisch– Paläontologisches Institut der Universität Hamburg*, 49, 135-146.
- Ulmer-Scholle, D. S., Scholle, P. A., Schieber, J., & Raine, R. J. (2014). *A color guide to the petrography of sandstones, siltstones, shales and associated rocks*: American Association of Petroleum Geologists.
- Vonderbank, K. (1970). Geologie und fauna der Tertiären Ablagerungen zentral-Spitzbergens.
- Vorren, T. O. (1993). *Arctic geology and petroleum potential : proceedings of the Norwegian Petroleum Society conference, 15-17 August 1990, Troms?, Norway* (Vol. no. 2). Amsterdam: Elsevier.
- Wanas, H. A. (2008). Calcite-cemented concretions in shallow marine and fluvial sandstones of the Birket Qarun Formation (Late Eocene), El-Faiyum depression, Egypt: Field, petrographic and geochemical studies: Implications for formation conditions. *Sedimentary Geology*, 212(1), 40-48.

- Wellner, R., Beaubouef, R., Van Wagoner, J., Roberts, H., & Sun, T. (2005). Jet-plume depositional bodies—the primary building blocks of Wax Lake Delta.
- Wilson, M., Deer, W., Howie, R., & Zussman, J. (2013). *Rock-Forming Minerals, Volume 3C, Sheet Silicates: Clay Minerals*. Paper presented at the Geological Society, London.
- Worsley, D. (2008). The post-Caledonian development of Svalbard and the western Barents Sea. *Polar Research*, 27(3), 298-317.
- Worsley, D., Aga, O. J., Statoil, & StatoilHydro. (1986). *The geological history of Svalbard : evolution of an arctic archipelago*. Stavanger: Den norske stats oljeselskap a.s.
- Zhang, P., Zhang, J., Lee, Y., Song, M., Zhang, M., Li, J., . . . Cheng, S. (2015). Diagenesis of braided fluvial sandstones and its implications for prediction of reservoir quality: a case study on the Neogene Shawan Formation, Junggar Basin, NW China. *Arabian Journal of Geosciences*, 8(1), 29-37.
- Zhou, W., & Wang, Z. L. (2007). *Scanning Microscopy for Nanotechnology: Techniques and Applications*. New York, NY: Springer New York: New York, NY.

Online resources

Norsk Polarinstitutt

<http://toposvalbard.npolar.no/> (accessed 02.12.2017)

Appendix A

Petrography data

In this appendix, Grain sizes for each sample is presented (A.1) in addition to raw data from the line scan analysis from the scanning electron microscope (SEM) for each of the studied samples (A.2).

A.1 Grain size chart

Measure of grain sizes displays great variety throughout the whole succession (Fig A.1). The majority of the samples in the marine environment are in the range 100-150 μm (very fine to fine sand). The floodplain environment in contrast, shows a variety in the dominant grain size from clay to fine sand. The largest dominant grain sizes are found in the channel systems with values of 200 μm representing the upper range of fine grain size.

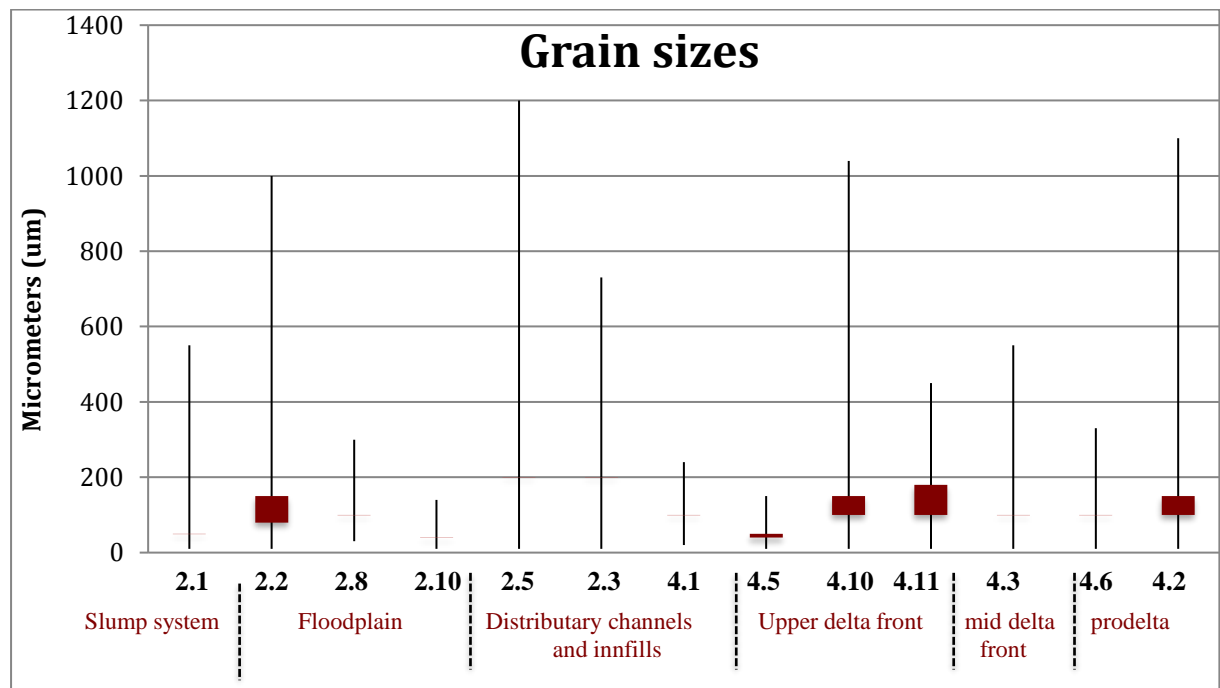


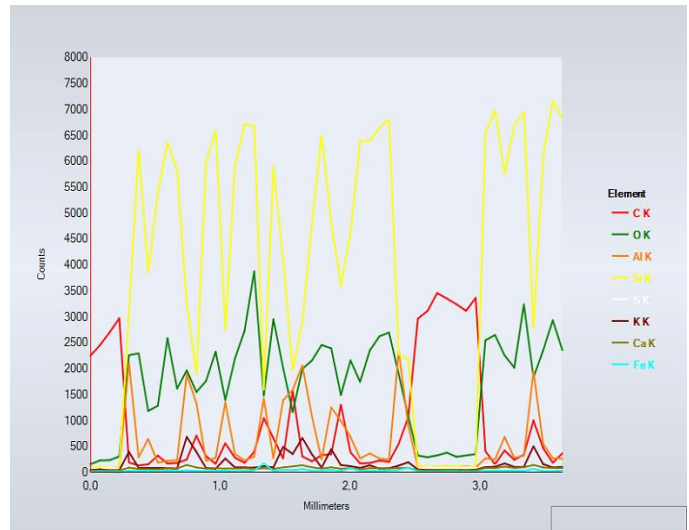
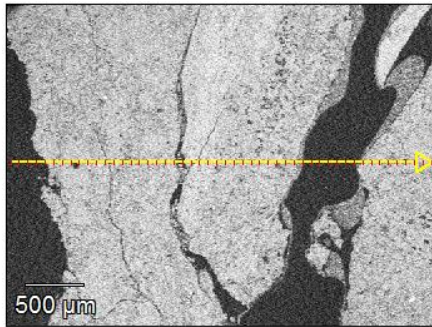
Fig A.1: Grain sizes for each sample, subdivided into depositional environments. The red box shows the distribution of dominant grain sizes per sample, whereas the black

vertical line exhibits the positive and negative size distributions from smallest measured grain size to the largest measured grain size per sample.

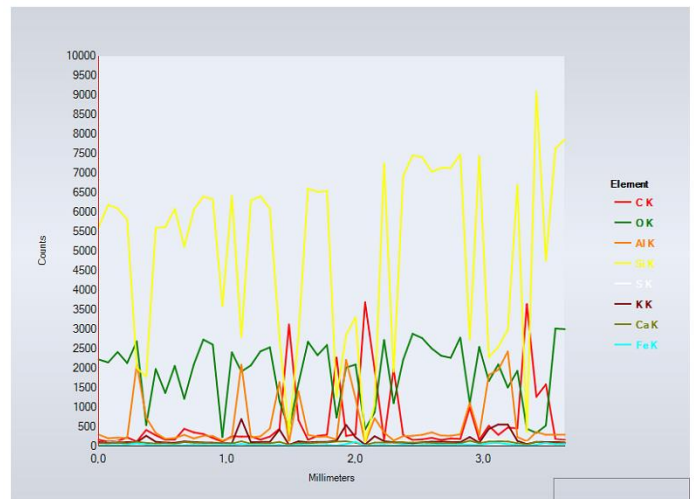
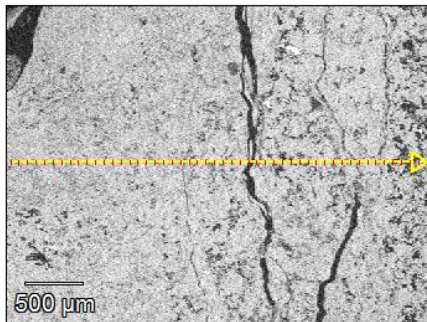
A.2 SEM scan lines (raw data)

Sample 2.1

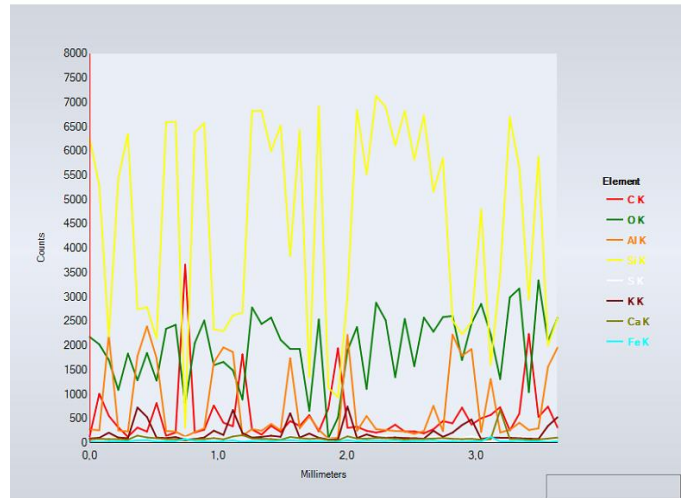
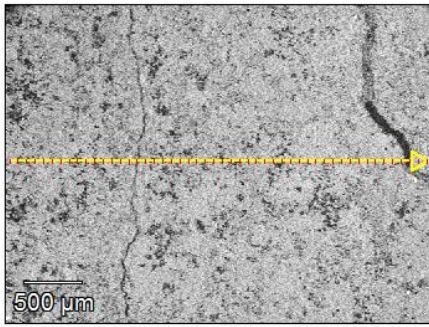
2-1(1)



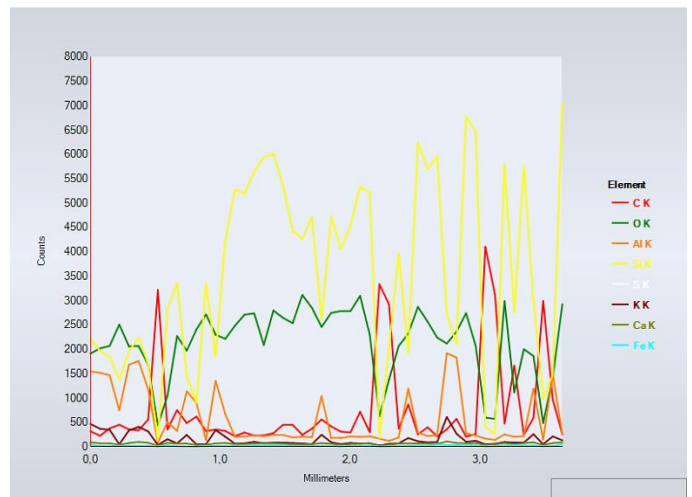
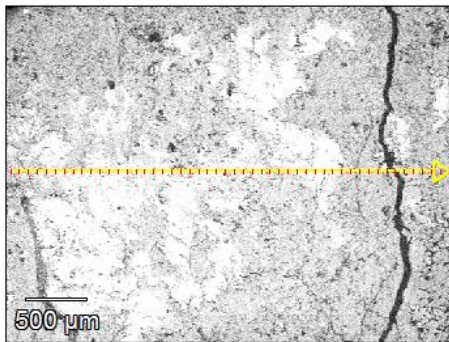
2-1(2)



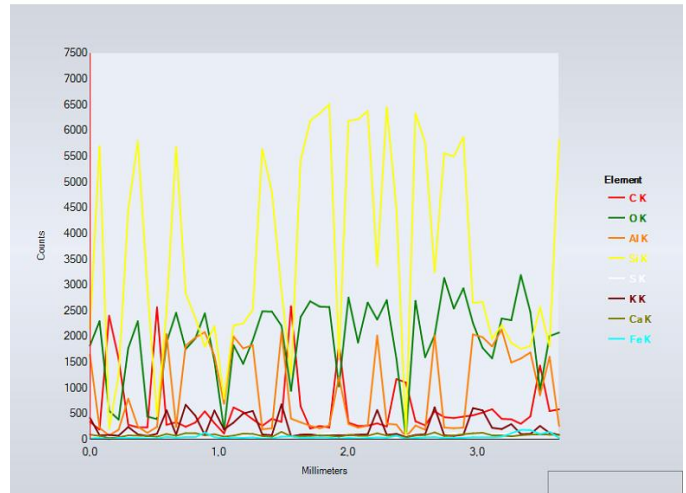
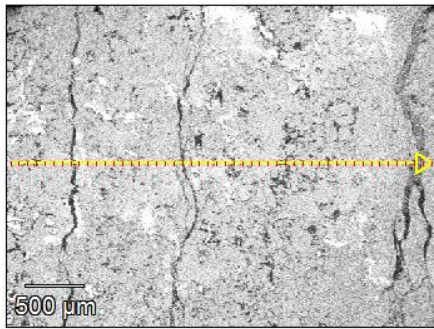
2-1(3)



2-1(4)



2-1(5)



2-1(6)

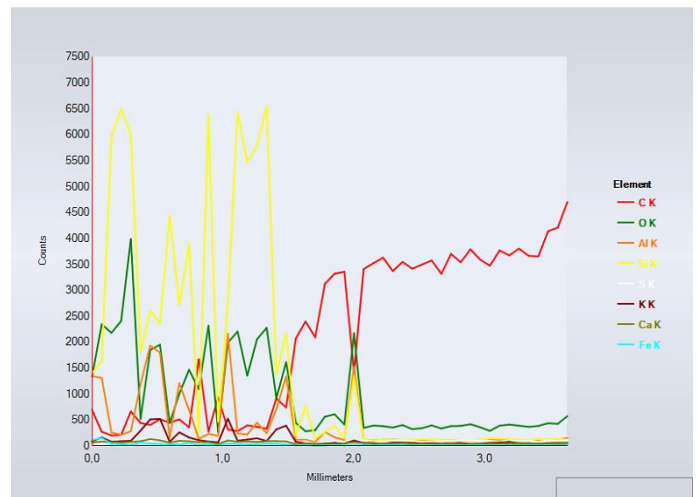
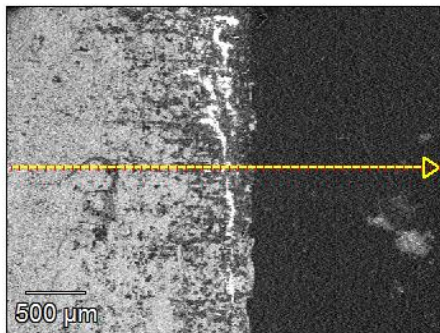
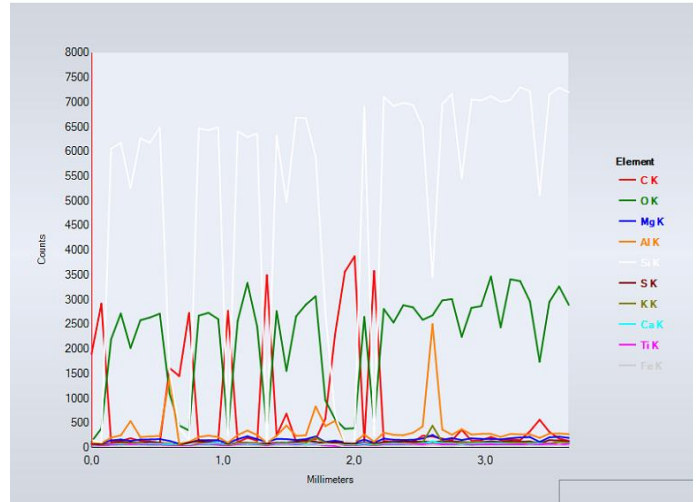
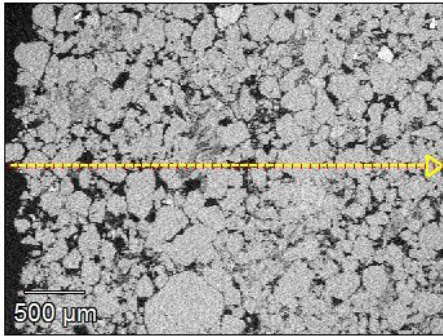


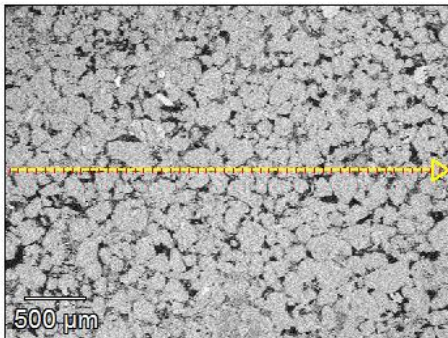
Figure A.2: Backscatter electron images and X-ray spectrums derived from line scans from sample 2.1

Sample 2.2

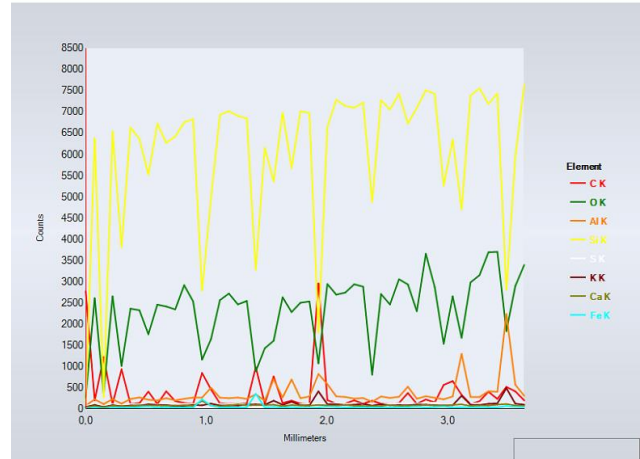
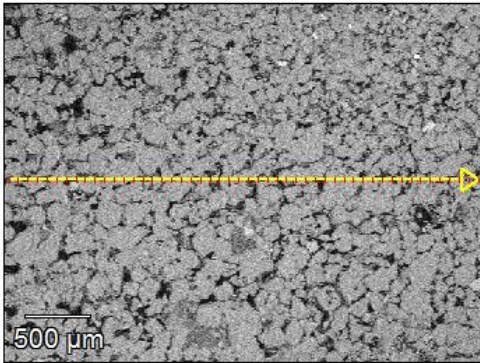
2-2 line(1)



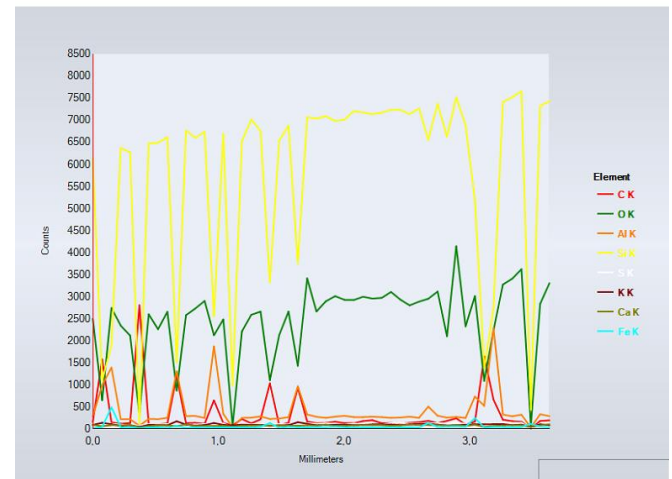
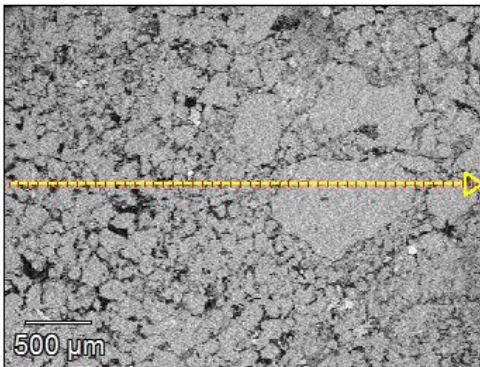
2-2 line(2)



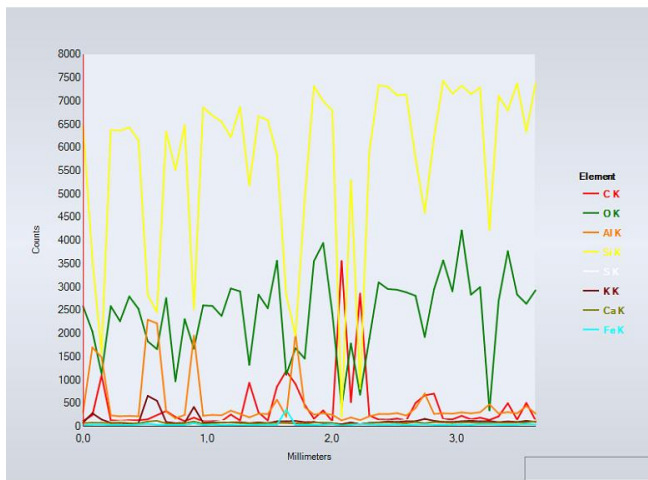
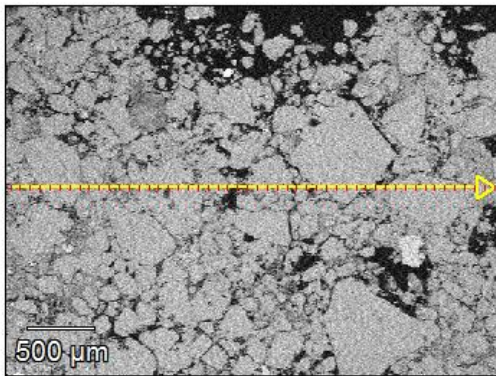
2-2 line(3)



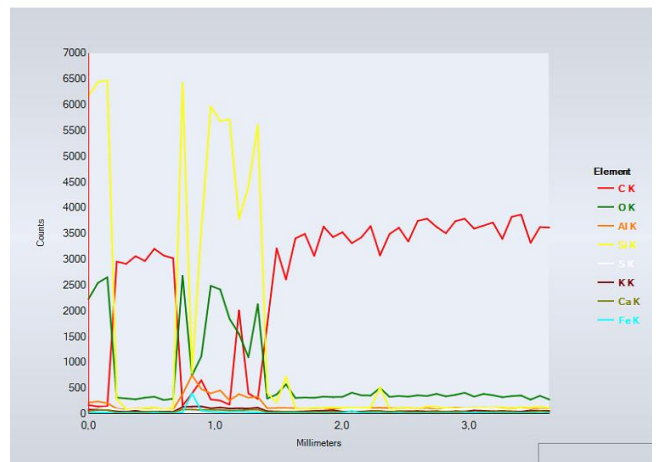
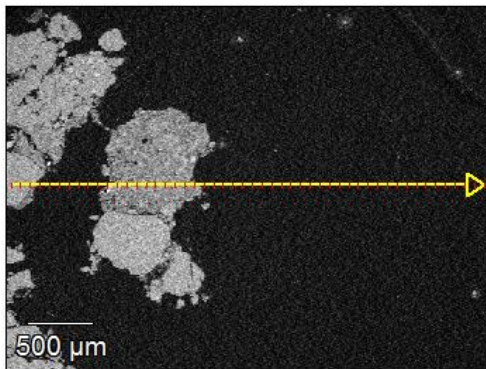
2-2 line(4)



2-2 line(5)



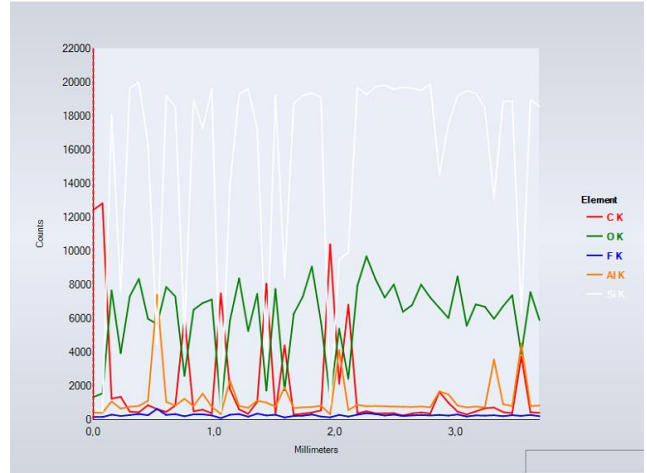
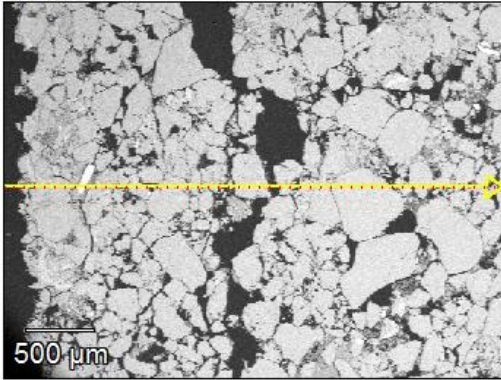
2-2 line(6)



Sample 2.3

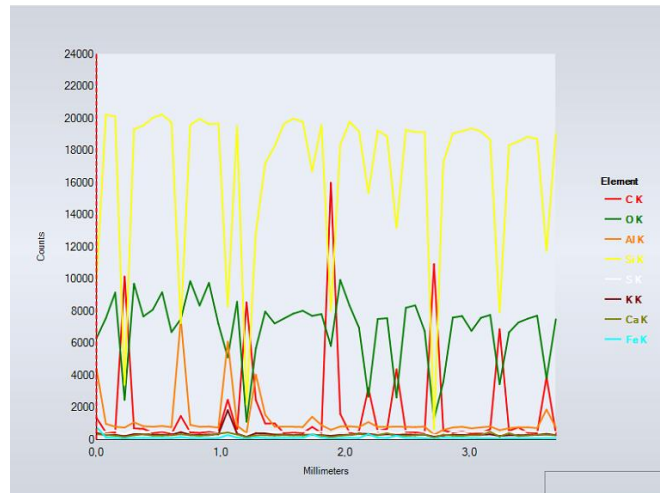
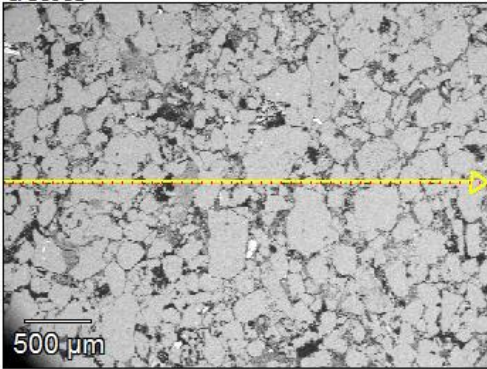
1(1)

X: 256 Y: 192
I: 54193



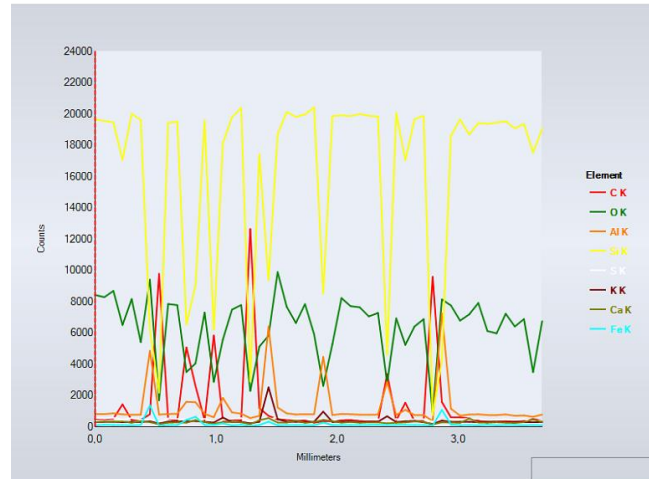
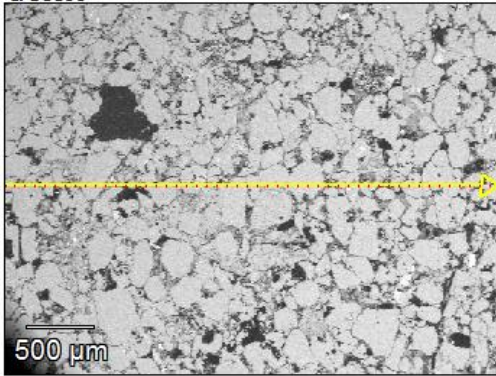
2(1)

X: 256 Y: 192
I: 50961



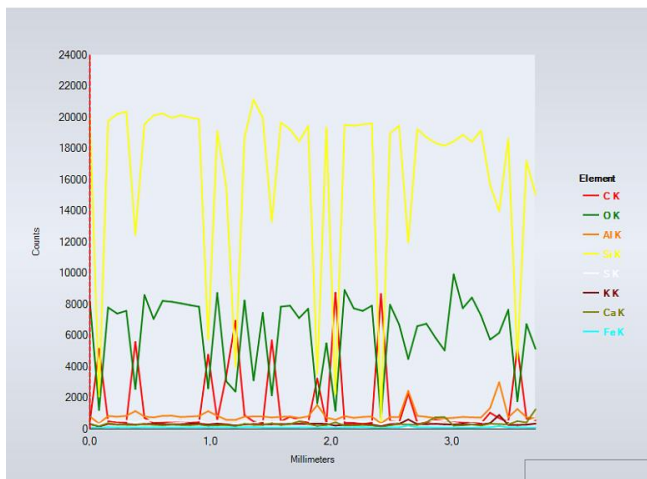
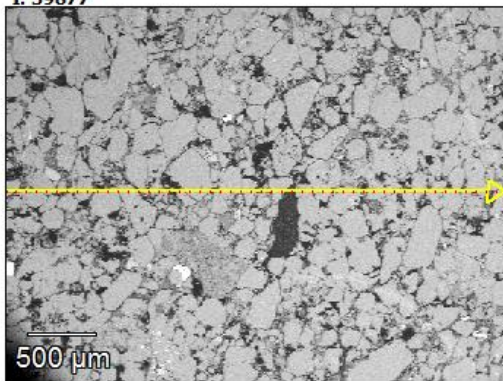
3(1)

X: 256 Y: 192
I: 58099



4(1)

X: 256 Y: 192
I: 39877



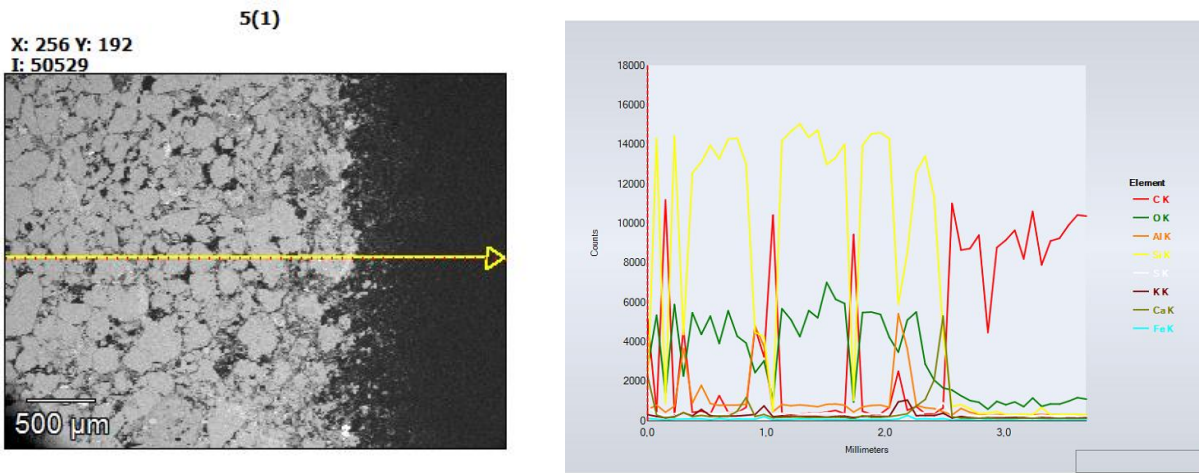
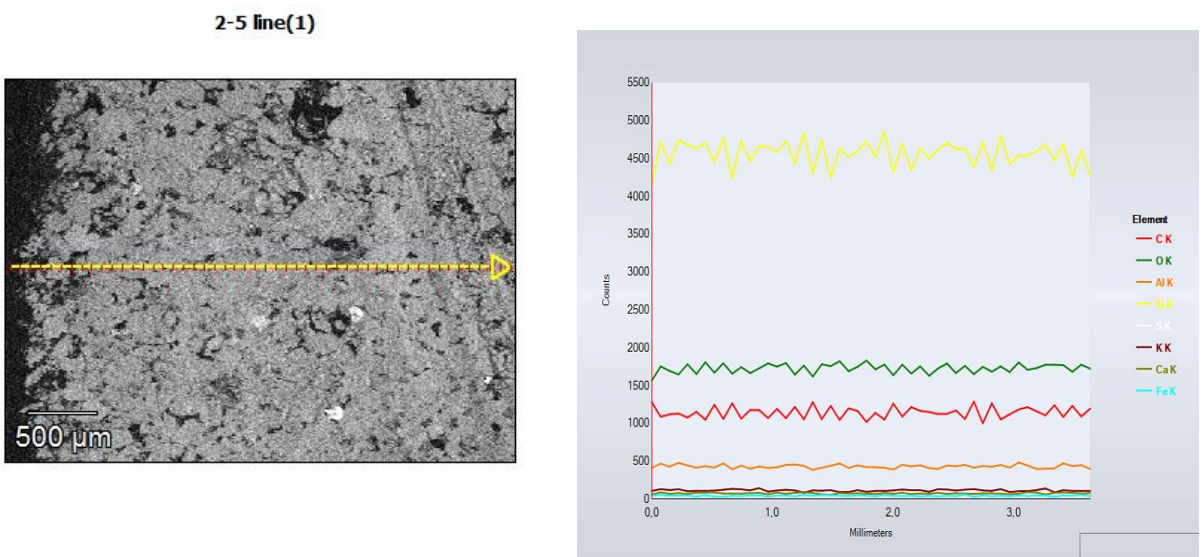
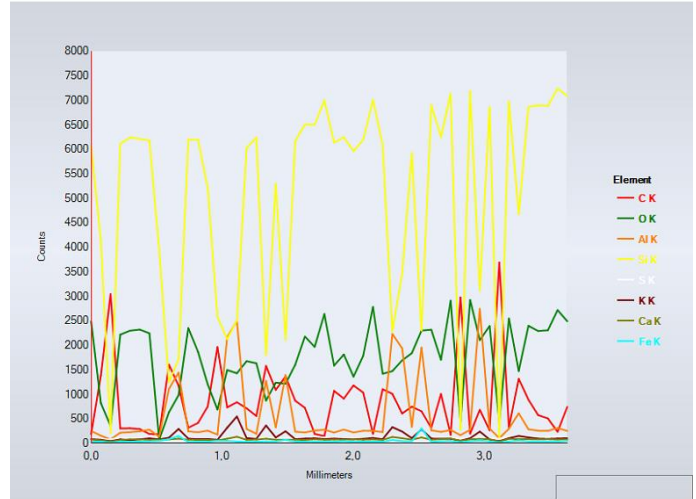
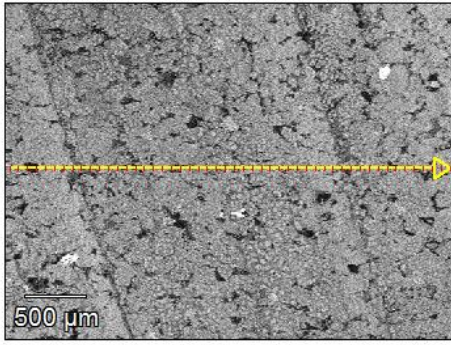


Figure A.4: Backscatter electron images and X-ray spectrums derived from line scans from sample 2.3

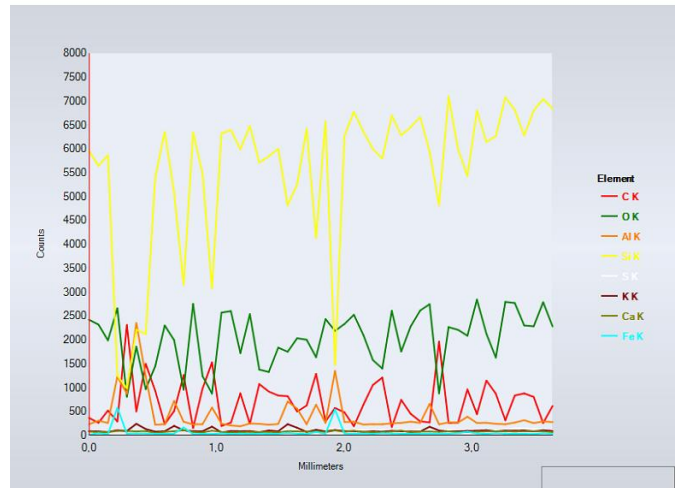
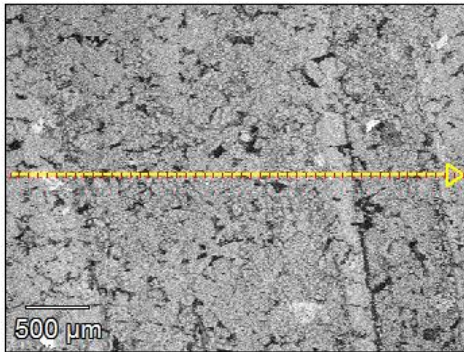
Sample 2.5



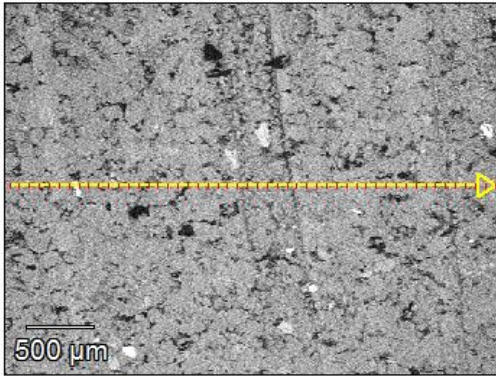
2-5 line(2)



2-5 line(3)



2-5 line(4)



2-5 line(5)

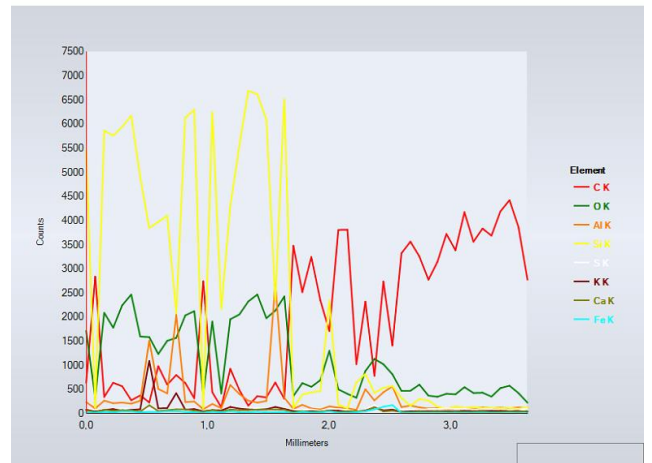
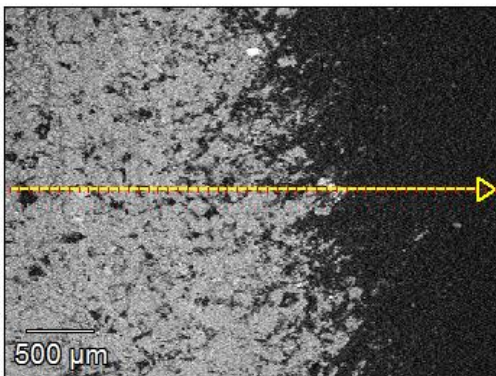
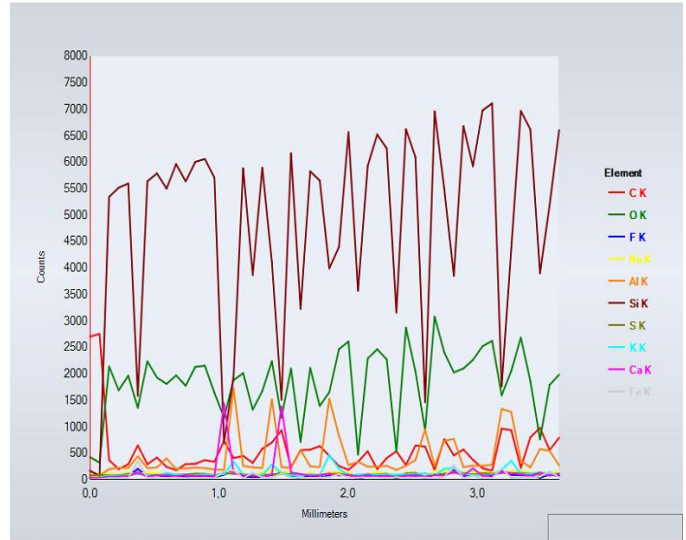
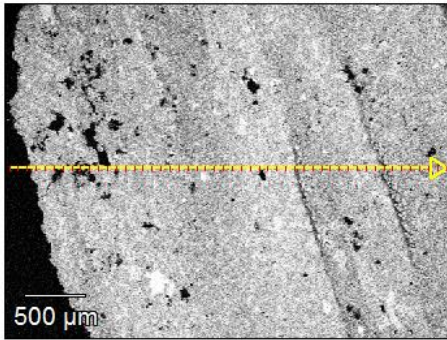


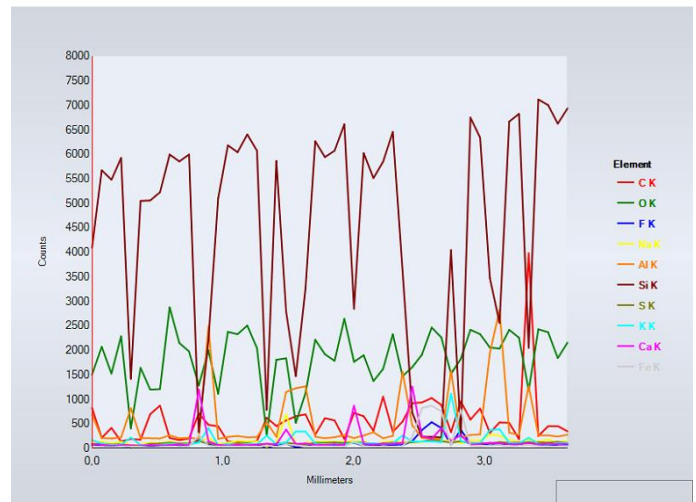
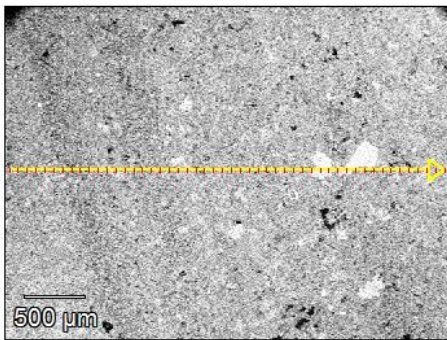
Figure A.5: Backscatter electron images and X-ray spectrums derived from line scans from sample 2.5

Sample 2.8

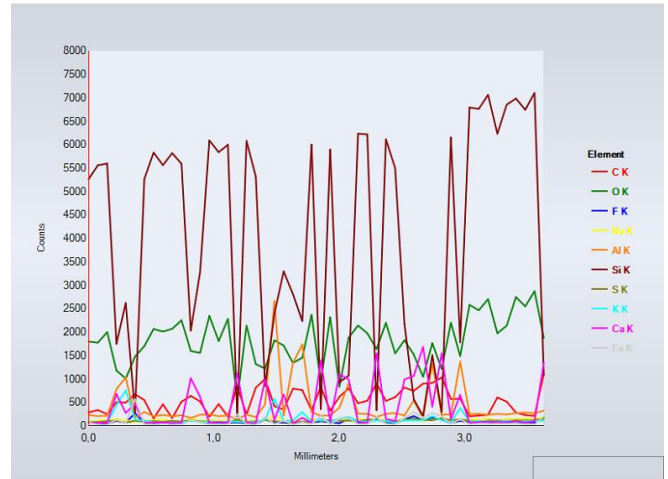
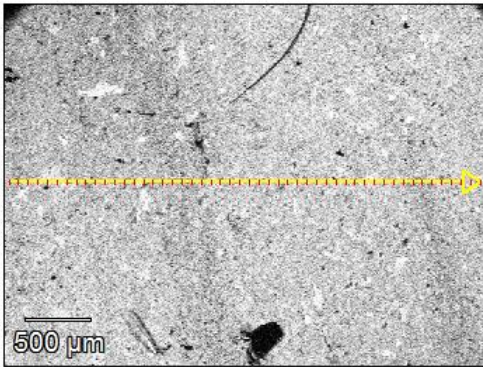
2-8 linecorrect(1)



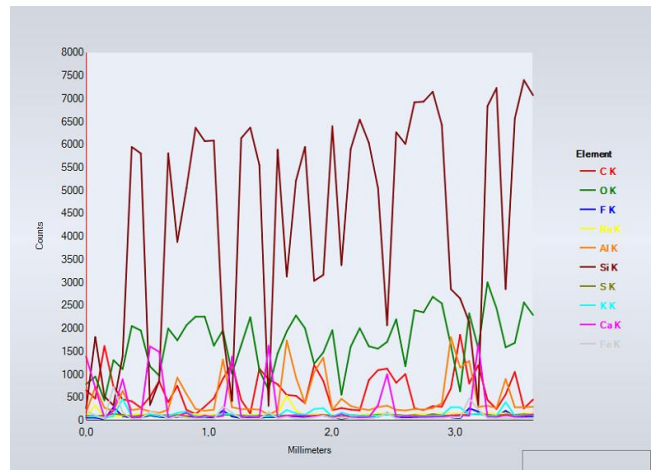
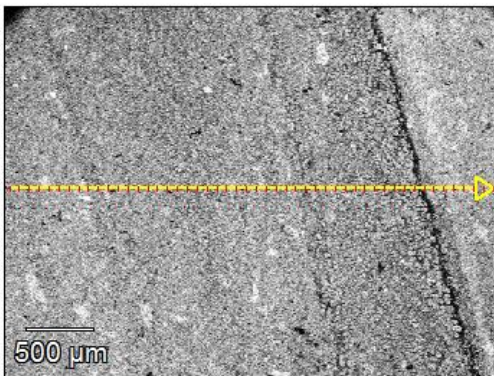
2-8 linecorrect(2)



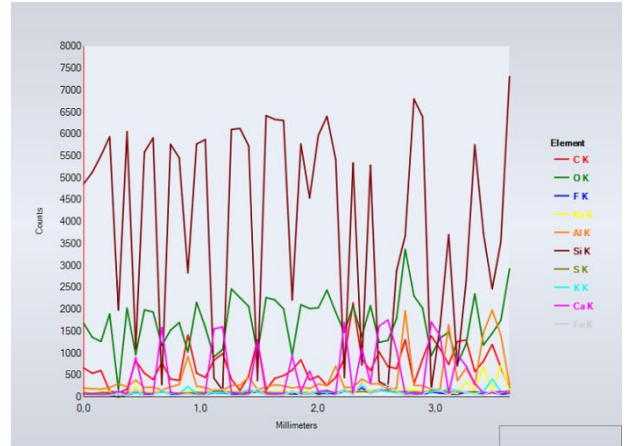
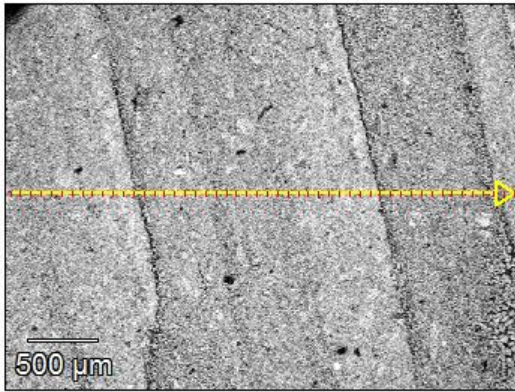
2-8 linecorrect(3)



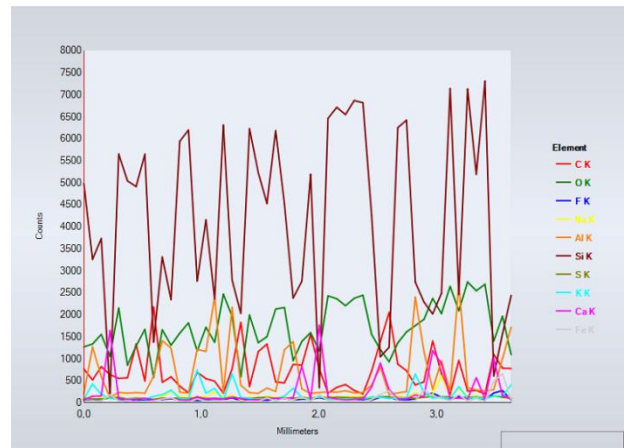
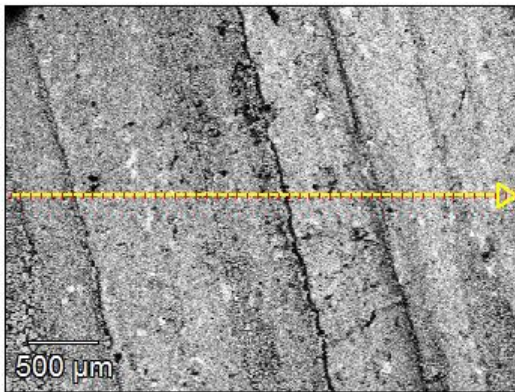
2-8 linecorrect(4)



2-8 linecorrect(5)



2-8 linecorrect(6)



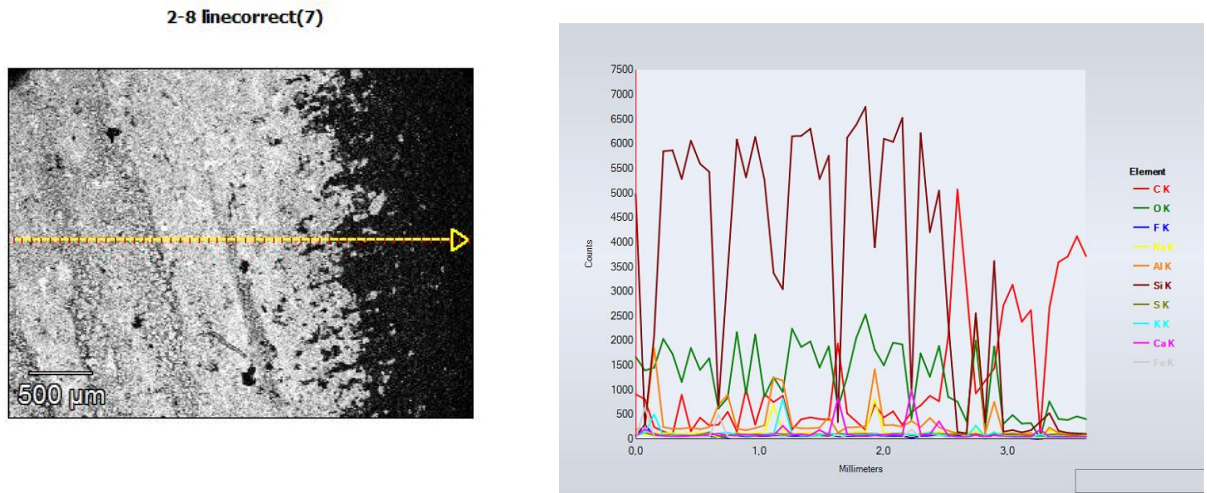
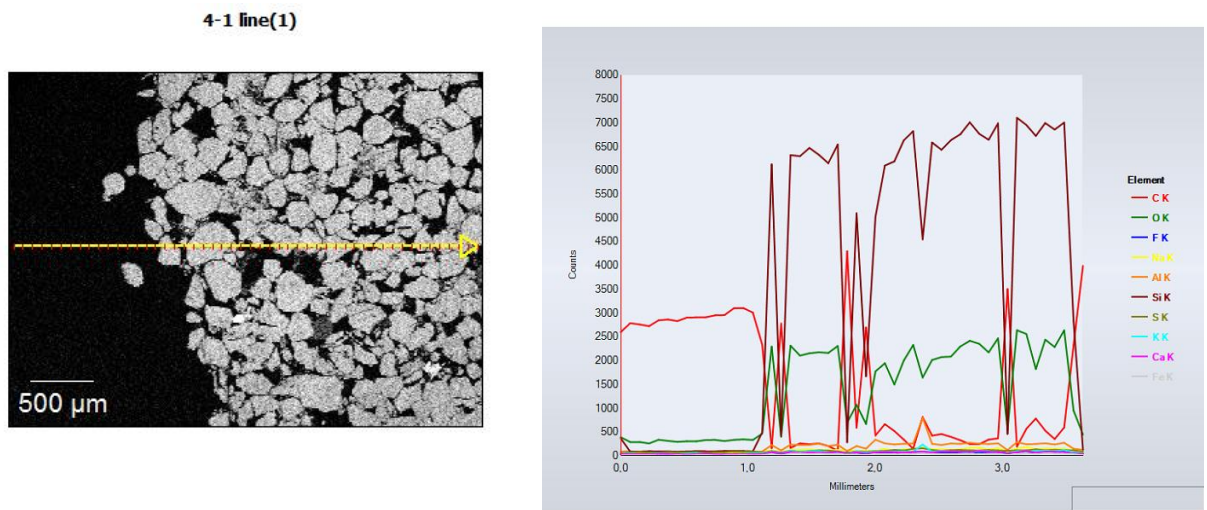
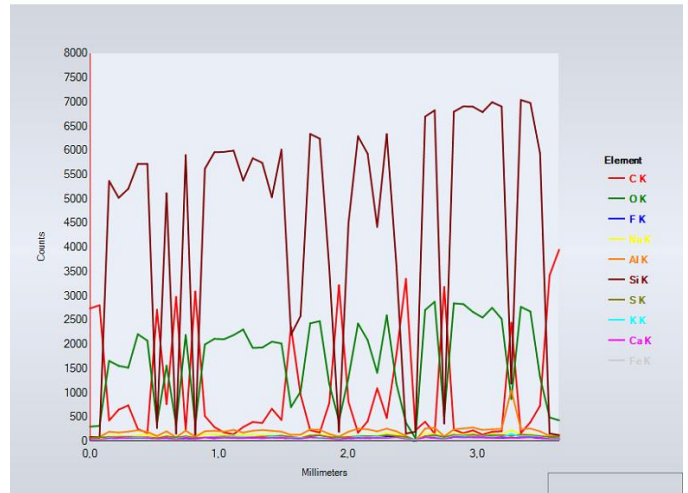
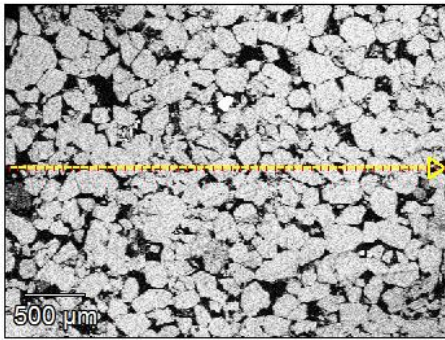


Figure A.6: Backscatter electron images and X-ray spectrums derived from line scans from sample 2.8

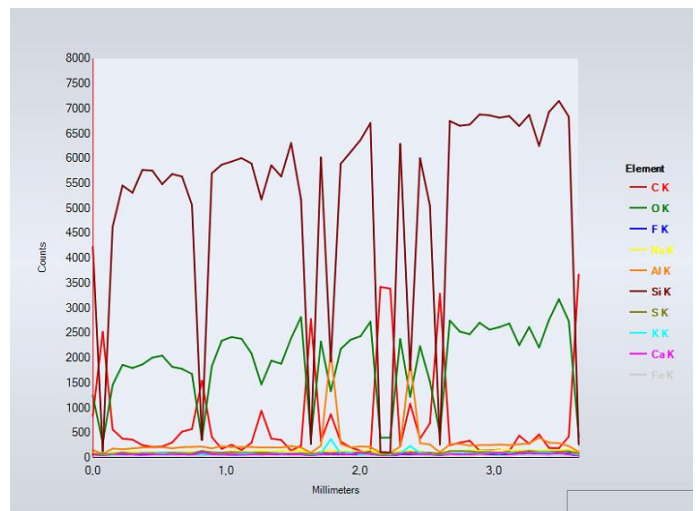
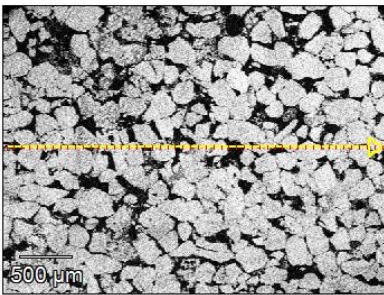
Sample 4.1



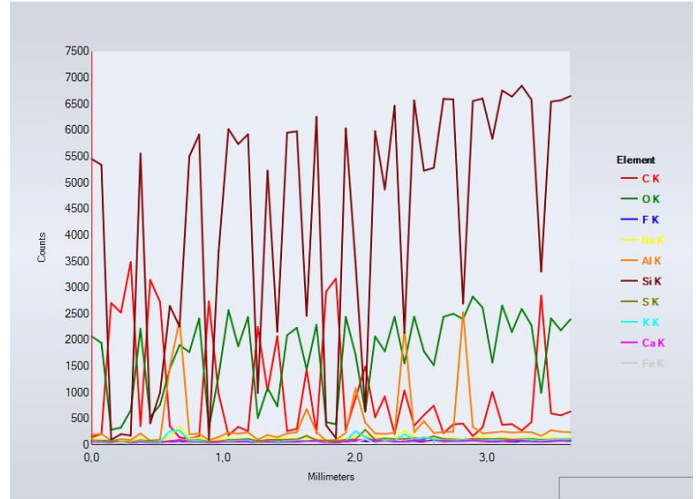
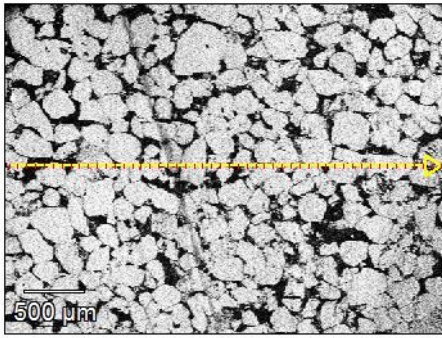
4-1 line(2)



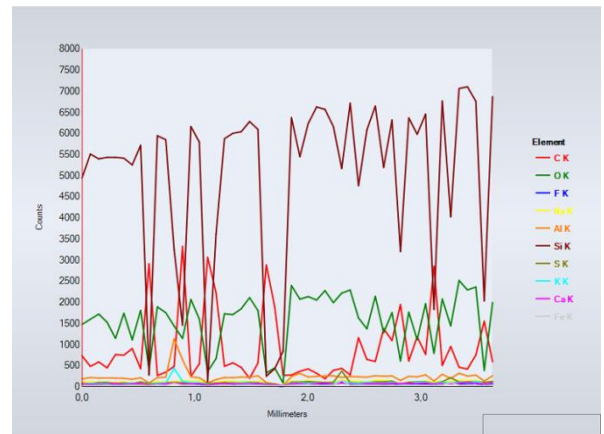
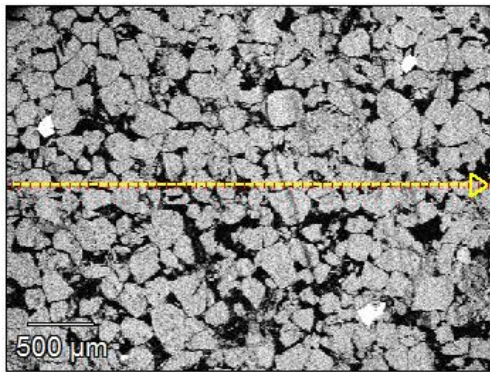
4-1 line(3)



4-1 line(4)

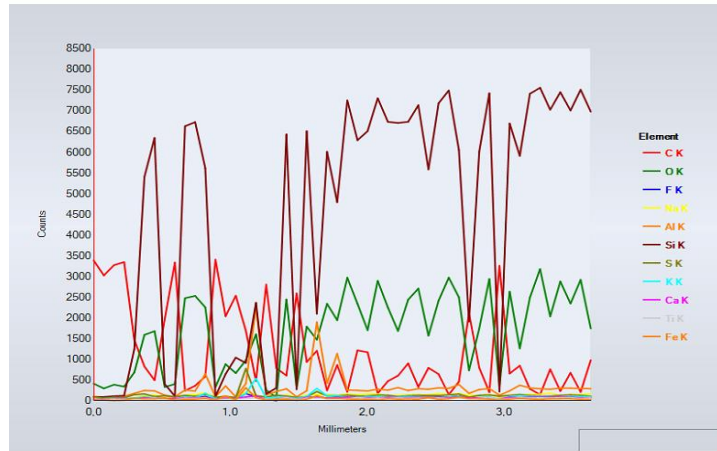
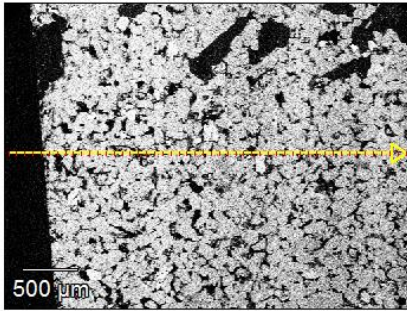


4-1 line(5)

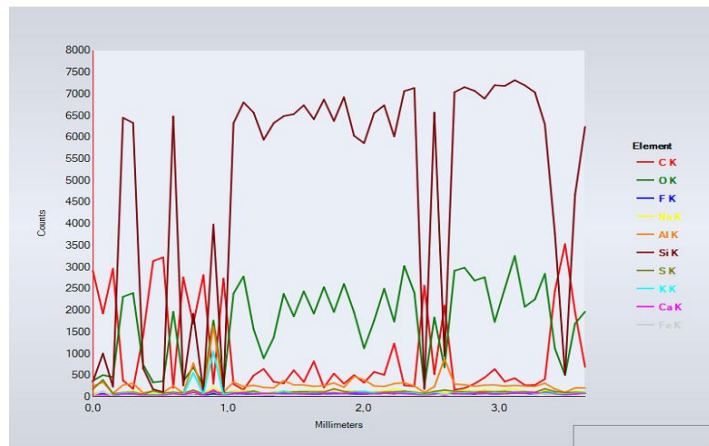
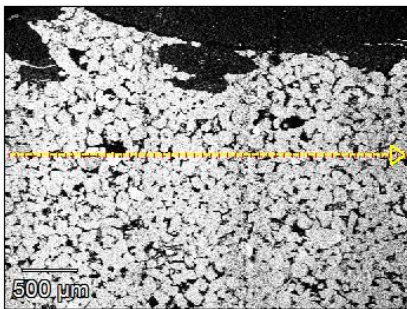


Sample 4.2

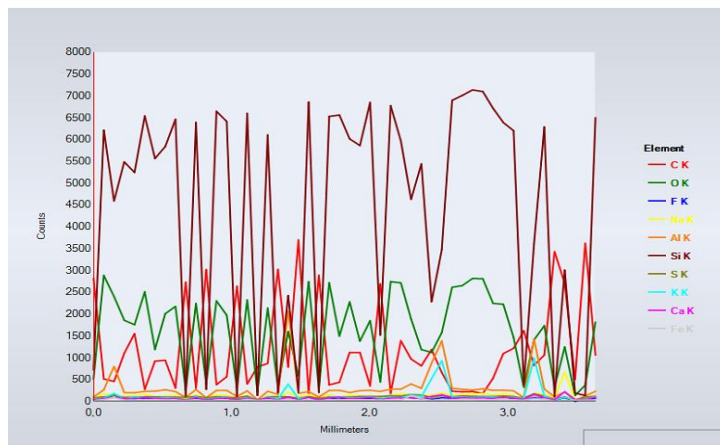
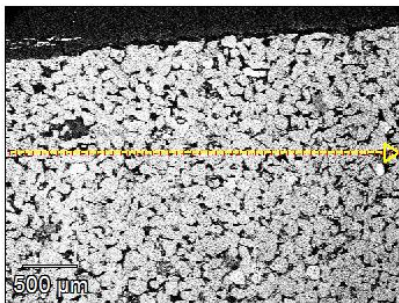
4-2 line scan(1)



4-2 line scan(2)

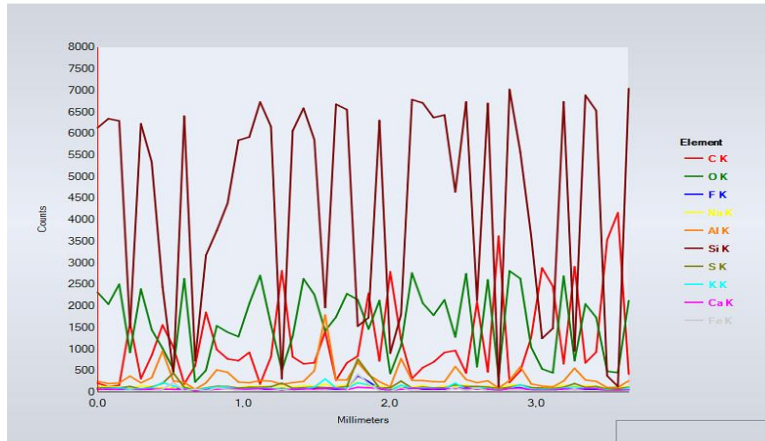
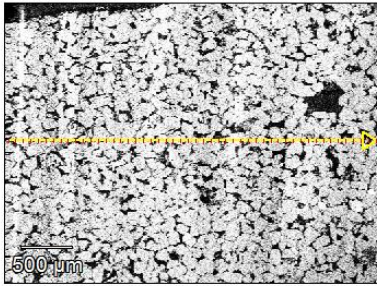


4-2 line scan(3)

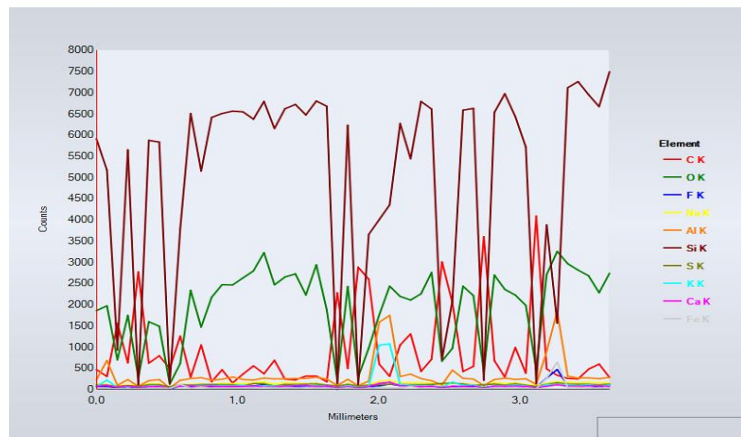
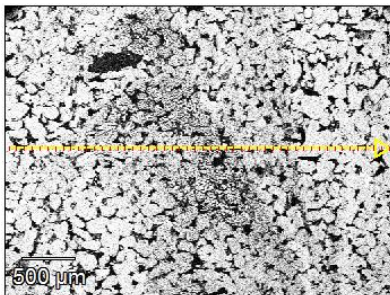


Appendix

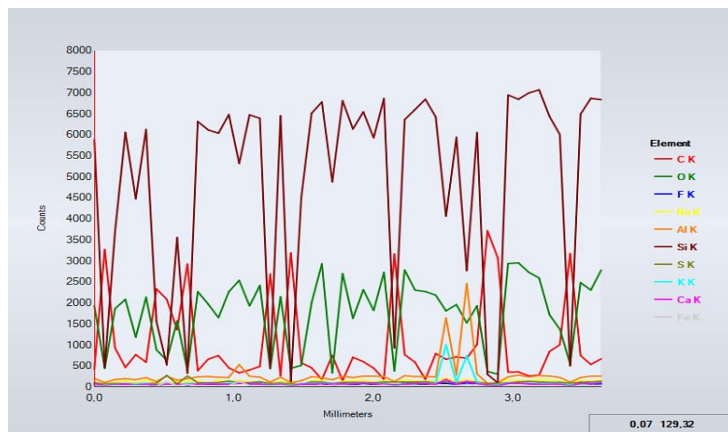
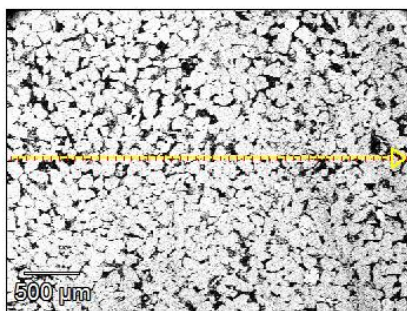
4-2 line scan(4)



4-2 line scan(5)



4-2 line scan(6)



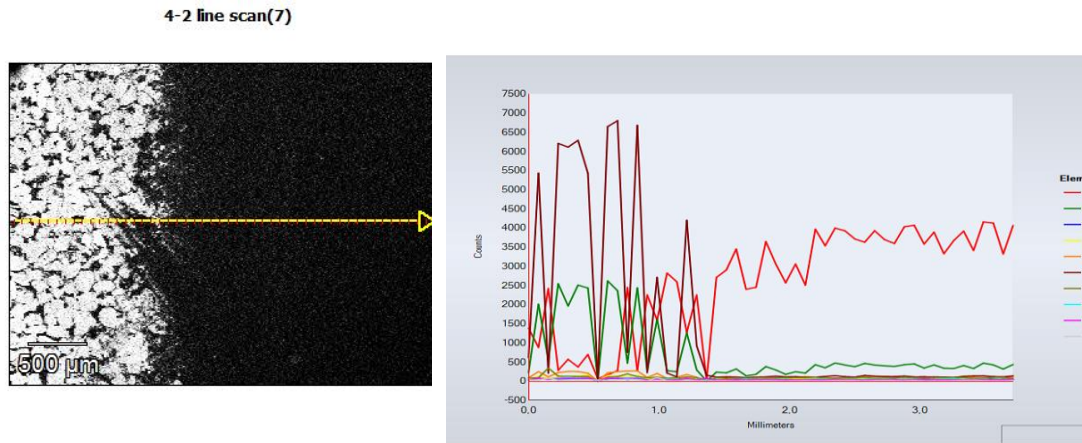
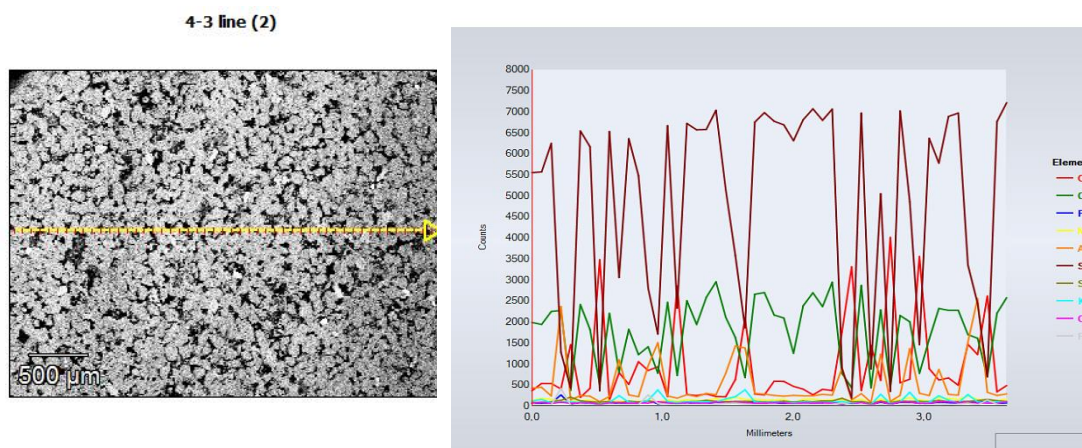
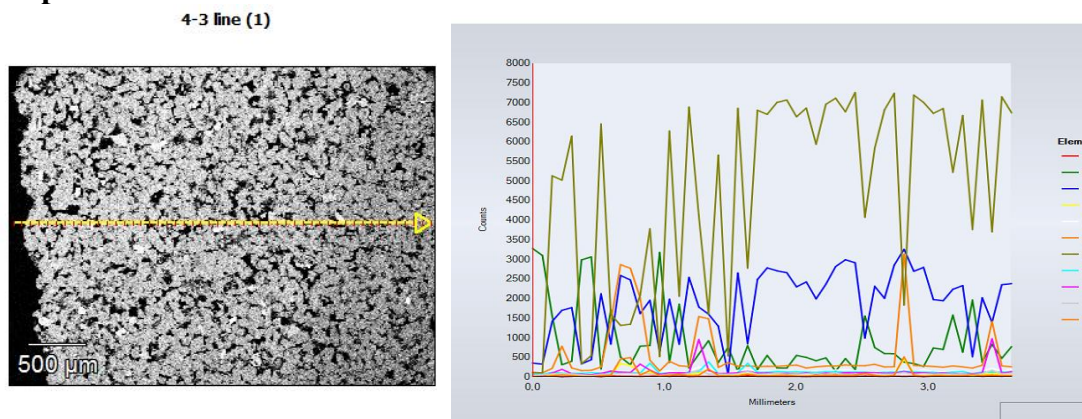
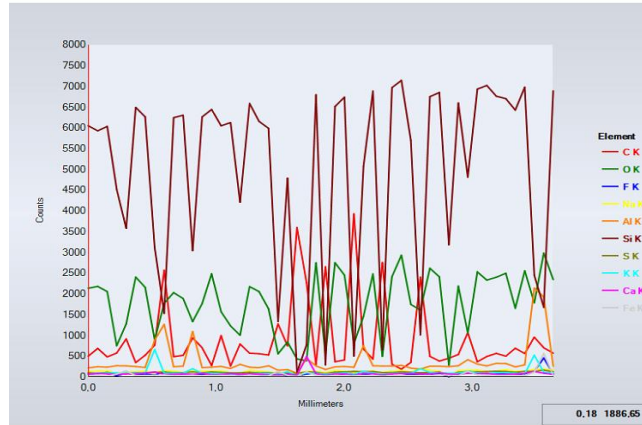
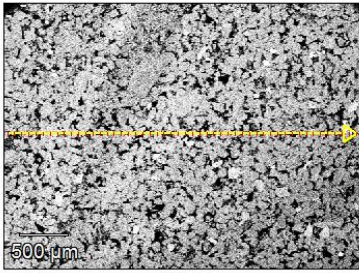


Figure A.8: Backscatter electron images and X-ray spectrums derived from line scans from sample 4.2

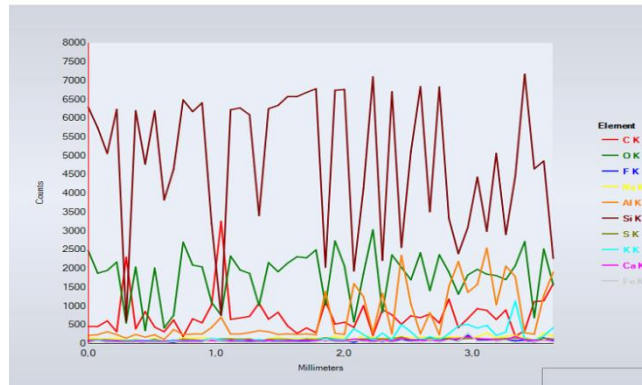
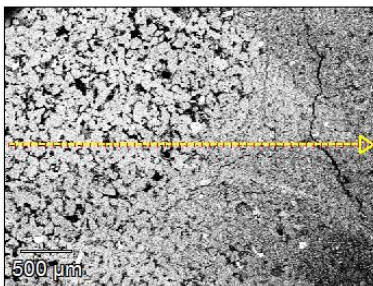
Sample 4.3



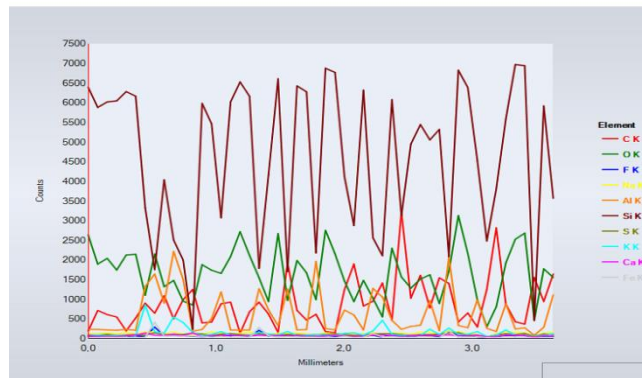
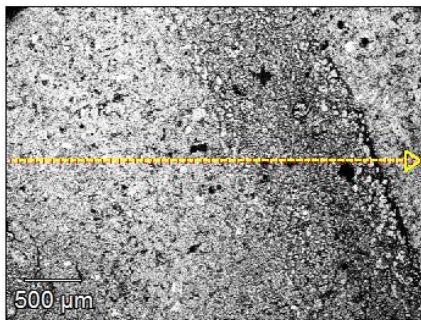
4-3 line (3)



4-3 line (4)



4-3 line (5)



4-3 line (6)

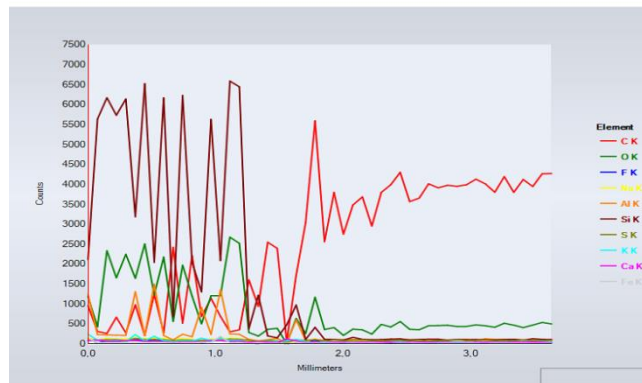
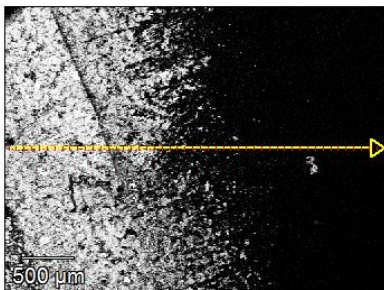


Figure A.9: Backscatter electron images and X-ray spectrums derived from line scans from sample 4.3

Sample 4.5

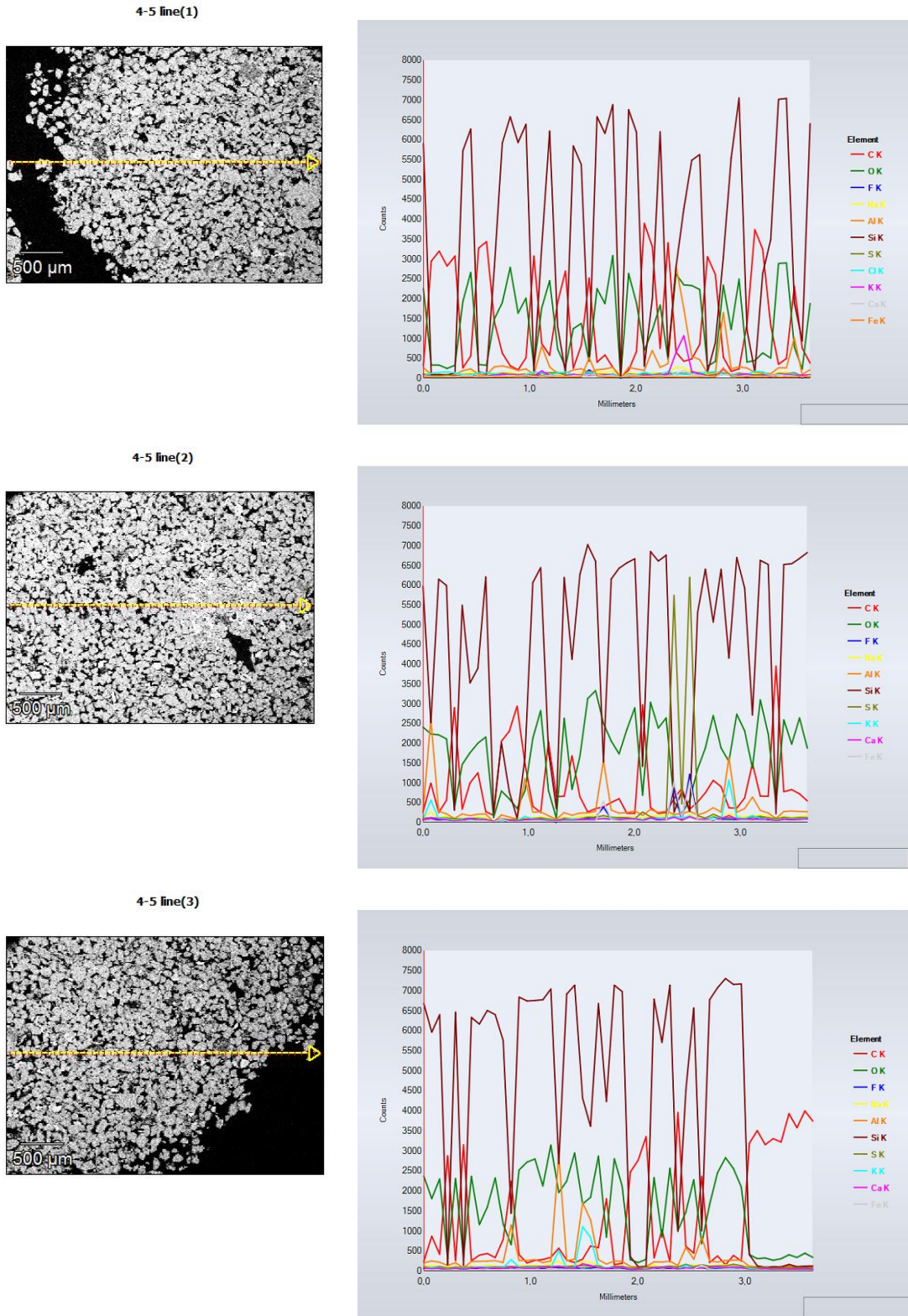
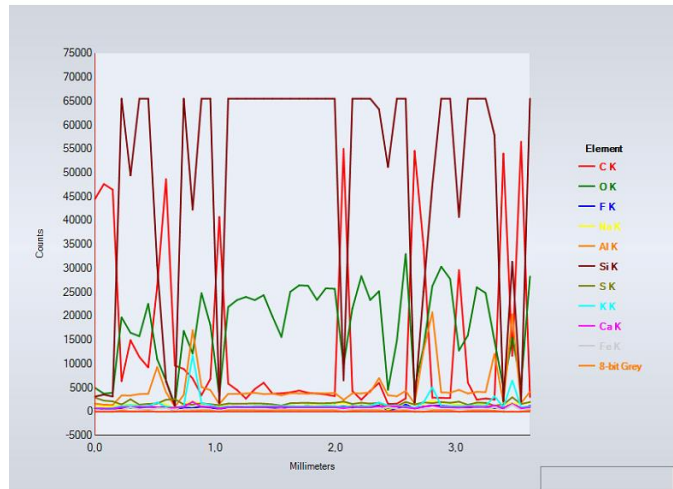
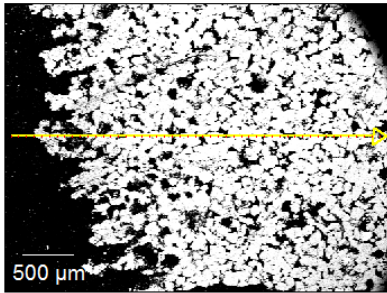


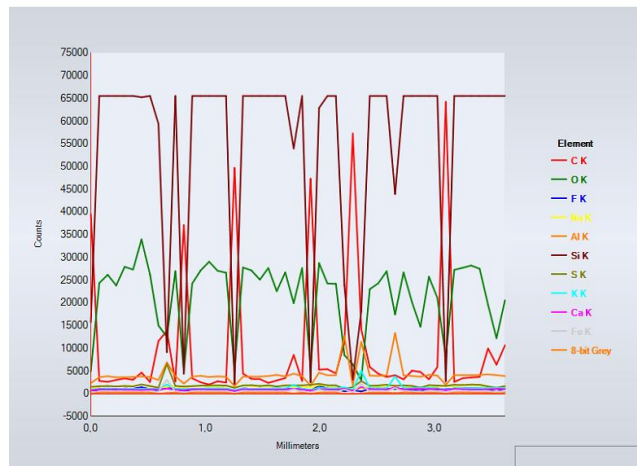
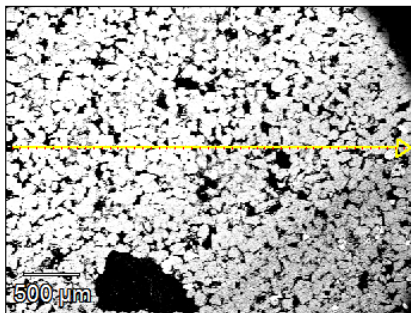
Figure A.10: Backscatter electron images and X-ray spectrums derived from line scans from sample 4.5

Sample 4.6

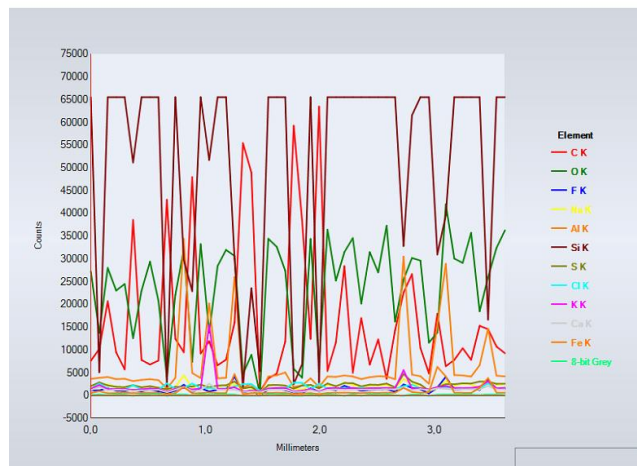
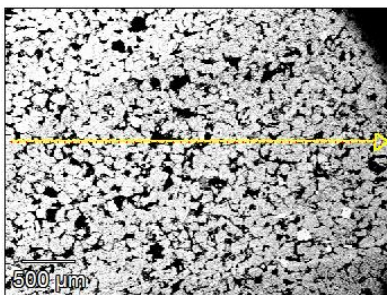
4-6 linescan(1)



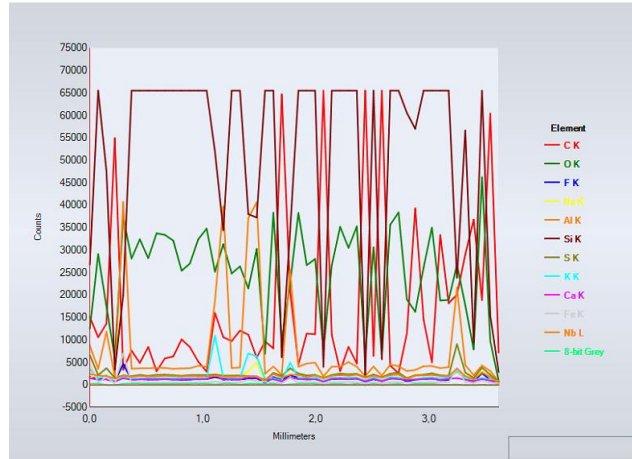
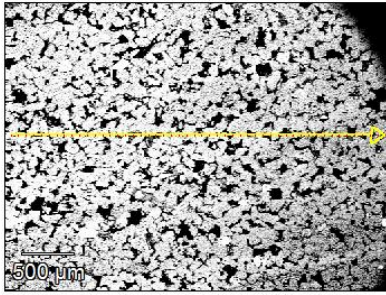
4-6 linescan(2)



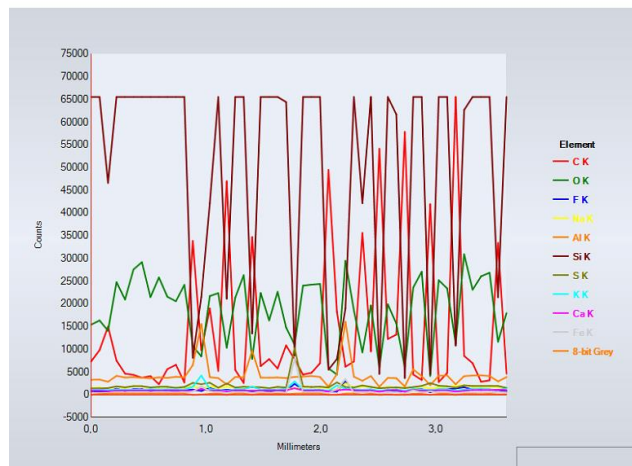
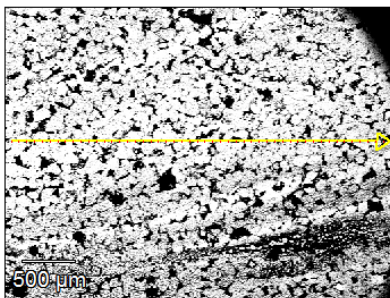
4-6 linescan(3)



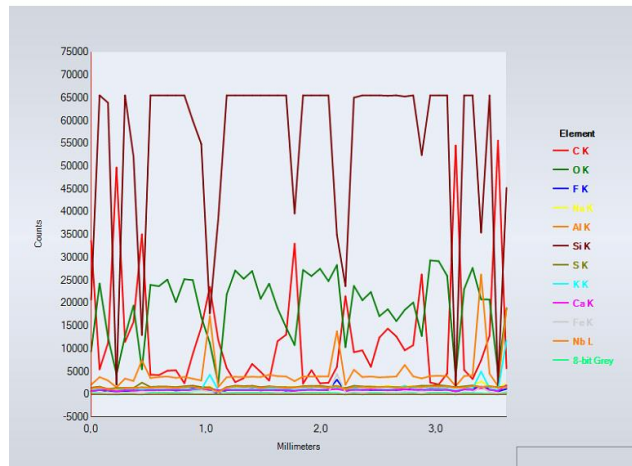
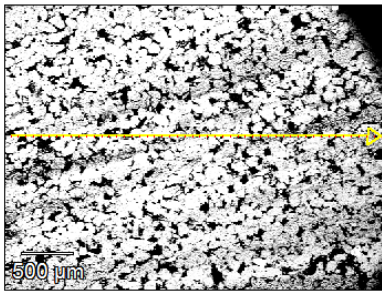
4-6 linescan(4)



4-6 linescan(5)



4-6 linescan(6)



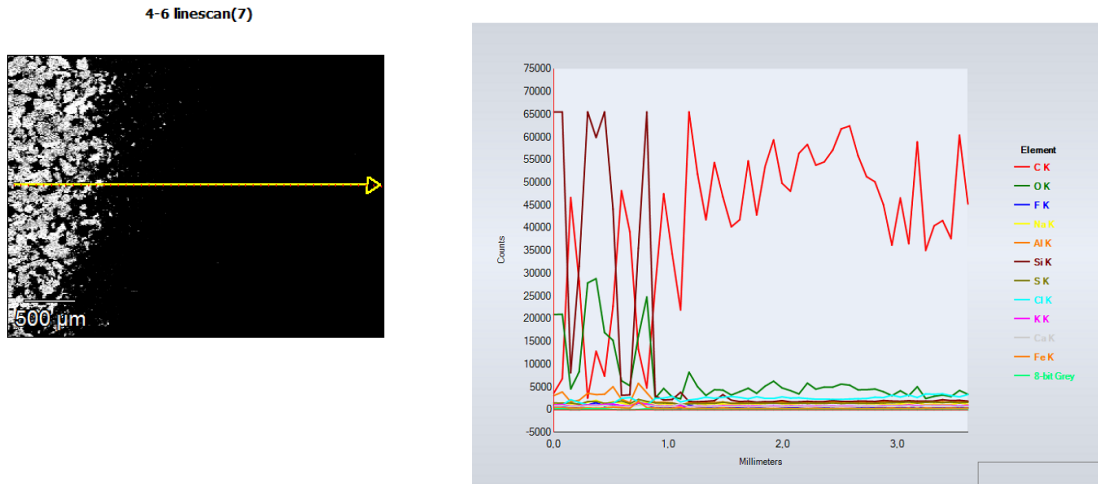
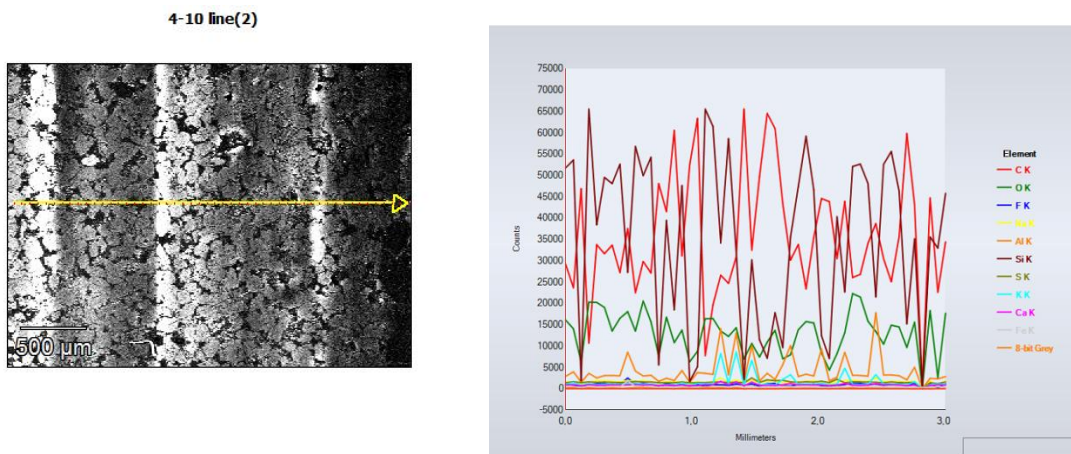
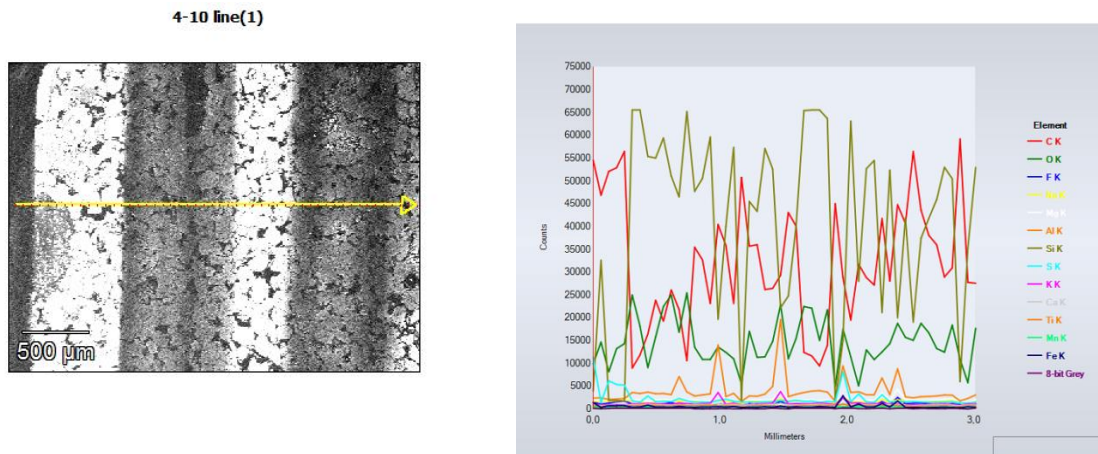
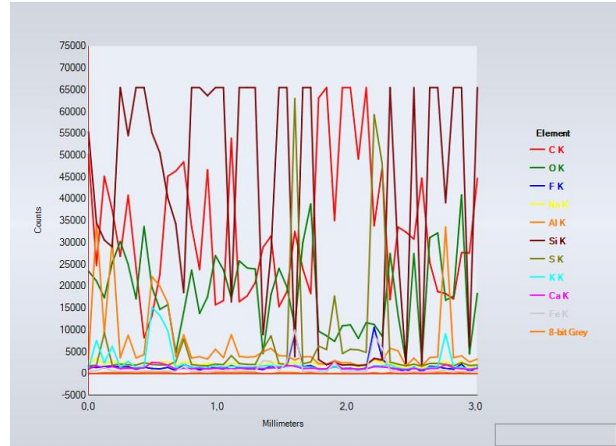
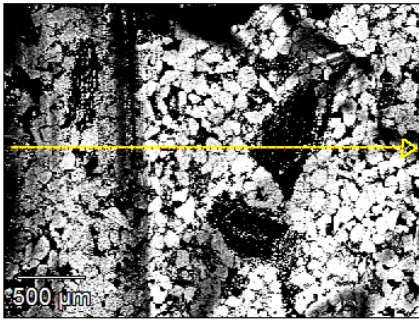


Figure A.11: Backscatter electron images and X-ray spectrums derived from line scans from sample 4.6

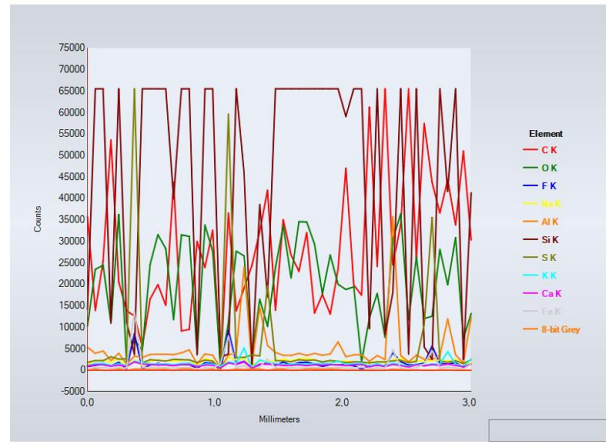
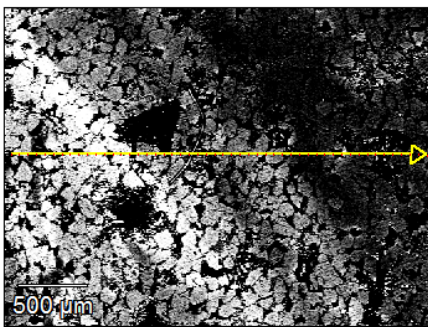
Sample 4.3



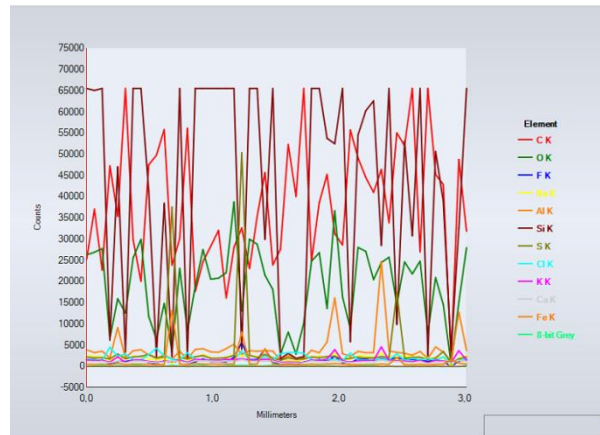
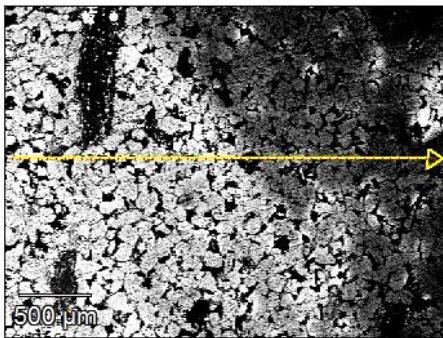
4-10 line(3)



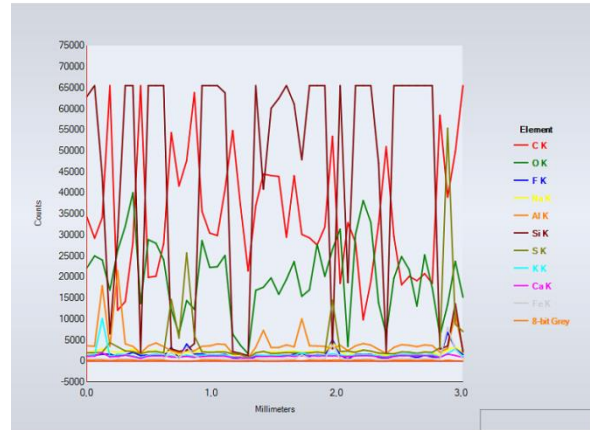
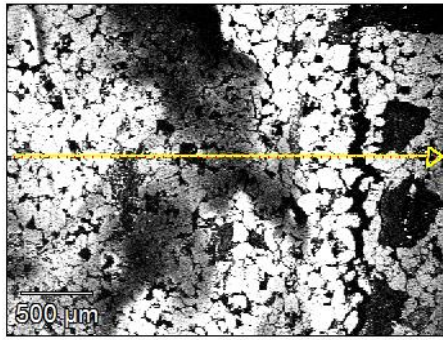
4-10 line(4)



4-10 line(5)



4-10 line(6)



4-10 line(7)

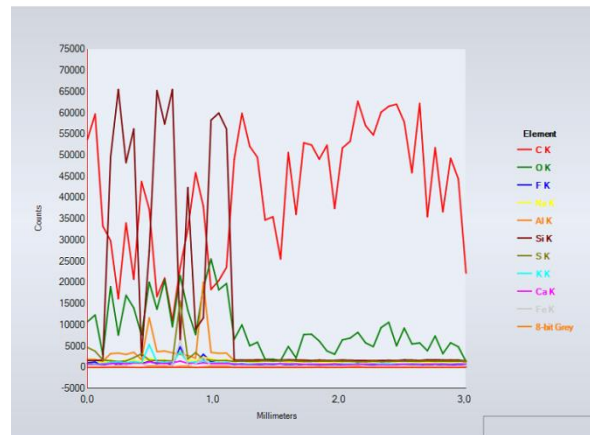
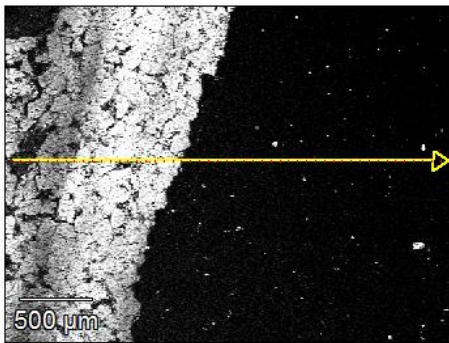
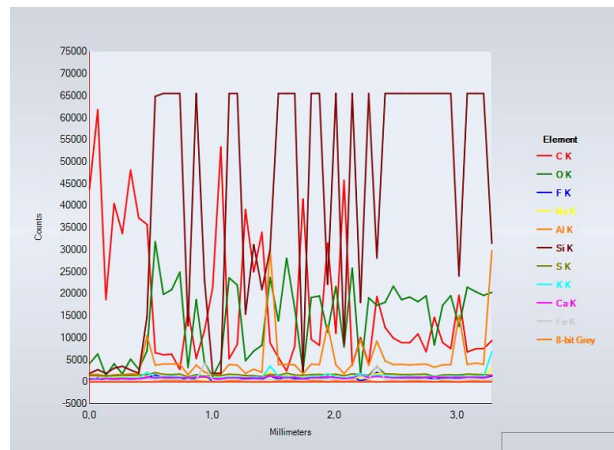
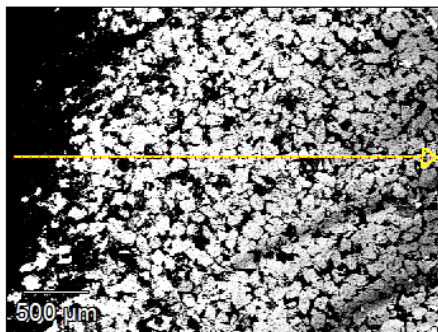


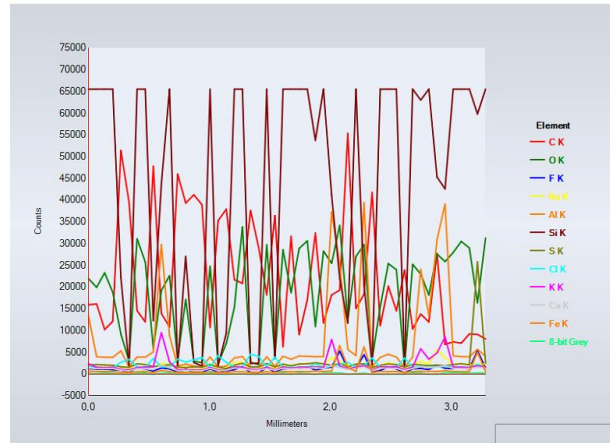
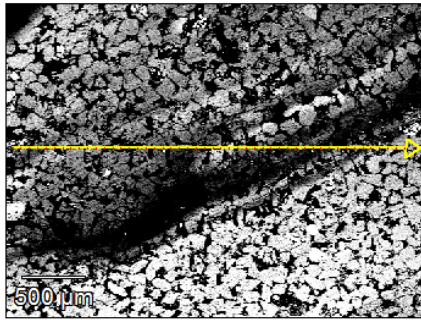
Figure A.12: Backscatter electron images and X-ray spectrums derived from line scans from sample 4.10

Sample 4.11

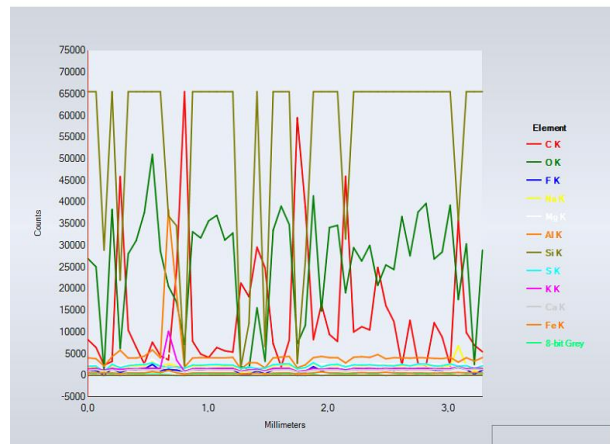
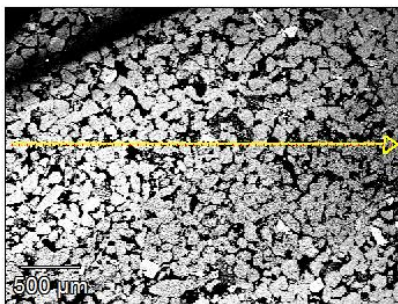
4-11 line(1)



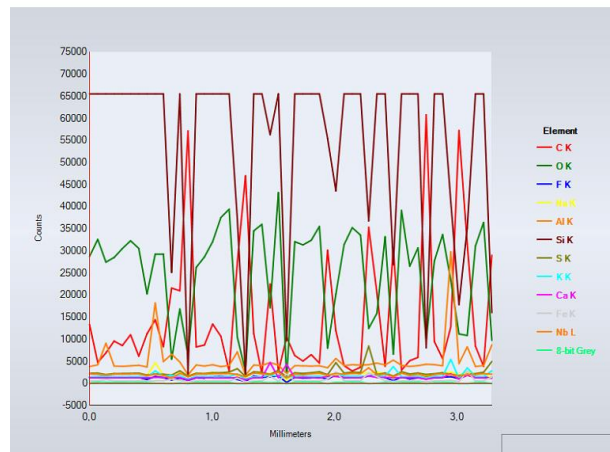
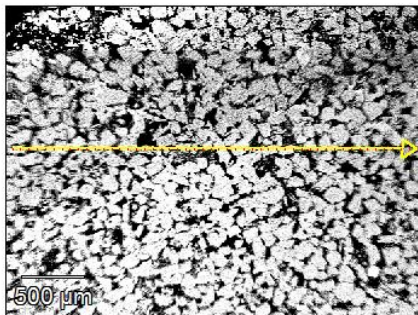
4-11 line(2)



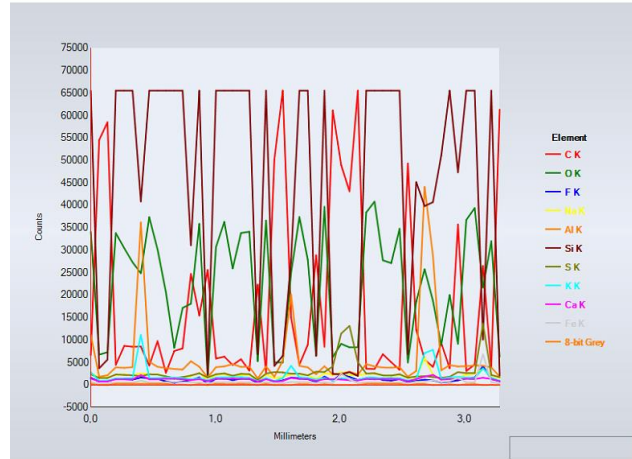
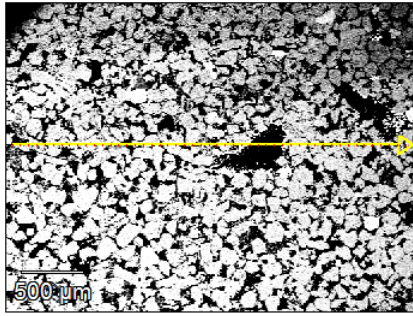
4-11 line(3)



4-11 line(4)



4-11 line(5)



4-11 line(6)

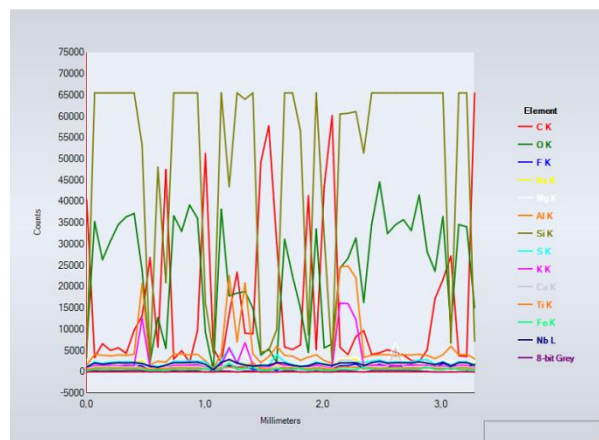
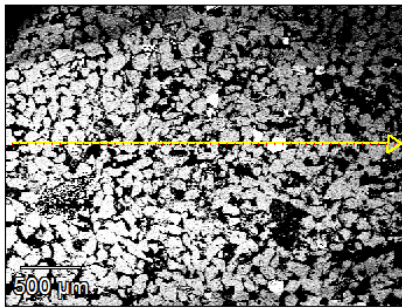



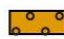






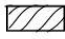





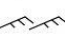

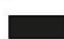


















Figure A.13: Backscatter electron images and X-ray spectrums derived from line scans from sample 4.11

Appendix B

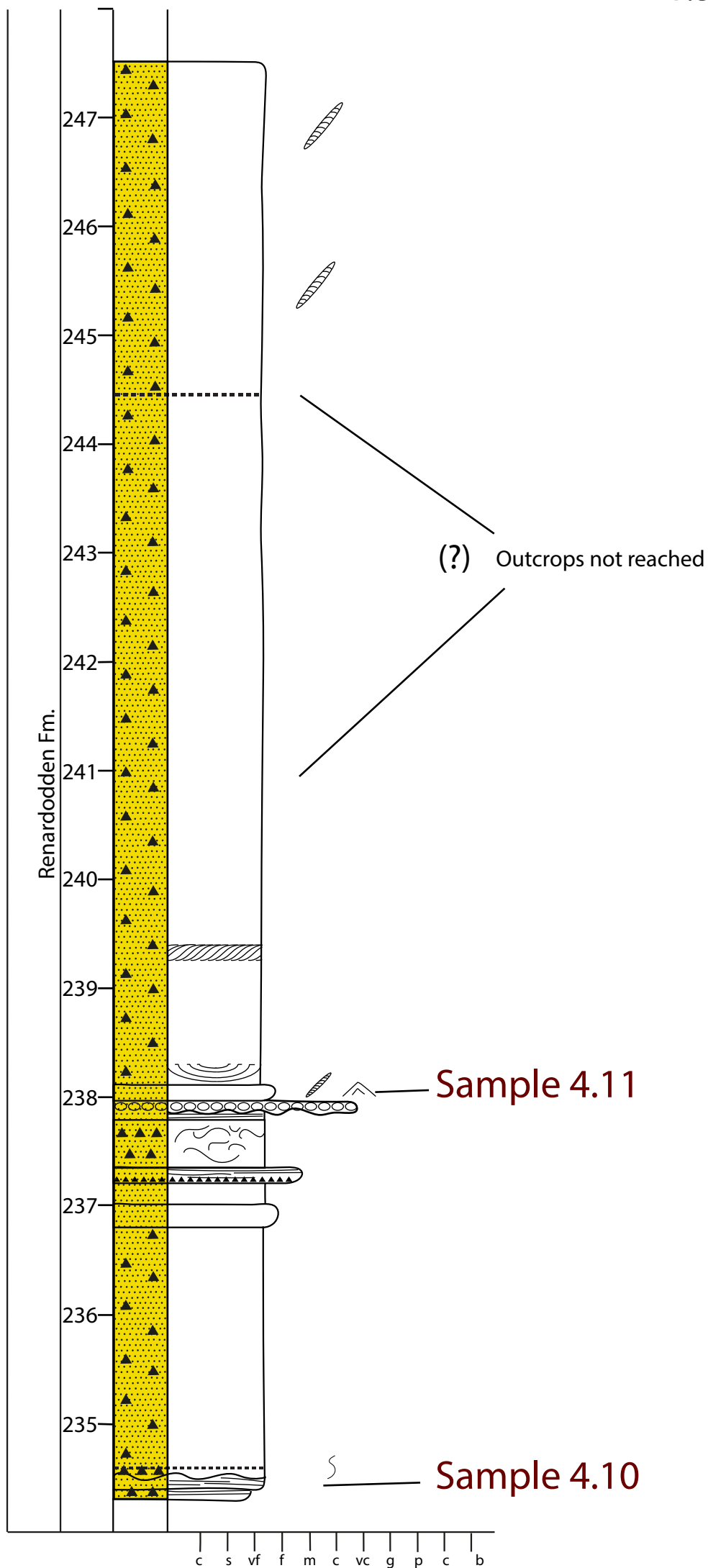
Lithostratigraphic logs

LEGEND

	Coal fragments		Trough cross-stratification		Rootlets
	Conglomerate		Crude laminations		Flaser bedding
	Sandstone		Plane parallel-stratification		Minor bioturbation
	Siltstone		Sigmoidal/tangential cross-stratification		Moderate bioturbation
	Sand/mud		Fractures		High bioturbation
	Mudstone		Current ripples		Palaeophycus
	Coal		Plane parallel laminations		Ophiomorpha
	Coaly shale		Soft sediment deformation		Teichichnus
	Gap		Wave ripples		Leaf traces
	Pyrite		Scouring		
	Granules		Load cast		
	Sandstone clast				
	Mudstone clast				
	Siderite concretion				
	Coal clast				

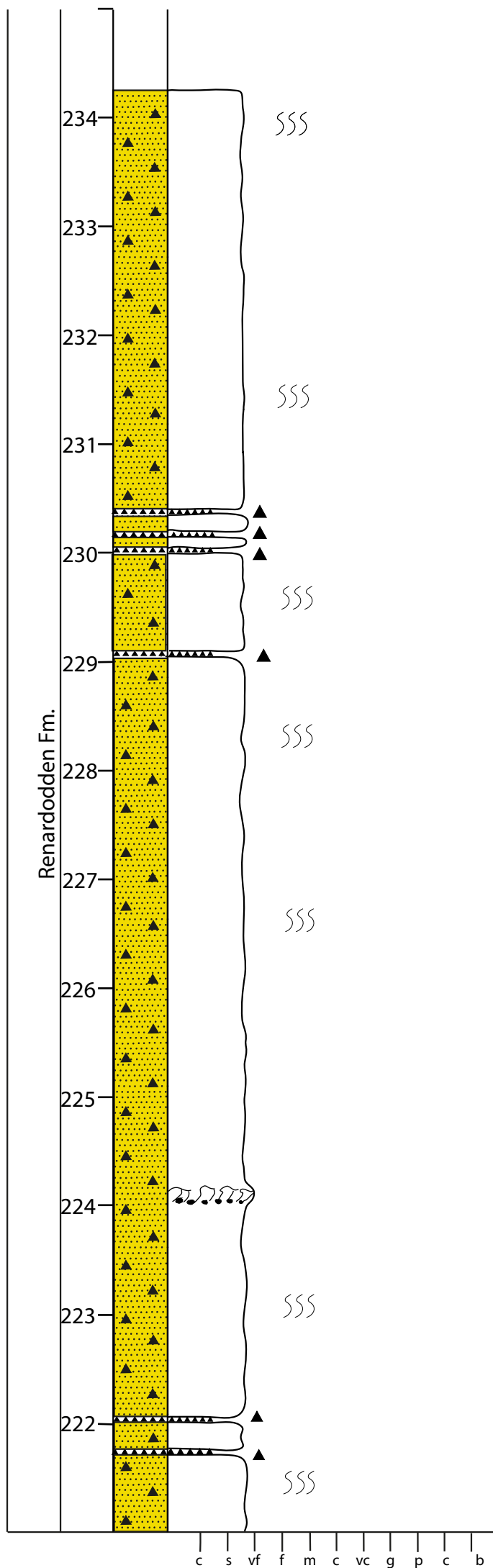
Fm. (m)

1:50

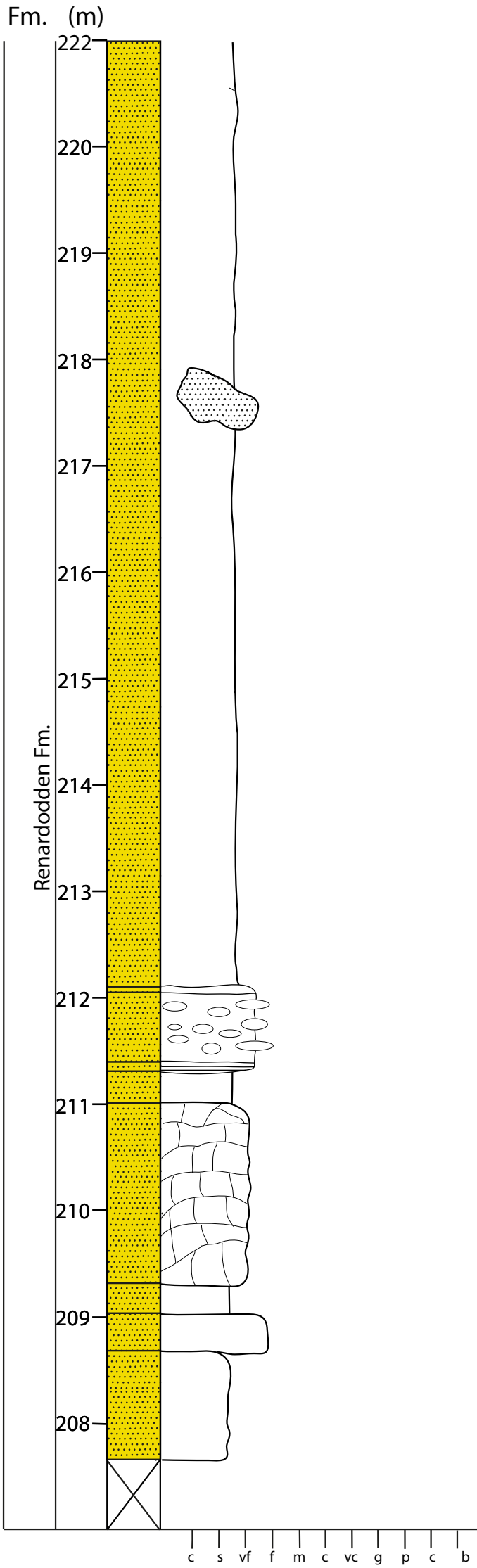


Fm. (m)

1:50

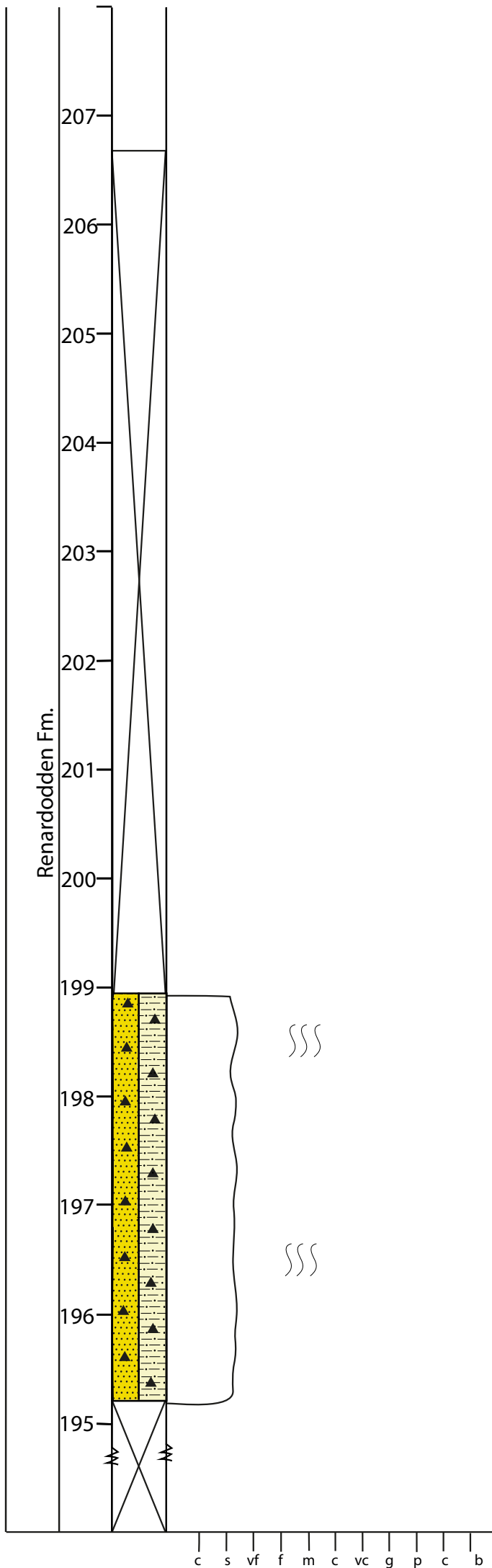


1:50



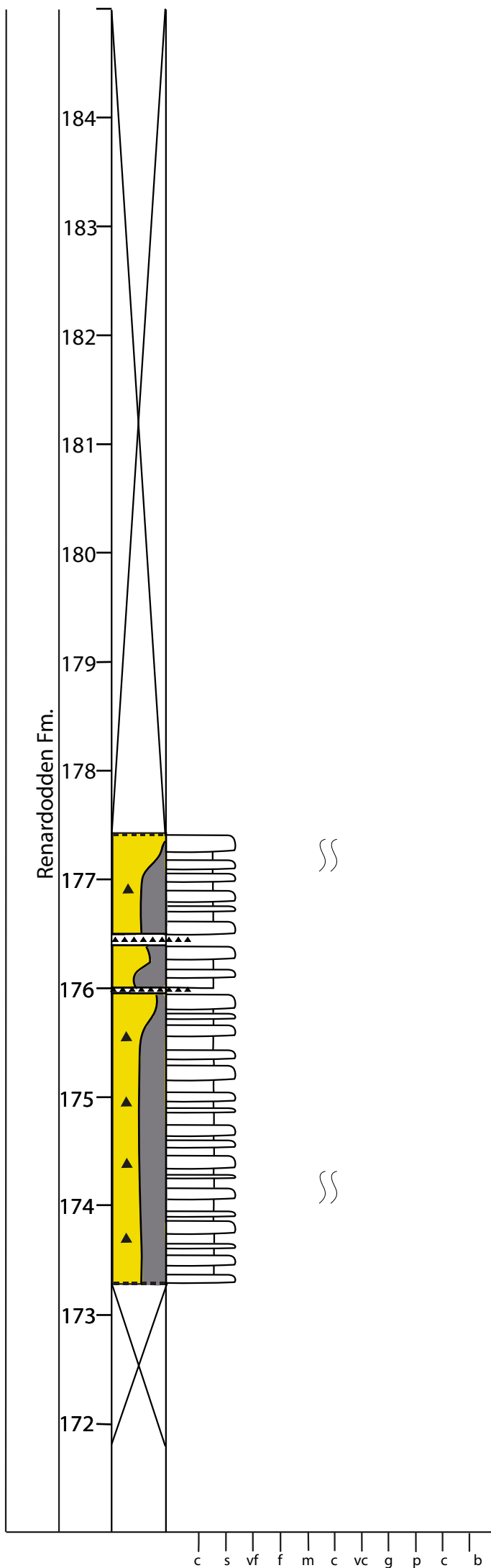
Fm. (m)

1:50



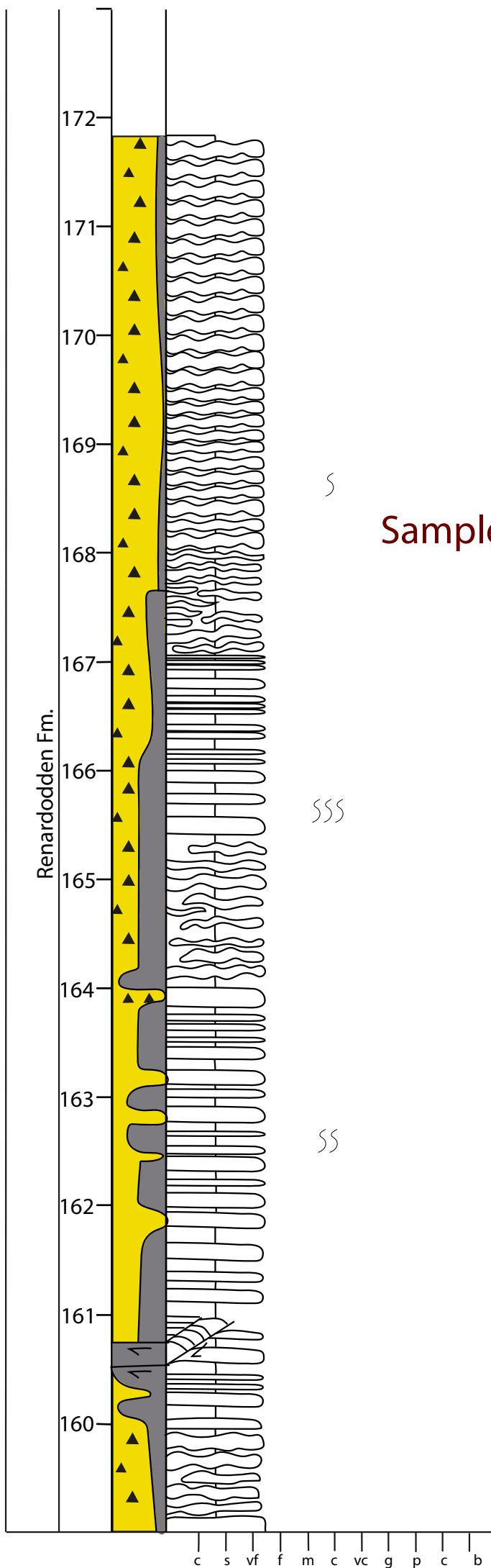
Fm. (m)

1:50

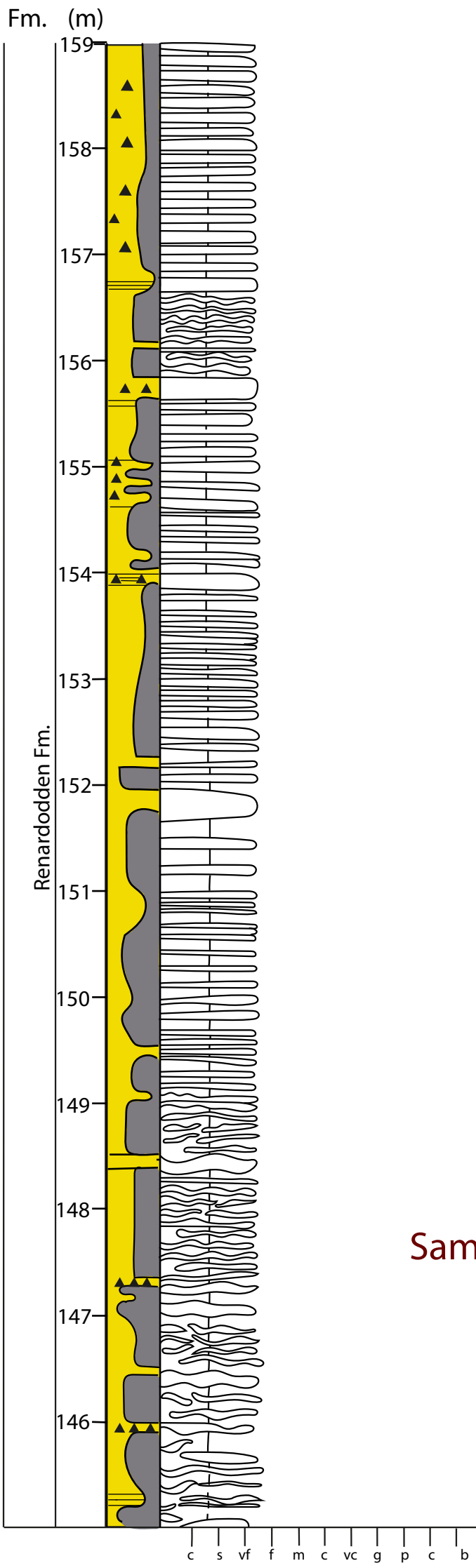


Fm. (m)

1:50



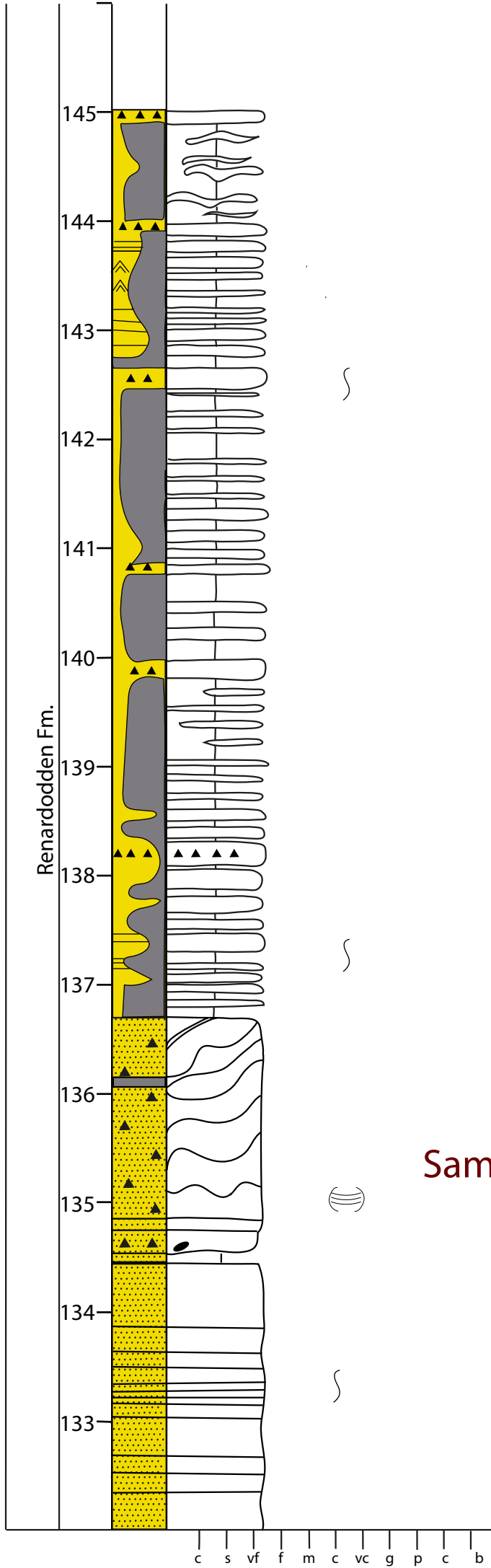
1:50



Sample 4.6

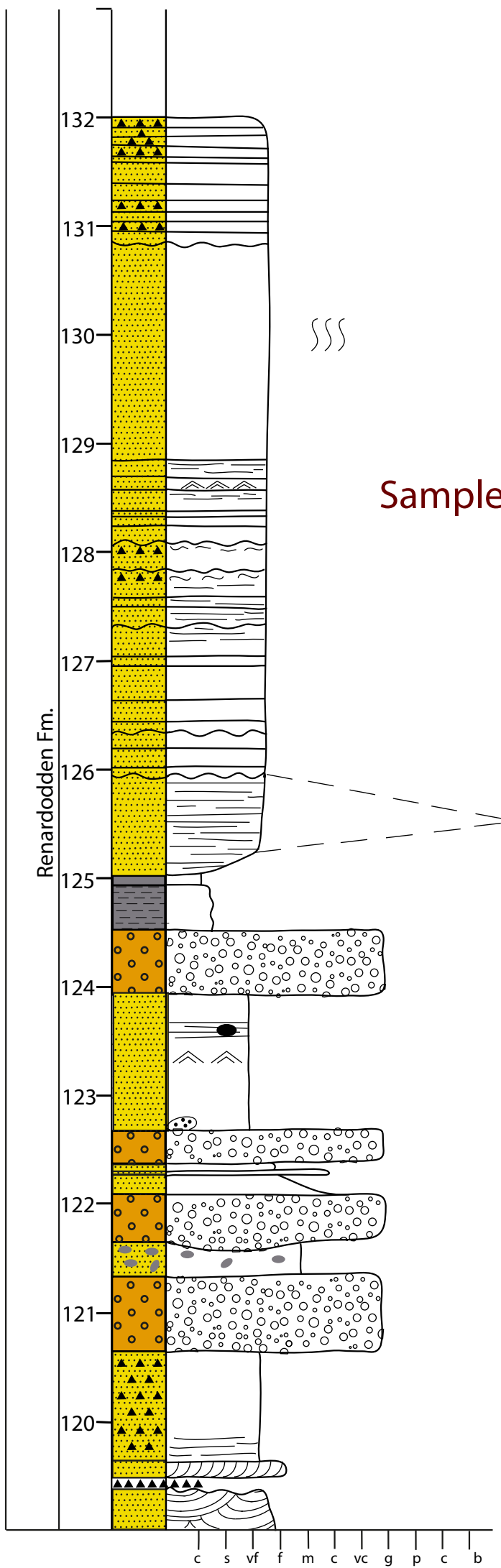
Fm. (m)

1:50

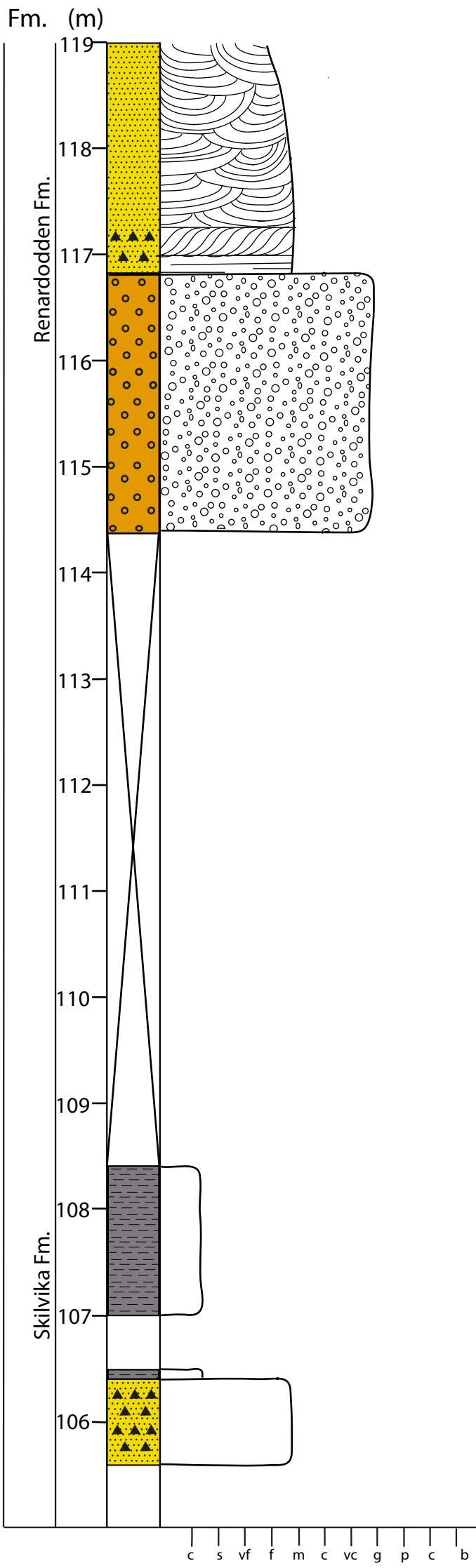


Fm. (m)

1:50

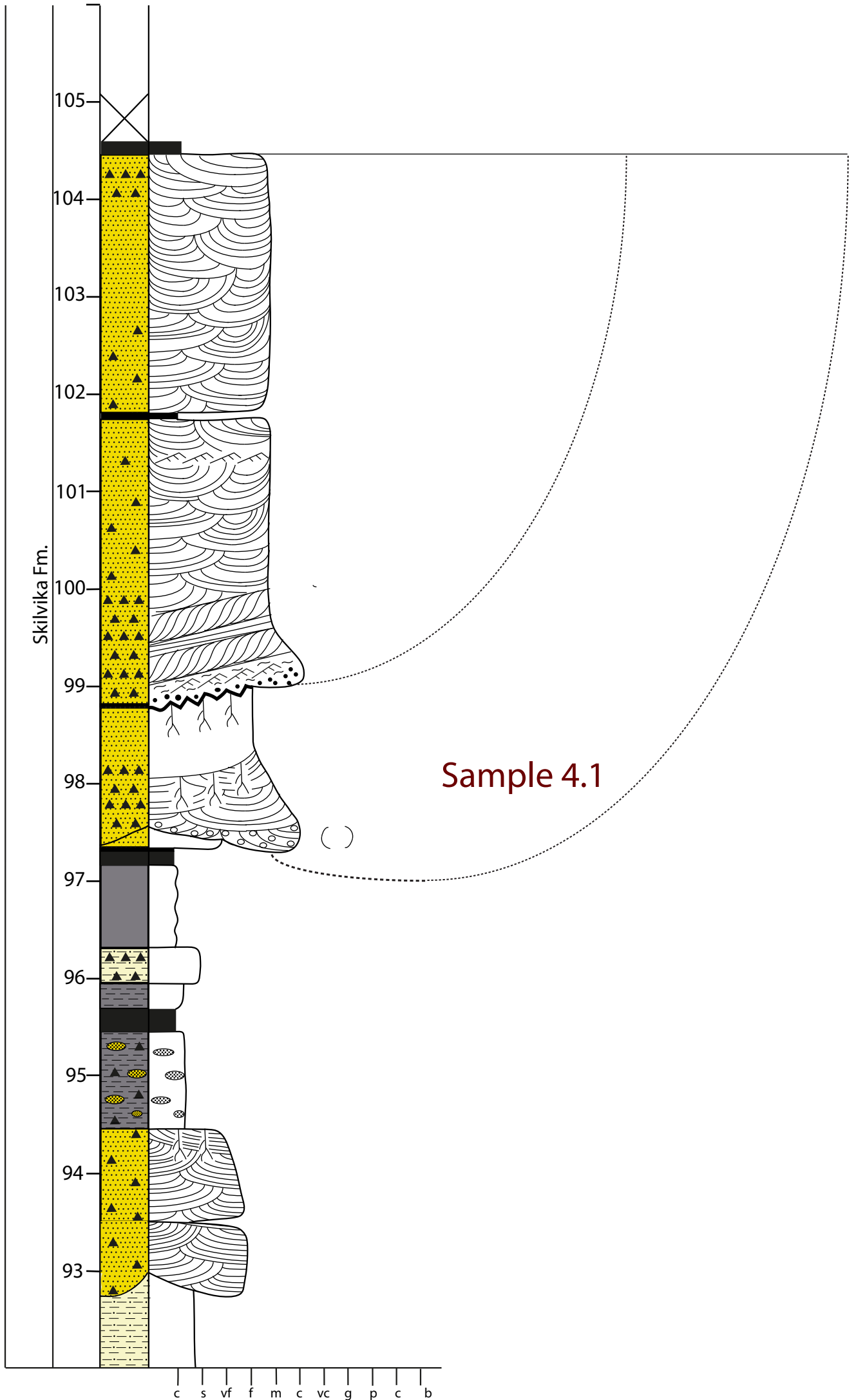


1:50



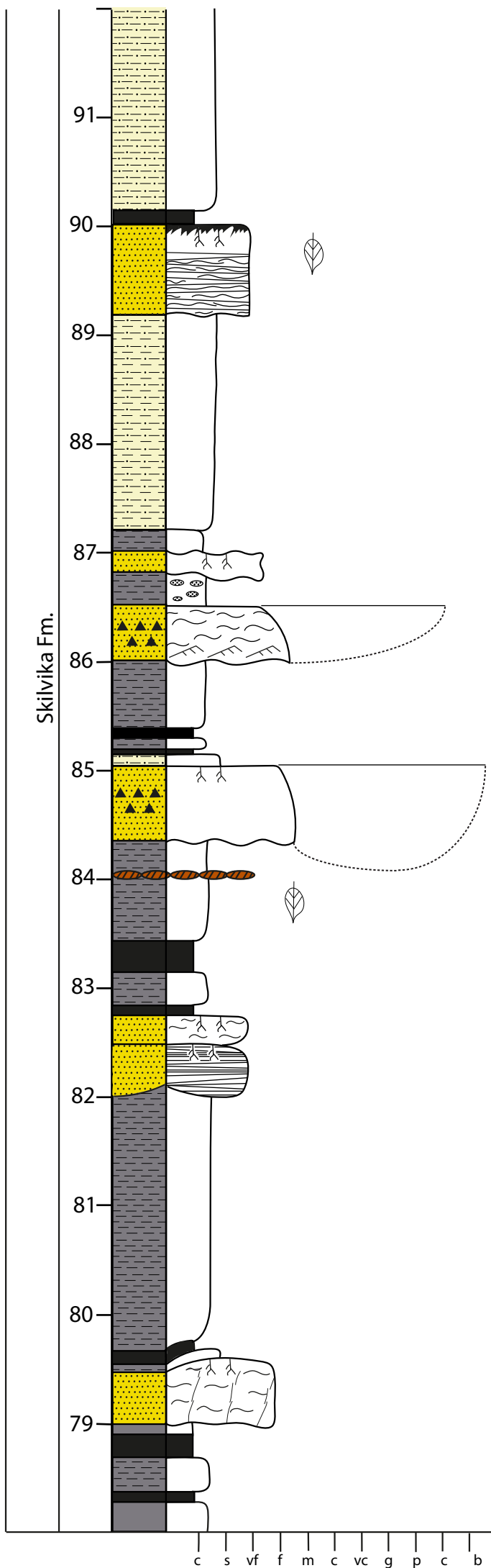
Fm. (m)

1:50



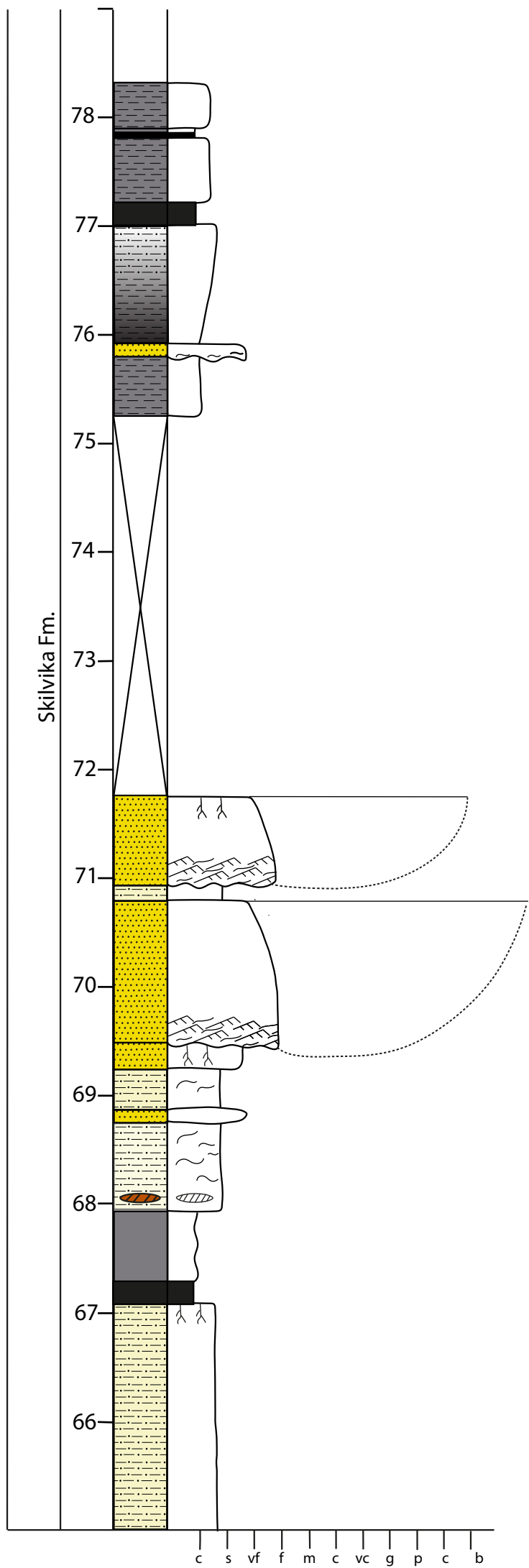
Fm. (m)

1:50

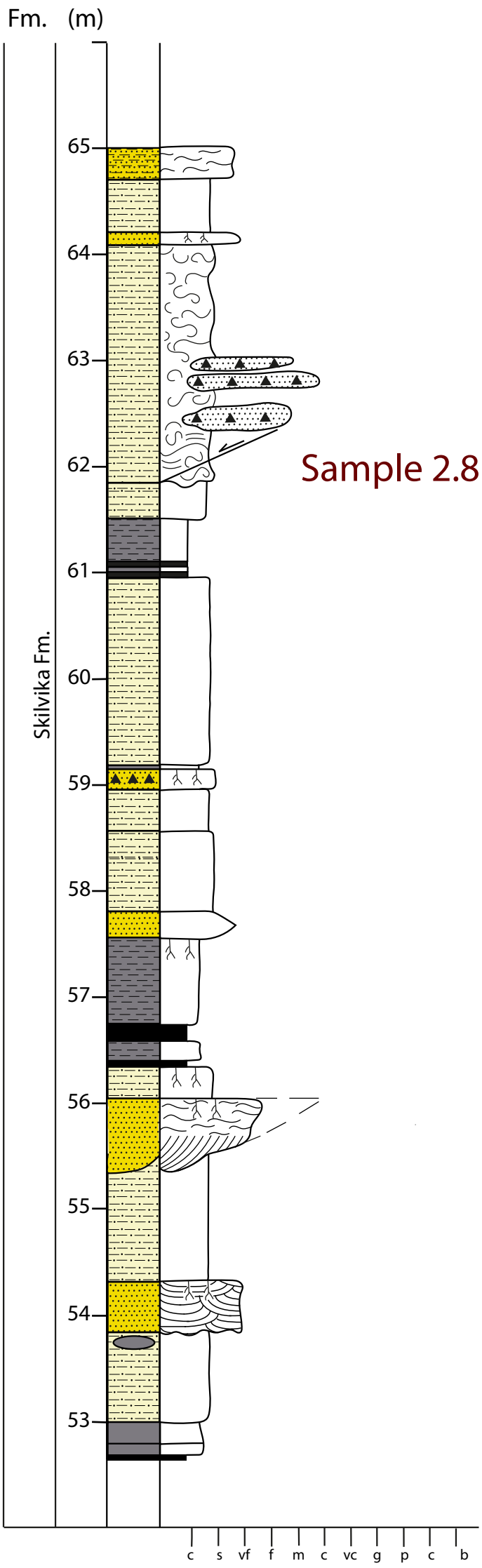


Fm. (m)

1:50

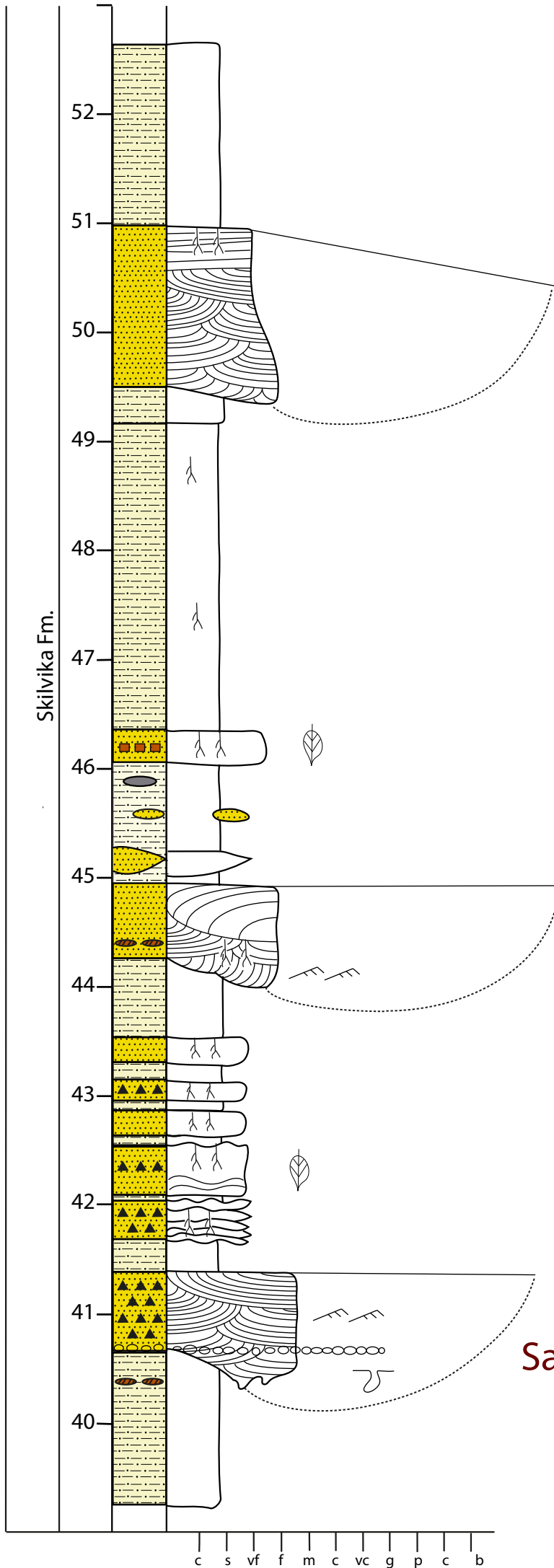


1:50



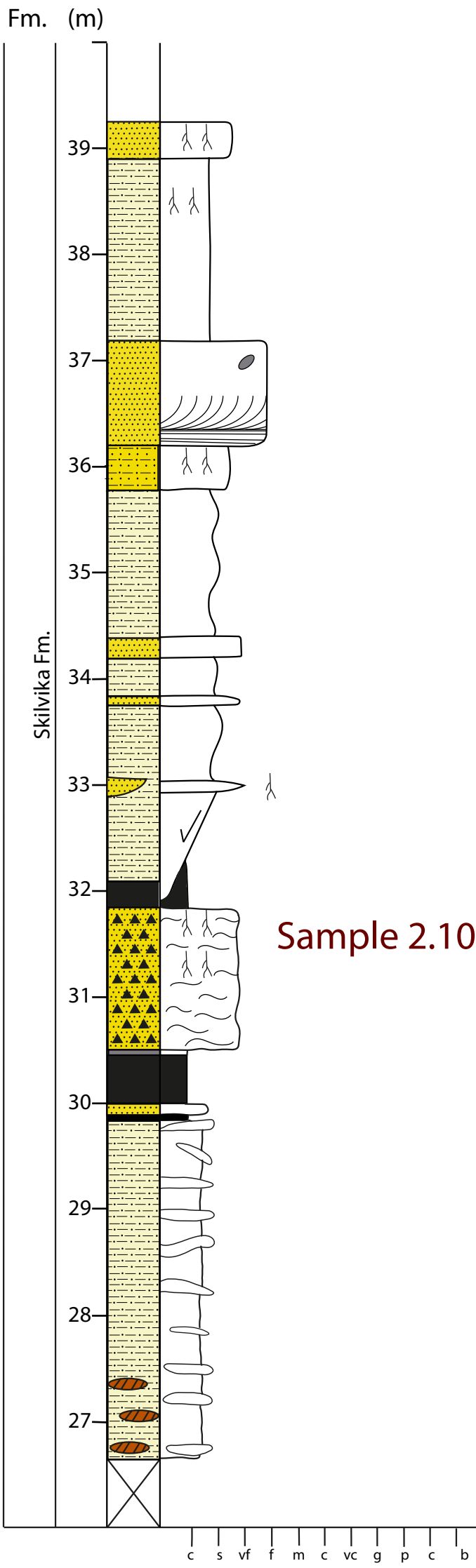
Fm. (m)

1:50



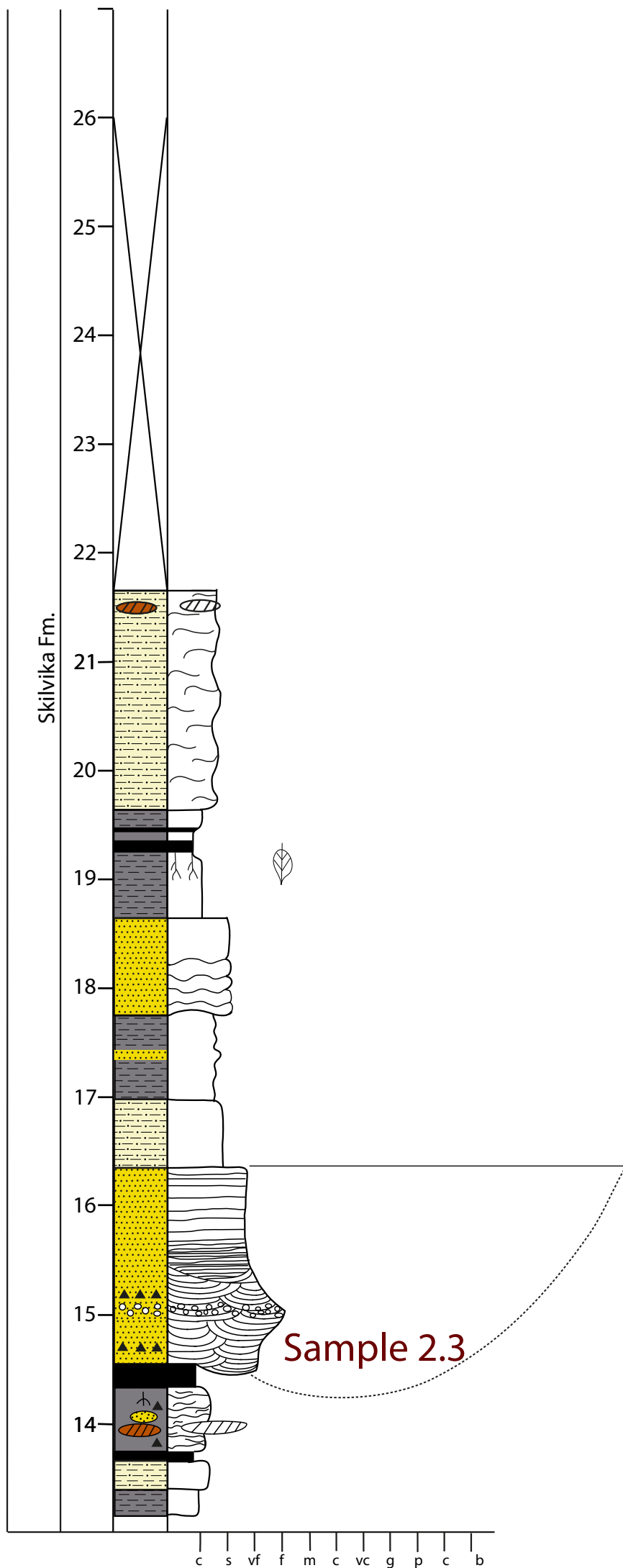
Sample 2.5

1:50



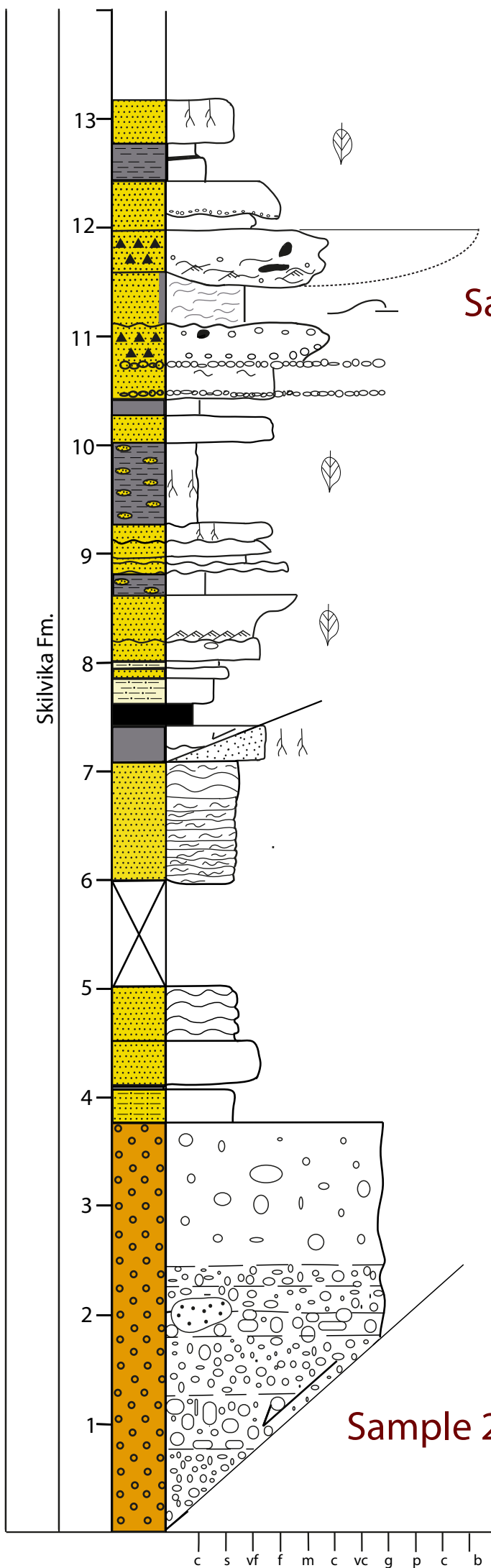
Fm. (m)

1:50



Fm. (m)

1:50



Sample 2.2

Sample 2.1

MPS=22.4